University of Zagreb

FACULTY OF SCIENCE
DEPARTMENT OF GEOLOGY

Erli Kovačević Galović

GEOCHEMICAL DISCRIMINATION OF BAUXITE HORIZONS IN THE REPUBLIC OF CROATIA

DOCTORAL THESIS

Zagreb, 2026

University of Zagreb

FACULTY OF SCIENCE
DEPARTMENT OF GEOLOGY

Erli Kovačević Galović

GEOCHEMICAL DISCRIMINATION OF BAUXITE HORIZONS IN THE REPUBLIC OF CROATIA

DOCTORAL THESIS

Supervisors:
Senior Research Assoc. Nikolina Ilijanić, PhD
Full Prof. Nenad Tomašić, PhD

Zagreb, 2026

Sveučilište u Zagrebu

PRIRODOSLOVNO-MATEMATIČKI FAKULTET

GEOLOŠKI ODSJEK

Erli Kovačević Galović

GEOKEMIJSKA DISKRIMINACIJA BOKSITNIH HORIZONATA U REPUBLICI HRVATSKOJ

DOKTORSKI RAD

Mentori:

dr. sc. Nikolina Ilijanić, viša znanstvena suradnica

dr. sc. Nenad Tomašić, redoviti profesor

Zagreb, 2026

This doctoral research was carried out at the Croatian Geological Survey under the guidance of Nikolina Ilijanić, PhD, Senior Research Associate at the Department for Mineral Resources and Marine Geology, and Nenad Tomašić, PhD, Full Professor at the University of Zagreb Faculty of Science, Department of Geology.

Mom padre-u, zbog kojeg sam zavoljela geologiju.

Od srca zahvaljujem svima koji su na bilo koji način pridonijeli izradi ovog rada:

... mentorici dr. sc. Nikolini Ilijanić na kontinuiranoj podršci tijekom izrade ove doktorske disertacije, na primjedbama i prijedlozima koji su poboljšali kvalitetu rada, na usmjeravanju, prenesenom znanju i strpljenju,

... mentoru prof. dr. sc. Nenadu Tomašiću na prihvaćanju mentorstva, brojnim savjetima i stručnom vodstvu kroz doktorski studij,

... članovima povjerenstva prof. dr. sc. Blanki Cvetko Tešović, izv. prof. dr. sc. Hani Fajković i akademiku Goranu Durnu na korisnim prijedlozima i pomoći kako bi se rad dodatno unaprijedio,

… svim kolegama iz Zavoda za mineralne sirovine i marinsku geologiju na prijateljstvu i dobroj dugogodišnjoj suradnji, a posebno kolegi i bivšem šefu dr. sc. Slobodanu Miki na konstruktivnim razgovorima i savjetima,

… kolegi dr. sc. Zoranu Pehu na tome što me uveo u svijet krških boksita te na nesebičnoj podršci, strpljenju i brojnim korisnim raspravama tijekom izrade znanstvenih radova,

… Slobodanu Radusinoviću i Ivoru Perkoviću na pomoći i korisnim savjetima,

... svim kolegama iz Instituta, a posebno Mireli, Jaci i Kosti te cimerima Ivoni, Ivi i Hrvoju na prijateljstvu, ugodnoj radnoj atmosferi i na tome što su bili uz mene u izazovnim trenucima u kojima nisu dopustili da izgubim motivaciju,

… HGI babama, zbog kojih mi je svaki dan na poslu ljepši. Tea, stani. Moram ti još nešto reći…,

… roditeljima, bratu i sestrama na bezuvjetnoj ljubavi i podršci. Hvala vam što ste bili moj oslonac na svim životnim putovanjima i što ste me uvijek poticali da širim vidike i pomičem vlastite granice,

… Damiru koji je sa mnom vjerojatno prošao najteži dio ovog puta, ali je izdržao, nadam se bez trauma. Gabrielu i Arji, na ljubavi i strpljenju. Uz vas je sve moguće!

Table of Contents

BASIC DOCUMENTATION CARD i
TEMELJNA DOKUMENTACIJSKA KARTICA ii
PROŠIRENI SAŽETAK iii
1. INTRODUCTION 1
1.1. Theoretical background 1
1.1.1. Karst bauxites 1
1.1.2. REE in bauxites 2
1.2. Thesis Rationale 4
1.3. Conceptual framework 6
2. METHODOLOGY 9
2.1. Study area 9
2.1.1. Geological setting and bauxite-bearing horizons of the Croatian Karst Dinarides 9
2.1.2. Geological setting of the Mamutovac-1a bauxite deposit 11
2.2. Field methods 13
2.3. Laboratory methods 14
2.4. Data analysis 16
3. DISCUSSION 18
3.1. Temporal geochemical variability of bauxites across horizons 18
3.2. Intra-deposit variability and vertical geochemical trends 21
3.3. Linking regional and deposit-scale processes 25
3.4. Controls on REE distribution and fractionation 28
3.5. Implications for resource potential of Croatian karst bauxites 30
4. CONCLUSION 32
5. REFERENCES 34
6. ORIGINAL SCIENTIFIC PAPERS 44
6.1. Geochemical records in subaerial exposure environments in Croatia using discriminant function analysis of bauxite data 44
6.2. Geochemical insights and mineral resource potential of rare earth elements (REE) in the Croatian karst bauxites 64
6.3. Mineralogical and geochemical variability of the Mamutovac-1a Upper Eocene karst bauxite deposit (Croatian Dinarides) and its CRM potential 92
7. BIOGRAPHY OF THE AUTHOR 136

List of Figures

Figure 1. Conceptual framework of the multi-scale approach applied to Croatian karst bauxites. The diagram illustrates the bauxite system as a depositional environment controlled by the temporal (stratigraphic) and spatial (geographic) dimensions. The temporal dimension is represented by stratigraphic horizons (BX1–BX8; Upper Triassic to Miocene), while the spatial dimension comprises the regional setting of the Croatian Karst Dinarides and the local setting of a representative deposit (Mamutovac-1a). Two analytical scales are distinguished: (1) regional scale analysis, based on the comparison of geochemical characteristics across stratigraphic horizons, and (2) deposit scale analysis, focused on intra-deposit variability within a single bauxite body. The integration of these scales enables interpretation of bauxite formation and evolution through the linkage of temporal and spatial geochemical patterns. 7
Figure 2. Geographical position of the study area (Croatian Karst Dinarides) showing locations of the sampled bauxite deposits from eight bauxite-bearing horizons from the Upper Triassic to the Miocene (BX1-BX8) and terra rossa (TR). (From Ilijanić et al., 2023) 10
Figure 3. a) Geological map of the Promina Municipality in Šibenik-Knin County, modified after Kruk et al. (2014), showing numerous bauxite deposits and occurrences, including the location of the Mamutovac-1a deposit. The geological units on the map (as well as on b) and c)) are as follows: 1 – Upper Cretaceous (Cenomanian – Turonian) limestones with dolomite intercalations ($K_2^{1,2}$), 2 – Upper Cretaceous (Turonian – Coniacian) rudist limestones ($K_2^{2,3}$), 3 – Paleogene Kozina beds (PcE_1), 4 – Paleogene foraminiferal limestones ($E_{1,2}$), 5 – Paleogene Jelar deposits – limestone breccias (E_2), 6 – Paleogene Promina beds – conglomerates, breccias, limestones, calcareous marls (E_3Ol_1), 7 – Paleogene Promina beds – limestones (E_3Ol_1), 8 – Paleogene Promina beds – marly limestone (E_3Ol_1), 9 – Quaternary – terra rossa with rock fragments ($Q_{1,2}$). The inset map shows the location of the studied area in Croatia; b) Geological column of the studied area with bauxite-bearing horizons. Modified after (Kruk et al., 2014). Bauxite occurrences in the wider region are associated with periods of emersion and occur within three stratigraphic horizons, while the studied Mamutovac-1a deposit is genetically linked to the Upper Eocene emersion phase. Note that the thickness of the geological units is not to scale; c) Detailed geological map and geological profile of the Mamutovac-1a bauxite deposit. The location of borehole B-1 is marked with the black and white dot in the detailed geological map. Modified after Lukšić et al. (2004). (From Kovačević Galović et al., 2026). 12
Figure 4. Discriminant function model (DFM) of clr-transformed geochemical data for Paleogene Croatian karst bauxites (BX5–BX7). (a) Scatterplot of variable loadings and (b) distribution of bauxite horizons in the reduced discriminant space defined by the first two discriminant functions (DF1–DF2). The model shows a clear separation between bauxites associated with geochemical characteristics consistent with a felsic-derived source material (positive DF1 values; BX5A) and those characterized by stronger mafic to ultramafic geochemical affinity (negative DF1 values; BX5D, BX6, BX7), including enrichment in trace elements and REE (From Kovačević Galović et al., 2025)..... 20
Figure 5. Vertical distribution of lithofacies, mineralogical composition, and selected geochemical parameters along the Mamutovac-1a bauxite core. Four facies-based zones are distinguished: Zone I (0–11 m; intraclastic–oolitic facies), Zone II (11–14 m; matrix-rich facies), Zone III (14–15.5 m; oolitic facies), and Zone IV (15.5–25 m; pelitomorphic facies). Major elements, trace elements, and REE parameters are shown as a function of depth. (Modified from Kovačević Galović et al., 2026). 22

BASIC DOCUMENTATION CARD

University of Zagreb
Faculty of Science
Department of Geology

Doctoral thesis

GEOCHEMICAL DISCRIMINATION OF BAUXITE HORIZONS IN THE REPUBLIC OF CROATIA

Erli Kovačević Galović

Croatian Geological Survey, Milana Sachsa 2, 10000 Zagreb

Abstract: Karst bauxites represent important archives of continental weathering, subaerial exposure, and tectonostratigraphic evolution, while also constituting a potential alternative source of critical raw materials, particularly rare earth elements (REE). This doctoral thesis investigates Croatian karst bauxites through a multi-scale approach integrating regional geochemical analysis, discriminant statistical modelling, mineralogical and petrographic investigations, and detailed characterization of the Upper Eocene Mamutovac-1a deposit. The study includes all eight stratigraphically defined bauxite-bearing horizons (BX1–BX8), ranging from the Upper Triassic to the Miocene, across the Croatian Karst Dinarides, to reconstruct the processes controlling bauxite formation and evaluate the distribution of rare earth elements (REE). The results demonstrate systematic geochemical variability between bauxite horizons, reflecting differences in provenance, weathering intensity, and depositional conditions during the evolution of the Croatian Karst Dinarides. Geochemical signatures indicate a general shift from predominantly felsic toward more mafic and ultramafic source affinities, particularly in Paleogene bauxites, which also show the highest trace element and REE enrichment. In contrast, Miocene bauxites display higher silica and clay contents, indicating less efficient desilicification. The Upper Eocene Mamutovac-1a deposit exhibits pronounced vertical variability related to reworking, fluid circulation, and evolving physicochemical conditions within the paleokarst system. The upper part of the profile reflects oxidizing, well-drained conditions, whereas the lower part shows stronger fluid influence, increased clay mineral abundance, and locally reducing conditions. Rare earth element distribution is controlled by provenance, pH-Eh conditions, fluid-mediated redistribution, and mineralogical hosts, with the positive correlation with P_2O_5 suggesting that phosphate minerals likely represent one of the principal hosts of REEs. Elevated concentrations of REE and other critical elements indicate that Croatian karst bauxites have promising resource potential as an alternative source of critical raw materials. Overall, this thesis establishes an integrated geochemical framework for understanding the formation and evolution of Croatian karst bauxites and highlights the importance of combining regional and deposit-scale approaches in studying karst bauxite systems.

(vii+137 pages, 4 figures, 98 references, original in English)

Keywords: karst bauxites; Croatian Karst Dinarides; geochemical variability; mineralogical composition; tectonostratigraphic evolution; rare earth elements (REE); critical raw materials (CRM)

Supervisor: Senior Research Associate Nikolina Ilijanić, PhD; Full Professor Nenad Tomašić, PhD

Reviewers: Full Professor Blanka Cvetko Tešović, PhD
Associate Professor Hana Fajković, PhD
Full Professor Goran Durn, PhD

Thesis accepted: 18.03.2025., 14.07.2026.

TEMELJNA DOKUMENTACIJSKA KARTICA

Sveučilište u Zagrebu **Doktorski rad**
Prirodoslovno-matematički fakultet
Geološki odsjek

GEOKEMIJSKA DISKRIMINACIJA BOKSITNIH HORIZONATA U REPUBLICI HRVATSKOJ

Erli Kovačević Galović

Hrvatski geološki institut, Milana Sachsa 2, 10000 Zagreb

Sažetak: Krški boksiti predstavljaju važne geološke pokazatelje procesa kontinentalnog trošenja, subaeralne izloženosti i tektonostratigrafske evolucije, a ujedno i potencijalni sekundarni izvor kritičnih sirovina, osobito elemenata rijetkih zemalja (REE). Ova doktorska disertacija istražuje hrvatske krške boksite primjenom višerazinskog pristupa koji uključuje regionalne geokemijske analize, diskriminantno statističko modeliranje, mineraloška i petrografska istraživanja te detaljnu karakterizaciju gornjoeocenskog ležišta Mamutovac-1a. Istraživanje obuhvaća svih osam stratigrafski definiranih boksitnih horizonata (BX1–BX8), od gornjeg trijasa do miocena, na području hrvatskih krških Dinarida, s ciljem rekonstrukcije procesa koji kontroliraju nastanak boksita i raspodjelu elemenata rijetkih zemalja. Rezultati pokazuju sustavnu geokemijsku varijabilnost između boksitnih horizonata, koja odražava razlike u provenijenciji, intenzitetu trošenja i uvjetima taloženja tijekom evolucije hrvatskih krških Dinarida. Geokemijski pokazatelji upućuju opći prijelaz od pretežno felzičnog prema mafičnom i ultramafičnom geokemijskom afinitetu izvorišnog materijala, osobito u paleogenskim boksitima, koji također pokazuju najveće obogaćenje elementima u tragovima i REE. Nasuprot tome, miocenski boksiti sadrže više silicija i glinovitih komponenti, što upućuje na manje učinkovitu desilicifikaciju. Gornjoeocensko ležište Mamutovac-1a pokazuje izraženu vertikalnu varijabilnost povezanu s pretaloživanjem materijala, cirkulacijom fluida i promjenjivim fizikalno-kemijskim uvjetima unutar paleokrškog sustava. Gornji dio profila odražava oksidacijske i dobro drenirane uvjete, dok donji dio karakterizira jači utjecaj fluida, povećana zastupljenost minerala glina i lokalno reducirajući uvjeti. Raspodjela elemenata rijetkih zemalja kontrolirana je provenijencijom, pH i redoks uvjetima, redistribucijom posredovanom fluidima te mineralnim fazama koje vežu REE, pri čemu pozitivna korelacija s P_2O_5 upućuje na to da fosfatni minerali vjerojatno predstavljaju jedan od glavnih nositelja REE. Povišene koncentracije REE i drugih kritičnih elemenata upućuju na resursni potencijal hrvatskih krških boksita kao mogućeg alternativnog izvora kritičnih sirovina. Ova disertacija uspostavlja integrirani geokemijski okvir za razumijevanje nastanka i evolucije hrvatskih krških boksita te naglašava važnost povezivanja regionalnih i ležišnih pristupa u istraživanju krških boksitnih sustava.

(vii+137 stranica, 4 slike, 98 literaturnih navoda, jezik izvornika engleski)

Ključne riječi: krški boksiti; hrvatski krški Dinaridi; geokemijska varijabilnost; mineraloški sastav; tektonostratigrafska evolucija; elementi rijetkih zemalja (REE); kritične sirovine (CRM)

Mentor: Dr. sc. Nikolina Ilijanić, viša znanstvena suradnica; Dr. sc. Nenad Tomašić, redoviti profesor

Ocjenjivači: Redoviti profesor dr.sc. Blanka Cvetko Tešović
Izvanredni profesor dr.sc. Hana Fajković
Redoviti profesor dr.sc. Goran Durn

Rad prihvaćen: 18.03.2025., 14.07.2026.

PROŠIRENI SAŽETAK

Uvod

Krški boksiti predstavljaju specifičan tip sedimentno-lateritnih ležišta nastalih intenzivnim kemijskim trošenjem alumosilikatnog materijala unutar karbonatnih paleokrških sustava tijekom faza subaeralne izloženosti. Njihov nastanak povezan je s djelovanjem klimatskih, tektonskih, paleogeografskih i geokemijskih čimbenika, zbog čega predstavljaju važne pokazatelje paleookolišnih uvjeta, tektonostratigrafskih diskontinuiteta i geodinamske evolucije karbonatnih platformi. Osim znanstvenog značaja u rekonstrukciji procesa trošenja i razvoja paleokrša, posljednjih godina krški boksiti privlače sve veću pozornost kao potencijalni sekundarni izvori kritičnih sirovina, osobito elemenata rijetkih zemalja (REE), što dodatno povećava važnost razumijevanja procesa koji kontroliraju njihovu geokemijsku evoluciju i raspodjelu kritičnih elemenata.

Na području hrvatskih krških Dinarida boksiti se pojavljuju unutar dobro definiranog tektonostratigrafskog okvira, a njihovo formiranje povezano je s višestrukim fazama emerzije tijekom mezozoika i kenozoika. Dosadašnja istraživanja hrvatskih krških boksita bila su pretežno usmjerena na pojedinačna ležišta, njihove gospodarske značajke ili lokalne mineraloške i geokemijske karakteristike. Iako su brojni radovi ukazali na važnost geokemijskih i mineraloških pokazatelja u interpretaciji geneze boksita, integrirani pristupi koji povezuju regionalnu geokemijsku varijabilnost različitih boksitonosnih horizonata s detaljnim istraživanjima pojedinačnih ležišta bili su ograničeni. Također, unatoč postojećim istraživanjima, raspodjela elemenata rijetkih zemalja i čimbenici koji kontroliraju njihovo obogaćenje u hrvatskim krškim boksitima još uvijek nisu dovoljno razjašnjeni.

Istraživanje provedeno u okviru ove doktorske disertacije temelji se na višerazinskom pristupu koji povezuje regionalnu i ležišnu skalu istraživanja. Regionalna razina obuhvatila je svih osam stratigrafski definiranih boksitonosnih horizonata (BX1–BX8), od gornjeg trijasa do miocena, na području hrvatskih krških Dinarida, dok je detaljna ležišna analiza provedena na gornjoeocenskom ležištu Mamutovac-1a u području Promine.

Ciljevi i hipoteze

Ciljevi istraživanja bili su interpretirati genezu boksita i njihov odnos prema karbonatnoj podlozi na osnovu geokemijskih podataka uzimajući u obzir postojeće tektonostratigrafske i klimatske uvjete te porijeklo ishodišnog materijala, kao i odrediti geološki eksploatacijski potencijal hrvatskih krških

boksita s naglaskom na udjele elemenata rijetkih zemalja (REE) kao gospodarski važnih elemenata i s posebnim osvrtom na ležište Mamutovac-1a. Istraživanje je provedeno na temelju hipoteze da se specifična tektonostratigrafska ograničenja i ukupna geodinamska evolucija krških Dinarida mogu utvrditi na temelju razlika u kemijskom i mineralnom sastavu među boksitnim ležištima različitih horizonata, kao i hipoteze da mineraloške i geokemijske karakteristike boksita unutar ležišta Mamutovac-1a odražavaju procese boksitizacije pri čemu dolazi do akumulacije minerala glina u dubljim dijelovima ležišta.

Metode i postupci

Terenska istraživanja provedena su na području Istre, Korduna, Like, sjevernojadranskih otoka i Dalmacije. Regionalno istraživanje obuhvatilo je ukupno 215 uzorkovanih lokaliteta iz svih osam boksitonosnih horizonata. Za detaljnu ležišnu analizu odabrano je ležište Mamutovac-1a, u kojem je izvedena istražna bušotina B-1 dubine 26,4 m s 25,1 m dobivene jezgre. Jezgra je detaljno dokumentirana te su uzorci sustavno prikupljani duž cijelog profila radi utvrđivanja vertikalne geokemijske i mineraloške varijabilnosti.

U laboratorijskom dijelu istraživanja provedene su geokemijske, mineraloške, petrografske analize i analize magnetskog susceptibiliteta. Koncentracije glavnih i elemenata u tragovima, uključujući REE, određene su metodama ICP-ES i ICP-MS nakon litij-metaboratne fuzije i kiselinske digestije. Mineraloški sastav određen je rendgenskom difrakcijom praha (XRD), dok je analiza minerala glina provedena na orijentiranim preparatima uz standardne tretmane etilenglikolom i žerenjem. Petrografska analiza provedena je na tankim izbruscima polarizacijskim mikroskopom, a magnetski susceptibilitet određen je na Bartington MS2 magnetometru. Dobiveni geokemijski podaci obrađeni su statističkim metodama, uključujući diskriminantnu funkcijsku analizu (DFA), Pearsonove korelacijske analize te interpretaciju različitih geokemijskih omjera i REE parametara. Integracija regionalnih geokemijskih podataka s detaljnim ležišnim istraživanjima omogućila je interpretaciju procesa boksitizacije na različitim prostornim skalama, od regionalne tektonostratigrafske evolucije do intra-ležišne redistribucije elemenata.

Rezultati i zaključci

Rezultati regionalnih geokemijskih istraživanja pokazali su izraženu varijabilnost između svih osam boksitonosnih horizonata (BX1–BX8), koja odražava razlike u provenijenciji, intenzitetu kemijskog trošenja, stupnju desilicifikacije i uvjetima taloženja tijekom geodinamske evolucije hrvatskih krških Dinarida. Diskriminantna funkcijska analiza pokazala je jasno razdvajanje pojedinih boksitonosnih

horizonata na temelju njihovih geokemijskih značajki, što upućuje na sustavne razlike povezane s paleookolišnim, provenijencijskim i tektonostratigrafskim uvjetima njihova nastanka. Svi istraživani boksiti pokazuju vrlo visoke vrijednosti kemijskog indeksa alteracije (CIA), što potvrđuje intenzivno kemijsko trošenje tijekom procesa boksitizacije, ali među pojedinim horizontima postoje značajne razlike u stupnju geokemijske evolucije. Gornjotrijaski boksiti (BX1) karakterizirani su povećanim sadržajem SiO_2 i glinovitih komponenti, što ukazuje na manje učinkovitu desilicifikaciju i izraženiji utjecaj alumosilikatnog ishodišnog materijala. Nasuprot tome, gornjokredni boksiti (BX4) pokazuju najviše sadržaje Al_2O_3 i najniže sadržaje SiO_2, što odražava optimalne uvjete boksitizacije i najučinkovitije procese desilicifikacije. Paleogenski horizonti (BX5–BX7), koji predstavljaju najopsežniju fazu razvoja boksita na području hrvatskih krških Dinarida, pokazuju povišene koncentracije elemenata u tragovima i elemenata rijetkih zemalja, osobito srednje- i gornjoeocenski boksiti. Miocenski boksiti (BX8) izdvajaju se povećanim sadržajem SiO_2 i glinovitih komponenti te geokemijskom sličnošću recentnim tlima tipa terra rossa, što ukazuje na niži stupanj razvijenosti boksitizacijskih procesa. Zr–Cr–Ga dijagram te geokemijski pokazatelji poput odnosa Cr–Ni, Eu anomalija i omjera TiO_2/Al_2O_3 upućuju na opći prijelaz od pretežno felzičnog prema mafičnom i ultramafičnom geokemijskom afinitetu ishodišnog materijala od gornjeg trijasa prema paleogenu. Takvu interpretaciju treba promatrati kao pokazatelj geokemijskog afiniteta mogućih izvorišnih stijena, a ne kao izravan dokaz njihove litološke provenijencije. Zajedno s rezultatima diskriminantne funkcijske analize, navedeni geokemijski pokazatelji potvrđuju hipotezu da razlike u kemijskom i mineralnom sastavu boksitnih horizonata odražavaju tektonostratigrafska ograničenja i geodinamsku evoluciju krških Dinarida.

Detaljna istraživanja ležišta Mamutovac-1a pokazala su izraženu vertikalnu zonaciju litofacijesnih, mineraloških i geokemijskih karakteristika unutar ležišta, što upućuje na složen višefazni razvoj paleokrškog sustava. Ležište ne predstavlja homogen profil trošenja, već rezultat izmjene procesa in situ boksitizacije, redepozicije i postdepozicijske redistribucije materijala tijekom evolucije paleokrškog okoliša. Vertikalna izmjena različitih facijesa odražava promjene u dinamici taloženja, intenzitetu redepozicije i stupnju očuvanosti primarno formiranog boksitnog materijala. Gornji i srednji dijelovi profila obilježeni su intenzivnijim redepozicijskim procesima i mehaničkim preoblikovanjem prethodno formiranog boksitnog materijala, dok donji dijelovi ležišta pokazuju homogeniju, sitnozrnatu matricu povezanu s većim utjecajem autigenih procesa i mirnijim uvjetima taloženja. Mineraloške i geokemijske promjene duž profila odražavaju evoluciju fizikalno-kemijskih uvjeta tijekom razvoja ležišta. U gornjim dijelovima profila dominiraju böhmit i hematit, uz niže

sadržaje SiO_2 i minerala glina, što ukazuje na učinkovitu desilicifikaciju, dobro drenirane oksidacijske uvjete i intenzivnije procese trošenja. Prema dubljim dijelovima profila povećava se sadržaj gibbsita, goethita i minerala glina, uz istovremeni porast SiO_2, što odražava smanjenu učinkovitost desilicifikacije, slabiju drenažu i jači utjecaj fluida unutar paleokrškog sustava. Takvi uvjeti pogodovali su očuvanju glinovitih i drugih sitnozrnatih alumosilikatnih komponenti te lokalnom razvoju hidratiziranijih i djelomično reducirajućih mikrookoliša. Ukupni vertikalni trend pokazuje prijelaz od dinamičnijih i oksidacijskih uvjeta u gornjem dijelu profila prema stabilnijim, fluidno kontroliranim i lokalno reducirajućim uvjetima u dubljim dijelovima ležišta. Petrografske, mineraloške i geokemijske značajke potvrđuju da intra-ležišna varijabilnost odražava kombinirani utjecaj redepozicije, cirkulacije fluida, promjenjivih redoks uvjeta i heterogenog ishodišnog materijala tijekom razvoja ležišta. Progresivno povećanje udjela minerala glina prema dubljim dijelovima profila potvrđuje da su procesi boksitizacije i desilicifikacije bili prostorno i vremenski neujednačeni, pri čemu je u dubljim dijelovima ležišta došlo do pojačanog očuvanja glinovitih komponenti uslijed smanjenog intenziteta ispiranja i jačeg utjecaja fluida.

Raspodjela elemenata rijetkih zemalja u hrvatskim krškim boksitima upućuje na to da njihovo ponašanje kontrolira kombinacija naslijeđenih geokemijskih značajki ishodišnog materijala i sekundarnih redistribucijskih procesa tijekom razvoja ležišta. U svim boksitonosnim horizontima utvrđeno je obogaćenje lakih REE u odnosu na teške REE, dok razlike u ukupnim koncentracijama između pojedinih horizonata odražavaju promjene provenijencije, intenziteta kemijskog trošenja i stupnja očuvanosti mineralnih faza. Najviše koncentracije REE utvrđene su u paleogenskim horizontima, osobito u srednje- i gornjoeocenskim boksitima, što se povezuje s povećanim doprinosom mafičnog i ultramafičnog ishodišnog materijala tijekom razvoja hrvatskih krških Dinarida. Frakcionacija REE dodatno je bila kontrolirana fizikalno-kemijskim uvjetima tijekom trošenja i boksitizacije, pri čemu pH uvjeti predstavljaju jedan od glavnih čimbenika njihove mobilnosti i retencije. Detaljna istraživanja ležišta Mamutovac-1a pokazala su da lokalna redistribucija REE dodatno ovisi o promjenama pH i Eh uvjeta, cirkulaciji fluida i vertikalnoj mineralnoj zonaciji unutar ležišta. Vertikalne promjene Ce anomalija ukazuju na promjenjive redoks uvjete tijekom evolucije ležišta, pri čemu gornji dijelovi profila odražavaju izraženije oksidacijske uvjete, dok dublji dijelovi pokazuju veći utjecaj fluidno posredovanih redistribucijskih procesa. Pozitivna korelacija između REE i P_2O_5 upućuje na to da fosfatni minerali vjerojatno predstavljaju jedne od glavnih nositelja REE, dok minerali glina imaju podređenu, ali lokalno značajnu ulogu.

Rezultati istraživanja upućuju na to da hrvatski krški boksiti imaju obećavajući resursni potencijal kao potencijalni alternativni izvor kritičnih sirovina, osobito elemenata rijetkih zemalja (REE). Paleogenski boksiti, posebno srednje- i gornjoeocenski horizonti, izdvajaju se kao najperspektivniji ciljevi za daljnja REE istraživanja i valorizaciju. Dobiveni rezultati pokazuju da resursni i istraživački potencijal hrvatskih krških boksita primarno ovisi o stratigrafskom položaju, mineralnim nositeljima REE i izraženoj intra-ležišnoj heterogenosti. Istraživanja ležišta Mamutovac-1a pokazala su da REE nisu ravnomjerno raspoređeni unutar ležišta, već su lokalno koncentrirani u pojedinim intervalima, osobito u dubljim dijelovima profila zahvaćenima intenzivnijim utjecajem fluida i promjenjivim fizikalno-kemijskim uvjetima. Takva vertikalna zonacija ukazuje da procjena mogućeg iskorištavanja resursa ne može biti temeljena isključivo na prosječnom kemijskom sastavu rude, nego zahtijeva detaljnu karakterizaciju prostorne raspodjele i kontinuiteta REE-obogaćenih zona unutar pojedinačnih ležišta. Osim REE, u hrvatskim krškim boksitima utvrđene su i povišene koncentracije drugih kritičnih elemenata, uključujući Ga, V i Sc, što dodatno povećava njihov resursni potencijal. Dobiveni rezultati pokazuju da procjena resursnog potencijala hrvatskih krških boksita zahtijeva integrirani pristup koji povezuje regionalne geokemijske trendove, mineralne nositelje elemenata i detaljna istraživanja na razini pojedinačnih ležišta. Izražena intra-ležišna heterogenost pokazuje da raspodjelu kritičnih elemenata unutar pojedinačnih ležišta kontrolira međudjelovanje regionalnih tektonostratigrafskih uvjeta, koji određuju početne geokemijske značajke boksita, i lokalnih postdepozicijskih procesa, koji taj signal naknadno modificiraju tijekom evolucije paleokrškog sustava. Procjena ekonomske isplativosti njihove eksploatacije nije bila predmet ove disertacije te bi zahtijevala zasebna geološka, tehnološka i ekonomska istraživanja.

1. INTRODUCTION

1.1. Theoretical background

1.1.1. Karst bauxites

Bauxite deposits form by intense chemical weathering of aluminosilicate-rich parent materials under specific climatic and geomorphological conditions (Valeton, 1972; Bárdossy, 1982). Their formation is associated with prolonged subaerial exposure, commonly exceeding ~100 ka, efficient drainage, and warm to tropical climates that promote leaching of mobile elements such as silica, alkali, and alkaline earth metals, while relatively immobile elements such as aluminium, iron, and titanium become enriched (Valeton, 1972; Bárdossy, 1982; Birkeland, 1985; D'Argenio and Mindszenty, 1995; Mindszenty et al., 1995). Two main genetic types are distinguished according to the nature of their bedrock: lateritic and karst bauxites (Bárdossy, 1982; MacLean et al., 1997; Deng et al., 2010). Lateritic bauxites develop in situ on silicate rocks and are characterized by thick weathering profiles and gradual vertical differentiation driven by leaching processes (Schellmann, 1994). In contrast, karst bauxites form within carbonate terrains and are associated with paleokarst surfaces developed during subaerial exposure (Bárdossy, 1982; D'Argenio and Mindszenty, 1992; Calagari and Abedini, 2007; Bogatyrev and Zhukov, 2009). They typically occur as infillings of karst depressions and form through accumulation and reworking of material derived from silicate rocks, volcanic ash, aeolian dust, or pre-existing lateritic profiles, together with insoluble carbonate residue, resulting in a polygenetic origin (Bárdossy, 1982; Bárdossy and Aleva, 1990; Valeton, 1991).

The formation and preservation of karst bauxites are closely linked to tectonostratigraphic controls. Phases of subaerial exposure enable the development of paleokarst surfaces and the accumulation of bauxitic material, whereas subsequent transgressions facilitate their preservation beneath younger sedimentary sequences (D'Argenio and Mindszenty, 1995). As a result, karst bauxites are commonly associated with regional unconformities and represent markers of stratigraphic discontinuities within carbonate platform successions. In this context, karst bauxites provide valuable records of coupled tectonic and climatic processes (Bárdossy and Combes, 1999). On a broader scale, episodes of widespread bauxite formation correspond to periods of elevated global humidity and temperature, often linked to enhanced volcanic activity, reflecting the interaction between climatic and geodynamic systems (D'Argenio and Mindszenty, 1992; Mindszenty, 2016).

Accordingly, karst bauxites are recognized as regional markers of global events recorded at specific intervals in the geological record, rather than solely as products of local weathering processes.

Karst bauxites show significant heterogeneity accross multiple scales, including variation between stratigraphic horizons, among deposits, and within individual bodies, reflecting differences in source material, hydrological conditions, basin morphology, and post-depositional processes (Maksimović and Pantó, 1991; Maksimović and Pantó, 1996; Mongelli and Acquafredda, 1999). This variability further underscores their polygenetic nature and the complex interplay of processes that control their formation and evolution (Bárdossy, 1982; Mameli et al., 2007; Maksimović and Pantó, 1996).

In the Croatian Karst Dinarides, karst bauxites developed within a long-lived carbonate platform system affected by multiple phases of emersion during the Mesozoic and Cenozoic (Vlahović et al., 2005; Korbar, 2009; Brlek et al., 2014). As such, they represent important archives of tectonostratigraphic evolution and provide a basis for reconstructing coupled climatic and geodynamic processes on carbonate platforms (Kovačević Galović et al., 2012; Peh and Kovačević Galović, 2014; Peh and Kovačević Galović, 2016; Brlek et al., 2021; Brčić et al., 2023; Ilijanić et al., 2023; Perković et al., 2024).

1.1.2. REE in bauxites

Rare earth elements (REE), comprising yttrium and the lanthanide series from La to Lu, are increasingly recognized as important geochemical tracers in bauxite deposits, as well as potential critical raw materials (Deady et al., 2014; Gamaletsos et al., 2019; Radusinović et al., 2017; Radusinović and Papadopoulos, 2021; Mondillo et al., 2019; Mongelli et al., 2017, Tomašić et al., 2021, Zhang et al., 2022, and others). Due to their relatively low mobility during chemical weathering, REE tend to become enriched in lateritic profiles, including bauxites, making them valuable indicators of weathering intensity, provenance, and post-depositional processes (Reinhardt et al., 2018; Mongelli et al., 2014).

In bauxite systems, REE are typically fractionated into light (LREE) and heavy (HREE) groups, which may exhibit different geochemical behavior depending on physicochemical conditions. Most bauxites are characterized by an enrichment of LREE relative to HREE, reflecting both the composition of the parent material and the effects of weathering processes (Mongelli et al., 2014; Ahmadnejad et al., 2017; Reinhardt et al., 2018). However, the degree of fractionation and total REE content can vary significantly between deposits and within individual profiles.

The distribution of REE in bauxites is controlled by several key factors, including the composition of the source material, intensity of weathering, and physicochemical conditions such as pH and redox potential (Nesbitt, 1979; Mongelli et al., 2014; Ahmadnejad et al., 2017; Ling et al., 2018; Abedini et al., 2019). Under acidic to mildly acidic conditions, REE can be mobilized and redistributed within the weathering profile, whereas under more neutral to alkaline conditions they tend to be immobilized and incorporated into secondary mineral phases (Ye et al., 2007; Wang et al., 2010; Mongelli et al., 2014; Liu et al., 2016; Ahmadnejad et al., 2017; Reinhardt et al., 2018). Redox conditions, particularly those affecting cerium, can lead to the development of characteristic Ce anomalies, which are widely used as indicators of paleoenvironmental conditions (Mongelli et al., 2014; Mondillo et al., 2022).

REE in bauxites may be associated with various mineral phases, including clay minerals, iron oxides and hydroxides, titanium-bearing phases such as anatase, and discrete REE-bearing minerals including phosphates and fluorocarbonates (Mordberg, 1999; Mordberg et al., 2000; Boulange et al., 1996; Laskou and Andreou, 2003; Kanazawa and Kamitani, 2006; Mongelli et al., 2014; Liu et al., 2016). The relative importance of these host phases remains a subject of ongoing research, particularly in karst bauxite systems where polygenetic processes may lead to complex redistribution and enrichment patterns (Maksimović and Pantó, 1983; Maksimović and Pantó, 1985; Mongelli, 1997; Mameli et al., 2007; Radusinović, 2017; Radusinović and Papadopoulos, 2021).

In addition to their significance as geochemical tracers, REE in bauxites have attracted considerable attention due to their economic potential. With increasing global demand for critical raw materials, bauxites and related lateritic deposits are increasingly being explored as alternative sources of REE and other critical metals (Boni et al., 2013; Deady et al., 2014; Goodenough et al., 2018; Gamaletsos et al., 2019). However, the economic viability of such resources depends not only on total REE concentrations but also on their mode of occurrence, mineralogical association, and extractability.

The study of REE distribution in bauxites therefore provides a unique opportunity to link geochemical processes with both paleoenvironmental reconstruction and resource evaluation. In karst bauxites, where multiple stages of weathering, transport, and redeposition may occur, REE behavior can offer important insights into the interplay between source material, weathering processes, and post-depositional modification (Maksimović and Pantó, 1991; Mongelli et al., 2014; Radusinović et al., 2017; Tomašić et al., 2021; Mondillo et al., 2022; Kovačević Galović et al., 2025).

1.2. Thesis Rationale

Karst bauxites represent important archives of continental weathering processes and are widely recognized as indicators of subaerial exposure, tectonic activity, and paleoenvironmental conditions (Bárdossy, 1982; D'Argenio and Mindszenty, 1995; Bárdossy and Combes, 1999; Retallack, 2010; Sinisi, 2018). Their formation reflects the combined influence of climate, tectonostratigraphic evolution, parent material, and hydrological conditions, resulting in complex and often polygenetic systems (Mameli et al., 2007; Peh and Kovačević Galović, 2014; Ahmadnejad et al., 2017; Mondillo et al., 2022). Within the Dinaric Karst region, karst bauxites occur within a well-defined tectonostratigraphic framework spanning from the Upper Triassic to the Miocene, reflecting multiple phases of emersion and karstification recorded in carbonate-platform successions (Šinkovec and Sakač, 1991; Vlahović et al., 2005; Ilijanić et al., 2023). As such, they represent key markers of regional geodynamic evolution and stratigraphic discontinuities within the Croatian Karst Dinarides.

Research on karst bauxites in Croatia has a long tradition. Early studies were primarily focused on the description, classification, and economic exploitation of deposits as a source of aluminium, while also addressing paleoclimate-related geochemical and mineralogical processes (e.g., Sakač et al., 1984; Šinkovec and Sakač, 1982; Šinkovec et al., 1985; Šušnjara et al., 1990; Sakač and Šinkovec, 1991; Šinkovec and Sakač, 1991; Šinkovec et al., 1994) and local tectonic controls (Blašković et al., 1989). The development of regional tectonostratigraphic models and paleogeographic reconstructions (Vlahović et al., 2005; Korbar, 2009) enabled a shift toward interpreting bauxites as indicators of emersion phases and broader geodynamic processes (D'Argenio and Mindszenty, 1995; Kovačević Galović et al., 2012; Peh and Kovačević Galović, 2014; Peh and Kovačević Galović, 2016; Brlek et al., 2021; Brčić et al., 2023; Ilijanić et al., 2023; Perković et al., 2024).

Geochemical approaches have further expanded the understanding of karst bauxites. Early studies demonstrated the usefulness of REE as tracers of source material and genetic processes (Maksimović and Roaldset, 1976; Crnički, 1987; Maksimović and Pantó, 1991; Maksimović et al., 1993), while more recent studies have employed multi-proxy approaches, including geochemistry and geochronology, to reconstruct paleoenvironmental conditions (Radusinović, 2017; Brlek et al., 2021; Radusinović and Papadopoulos, 2021; Brčić et al., 2023). The mathematical modelling with application of multivariate statistical methods, such as discriminant analysis, has also been explored in regional studies (Kovačević Galović et al., 2012; Peh and Kovačević Galović, 2014; Peh and

Kovačević Galović, 2016; Ilijanić et al., 2023), highlighting their potential for distinguishing between geochemical groups of bauxites.

Despite these advances, significant gaps remain. Most studies have focused either on individual deposits or on specific stratigraphic intervals, and integrated approaches that combine regional-scale geochemical variability with detailed intra-deposit investigations are still limited. Consequently, the relationships between different bauxite horizons, their source material, and the controlling tectonic and climatic factors remain only partially understood.

In addition to their significance as paleoenvironmental indicators, karst bauxites have recently gained attention as potential sources of critical raw materials, particularly REE (e.g., Deady et al., 2014; Goodenough et al., 2016; Gamaletsos et al., 2019). Although elevated REE concentrations have been reported in numerous bauxite deposits, the mechanisms controlling their distribution, fractionation, and potential extractability remain debated (Mameli et al., 2007; Mongelli et al., 2014; Tomašić et al., 2021). In particular, integrated studies linking regional geochemical patterns with intra-deposit variability are still limited, which hampers both genetic interpretations and resource evaluation (Ilijanić et al., 2023; Kovačević Galović et al., 2026).

Based on these knowledge gaps, this doctoral research adopts a multi-scale approach to investigate Croatian karst bauxites, integrating regional geochemical analysis, statistical modelling, and detailed deposit-scale investigations.

The main objectives of this thesis are:

(1) Interpret the genesis of bauxites and their relationship to the carbonate substrate based on geochemical data, taking into account existing tectonostratigraphic and climatic conditions, as well as the origin of the source material; and

(2) Determine the geological exploitation potential of Croatian karst bauxites, with emphasis on the content of rare earth elements (REE) as economically important elements, with special reference to the Mamutovac-1a deposit.

The first objective is addressed through the analysis of compositional and mineralogical variations among bauxite deposits of different stratigraphic horizons, with the aim of identifying the key controls governing their formation and evolution (Ilijanić et al., 2023; Kovačević Galović et al., 2025). The second objective focuses on the distribution and behavior of REE and other critical elements,

including their vertical variability within a representative deposit, as well as their potential extractability (Kovačević Galović et al., 2026).

The research is guided by the following hypotheses:

(1) Differences in the chemical and mineral composition of bauxite deposits from different horizons can infer specific tectonostratigraphic constraints and the overall geodynamic evolution of the Karst Dinarides.; and

(2) The mineralogical and geochemical characteristics of bauxites within the Mamutovac-1a deposit reflect the processes of bauxitization in the deposit, leading to the accumulation of clay minerals in the deeper parts.

By addressing these objectives and hypotheses, this thesis aims to provide an integrated understanding of the processes governing the formation of Croatian karst bauxites and to evaluate their significance both as paleoenvironmental archives and as potential sources of critical raw materials.

1.3. Conceptual framework

The formation and evolution of karst bauxites represent complex processes controlled by the interaction of tectonostratigraphic, climatic, and geochemical factors operating across different spatial and temporal scales (Bárdossy, 1982; D'Argenio and Mindszenty, 1995). Therefore, understanding these systems requires an integrated approach that links regional geological evolution with local depositional processes and geochemical characteristics.

In this study, a multi-scale conceptual framework based on a systems approach is adopted to investigate Croatian karst bauxites. This framework distinguishes between two main levels of analysis: (1) the regional (tectonostratigraphic) scale and (2) the deposit (intra-core) scale (Figure 1). It is based on the integration of results obtained from regional-scale geochemical analyses and statistical modelling, as well as detailed deposit-scale investigations conducted in this study (Ilijanić et al., 2023; Kovačević Galović et al., 2025; Kovačević Galović et al., 2026).

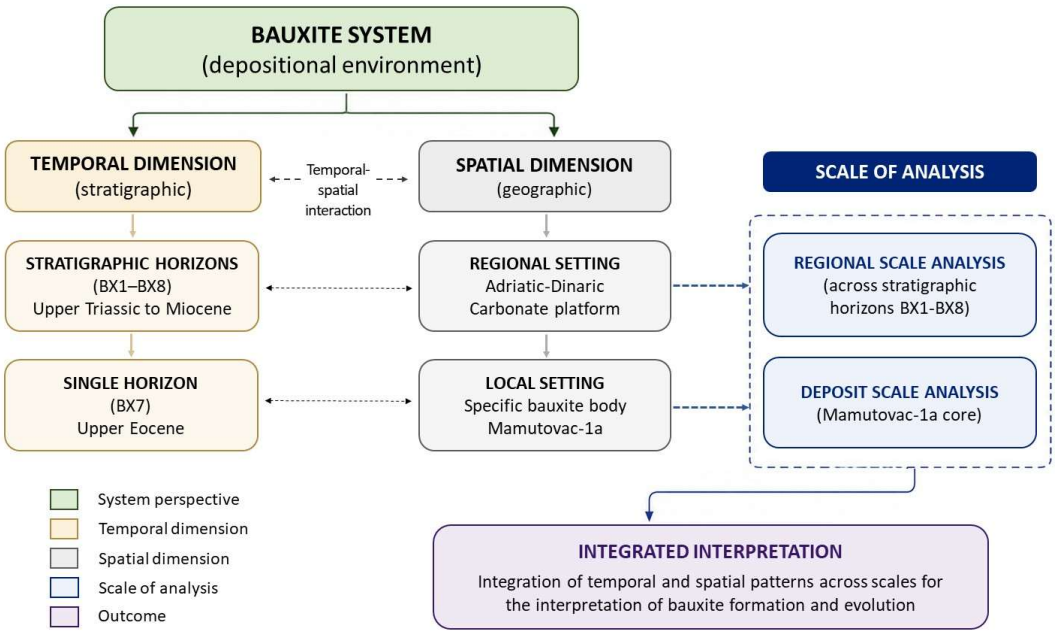

Figure 1. Conceptual framework of the multi-scale approach applied to Croatian karst bauxites. The diagram illustrates the bauxite system as a depositional environment controlled by the temporal (stratigraphic) and spatial (geographic) dimensions. The temporal dimension is represented by stratigraphic horizons (BX1–BX8; Upper Triassic to Miocene), while the spatial dimension comprises the regional setting of the Croatian Karst Dinarides and the local setting of a representative deposit (Mamutovac-1a). Two analytical scales are distinguished: (1) regional scale analysis, based on the comparison of geochemical characteristics across stratigraphic horizons, and (2) deposit scale analysis, focused on intra-deposit variability within a single bauxite body. The integration of these scales enables interpretation of bauxite formation and evolution through the linkage of temporal and spatial geochemical patterns.

At the regional scale, bauxite deposits are analysed according to their stratigraphic affiliation (BX1–BX8; stratigraphic bauxite horizons ranging from the Upper Triassic to the Miocene) to evaluate differences among bauxite groups. This approach enables the comparison of geochemical characteristics among horizons and the identification of compositional variability at the scale of the Croatian Karst Dinarides (Ilijanić et al., 2023; Kovačević Galović et al., 2025).

At the deposit scale, vertical variability was analysed within the representative Mamutovac-1a bauxite core. Changes in mineralogical and geochemical composition with depth were used to characterize intra-deposit variability and to document vertical trends within the bauxite body (Kovačević Galović et al., 2026).

Geochemical data, including major and trace elements and REE, represent the primary dataset used for quantitative analysis across both spatial scales. These data are analysed using statistical methods

and selected element ratios to both identify relationships between variables and to distinguish between different groups of samples. Mineralogical, petrographic, and magnetic susceptibility data provide complementary information that is used to support the interpretation of geochemical patterns.

The two scales are interrelated. Regional analysis provides a framework for comparing bauxite deposits across different stratigraphic horizons, while deposit-scale analysis captures vertical variability within individual (single horizon) bauxite bodies. By integrating these two levels of analysis, it becomes possible to relate regional geochemical patterns to intra-deposit variability and to evaluate the processes controlling bauxite formation across different spatial scales. This integrated approach forms the basis for the interpretation of bauxite formation processes presented in the following chapters.

2. METHODOLOGY

2.1. Study area

2.1.1. Geological setting and bauxite-bearing horizons of the Croatian Karst Dinarides

The study area is located within the Croatian Karst Dinarides, forming part of the External Dinarides and comprising a thick carbonate succession characterized by a complex tectonostratigraphic evolution (Tišljar et al., 2002; Vlahović et al., 2002; Vlahović et al., 2005; Schmid et al., 2008; Korbar, 2009; Schmid et al., 2020). The carbonate succession reaches thicknesses exceeding 8000 m and records more than 270 million years of deposition, extending from at least the Middle Permian to the Late Eocene. It consists predominantly of shallow-marine carbonate deposits that accumulated through multiple phases of platform development, emersion, and karstification, forming the geological framework of the Croatian Karst Dinarides.

The tectonostratigraphic evolution of the Croatian Karst Dinarides was controlled by a combination of eustatic sea-level fluctuations and regional tectonic processes, including the separation of the Adria microplate during the Triassic and subsequent tectonic reorganization of the carbonate system during the Jurassic (Vlahović et al., 2005; Korbar, 2009). Later tectonic activity resulted in the development of regional subaerial unconformities, including flexural uplift (forebulge development) associated with the advance of the Dinaric orogen (Peh and Kovačević Galović, 2014). These processes produced repeated phases of emersion, during which karstification and bauxitization took place, commonly in association with regional unconformities and major tectonic events (D'Argenio and Mindszenty, 1995; Mindszenty et al., 1995; Brlek et al., 2014; Brčić et al., 2023).

In Croatia, bauxite deposits occur as karst-type bauxites formed within carbonate successions during these emersion phases. They are widely distributed and represent important indicators of paleoclimatic and tectonic conditions, particularly reflecting warm and humid climates combined with tectonically controlled subaerial exposure (Bárdossy, 1982; D'Argenio and Mindszenty, 1995; Ilijanić et al., 2023).

Bauxite deposits in the Croatian Dinarides are grouped into eight stratigraphically defined horizons, representing successive phases of subaerial exposure and karstification from the Upper Triassic to the Miocene (Šinkovec and Sakač, 1991; Ilijanić et al., 2023). These include: Upper Triassic (BX1),

Upper Jurassic (BX2), Lower Cretaceous (BX3), Upper Cretaceous (BX4), Paleocene (BX5), Middle Eocene (BX6), Upper Eocene (BX7), and Miocene (BX8) (Figure 2).

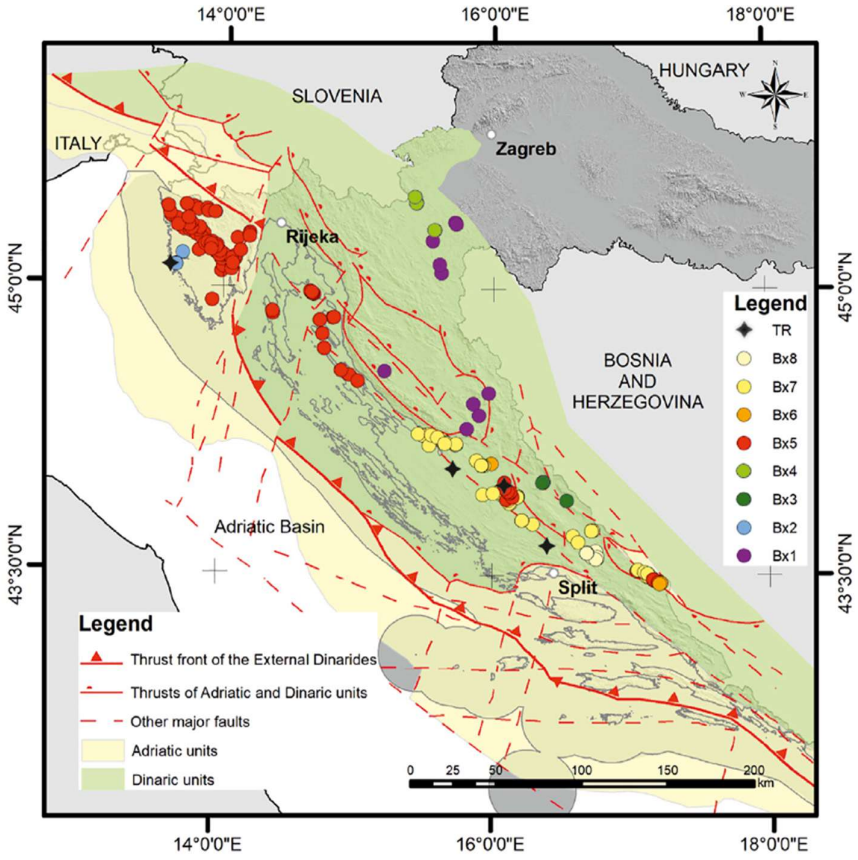

Figure 2. Geographical position of the study area (Croatian Karst Dinarides) showing locations of the sampled bauxite deposits from eight bauxite-bearing horizons from the Upper Triassic to the Miocene (BX1-BX8) and terra rossa (TR). (From Ilijanić et al., 2023)

The Upper Triassic horizon (BX1), developed in Lika, Kordun, and northern Dalmatia, is associated with early emersion phases linked to initial tectonic activity and is typically composed of clay-rich bauxites derived from weathering of clastic and pyroclastic material (Šinkovec et al., 1985). Upper Jurassic bauxites (BX2), mainly developed in Istria, formed on carbonate substrates with aeolian input and are generally characterized by higher silica content (Šinkovec, 1974). Lower Cretaceous (BX3) deposits, occurring in central Dalmatia, are relatively small and clay-rich, reflecting incomplete bauxitization processes (Sakač and Šinkovec, 1991). In contrast, Upper Cretaceous (BX4) bauxites, typical of the Kordun area, are generally Al-rich but occur as limited lens-shaped bodies (Sakač and Šinkovec, 1991).

The Paleogene interval represents the most extensive phase of bauxitization within the Croatian Karst Dinarides (Šinkovec and Sakač, 1982). Paleocene bauxites (BX5) are widespread across Istria, northern Adriatic islands, and Dalmatia and represent economically important deposits. They formed during post-Laramian emersion and are commonly associated with transgressive Kozina deposits (Sakač and Šinkovec, 1991). Middle Eocene bauxites (BX6), developed in Dalmatia, occur as relatively small deposits. In contrast, Upper Eocene bauxites (BX7) form the most economically significant and laterally extensive bodies, also in Dalmatia, and are associated with major tectonic uplift and the development of paleorelief (Šinkovec and Sakač, 1991; Brčić et al., 2023).

The youngest Miocene bauxites (BX8), occurring mainly in Dalmatia and Kordun, are predominantly clay-rich deposits formed during the final phases of regional tectonosedimentary evolution, often developed in situ on karstified substrates and associated with clastic cover sequences and locally influenced by paleorelief-controlled accumulation (Šušnjara et al., 1990; Brlek et al., 2021).

Geochemical differences between the horizons reflect variations in parent material, paleogeographic setting, and physicochemical conditions during bauxitization. In particular, Eocene bauxites (BX6–BX7) show enrichment in trace elements and REE, indicating more complex geodynamic and weathering conditions compared to older horizons (Ilijanić et al., 2023).

2.1.2. Geological setting of the Mamutovac-1a bauxite deposit

The Mamutovac-1a bauxite deposit is located in the Promina area (Šibenik–Knin County, Croatia), southwest of the village of Oklaj, representing one of ten deposits within the former Mamutovac bauxite exploitation field (Figure 3a). In the wider study area, bauxite deposits are associated with three stratigraphic horizons related to phases of emersion (Figure 3b). Upper Cretaceous rudist limestones form the basement and are overlain by Paleogene Kozina deposits and foraminiferal limestones (Velić and Vlahović, 2009; Španiček et al., 2017; Babić and Zupanič, 2016; Ćosović et al., 2018). The bauxite deposits are situated within a shallow syncline, part of a NW–SE-trending fold system characteristic of the External Dinarides (Korbar, 2009) and occur as irregular, lens-shaped bodies. The geometry and distribution of the bauxite bodies are related to synclinal structures and the morphology of the karstified substrate (Babić and Zupanič, 2012; Ćosović et al., 2018).

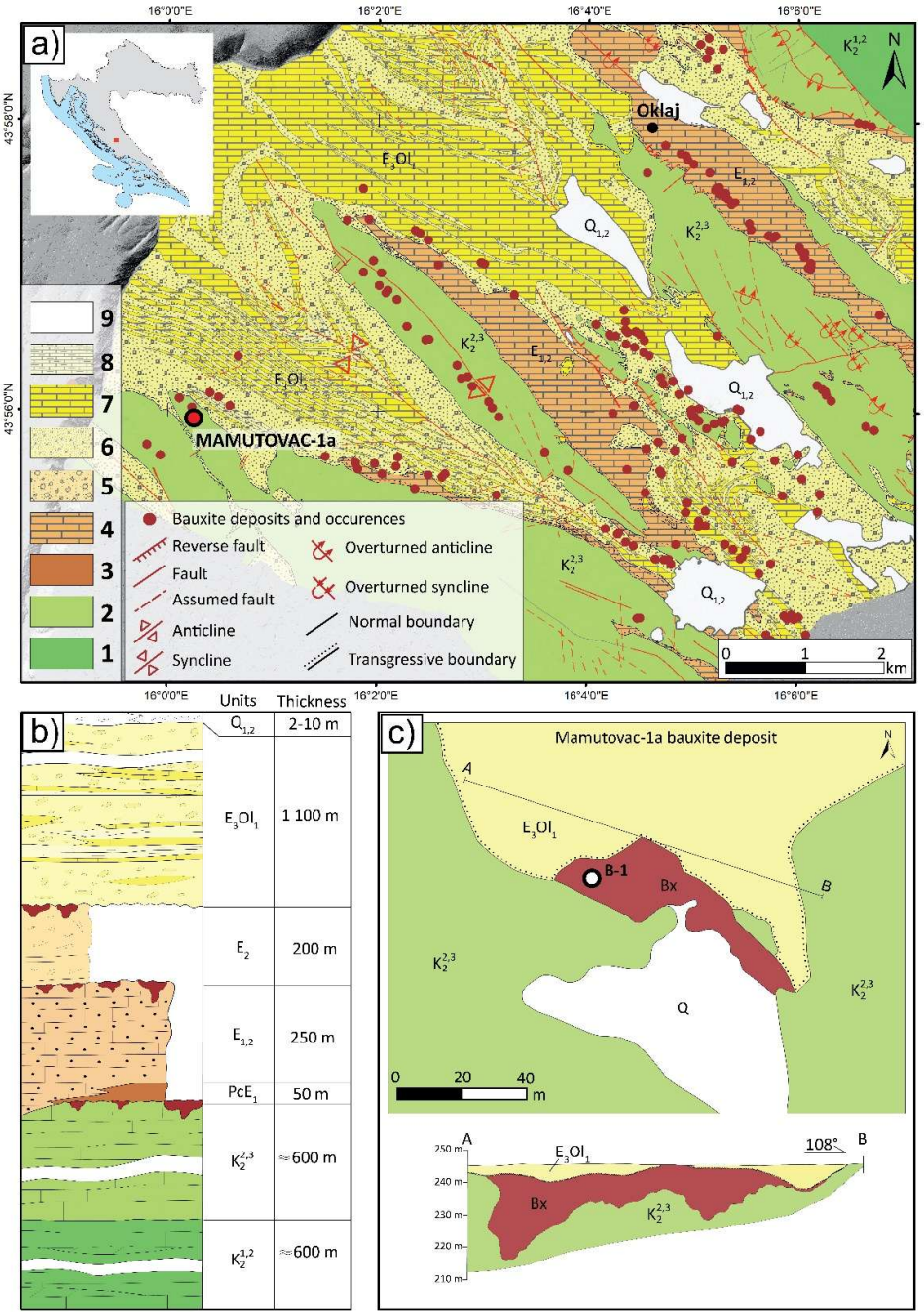

Figure 3. a) Geological map of the Promina Municipality in Šibenik-Knin County, modified after Kruk et al. (2014), showing numerous bauxite deposits and occurrences, including the location of the Mamutovac-1a deposit. The geological units on the map (as well as on b) and c)) are as follows: 1 – Upper Cretaceous (Cenomanian – Turonian) limestones with dolomite intercalations ($K_2^{1,2}$), 2 – Upper Cretaceous (Turonian – Coniacian) rudist limestones ($K_2^{2,3}$), 3 – Paleogene Kozina beds (PcE_1), 4 – Paleogene foraminiferal limestones ($E_{1,2}$), 5 – Paleogene Jelar deposits – limestone breccias (E_2), 6 – Paleogene Promina beds – conglomerates, breccias, limestones, calcareous marls (E_3Ol_1), 7 – Paleogene Promina beds – limestones (E_3Ol_1), 8 – Paleogene Promina beds – marly limestone (E_3Ol_1), 9 – Quaternary – terra rossa with rock fragments ($Q_{1,2}$). The inset map shows the location of the studied area in Croatia; b) Geological column of the studied area with bauxite-bearing horizons. Modified after (Kruk et al., 2014). Bauxite occurrences in the wider region

are associated with periods of emersion and occur within three stratigraphic horizons, while the studied Mamutovac-1a deposit is genetically linked to the Upper Eocene emersion phase. Note that the thickness of the geological units is not to scale; c) Detailed geological map and geological profile of the Mamutovac-1a bauxite deposit. The location of borehole B-1 is marked with the black and white dot in the detailed geological map. Modified after Lukšić et al. (2004). (From Kovačević Galović et al., 2026).

According to its stratigraphic position, the Mamutovac-1a deposit belongs to the Upper Eocene (BX7) bauxite horizon (Ilijanić et al., 2023; Kovačević Galović et al., 2025). The deposit formed during a regional emersion phase in the Middle to Late Eocene, accompanied by uplift, erosion, and development of a regional unconformity that controlled bauxite distribution in the Promina area (Marković, 2002; Kruk et al., 2014). The deposit is formed on Upper Cretaceous rudist limestones (Figure 3c) that were subjected to subaerial exposure and karstification before bauxite formation (Brčić et al., 2023). The Mamutovac-1a deposit forms an elongated trough developed on the karstified limestone surface. The basal contact is irregular and follows the morphology of karst depressions. The exposed part of the deposit measures approximately 80 × 10–25 m, while the ore body extends an additional 30–80 m beneath the overlying sedimentary cover toward the northeast. In its central part, the deposit reaches a thickness of up to ~30 m and gradually thins toward its margins (Lukšić et al., 2004). In addition to in situ weathering, the bauxitic material includes contributions from externally derived detritus, including material potentially derived from volcaniclastic sources and transported by aeolian and fluvial processes (Boni et al., 2012; Brlek et al., 2021; Brčić et al., 2023). Following bauxite formation, the deposit was covered by Promina deposits of Eocene–Oligocene age, composed predominantly of conglomerates with subordinate marls and limestones (Babić et al., 1995). In the southeastern part of the area, the succession is locally overlain by a thin cover of Quaternary terra rossa (Lukšić et al., 2004).

2.2. Field methods

Field investigations were conducted across the Croatian Karst Dinarides with the aim of capturing both regional-scale variability among bauxite horizons and detailed intra-deposit variability within a representative core.

At the regional scale, sampling was carried out along approximately 400 km of the Croatian Karst Dinarides, covering all eight recognized bauxite-bearing horizons (BX1–BX8). Sampling sites were distributed across the main bauxite-bearing regions, including Istria, Kordun, Lika, North Adriatic islands, and Dalmatia (Figure 2), and targeted deposits associated with major regional

unconformities to capture variability between tectonostratigraphic horizons. A total of 215 sampling locations were investigated during multiple field campaigns, with each site represented by a single composite sample. This approach was adopted to obtain a representative bulk geochemical signature of each bauxite deposit, independent of the precise position of the sampled material within the bauxite body.

The regional sampling strategy was based on the assumption that bulk geochemical data from multiple deposits can be used to identify the principal geochemical processes controlling bauxite formation in both vertical (temporal or stratigraphic) and horizontal (spatial) dimensions. This approach enabled comparison of geochemical characteristics between different horizons and the identification of large-scale trends related to tectonostratigraphic evolution.

At the deposit scale, detailed field investigations were conducted at the Mamutovac-1a bauxite deposit. To investigate vertical variability within the ore body, exploratory drilling was carried out at a representative location selected based on previous geological studies (Figure 3c). A vertical borehole (B-1) was drilled through the bauxite body, reaching a total depth of 26.4 m, with 25.1 m of recovered core. The recovered core was documented through detailed macroscopic logging, including the description of lithological variations and color determination using Munsell Soil Color Charts (Munsell Color Company, 1994). Based on these observations, samples were systematically collected along the core at regular depth intervals to characterize the vertical mineralogical and geochemical variability of the deposit.

2.3. Laboratory methods

Collected samples were subjected to a series of laboratory analyses aimed at determining their physical, mineralogical, and geochemical characteristics, as well as their interrelationships. The selection of analytical methods was guided by the objectives of this study, particularly to constrain the origin of the source material, reconstruct weathering and depositional processes, and evaluate the behavior of trace elements, including REE.

Prior to analysis, all samples were oven-dried and homogenized by grinding in an agate mortar to obtain representative bulk material and minimize sample heterogeneity.

Magnetic susceptibility measurements were performed exclusively on samples from the Mamutovac-1a deposit at the Croatian Geological Survey using a Bartington MS2 susceptibility meter with an MS2B dual-frequency sensor. Pulverized and homogenized samples from different

depth intervals of the bauxite drill core were packed into 10 cm^3 plastic containers, weighed, and measured first at low frequency (0.465 kHz) and subsequently at high frequency (4.65 kHz). The obtained results were used to determine mass-specific magnetic susceptibility values at low frequency (χ_{lf}), as well as frequency-dependent magnetic susceptibility (χ_{fd}), expressed as percentages.

Mineralogical composition of selected bulk samples was determined by qualitative powder X-ray diffraction (XRD) analysis at the Croatian Geological Survey using a PANalytical X'Pert Powder diffractometer equipped with a Cu ceramic X-ray tube (CuKα radiation, λ = 1.5406 Å), a vertical θ–θ goniometer, graphite monochromator, and PIXcel detector. Measurements were performed at 45 kV and 40 mA over the 5–66°2θ range, with a step size of 0.02°2θ and a counting time of 100 s per step. Prior to analysis, powdered samples were crushed in an agate mortar and prepared as random mounts on Al holders using the back-loading method. Diffraction patterns were interpreted using X'Pert HighScore Plus software in combination with the ICDD PDF-4/Minerals database. Major mineral phases, including aluminium hydroxides, iron oxides, and accessory minerals, were identified using this method.

For a more detailed characterization of fine-grained mineral phases, clay mineral analysis was carried out exclusively on selected samples from the Mamutovac-1a deposit at the Croatian Geological Survey. Oriented aggregates were prepared from selected bauxite samples to obtain detailed insight into clay mineral composition. The clay mineral fraction (<2 µm) was separated by centrifugation, and the suspension was deposited onto glass slides and air-dried at room temperature to obtain oriented mounts. A series of standard treatments was then applied following Moore and Reynolds (1998), including air-dried (AD), ethylene glycol-solvated (EG), and heated samples (400 °C and 550 °C). X-ray diffraction measurements were subsequently performed in the 4–30°2θ range. These procedures were used to differentiate clay minerals with overlapping basal reflections and to identify mixed-layer phases.

Petrographic analysis was also conducted exclusively on samples from the Mamutovac-1a deposit at the Croatian Geological Survey. Thin sections were prepared and examined under a polarizing microscope to identify textures and microstructures related to transport processes, degree of reworking, and the autochthonous or allochthonous origin of the material.

Geochemical analyses were performed at an accredited external laboratory (Bureau Veritas Minerals / ACME Analytical Laboratories, Canada). Concentrations of major oxides and trace

elements were determined using inductively coupled plasma emission spectroscopy (ICP-ES) and inductively coupled plasma mass spectrometry (ICP-MS) following lithium metaborate/tetraborate fusion and subsequent acid dissolution. Major elements were analysed by ICP-ES, whereas trace elements, including REE, were determined by ICP-MS.

Magnetic susceptibility data provided information on the concentration and grain-size distribution of magnetic minerals, primarily iron-bearing phases. Bulk and clay mineralogical analyses enabled characterization of major mineral assemblages and fine-grained clay fractions sensitive to physicochemical conditions during bauxitization, while the obtained mineralogical data were used to constrain weathering intensity and post-depositional processes. Petrographic observations provided complementary information to mineralogical and geochemical data, particularly in recognizing depositional and diagenetic features at the microscale. Geochemical analyses provided quantitative bulk compositional data used to evaluate source material, degree of weathering, and geochemical differentiation, including the distribution and behavior of trace elements and REE. The integration of magnetic, mineralogical, petrographic, and geochemical data provided a comprehensive basis for interpreting bauxite formation processes across multiple spatial scales and linking regional geochemical trends with intra-deposit variability.

2.4. Data analysis

Geochemical data were processed using statistical methods to identify relationships between variables and to distinguish compositional patterns among bauxite samples. Basic statistical parameters were calculated for all analysed elements to characterize the geochemical dataset. Pearson correlation coefficients were used to evaluate relationships between selected major and trace elements, including REE. Selected elemental ratios and REE parameters were calculated to support the interpretation of provenance, weathering processes, and physicochemical conditions during bauxitization. REE concentrations were normalised to chondrite and Upper Continental Crust (UCC) reference values to compare REE distribution patterns and fractionation between samples.

Multivariate statistical analysis was applied to the geochemical dataset to distinguish between predefined groups of Croatian karst bauxites and to characterize their geochemical variability. DFA is a supervised multivariate statistical technique in which group membership is defined a priori on the basis of geological criteria. For the regional dataset, samples were grouped according to the eight stratigraphically defined bauxite-bearing horizons (BX1–BX8), while terra rossa samples were included as an additional reference group. In the analysis of Paleogene bauxites, the dataset was

subdivided into the stratigraphic groups BX5A, BX5D, BX6, and BX7. Because whole-rock geochemical data are compositional data (CoDa), in which the individual components represent parts of a constant whole and are therefore not statistically independent, all geochemical variables were transformed using the centered log-ratio (clr) transformation (Aitchison, 1986) prior to multivariate statistical analysis. This transformation removes the closure effect and allows meaningful statistical analysis of relationships among geochemical variables. The clr transformation was applied only for the discriminant function analyses, whereas conventional geochemical diagrams, elemental ratios, and REE parameters were calculated and interpreted using the original concentration data, following the standard methodologies by which these geochemical proxies have been established and are commonly applied in geochemical studies. Whole-rock major- and trace-element geochemical data, including ΣLREE and ΣHREE variables, were used as predictor variables to characterize the geochemical variability between the studied bauxite horizons. The discriminant model was constructed using the clr-transformed predictor variables. DFA identifies the linear combinations of variables that maximize separation between predefined groups while minimizing variability within each group, thereby providing the most effective discrimination of the studied bauxite horizons. The resulting discriminant functions and associated variable loadings were then examined to identify which geochemical variables contributed most strongly to group separation. The discriminant model was interpreted together with independent geochemical indicators, including elemental ratios, discrimination diagrams, and REE parameters, to infer provenance, weathering processes, and paleoenvironmental evolution. The predictive performance of the discriminant model was assessed using the proportion of correctly classified samples and the corresponding misclassification rate, providing an estimate of the model's classification accuracy.

All basic statistical analyses, including descriptive statistics, Pearson correlation coefficients, elemental ratios, REE normalization, and geochemical diagrams, were performed using Microsoft Excel. Box-and-whisker plots and discriminant function analyses were performed using the STATISTICA software package, Release 7.1 (StatSoft, Inc., 2006).

3. DISCUSSION

3.1. Temporal geochemical variability of bauxites across horizons

Geochemical data from Croatian karst bauxites indicate a structured variability across the eight stratigraphic horizons (BX1–BX8), reflecting the long-term tectonostratigraphic evolution of the Croatian Karst Dinarides from the Late Triassic to the Miocene (Ilijanić et al., 2023; Kovačević Galović et al., 2025). Rather than representing a simple linear progression, this variability results from the combined effects of changing provenance, weathering processes, and depositional conditions acting under different tectonostratigraphic settings, as commonly observed in polygenetic karst bauxite systems (Bárdossy, 1982; D'Argenio and Mindszenty, 1995; Mameli et al., 2007). At the regional scale, discriminant function analysis (DFA) performed on the complete dataset (BX1–BX8) demonstrates that the main geochemical variability is organized along a temporal axis, capturing systematic differences between bauxite horizons formed during distinct episodes of subaerial exposure (Ilijanić et al., 2023). This pattern enables interpretation of bauxite formation as a function of evolving environmental conditions, without implying direct temporal continuity between individual deposits.

It is important to emphasize that the studied bauxite horizons do not represent a continuous evolutionary sequence, but rather discrete episodes of bauxitization formed under different geological conditions. Consequently, the observed geochemical variability between horizons cannot be attributed solely to differences in the duration of emersion. While the duration of exposure controls the degree of weathering within individual deposits, variations between horizons primarily reflect differences in the environmental conditions under which bauxitization occurred, including climatic regime, source material, and tectonostratigraphic setting. In this context, climatic conditions can be interpreted as a key modulating factor influencing the intensity of chemical weathering and desilicification, while the duration of emersion determines the extent to which these processes develop within individual deposits.

Weathering processes recorded in the bauxites vary between horizons but do not define a simple progressive trend. All bauxite samples are characterized by high chemical index of alteration (CIA) values, indicating intense chemical weathering during bauxitization (Nesbitt and Young, 1982). Differences between horizons are instead reflected in variations in desilicification, ferralitization, and related geochemical processes identified through discriminant functions (DF2 and DF3). The Upper Triassic bauxites (BX1) are distinguished by elevated contents of SiO_2 and clay-related

components, reflecting a strong influence of clay-rich precursor material and less effective desilicification. In contrast, the Upper Cretaceous bauxites (BX4) show the highest Al_2O_3 and lowest SiO_2 contents, indicating the most efficient desilicification and optimal conditions for bauxitization (Bárdossy, 1982). These deposits therefore represent the most geochemically evolved bauxites within the studied dataset, rather than a stage in a continuous evolutionary sequence.

The Paleogene interval (BX5–BX7), which represents the most extensive phase of bauxite formation, forms a relatively coherent geochemical cluster in the discriminant function model (Ilijanić et al., 2023). This reflects broadly similar tectonostratigraphic and environmental conditions during repeated episodes of subaerial exposure affecting different parts of the study area (D'Argenio and Mindszenty, 1995). Nevertheless, this interval is characterized by elevated concentrations of trace elements, including transition metals and rare earth elements, particularly in the Middle and Upper Eocene bauxites (BX6–BX7) (Kovačević Galović et al., 2025). Comparable enrichment patterns have been documented in other Mediterranean karst bauxite provinces and are commonly interpreted as reflecting variations in parent material and the contribution of externally derived detrital components (Bárdossy, 1982; Maksimović and Pantó, 1991; Mongelli and Acquafredda, 1999; Mameli et al., 2007; Boni et al., 2012; Boni et al., 2013; Deady et al., 2014; Mongelli et al., 2014; Mondillo et al., 2022).

The youngest Miocene bauxites (BX8) display a distinct geochemical signature characterized by higher contents of SiO_2 and clay-related components, as well as a closer affinity to modern terra rossa soils (Ilijanić et al., 2023). This indicates less efficient desilicification and incomplete bauxitization, likely reflecting shorter exposure times or less favorable environmental conditions (Schellmann, 1994). Their geochemical similarity to soils further supports the interpretation that Miocene bauxites represent only weakly transformed proto-bauxitic material.

The observed geochemical variability also suggests changes in the nature of the source material through time. Multiple independent geochemical proxies indicate a general shift from predominantly felsic to increasingly mafic and ultramafic geochemical signatures suggesting corresponding changes in the nature of the source material from the Upper Triassic to the Paleogene (Ilijanić et al., 2023; Kovačević Galović et al., 2025). Upper Triassic bauxites display geochemical characteristics consistent with predominantly felsic to intermediate source rocks, whereas Jurassic and Lower Cretaceous deposits show compositions close to the average upper continental crust. From the Upper Cretaceous onwards, geochemical characteristics become

progressively more consistent with mafic and ultramafic source rocks, with Upper Eocene bauxites (BX7) displaying the highest affinity toward ultramafic source compositions. This trend is supported by the combined evidence from the Zr–Cr–Ga ternary discrimination diagram and trace element systematics, including Cr–Ni relationships, Eu anomalies, and TiO_2/Al_2O_3 ratios, which are widely used as provenance indicators in bauxite studies (Mameli et al., 2007; Ahmadnejad et al., 2017; Radusinović et al., 2017), whereas the discriminant function analysis independently confirms the presence of systematic geochemical differences between the studied horizons (Ilijanić et al., 2023; Kovačević Galović et al., 2025). However, the youngest Miocene bauxites (BX8) deviate from this general trend, showing a shift toward intermediate compositions, suggesting renewed input of material with a more felsic geochemical affinity or a change in sediment sourcing.

DFA performed on Paleogene bauxites (BX5–BX7) (Figure 4) further refines this provenance pattern by distinguishing between geochemical domains across these closely spaced stratigraphic horizons within the Paleogene interval (Kovačević Galović et al., 2025).

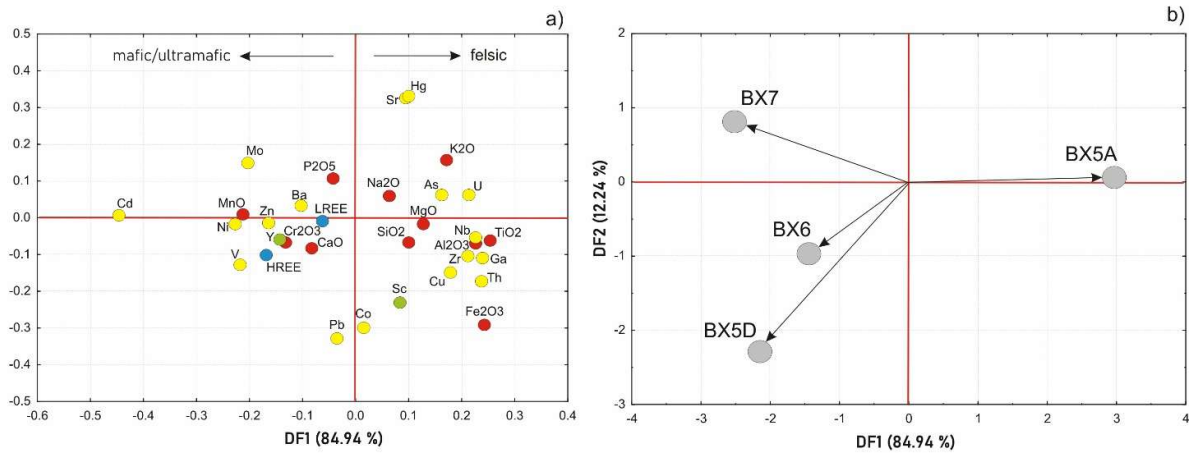

Figure 4. Discriminant function model (DFM) of clr-transformed geochemical data for Paleogene Croatian karst bauxites (BX5–BX7). (a) Scatterplot of variable loadings and (b) distribution of bauxite horizons in the reduced discriminant space defined by the first two discriminant functions (DF1–DF2). The model shows a clear separation between bauxites associated with geochemical characteristics consistent with a felsic-derived source material (positive DF1 values; BX5A) and those characterized by stronger mafic to ultramafic geochemical affinity (negative DF1 values; BX5D, BX6, BX7), including enrichment in trace elements and REE (From Kovačević Galović et al., 2025).

In particular, it separates bauxites characterized by geochemical characteristics consistent with a stronger felsic contribution from those displaying geochemical characteristics indicative of greater mafic to ultramafic input and enriched in trace elements, including rare earth elements (REE). As shown in Figure 4a, the positive side of DF1 is associated with geochemical components typical of

aluminosilicate-rich and felsic-derived source materials (SiO_2, Al_2O_3, K_2O, Na_2O), whereas the negative side reflects a stronger affinity toward mafic and ultramafic source components characterized by Cr, Ni, V, MnO, and P_2O_5. Rare earth elements are also associated with this mafic–ultramafic geochemical domain, indicating that source composition represents one of the principal controls on REE enrichment within the studied Paleogene bauxites. The discrimination along DF1 additionally demonstrates that even Paleocene bauxites of similar age, but formed within different paleogeographic and tectonic settings (BX5A and BX5D), exhibit markedly different geochemical signatures. This distinction emphasizes the importance of regional-scale variability in sediment input and paleogeographic setting, consistent with polygenetic models of karst bauxite formation involving both residual and allochthonous components (Bárdossy, 1982; Mameli et al., 2007; Mongelli et al., 2014).

Overall, the geochemical variability of Croatian karst bauxites reflects a complex interplay between provenance, weathering regimes, and evolving depositional and tectonostratigraphic conditions (Bárdossy, 1982; D'Argenio and Mindszenty, 1995; Mongelli et al., 2014). Variability in weathering-related processes, differences in desilicification efficiency, and the distinct character of individual horizons demonstrate that the studied bauxite horizons do not represent a single continuous evolutionary sequence, but rather discrete episodes of bauxitization formed under different environmental and tectonostratigraphic conditions. At the same time, the observed shift from geochemical characteristics typical of felsic compositions toward those more consistent with mafic and ultramafic compositions suggests long-term changes in source material and paleogeographic conditions through time. The obtained regional-scale geochemical patterns therefore support the interpretation that differences in the chemical and mineral composition of bauxite horizons reflect tectonostratigraphic constraints and the overall geodynamic evolution of the Croatian Karst Dinarides (hypothesis 1). Each horizon consequently represents a geochemically distinct response to specific regional environmental conditions during discrete episodes of subaerial exposure and karstification (Ilijanić et al., 2023; Kovačević Galović et al., 2025).

3.2. Intra-deposit variability and vertical geochemical trends

The Mamutovac-1a bauxite core exhibits pronounced vertical variability that reflects the interplay of depositional processes, post-depositional modification, and evolving physicochemical conditions within the karst system (Valeton, 1991; Mongelli et al., 2016). Rather than representing a uniform weathering profile, the deposit records a multi-stage evolution characterized by alternating phases

of in-situ bauxitization and episodic reworking and redistribution of bauxitic material (Bárdossy, 1982; Valeton, 1991; D'Argenio and Mindszenty, 1995; Mongelli et al., 2014; Kovačević Galović et al., 2026). This variability is most clearly expressed through the vertical succession of facies, ranging from intraclastic–oolitic and oolitic intervals to matrix-dominated and pelitomorphic facies. The predominance of coated grains, intraclasts, and micro-pebbles in the upper and middle parts of the core indicates significant reworking of previously formed bauxitic material, whereas the lower part, characterized by a finer and more homogeneous matrix, reflects a greater contribution of authigenic processes (Bárdossy, 1982; Valeton, 1991; D'Argenio and Mindszenty, 1995; Kovačević Galović et al., 2026). This alternation indicates discontinuous accumulation controlled by repeated redistribution within karst depressions (Valeton, 1991; Maksimović and Pantó, 1996; Mongelli et al., 2014; Abedini and Khosravi, 2024).

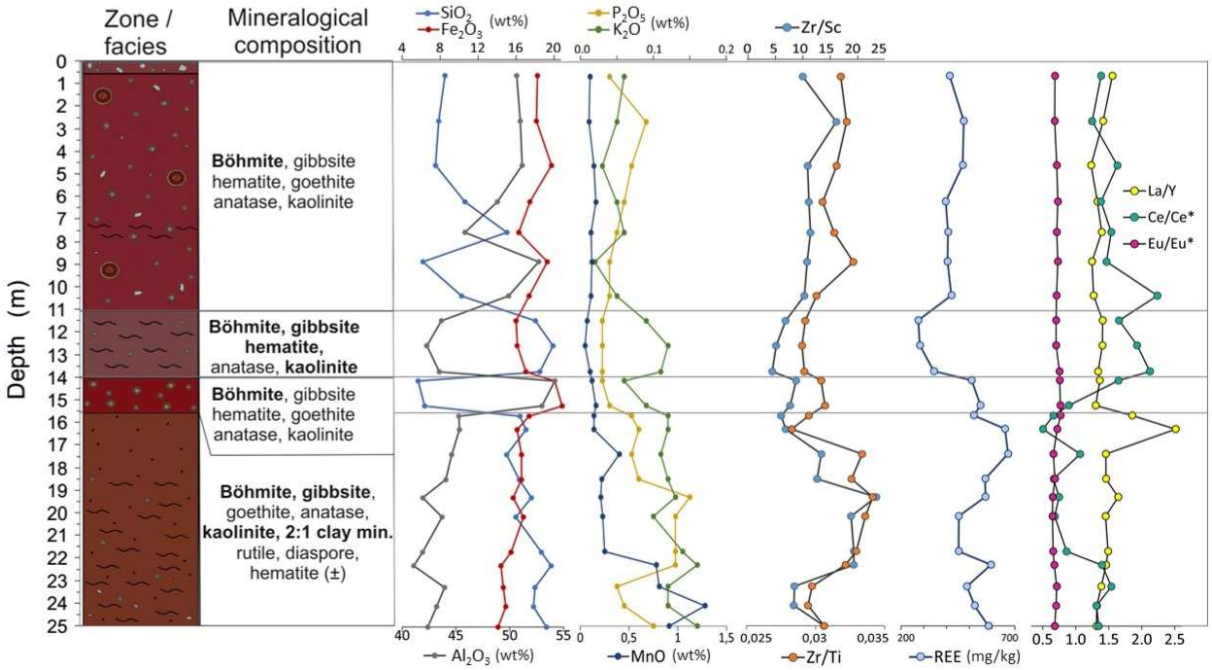

Figure 5. Vertical distribution of lithofacies, mineralogical composition, and selected geochemical parameters along the Mamutovac-1a bauxite core. Four facies-based zones are distinguished: Zone I (0–11 m; intraclastic–oolitic facies), Zone II (11–14 m; matrix-rich facies), Zone III (14–15.5 m; oolitic facies), and Zone IV (15.5–25 m; pelitomorphic facies). Major elements, trace elements, and REE parameters are shown as a function of depth. (Modified from Kovačević Galović et al., 2026).

Mineralogical variations reflect a clear vertical differentiation in physicochemical conditions within the deposit. The upper and middle parts of the core are dominated by böhmite and hematite, indicating predominantly oxidizing and relatively dehydrated conditions, associated with enhanced

diagenetic transformation and more dynamic depositional environments, including reworking of previously formed bauxitic material (Valeton, 1972; Bárdossy and Aleva, 1990; Temur and Kansun, 2006). The lower abundance and poorer crystallinity of clay minerals in these intervals further support more efficient leaching and desilicification under well-drained conditions. In contrast, the lower part of the core is characterized by increased abundance of gibbsite, the presence of minor diaspore, higher proportions of goethite, and a greater contribution of clay minerals, reflecting more stable, hydrated conditions with reduced drainage efficiency. These conditions likely promoted preservation of earlier-formed phases, limited dehydration, and localized development of reducing and possibly alkaline microenvironments, as indicated by the occurrence of diaspore and the shift toward goethite-dominated Fe assemblages (Bárdossy, 1982; D'Argenio and Mindszenty, 1995; Liu et al., 2013; Mamedov et al., 2022). Overall, this vertical transition indicates a shift from oxidizing, well-drained, and more dynamic conditions in the upper part of the profile toward more water-influenced, chemically buffered, and locally reducing environments at depth, reflecting increasing control of fluid-mediated processes within the paleokarst system.

These mineralogical changes are accompanied by systematic geochemical trends reflecting variations in the efficiency of desilicification and element redistribution along the profile. The upper and middle parts of the core are characterized by lower SiO_2 and elevated Al_2O_3 and Fe_2O_3 contents, indicating more efficient silica removal and residual enrichment of Al and Fe under well-drained conditions, typical of advanced bauxitization stages (Bárdossy, 1982; Bárdossy and Aleva, 1990; Schellmann, 1994; D'Argenio and Mindszenty, 1995). In contrast, the lower part of the core shows higher SiO_2 contents and lower Al_2O_3 and Fe_2O_3 values, indicating less efficient desilicification and a greater contribution of less altered material, consistent with incomplete bauxitization (Schellmann, 1994). This reflects reduced leaching intensity and drainage efficiency, as well as enhanced retention of clay-related components and possible detrital input, consistent with polygenetic karst bauxite systems (Bárdossy, 1982). Overall, the vertical pattern indicates a transition from efficient desilicification and advanced weathering in the upper part of the profile toward less intensive leaching and greater influence of detrital and fluid-controlled processes at depth. This is further reflected in the increased abundance and preservation of clay minerals in the lower part of the profile, indicating their accumulation under conditions of reduced leaching and enhanced fluid influence.

Trace element distribution further reflects changes in dominant geochemical controls along the core. In the upper part, trace elements are primarily associated with Fe oxy-hydroxides, indicating

their incorporation during ferruginization under oxidizing conditions (Ahmadnejad et al., 2017; Abedini et al., 2019; Abedini and Khosravi, 2020; Kovačević Galović et al., 2026). Toward the base of the deposit, this control shifts, as enrichment of Mn, Ni, and Co indicates mobilization of Mn in solution and its subsequent reprecipitation as Mn oxides, which act as effective scavengers for trace elements. This behaviour reflects more reducing and hydrated conditions, under which Mn becomes mobile and is subsequently redistributed within the ore body (Kovačević Galović et al., 2026; Mondillo et al., 2022). The transition therefore indicates an increasing influence of fluid-mediated redistribution processes with depth, rather than simple residual concentration, consistent with redistribution models proposed for karst bauxite systems (Abedini et al., 2019; Mondillo et al., 2022). Interaction with the underlying carbonate basement may have additionally influenced fluid chemistry and acted as a local geochemical barrier promoting trace element fixation (Maksimović and Pantó, 1996).

The strong correlation between Zr and Ti confirms their conservative behavior during bauxitization, indicating that these elements reliably preserve source-related information. However, depth-dependent variations in Zr/Ti and Zr/Sc ratios indicate that the deposit was not derived from a single homogeneous source, but instead reflects compositional heterogeneity and variable input of source material. The heterogeneous distribution of Zr/Sc ratios suggests that the contribution of compositionally mature or recycled material was not uniform throughout the core, but varied in response to changes in sediment input and reworking intensity. Additional constraints on possible source compositions are provided by trace-element systematics, particularly the distribution of samples in the Zr–Cr–Ga discrimination diagram, which suggestsgeochemical affinities with compositionally diverse parent rocks. The observed variations are consistent with contributions from intermediate to ultramafic source components, with no evidence for a single dominant precursor lithology. This interpretation is further supported by Eu anomalies and TiO_2/Al_2O_3 ratios, which show a shift toward more mafic-influenced compositions relative to the upper continental crust. Together, these data support the interpretation of a heterogeneous and mixed provenance, reflecting multiple source contributions and subsequent redistribution processes rather than a simple residual origin.

The behavior of rare earth elements provides further insight into the combined effects of inheritance and post-depositional modification. REE concentrations increase with depth despite decreasing Al_2O_3 and Fe_2O_3 contents, indicating that their distribution is not controlled by the main bauxitic phases but rather reflects redistribution during later stages of evolution (Kovačević Galović

et al., 2026; Reinhardt et al., 2018). The consistent enrichment of LREE relative to HREE across the core suggests preferential retention of LREE, whereas variations in fractionation indices indicate changes in mobility linked to evolving physicochemical conditions.

In particular, the vertical variability of Ce anomalies records changes in redox conditions and fluid circulation within the deposit. Predominantly positive anomalies in the upper part reflect oxidizing conditions typical of vadose environments, whereas the transition to negative anomalies at intermediate depths indicates downward migration of Ce-depleted fluids, likely associated with repeated dissolution–transport–precipitation cycles during fluctuating groundwater conditions (Kovačević Galović et al., 2026; Mongelli et al., 2014; Mondillo et al., 2022). The reappearance of positive anomalies in the lowermost part of the core suggests localized conditions favoring Ce fixation, likely related to interaction with the carbonate basement and changes in pore-water chemistry. In contrast, the consistently negative Eu anomaly across the core indicates a strong inherited signal from the parent material, largely unaffected by weathering and diagenetic processes (Kovačević Galović et al., 2026; Mongelli et al., 2014).

Generally, the vertical trends observed in the Mamutovac-1a deposit demonstrate that intra-deposit variability reflects the combined influence of depositional processes, degree of reworking, fluid circulation, and evolving physicochemical conditions within the paleokarst system. The core records a transition from more dynamic, reworked, and oxidizing conditions in the upper part toward more stable, fluid-influenced, and locally reducing environments at depth. The observed vertical mineralogical and geochemical zonation indicates that bauxitization processes varied significantly throughout the profile, resulting in systematic changes in mineral assemblages and major-element composition with depth. In particular, the progressive increase in clay mineral abundance toward the lower part of the profile reflects reduced desilicification efficiency, stronger fluid influence, and enhanced preservation of fine-grained phases within deeper parts of the paleokarst system (hypothesis 2).

3.3. Linking regional and deposit-scale processes

The integration of regional-scale geochemical patterns with deposit-scale variability provides a coherent framework for understanding the processes governing the formation of Croatian karst bauxites. While regional data define broad temporal trends related to long-term geological evolution, the Mamutovac-1a core reveals the mechanisms through which these large-scale controls are expressed at the level of an individual deposit.

At the regional scale, bauxite horizons exhibit systematic geochemical differences reflecting changes in provenance, weathering intensity, and depositional conditions throughout the geological evolution of the Croatian Karst Dinarides (Ilijanić et al., 2023; Kovačević Galović et al., 2025). These differences define a clear temporal structure, in which older and younger horizons are distinguished by contrasting geochemical signatures consistent with changes in source material and paleoenvironmental conditions. However, such large-scale patterns alone do not fully explain the internal complexity observed within individual deposits.

The Mamutovac-1a core demonstrates that these regional signals are not preserved simply or uniformly but are modified by local depositional and post-depositional processes. Vertical variability within the ore body reflects repeated reworking, redistribution, and in-situ transformation of bauxitic material, indicating that the geochemical signature of a given horizon represents not only primary weathering products but also the cumulative effect of subsequent processes operating within karst depressions (Kovačević Galović et al., 2026; Bárdossy, 1982; D'Argenio and Mindszenty, 1995).

This relationship between scales suggests that regional geochemical trends define the initial conditions for bauxite formation, particularly the geochemical characteristics of the source material and the general climatic and tectonic framework, whereas deposit-scale processes control the degree to which these signals are preserved, modified, or redistributed. In this context, the variability observed within the Mamutovac-1a deposit can be interpreted as a local expression of broader regional controls, filtered through the dynamics of karst environments.

The link between scales is particularly evident in the behavior of immobile and relatively conservative elements. At the regional level, geochemical patterns are defined by multi-element systematics and statistical relationships that are consistent with changes in provenance and tectonostratigraphic evolution (Ilijanić et al., 2023; Kovačević Galović et al., 2025). At the deposit scale, however, immobile elements such as Zr, Ti, and Sc provide additional constraints on source-related characteristics. Their distribution reflects not only variations in the geochemical characteristics of the source material but also variations in sediment input and the degree of recycling and reworking, as indicated by fluctuating Zr/Ti and Zr/Sc ratios (Kovačević Galović et al., 2026). This indicates that even conservative geochemical indicators, although largely immobile during weathering, may exhibit significant variability and therefore do not necessarily reflect a single, well-defined source signature at the deposit scale.

A similar relationship is observed in the distribution of rare earth elements. Regional-scale patterns show that REE concentrations and fractionation vary systematically between horizons and are interpreted to reflect the combined influence of both provenance and physicochemical conditions during bauxitization (Kovačević Galović et al., 2025). At the deposit scale, however, REE distribution reflects additional controls, including fluid circulation, redox gradients, and interaction with the carbonate substrate (Kovačević Galović et al., 2026). This interaction highlights the active role of the carbonate substrate in controlling the geochemical evolution of bauxite deposits. The karstified carbonate basement influences fluid circulation pathways, buffering capacity, and pH conditions, thereby affecting element mobility, mineral stability, and the redistribution of both major and trace elements (D'Argenio and Mindszenty, 1995; Bárdossy and Combes, 1999; Abedini and Khosravi, 2024). In addition, variations in weathering intensity observed at the regional scale reflect not only changes in source material and tectonostratigraphic setting, but also the influence of broader climatic conditions that governed the efficiency of leaching and desilicification during different stages of platform evolution. The vertical zonation of REE within the Mamutovac-1a core thus represents a superposition of inherited geochemical characteristics and localized redistribution processes.

In this context, regional and deposit-scale processes can be viewed as operating within a hierarchical system. Tectonostratigraphic evolution governs the timing and conditions of subaerial exposure, determining the availability and nature of source material, while local hydrological and geochemical conditions within the karst depressions control the redistribution and preservation of that material. As a result, each bauxite deposit represents a site-specific realization of regionally controlled processes.

This multi-scale perspective highlights the polygenetic nature of karst bauxites and underscores the importance of integrating different levels of analysis. Regional datasets alone may obscure local variability, whereas deposit-scale studies without regional context may overlook the broader controls on bauxite formation. By combining both approaches, it becomes possible to distinguish between inherited geochemical signals and those generated or modified during later stages of evolution.

Overall, the integration of regional and deposit-scale data indicates that the genesis of Croatian karst bauxites was controlled by the interaction of tectonostratigraphic evolution, climatic and paleoenvironmental conditions, and variations in source material. Temporal geochemical trends

recorded among the studied bauxite horizons are consistent with shifts in provenance and depositional regimes through time, while intra-deposit variability captures the influence of local karst processes, including reworking, fluid circulation, and redox-controlled redistribution. Together, these multi-scale relationships link large-scale geodynamic evolution with localized depositional and diagenetic processes, providing a comprehensive geochemical framework for interpreting bauxite formation within the karst paleoenvironment.

3.4. Controls on REE distribution and fractionation

The distribution and fractionation of rare earth elements (REE) in Croatian karst bauxites reflect a combined influence of provenance, physicochemical conditions during weathering, and post-depositional processes operating across both regional and deposit scales (Ilijanić et al., 2023; Kovačević Galović et al., 2025). Regional geochemical data show that REE concentrations vary systematically across bauxite horizons, with the lowest ΣREE values in the Upper Triassic (BX1) and significantly higher concentrations in the Paleogene, particularly in the Middle and Upper Eocene (BX6–BX7), where median values exceed 550 mg/kg (Kovačević Galović et al., 2025). This pattern is consistent with changes in both source material and depositional setting, with an increased geochemical contribution from mafic to ultramafic material, possibly related to the Dinaridic ophiolite belt, representing one of the principal controls on REE enrichment (Mameli et al., 2007; Radusinović et al., 2017; Ilijanić et al., 2023; Kovačević Galović et al., 2025). However, regional trends also suggest that provenance alone is insufficient to explain the observed variability, as REE distribution is further modified by processes operating during bauxitization and diagenesis.

All horizons exhibit enrichment of LREE relative to HREE (ΣLREE/ΣHREE ≈ 6.8–10.5; Kovačević Galović et al., 2025), reflecting differential mobility of REE during weathering, similar to fractionation patterns reported from Mediterranean karst bauxites by Karadağ et al. (2009). Fractionation is primarily controlled by pH-dependent processes: under acidic conditions, REE are more mobile, and HREE are preferentially leached due to their stronger complexation, whereas under neutral to alkaline conditions, REE retention increases, modifying fractionation patterns (Kovačević Galović et al., 2025). This control is reflected in La/Y ratios, which indicate more acidic conditions for BX1 and BX6 and more neutral to alkaline conditions for the remaining horizons (Kovačević Galović et al., 2025). At the deposit scale, the Mamutovac-1a core refines this pattern, showing non-uniform fractionation trends with depth, consistent with evolving fluid conditions and interaction with the carbonate substrate (Kovačević Galović et al., 2026), as also observed in other Mediterranean karst

bauxite profiles (Karadağ et al., 2009). Together, these relationships indicate that pH was likely one of the primary controls on REE fractionation across both spatial scales.

Redox conditions exert an additional control, particularly through the behavior of Ce. Predominantly positive Ce anomalies at the regional scale indicate oxidizing conditions during bauxitization (Kovačević Galović et al., 2025), consistent with well-drained vadose environments where Ce^{3+} is oxidized to Ce^{4+} and preferentially removed from solution. Within the Mamutovac-1a core, however, Ce anomalies show pronounced vertical variability, with positive values in the upper part, negative anomalies at intermediate depths, and renewed positive anomalies near the base (Kovačević Galović et al., 2026). This pattern reflects progressive redistribution during post-depositional evolution, where downward percolation of Ce-depleted fluids produces negative anomalies, while renewed fixation near the carbonate basement suggests localized geochemical conditions favoring Ce precipitation (Wang et al., 2013; Abedini and Khosravi, 2024). In contrast, consistently negative Eu anomalies across all horizons indicate that Eu behavior is largely independent of weathering conditions and preserves a strong inherited geochemical signal consistent with predominantly felsic to intermediate source material (Kovačević Galović et al., 2025; Kovačević Galović et al., 2026), as supported by additional provenance proxies such as TiO_2/Al_2O_3 and Sm/Nd ratios.

The distribution of REE is strongly influenced by their association with specific mineral phases and by fluid-mediated redistribution (Mordberg et al., 2000; Laskou and Andreou, 2003; Liu et al., 2016). Regional observations suggest multiple potential hosts (Kovačević Galović et al., 2025), while data from the Mamutovac-1a core indicate that REE are not directly linked to the main bauxitic components (Al_2O_3, Fe_2O_3), and instead reflect more complex controls (Kovačević Galović et al., 2026). A positive relationship between REE and P_2O_5 suggests that phosphate minerals were likely the principal, and possibly dominant, hosts in the studied bauxites, consistent with the occurrence of authigenic REE-bearing phosphate minerals, such as monazite and xenotime reported from Mediterranean karst bauxites (Mondillo et al., 2011; Radusinović et al., 2017; Tomašić et al., 2021; Kovačević Galović et al., 2026). However, direct mineralogical confirmation of the REE-bearing phases was beyond the scope of the present study. Clay minerals may additionally contribute to REE retention through adsorption processes, particularly in fine-grained weathering products, although their role in the studied deposit appears secondary (Mongelli et al., 2014; Liu et al., 2016; Estrade et al., 2019). These relationships indicate that REE distribution is largely decoupled from the main ore-forming phases and controlled by the abundance and stability of specific mineral hosts.

Vertical trends within the Mamutovac-1a core highlight the importance of fluid–rock interaction, particularly in the lower part of the deposit where increasing REE concentrations coincide with changing physicochemical conditions and interaction with the carbonate basement (Kovačević Galović et al., 2026). Such interaction modifies pore-water chemistry (Calagari and Abedini, 2007), influencing pH and carbonate complexation, and promotes redistribution and localized enrichment of REE (Maksimović and Pantó, 1996). The elevated and more variable La/Y ratios in the lowermost zone further support the development of more alkaline conditions and enhanced fluid influence. REE behavior in Croatian karst bauxites is best interpreted as reflecting the combined effects of inherited geochemical signatures and secondary modification through fluid-mediated processes, demonstrating that their distribution cannot be explained by a single controlling factor but rather by the interaction of multiple processes operating across different scales.

3.5. Implications for resource potential of Croatian karst bauxites

The results of this study indicate that Croatian karst bauxites have promising resource potential as aa alternative source of critical raw materials, particularly REE, consistent with recent assessments of Mediterranean karst bauxites as emerging unconventional resources of critical metals (Boni et al., 2013; Deady et al., 2014; Gamaletsos et al., 2019). Their resource and exploration potential is primarily controlled by stratigraphic position, mineralogical hosting, and intra-deposit variability.

At the regional scale, REE distribution shows systematic differences between bauxite horizons, with the highest concentrations consistently recorded in Paleogene deposits, particularly the Middle Eocene (BX6) and Upper Eocene (BX7) horizons (Kovačević Galović et al., 2025; Crnički and Jurković, 1990; Tomašić et al., 2021; Brčić et al., 2023). These horizons therefore represent the most prospective targets for REE exploration. The observed enrichment reflects the combined influence of source material and tectonostratigraphic setting, indicating that specific phases of geological evolution created favorable conditions for REE accumulation. Consequently, the regional geological framework represents a first-order control on the exploration potential of Croatian karst bauxites.

At the deposit scale, the Mamutovac-1a case study demonstrates that REE distribution within a single bauxite body is highly heterogeneous and cannot be reliably assessed using bulk compositions alone (Kovačević Galović et al., 2026). REE concentrations increase with depth despite decreasing Al_2O_3 and Fe_2O_3 contents, indicating that their distribution is controlled by specific mineral hosts rather than the main bauxitic phases. As discussed in the previous section, the positive relationship with P_2O_5 suggests that phosphate minerals are likely to represent the principal REE hosts

(Mordberg, 1999; Liu et al., 2016; Laskou and Andreou, 2003), although their direct identification requires further mineralogical investigation. From a resource perspective, this inferred mineralogical control is important because REE hosted in phosphate phases may require different processing approaches compared to those associated with clay minerals or Fe oxides (Kanazawa and Kamitani, 2006).

The vertical zonation observed in the Mamutovac-1a core further indicates that REE enrichment is not uniformly distributed, but concentrated in specific intervals, particularly in the lower parts of the deposit affected by fluid circulation and evolving physicochemical conditions (Kovačević Galović et al., 2026). This heterogeneity indicates that any future assessment of resource utilization would require detailed characterization of the spatial distribution and continuity of REE-enriched zones within individual deposits.

In addition to REE, the presence of other critical elements, including Ga, V, and Sc, further enhances the resource potential of Croatian karst bauxites. Their distribution is linked to specific mineral phases and geochemical environments, while partial recovery of La, Ga, and V through aqua regia extraction demonstrates their chemical extractability under laboratory conditions and suggests that primary bauxite may represent a potential source of critical raw materials. Although the similar aqua regia extractability of V and Fe may suggest that V is at least partly associated with Fe-bearing mineral phases, the lack of clear correlations with major or trace elements means that its mineralogical host cannot be unambiguously constrained from the available data. More generally, the results of the aqua regia extraction should be regarded as preliminary indicators of resource potential rather than evidence of technical or economic feasibility, which would require dedicated technological and economic investigations.

Overall, Croatian karst bauxites exhibit moderate to locally high resource -potential for REE, with the greatest exploration potential associated with Paleogene horizons and deposits characterized by favorable mineralogical hosting and fluid-controlled enrichment. However, reliable evaluation of this resource potential is strongly dependent on intra-deposit variability, mineralogical controls, and the spatial distribution of enriched zones, requiring detailed deposit-scale investigations. The resource potential identified in this study should not be interpreted as evidence of economic feasibility, and assessment of potential exploitation would require additional geological, technological, and economic investigations beyond the scope of this dissertation.

4. CONCLUSION

This doctoral thesis provides an integrated geochemical and mineralogical framework for understanding the formation, evolution, and resource potential of Croatian karst bauxites developed within the Croatian Karst Dinarides. By combining regional-scale geochemical datasets with detailed investigation of the Upper Eocene Mamutovac-1a deposit, the study demonstrates that Croatian karst bauxites represent complex polygenetic systems controlled by the interaction of tectonostratigraphic evolution, provenance, weathering processes, depositional conditions, and post-depositional modification.

At the regional scale, systematic geochemical variability between bauxite horizons (BX1–BX8) reflects major changes in source material and environmental conditions during successive phases of subaerial exposure from the Upper Triassic to the Miocene. The results indicate a general shift from predominantly felsic toward increasingly mafic and ultramafic geochemical signatures, suggesting corresponding changes in the nature of the source material, particularly during the Paleogene, accompanied by enrichment in trace elements and rare earth elements (REE). Variations in desilicification efficiency and major-element composition further demonstrate that individual horizons formed under different physicochemical and paleogeographic conditions rather than representing a single continuous evolutionary sequence.

Discriminant function analysis proved to be an effective tool for distinguishing geochemically different bauxite groups and identifying the principal controls governing their variability. The obtained discriminant models clearly separate horizons according to their overall geochemical characteristics, highlighting systematic differences associated with tectonostratigraphic and paleogeographic evolution. In particular, the Paleogene horizons record distinct differences between felsic- and mafic–ultramafic-related geochemical domains, emphasizing the heterogeneous and polygenetic nature of the Croatian karst bauxite system.

The Mamutovac-1a deposit exhibits pronounced vertical mineralogical and geochemical variability reflecting the combined influence of reworking, fluid circulation, and evolving physicochemical conditions within the paleokarst environment. The upper part of the deposit is characterized by more oxidizing and well-drained conditions associated with efficient desilicification and enrichment of Al and Fe phases, whereas the lower part records increased clay mineral abundance, stronger fluid influence, and locally reducing conditions. These trends demonstrate that intra-deposit

variability is controlled by both depositional processes and post-depositional redistribution within the karst system.

The distribution and fractionation of REE are controlled by multiple interacting factors operating across both regional and deposit scales. Geochemical characteristics of the source material represent one of the principal controls on REE enrichment, particularly in Paleogene bauxites showing stronger mafic and ultramafic geochemical affinities. However, the results additionally show that REE behavior is strongly influenced by pH and redox conditions, fluid-mediated redistribution, and mineralogical hosts. The positive correlation between REE and P_2O_5 suggests that phosphate minerals likely represent one of the principal REE hosts, whereas clay minerals play subordinate but locally important roles. Vertical variations in Ce anomalies within the Mamutovac-1a core further indicate changing redox conditions and fluid circulation during post-depositional evolution.

The results confirm that Croatian karst bauxites have promising resource potential as an alternative source of critical raw materials, particularly REE, as well as other critical elements such as Ga, V, and Sc. The greatest exploration and resource potential is associated with Paleogene horizons and deposits characterized by favorable mineralogical hosting and localized fluid-controlled enrichment. However, reliable assessment of this resource potential depends on detailed characterization of intra-deposit heterogeneity, mineralogical controls, and the spatial distribution of enriched zones, emphasizing the importance of detailed deposit-scale investigations in resource evaluation. The resource potential identified here should not be interpreted as evidence of economic feasibility, which would require additional geological, technological, and economic investigations beyond the scope of this dissertation.

Overall, this research demonstrates that the genesis of Croatian karst bauxites cannot be explained by a single process or source, but instead reflects a multi-stage evolution controlled by the interaction of regional geodynamic processes and local karst-related mechanisms. The integration of regional and deposit-scale approaches provides a comprehensive basis for interpreting bauxite formation within karst paleoenvironments and contributes to a broader understanding of karst bauxite systems as both paleoenvironmental archives and potential alternative resources of critical raw materials.

5. REFERENCES

Abedini, A., Khosravi, M. (2020): Geochemical constraints on the Triassic–Jurassic Amir-Abad karst-type bauxite deposit, NW Iran. – Journal of Geochemical Exploration, 211, 106489. https://doi.org/10.1016/j.gexplo.2020.106489

Abedini, A., Khosravi, M. (2024): Geochemical characteristics of aluminum-bearing iron ores: A case study from the Kolijan karst-type bauxite deposit, northwestern Iran. – Minerals, 14, 151. https://doi.org/10.3390/min14020151

Abedini, A., Khosravi, M., Calagari, A.A. (2019): Geochemical characteristics of the Arbanos karst-type bauxite deposit, NW Iran: Implications for parental affinity and factors controlling the distribution of elements. – Journal of Geochemical Exploration, 200, 249–265. https://doi.org/10.1016/j.gexplo.2018.09.004

Ahmadnejad, F., Zamanian, H., Taghipour, B., Zarasvandi, A., Buccione, R., Ellahi, S.S. (2017): Mineralogical and geochemical evolution of the Bidgol bauxite deposit, Zagros Mountain Belt, Iran: Implications for ore genesis, rare earth elements fractionation and parental affinity. – Ore Geology Reviews, 86, 755–783. https://doi.org/10.1016/j.oregeorev.2017.04.006

Aitchison, J. (1986): The Statistical Analysis of Compositional Data. – Chapman & Hall, London, 416 p.

Babić, L., Zupanič, J. (2016): The youngest stage in the evolution of the Dinaric carbonate platform: The Upper nummulitic limestones in the North Dalmatian foreland, Middle Eocene, Croatia. – Natura Croatica, 25(1), 55–71. doi:10.20302/nc.2016.25.3. https://doi.org/10.20302/NC.2016.25.3

Babić, L., Zupanić, J., Kurtanjek, D. (1995): Sharply-topped alluvial gravel sheets in the Palaeogene Promina basin (Dinarides, Croatia). – Geologia Croatica, 48(1), 33–48. https://doi.org/10.4154/GC.1995.04

Bárdossy, G. (1982): Karst Bauxites: Bauxite Deposits on Carbonate Rocks. – Elsevier, Amsterdam, 441 p.

Bárdossy, G., Aleva, G.J.J. (1990): *Lateritic Bauxites*. – Developments in Economic Geology, 27, Elsevier Scientific Publication, Amsterdam, 624 p.

Bárdossy, G., Combes, P.J. (1999): Karst bauxites: Interfingering of deposition and palaeoweathering. – Special Publication of the International Association of Sedimentologists, 27, 189–206. https://doi.org/10.1002/9781444304190.ch7

Birkeland, P.W. (1985): Soils and Geomorphology. – Oxford University Press, New York, 372 p. https://doi.org/10.1017/S0016756800031617

Blašković, I., Dragičević, I., Pokrajčić, I. (1989): Tectonic control of the origin of the paleorelief for bauxite deposits in western Herzegovina, Yugoslavia. – Travaux ICSOBA, 19, 230–238.

Bogatyrev, B.A., Zhukov, V.V. (2009): Bauxite provinces of the world. – Geology of Ore Deposits, 51, 339–355. https://doi.org/10.1134/S1075701509050018

Boni, M., Reddy, S.M., Mondillo, N., Balassone, G., Taylor, R. (2012): A distant magmatic source for Cretaceous karst bauxites of Southern Apennines (Italy), revealed through SHRIMP zircon age dating. – Terra Nova, 24, 326–332. https://doi.org/10.1111/j.1365-3121.2012.01068.x

Boni, M., Rollinson, G., Mondillo, N., Balassone, G., Santoro, L. (2013): Quantitative mineralogical characterization of karst bauxite deposits in the Southern Apennines, Italy. – Economic Geology, 108, 813–833. https://doi.org/10.2113/econgeo.108.4.813

Brčić, V., Dunkl, I., Mindszenty, A., Brlek, M., Trinajstić, N., Bajo, P., Bauluz, B., Mišur, I., Karius, V., Šuica, S., Kukoč, D., Yuste, A., Laita, E., von Eynatten, H., Zeh, A. (2023): A time-space window between Eocene karst bauxite genesis and the first molasse deposition in the Dinaric Foreland Basin in North Dalmatia, Croatia. – Frontiers in Earth Science, 11, 1224164. https://doi.org/10.3389/feart.2023.1224164

Brlek, M., Gaynor, S.P., Mongelli, G., Bauluz, B., Sinisi, R., Brčić, V. (2021): Karst bauxite formation during Miocene climatic optimum (Central Dalmatia, Croatia): Mineralogical, compositional and geochronological perspectives. – International Journal of Earth Sciences, 110, 2899–2922. https://doi.org/10.1007/s00531-021-02091-z

Brlek, M., Korbar, T., Košir, A., Glumac, B., Grizelj, A., Otoničar, B. (2014): Discontinuity surfaces in Upper Cretaceous to Paleogene carbonates of central Dalmatia (Croatia): Glossifungites ichnofacies, biogenic calcretes, and stratigraphic implications. – Facies, 60, 467–487. https://doi.org/10.1007/s10347-013-0378-9

Calagari, A.A., Abedini, A. (2007): Geochemical investigations on Permo–Triassic bauxite horizon at Kanisheeteh, east of Bukan, West-Azarbaidjan, Iran. – Journal of Geochemical Exploration, 94, 1–18. https://doi.org/10.1016/j.gexplo.2007.04.003

Ćosović, V., Mrinjek, E., Nemec, W., Španiček, J., Terzić, K. (2018): Development of transient carbonate ramps in an evolving foreland basin. – Basin Research, 30, 746–765. https://doi.org/10.1111/bre.12274Digital Object Identifier (DOI)

Crnički, J. (1987): Raspodjela lantanida u boksitima Hrvatske i njihovo značenje za genezu boksita. – PhD Thesis, University of Zagreb, Zagreb, Croatia.

D'Argenio, B., Mindszenty, A. (1992): Tectonic and climatic control on paleokarst and bauxites. – Giornale di Geologia, 54(1), 207–218.

D'Argenio, B., Mindszenty, A. (1995): Bauxites and related paleokarst: tectonic and climatic event markers at regional unconformities. – Eclogae Geologicae Helvetiae, 88(3), 453–499.

Deady, D., Mochos, E., Goodenough, K., Williamson, B., Wall, F. (2014): Rare earth elements in karst-bauxites: A novel untapped European resource? – In: Proceedings of the 1st European Rare Earth Resources Conference (ERES2014), Milos, Greece, 4–7 September 2014, 1–12.

Deng, J., Wang, Q.F., Yang, S.J., Liu, X.F., Zhang, Q.Z., Yang, L.Q., Yang, Y.H. (2010): Genetic relationship between the Emeishan plume and the bauxite deposits in western Guangxi, China: Constraints from U–Pb and Lu–Hf isotopes of the detrital zircons in bauxite ores. – Journal of Asian Earth Sciences, 37(5–6), 412–424. https://doi.org/10.1016/j.jseaes.2009.10.005

Estrade, G., Marquis, E., Smith, M., Goodenough, K., Nason, P. (2019): REE concentration processes in ion adsorption deposits: Evidence from the Ambohimirahavavy alkaline complex in Madagascar. – Ore Geology Reviews, 112, 103027. https://doi.org/10.1016/j.oregeorev.2019.103027

Gamaletsos, P.N., Godelitsas, A., Filippidis, A., Pontikes, Y. (2019): The rare earth elements potential of Greek bauxite active mines in the light of a sustainable REE demand. – Journal of Sustainable Metallurgy, 5, 20–47. https://doi.org/10.1007/S40831-018-0192-2

Goodenough, K.M., Wall, F., Merriman, D. (2018): The Rare Earth Elements: Demand, Global Resources, and Challenges for Resourcing Future Generations. – Natural Resources Research, 27, 201–216. https://doi.org/10.1007/s11053-017-9336-5

Ilijanić, N., Kovačević Galović, E., Gizdavec, N., Ivkić Filipović, I., Miko, S., Peh, Z. (2023): Geochemical records in subaerial exposure environments in Croatia using discriminant function analysis of bauxite data. – Frontiers in Earth Science, 10, 1055435. https://doi.org/10.3389/feart.2022.1055435

Kanazawa, Y., Kamitani, M. (2006): Rare earth minerals and resources in the world. – Journal of Alloys and Compounds, 408–412, 1339–1343. https://doi.org/10.1016/j.jallcom.2005.04.033

Karadağ, M.M., Küpeli, S., Arýk, F., Ayhan, A., Zedef, V., Döyen, A. (2009): Rare earth element (REE) geochemistry and genetic implications of the Mortaş bauxite deposit (Seydişehir/Konya – southern Turkey). – Geochemistry, 69(2), 143–159. https://doi.org/10.1016/j.chemer.2008.04.005

Korbar, T. (2009): Orogenic evolution of the external Dinarides in the NE Adriatic region: A model constrained by tectonostratigraphy of Upper Cretaceous to Paleogene carbonates. – Earth-Science Reviews, 96, 296–312. https://doi.org/10.1016/j.earscirev.2009.07.004

Kovačević Galović, E., Ilijanić, N., Fajković, H., Miko, S., Tomašić, N., Ivkić Filipović, I., Gizdavec, N., Peh, Z., Teskera, D. (2026): Mineralogical and Geochemical Variability of the Mamutovac-1a Upper Eocene Karst Bauxite Deposit (Croatian Dinarides) and Its CRM Potential. – Minerals, 16(5), 547. https://doi.org/10.3390/min16050547

Kovačević Galović, E., Ilijanić, N., Gizdavec, N., Miko, S., Peh, Z. (2025): Geochemical insights and mineral resource potential of rare earth elements (REE) in the Croatian karst bauxites. – Minerals, 15(2), 192. https://doi.org/10.3390/min15020192

Kovačević Galović, E., Ilijanić, N., Peh, Z., Miko, S., Hasan, O. (2012): Geochemical discrimination of early Palaeogene bauxites in Croatia. – Geologia Croatica, 65, 53–65. https://doi.org/10.4154/GC.2012.04

Kruk, B., Dedić, Ž., Kovačević Galović, E., Kruk, L. (2014): Osnove gospodarenja mineralnim sirovinama na području općine Promina u Šibensko-kninskoj županiji. – Croatian Geological Survey, Zagreb, 124 p. (unpublished report).

Laskou, M., Andreou, G. (2003): Rare earth elements distribution and REE-minerals from the Parnassos–Ghiona bauxite deposits, Greece. In: Eliopoulos, D. et al. (eds.): *Mineral Exploration and Sustainable Development, 7th Biennial SGA Meeting*. – Mill Press, Rotterdam, 89–92.

Ling, K.Y., Zhu, X.Q., Tang, H.S., Du, S.J., Gu, J. (2018): Geology and geochemistry of the Xiaoshanba bauxite deposit, Central Guizhou Province, SW China: Implications for the behavior of trace and rare earth elements. – Journal of Geochemical Exploration, 190, 170–186. https://doi.org/10.1016/j.gexplo.2018.03.007

Liu, X., Wang, Q., Zhang, Q., Zhang, Y., Li, Y. (2016): Genesis of REE minerals in the karstic bauxite in western Guangxi, China, and its constraints on the deposit formation conditions. – Ore Geology Reviews, 75, 100–115. https://doi.org/10.1016/j.oregeorev.2015.12.015

Liu, X., Wang, Q., Feng, Y., Li, Z., Cai, S. (2013): Genesis of the Guangou karstic bauxite deposit in western Henan, China. – Ore Geology Reviews, 55, 162–175. https://doi.org/10.1016/j.oregeorev.2013.06.002

MacLean, W.H., Bonavia, F.F., Sanna, G. (1997): Argillite debris converted to bauxite during karst weathering: Evidence from immobile element geochemistry at the Olmedo Deposit, Sardinia. – Mineralium Deposita, 32, 607–616. https://doi.org/10.1007/s001260050126

Maksimović, Z., Pantó, G. (1983): Mineralogy of yttrium and lanthanide elements in karstic bauxite deposits. – Travaux ICSOBA, 18, 191–200.

Maksimović, Z., Pantó, G. (1985): Hydroxy-bastnaesite-(Nd), a new mineral from Montenegro, Yugoslavia. – Mineralogical Magazine, 49, 717–720.

Maksimović, Z., Pantó, G. (1991): Contribution to the geochemistry of the rare earth elements in the karst-bauxite deposits of Yugoslavia and Greece. – Geoderma, 51, 93–109.

Maksimović, Z., Pantó, G. (1996): Authigenic rare earth minerals in karst-bauxites and karstic nickel deposits. In: Jones, A.P., Wall, F., Williams, C.T. (eds.): *Rare Earth Minerals, Chemistry, Origin and Ore Deposits*. – Mineralogical Society Series, Chapman & Hall, London, Chapter 10, 199–220.

Maksimović, Z., Roaldset, E. (1976): Lanthanide elements in some Mediterranean karstic bauxite deposits. – Travaux ICSOBA, 13, 199–220.

Maksimović, Z., Skarpelis, N., Pantó, G. (1993): Mineralogy and geochemistry of the rare earth elements in the karstic nickel deposits of Lokris area, Greece. – Acta Geologica Hungarica, 36(3), 331–342.

Mamedov, V., Boeva, N., Makarova, M., Shipilova, E., Melnikov, P. (2022): The problem of the formation of boehmite and gibbsite in bauxite-bearing lateritic profiles. – Minerals, 12, 389. https://doi.org/10.3390/min12030389

Mameli, P., Mongelli, G., Oggiano, G., Dinelli, E. (2007): Geological, geochemical and mineralogical features of some bauxite deposits from Nurra (Western Sardinia, Italy): Insights on conditions of formation and parental affinity. – International Journal of Earth Sciences, 96, 887–902. https://doi.org/10.1007/s00531-006-0142-2

Marković, S. (2002): Hrvatske mineralne sirovine. – Institut za geološka istraživanja, Zavod za geologiju, Zagreb, 544 p.

Mindszenty, A. (2016): Bauxites: feedbacks of system earth at greenhouse times. – Geologia Croatica, 69, 79–87. https://doi.org/10.4154/GC.2016.07

Mindszenty, A., D'Argenio, B., Aiello, G. (1995): Lithospheric bulges recorded by regional unconformities: The case of Mesozoic–Tertiary Apulia. – Tectonophysics, 252, 137–161. https://doi.org/10.1016/0040-1951(95)00091-7

Mondillo, N., Balassone, G., Boni, M., Chelle-Michou, C., Cretella, S., Mormone, A. (2019): Rare earth elements (REE) in Al- and Fe-(oxy)-hydroxides in bauxites of Provence and Languedoc (southern

France): Implications for the potential recovery of REEs as by-products of bauxite mining. – Minerals, 9, 504. https://doi.org/10.3929/ethz-b-000362745

Mondillo, N., Di Nuzzo, M., Kalaitzidis, S., Boni, M., Santoro, L., Balassone, G. (2022): Petrographic and geochemical features of the B3 bauxite horizon (Cenomanian–Turonian) in the Parnassos–Ghiona area: A contribution towards the genesis of the Greek karst bauxites. – Ore Geology Reviews, 143, 104759. https://doi.org/10.1016/j.oregeorev.2022.104759

Mongelli, G. (1997): Ce-anomalies in the textural components of Upper Cretaceous karst bauxites from the Apulian Carbonate Platform (southern Italy). – Chemical Geology, 140, 69–79. https://doi.org/10.1016/S0009-2541(97)00042-9

Mongelli, G., Acquafredda, P. (1999): Ferruginous concretions in a Late Cretaceous karst bauxite: Composition and conditions of formation. – Chemical Geology, 158, 315–320. https://doi.org/10.1016/S0009-2541(99)00061-3

Mongelli, G., Boni, M., Buccione, R., Sinisi, R. (2014): Geochemistry of the Apulian karst bauxites (southern Italy): Chemical fractionation and parental affinities. – Ore Geology Reviews, 63, 9–21. https://doi.org/10.1016/j.oregeorev.2014.04.012

Mongelli, G., Boni, M., Oggiano, G., Mameli, P., Sinisi, R., Buccione, R. (2017): Critical metals distribution in Tethyan karst bauxite: The Cretaceous Italian ores. – Ore Geology Reviews, 86, 526–536. https://doi.org/10.1016/j.oregeorev.2017.03.017

Moore, D.M., Reynolds, R.C. Jr. (1998): X-ray diffraction and the identification and analysis of clay minerals, 2nd ed. – Oxford University Press, New York.

Mordberg, L.E. (1999): Geochemical evolution of a Devonian diaspore–crandallite–svanbergite-bearing weathering profile in the Middle Timan, Russia. – Journal of Geochemical Exploration, 66, 353–361. https://doi.org/10.1016/S0375-6742(99)00021-7

Mordberg, L.E., Stanley, C.J., Germann, K. (2000): Rare earth element anomalies in crandallite group minerals from the Schugorsk bauxite deposit, Timan, Russia. – European Journal of Mineralogy, 12, 1229–1243. https://doi.org/10.1127/ejm/12/6/1229

Munsell Color Company (1994): Munsell Soil Color Charts; Munsell Color Company: Baltimore, MD, USA, pp. 12

Nesbitt, H.W. (1979): Mobility and fractionation of rare earth elements during weathering of a granodiorite. – Nature, 279, 206–210. https://doi.org/10.1038/279206a0

Nesbitt, H.W., Young, G.M. (1982): Early Proterozoic climates and plate motions inferred from major element chemistry of lutites. – Nature, 299, 715–717. https://doi.org/10.1038/299715a0

Onac, B.P., Ettinger, K., Kearns, J., Balasz, I.I. (2005): A modern, guano-related occurrence of foggite, CaAl(PO4)(OH)2·H2O and churchite-(Y), YPO4·2H2O in Cioclovina Cave, Romania. – Mineralogy and Petrology, 85, 291–302. https://doi.org/10.1007/s00710-005-0106-4

Peh, Z., Kovačević Galović, E. (2014): Geochemistry of Istrian Lower Palaeogene bauxites – Is it relevant to the extent of subaerial exposure during Cretaceous times? – Ore Geology Reviews, 63, 296–306. https://doi.org/10.1016/j.oregeorev.2014.05.020

Peh, Z., Kovačević Galović, E. (2016): Geochemistry of Lower Palaeogene bauxites – Unique signature of the tectonostratigraphic evolution of a part of the Croatian Karst. – Geologia Croatica, 69, 269–279. https://doi.org/10.4154/gc.2016.24

Perković, I., Martinuš, M., Cvetko Tešović, B., Vlahović, I., Matešić, D., Newton, R.J., He, T., Šoufek, M., Razum, I., Durn, G. (2024): Tracing the evolution of the world's first mined bauxite from palaeotopography to pyritization: Insights from Minjera deposits, Istria, Croatia. – Geologia Croatica, 77(2), 159–178. https://doi.org/10.4154/gc.2024.12

Radusinović, S.S. (2017): Metalogenija jurskih karstnih boksita rudnih rejona Vojnik-Maganik i Prekornica, Crna Gora. Doktorska disertacija, Univerzitet u Beogradu, Rudarsko-geološki fakultet, Beograd, 425 p.

Radusinović, S., Jelenković, R., Pačevski, A., Simić, V., Božović, D., Holclajtner-Antunović, I., Životić, D. (2017): Content and mode of occurrence of rare earth elements in the Zagrad karstic bauxite deposit (Nikšić area, Montenegro). – Ore Geology Reviews, 80, 406–428. https://doi.org/10.1016/j.oregeorev.2016.05.026

Radusinović, S., Papadopoulos, A. (2021): The potential for REE and associated critical metals in karstic bauxites and bauxite residue of Montenegro. – Minerals, 11, 975. https://doi.org/10.3390/min11090975

Reinhardt, N., Proenza, J., Villanova-de-Benavent, C., Aiglsperger, T., Bover-Arnal, T., Torró, L. (2018): Geochemistry and mineralogy of rare earth elements (REE) in bauxitic ores of the Catalan Coastal Range, NE Spain. – Minerals, 8, 562. https://doi.org/10.3390/min8120562

Retallack, G.J. (2010): Lateritization and bauxitization events. – Economic Geology, 105, 655–667. https://doi.org/10.2113/gsecongeo.105.3.655

Sakač, K., Šinkovec, B. (1991): The bauxites of the Dinarides. – Travaux ICSOBA, 21, 1–11.

Sakač, K., Šinkovec, B., Jungwirth, E., Lukšić, B. (1984): Opća obilježja geološke građe i ležišta boksita područja Imotskog. – Geološki vjesnik, 37, 153–174.

Schellmann, W. (1994): Geochemical differentiation in laterite and bauxite formation. – Catena, 21, 131–143. https://doi.org/10.1016/0341-8162(94)90007-8

Schmid, S.M., Bernoulli, D., Fügenschuh, B., Matenco, L., Schefer, S., Schuster, R., et al. (2008): The Alpine–Carpathian–Dinaridic orogenic system: Correlation and evolution of tectonic units. – Swiss Journal of Geosciences, 101, 139–183. https://doi.org/10.1007/s00015-008-1247-3

Schmid, S.M., Fügenschuh, B., Kounov, M., Matenco, L., Nievergelt, P., Oberhänsli, R., et al. (2020): Tectonic units of the Alpine collision zone between Eastern Alps and western Turkey. – Gondwana Research, 78, 308–374. https://doi.org/10.1016/j.gr.2019.07.005

Sinisi, R. (2018): Mineralogical and geochemical features of Cretaceous bauxite from San Giovanni Rotondo (Apulia, Southern Italy): A provenance tool. – Minerals, 8, 567. https://doi.org/10.3390/min8120567

StatSoft, Inc. (2006): STATISTICA (data analysis software system), version 7.1. – StatSoft, Inc., Tulsa, OK, USA.

Šinkovec, B. (1974): Jurski glinoviti boksiti zapadne Istre. – Geološki vjesnik, 27, 217–226.

Šinkovec, B., Sakač, K. (1982): The Paleogene bauxites of Dalmatia. – Travaux ICSOBA, 12, 293–331.

Šinkovec, B., Sakač, K. (1991): Bauxite deposits of Yugoslavia—The state of the art. In: Haas, J., Bárdossy, G., Mindszenty, A. (eds.): Tethyan Bauxites, IGCP-287, II. – Acta Geologica Academiae Scientiarum Hungaricae, 34, 307–315.

Šinkovec, B., Sakač, K., Durn, G. (1994): Pyritized bauxites from Minjera, Istria, Croatia. – Natura Croatica, 3(1), 41–65.

Šinkovec, B., Šušnjara, A., Sakač, K. (1985): Boksiti Korduna i susjednih područja. – Geološki vjesnik, 38, 215–233.

Španiček, J., Ćosović, V., Mrinjek, E., Vlahović, I. (2017): Early Eocene evolution of carbonate depositional environments recorded in the Čikola Canyon (North Dalmatian Foreland Basin, Croatia). – Geologia Croatica, 70, 11–25. https://doi.org/10.4154/gc.2017.05

Šušnjara, A., Sakač, K., Gabrić, A., Šinkovec, B. (1990): Boksiti područja Sinja u Srednjoj Dalmaciji. – Geološki vjesnik, 43, 169–179.

Temur, S., Kansun, G. (2006): Geology and petrography of the Masatdagi diasporic bauxites, Alanya, Antalya, Turkey. – Journal of Asian Earth Sciences, 27, 512–522. https://doi.org/10.1016/j.jseaes.2005.07.001

Tišljar, J., Vlahović, I., Velić, I., Sokač, B. (2002): Carbonate platform megafacies of the Jurassic and Cretaceous deposits of the Karst Dinarides. – Geologia Croatica, 55, 139–170. https://doi.org/10.4154/gc.2002.14

Tomašić, N., Čobić, A., Bedeković, M., Miko, S., Ilijanić, N., Gizdavec, N., Matošević, M. (2021): Rare earth elements enrichment in the Upper Eocene Tošići–Dujići bauxite deposit, Croatia, and relation to REE mineralogy, parent material and weathering pattern. – Minerals, 11, 1260. https://doi.org/10.3390/min11111260

Valeton, I. (1972): Bauxites. Developments in Soil Science, 1, Elsevier Publishing Company, Amsterdam, 226 p.

Velić, I., Vlahović, I. (2009): Tumač geološke karte Republike Hrvatske : 1:300.000. – Croatian Geological Survey, Zagreb.

Vlahović, I., Tišljar, J., Velić, I., Matičec, D. (2002): The Karst Dinarides are composed of relics of a single Mesozoic platform: Facts and consequences. – Geologia Croatica, 55, 171–183. https://doi.org/10.4154/gc.2002.15

Vlahović, I., Tišljar, J., Velić, I., Matičec, D. (2005): Evolution of the Adriatic Carbonate Platform: Palaeogeography, main events and depositional dynamics. – Palaeogeography, Palaeoclimatology, Palaeoecology, 220, 333–360. https://doi.org/10.1016/j.palaeo.2005.01.011

Wang, Q., Deng, J., Liu, X., Zhang, Q., Sun, S., Jiang, C., Zhou, F. (2010): Discovery of the REE minerals and its geological significance in the Quyang bauxite deposit, West Guangxi, China. – Journal of Asian Earth Sciences, 39, 701–712. https://doi.org/10.1016/j.jseaes.2010.05.005

Wang, X., Jiao, Y., Du, Y., Ling, W., Wu, L., Cui, T., Zhou, Q., Jin, Z., Lei, Z., Weng, S. (2013): REE mobility and Ce anomaly in bauxite deposits of northern Guizhou, China. – Journal of Geochemical Exploration, 133, 103–117. https://doi.org/10.1016/j.gexplo.2013.08.009

Ye, L., Cheng, Z.T., Pan, Z.P. (2007): The REE geochemical characteristics of the Xiaoshanba bauxite deposit, Guizhou. – Bulletin of Mineralogy, Petrology and Geochemistry, 26(3), 228–233. https://doi.org/10.1016/j.gexplo.2018.03.007

Zhang, S., Zhao, F., Liu, D., Zhao, L., Zhang, X., Lin, J., Dong, H., Zhao, S., Liu, X., Zan, M. (2022): Modes of occurrence of critical metal elements (Li, REEs, and other critical elements) in low-grade bauxite from southern Shanxi Province, China. – Minerals, 12, 990. https://doi.org/10.3390/min12080990

6. ORIGINAL SCIENTIFIC PAPERS

6.1. Geochemical records in subaerial exposure environments in Croatia using discriminant function analysis of bauxite data

By Ilijanić*, N., Kovačević Galović, E., Gizdavec, N., Ivkić Filipović, I., Miko, S.*, Peh, Z.

Published in Frontiers in Earth Science 2023, 10, 1055435.

DOI: https://doi.org/10.3389/feart.2022.1055435

This paper investigates the geochemical variability of Croatian karst bauxites across all eight bauxite-bearing horizons (BX1–BX8) of the Adriatic–Dinaric Carbonate Platform, spanning the period from the Upper Triassic to the Miocene. Using discriminant function analysis applied to major- and trace-element geochemical data, the study identifies systematic geochemical patterns related to weathering intensity, environmental conditions, and variations in the geochemical characteristics of the source material during platform evolution. The results demonstrate that bauxite geochemistry preserves a record of tectonostratigraphic and paleogeographic changes, enabling clear differentiation between individual bauxite horizons. A general shift from clay-rich compositions toward geochemical signatures indicative of increasing mafic and ultramafic affinity is recognized, while the discriminant functions highlight the importance of desilicification and ferrallitization processes in bauxite formation. The study provides the regional geochemical framework for understanding the evolution of Croatian karst bauxites and forms the basis for testing the first hypothesis of this doctoral dissertation.

frontiers | Frontiers in Earth Science

TYPE Original Research
PUBLISHED 04 January 2023
DOI 10.3389/feart.2022.1055435

Check for updates

OPEN ACCESS

EDITED BY
Francesco Perri,
University of Calabria, Italy

REVIEWED BY
George Iliopoulos,
University of Patras, Greece
Giovanni Mongelli,
University of Basilicata, Italy

*CORRESPONDENCE
Nikolina Ilijanić,
nilijanic@hgi-cgs.hr
Slobodan Miko,
smiko@hgi-cgs.hr

SPECIALTY SECTION
This article was submitted to Sedimentology, Stratigraphy and Diagenesis, a section of the journal Frontiers in Earth Science

RECEIVED 27 September 2022
ACCEPTED 05 December 2022
PUBLISHED 04 January 2023

CITATION
Ilijanić N, Kovačević Galović E, Gizdavec N, Ivkić Filipović I, Miko S and Peh Z (2023), Geochemical records in subaerial exposure environments in Croatia using discriminant function analysis of bauxite data.
Front. Earth Sci. 10:1055435.
doi: 10.3389/feart.2022.1055435

COPYRIGHT
© 2023 Ilijanić, Kovačević Galović, Gizdavec, Ivkić Filipović, Miko and Peh. This is an open-access article distributed under the terms of the Creative Commons Attribution License (CC BY). The use, distribution or reproduction in other forums is permitted, provided the original author(s) and the copyright owner(s) are credited and that the original publication in this journal is cited, in accordance with accepted academic practice. No use, distribution or reproduction is permitted which does not comply with these terms.

Geochemical records in subaerial exposure environments in Croatia using discriminant function analysis of bauxite data

Nikolina Ilijanić*, Erli Kovačević Galović, Nikola Gizdavec, Ivona Ivkić Filipović, Slobodan Miko* and Zoran Peh

Croatian Geological Survey, Zagreb, Croatia

Croatian bauxites are long known for their chemical and physical diversity arisen from their characteristic origin and emplacement within the area of the Adriatic–Dinaric carbonate platform (ADCP). They include eight horizons spanning the period between the Upper Triassic (Carnian) and the Miocene, formed on subaerially exposed platform paleoenvironments. The bauxite genesis is recorded in the bauxite geochemical composition as a unique signature of tectonostratigraphic evolution of the different parts of the Croatian Karst, including, for example, the forebulge unconformity typical for the Istrian area. In this work, an explanation of the typical patterns of bauxite formation is based on the construction of a discriminant function model (DFM) resulting from the compositional data (CoDa) analysis of bauxite geochemical data (major and trace elements). The model shows that the greatest part of the variation contained in the analyzed bauxite data (the first discriminant function, DF1) is associated with systematic alteration of geochemical composition in time, emphasizing characteristic decrease in clay component and gradual enrichment in heavy metals from oldest (Upper Triassic) to the youngest (Miocene) bauxites. In the general scheme, particular bauxite horizons represent standalone groups (Upper Triassic) while others form clusters showing increase and/or decrease of a particular set of elements signaling the changes in environmental conditions during the considered geological history of ADCP. Other discriminant functions (DF2 and DF3) also contribute to the all-inclusive distinction between the eight a priori defined bauxite groups discriminated by the characteristic set of geochemical variables where DF2 typically refers to the process of desilication, while DF3 to that of deferralitization.

KEYWORDS

bauxite geochemistry, compositional data, discriminant function model, Adriatic-Dinaric carbonate platform, Croatia

Introduction

The karst bauxites are broadly recognized as regional markers of diverse largescale events impacting the carbonate platforms in particular periods of their geological history when warm and humid climates conjoined to their tectonically controlled subaerial exposure (D'Argenio and Mindszenty, 1992; Mindszenty et al., 1995). Thus, the karst bauxites in general, and those originated in the plate-interior settings such as the Croatian Karst Dinarides in particular, assume the typical geochemical signature that may help elucidate specific issues concerning their genesis. In Croatia, however, regardless of extensive bauxite research and mining activities during more than half a century that generated copious mineralogical and chemical records, the question of bauxite genesis, especially on the subject of paleokarst and its tectonostratigraphic constraints, has been greatly unappreciated. Most probably, this disadvantageous position resulted from former predominant perceptions of bauxites as predominantly an aluminum ore, focusing all research efforts on the appraisal of aspects concerning their finding, exploitation and refinement. Sometimes, they were considered in broader perspective of local tectonics (Blašković et al., 1989), as well as paleoclimate related mineralogical and geochemical processes (e.g., Šinkovec and Sakač, 1982; 1991; Sakač and Šinkovec, 1991) but their tectonically instigated origin was brought to a focus only after the construction of new models of orogenic evolution of the Adriatic (Adriatic/Dinaric) Carbonate Platform (ADCP). The latter referred specifically to the External Dinarides of the NE Adriatic region (Vlahović et al., 2005; Korbar, 2009; Brlek et al., 2014) taking also into account new ideas of "forebulge related unconformities associated with early stages of foreland basin development" (Crampton and Allen, 1995) that emphasized the importance of manifold stratigraphic gaps appearing in the Mesozoic-Tertiary successions of the Croatian Dinarides, as well as new insights into a potential source of the parent material (Merino and Banerjee, 2008; Šušteršič et al., 2009; Banerjee and Merino, 2011). That said, the complex investigation of bauxites as "tectonic and climatic event markers at regional unconformities" (D'Argenio and Mindszenty, 1995) became indispensable in search for a new lithostratigraphic scheme, setting the foundation for the regional correlation studies over the whole platform.

The basic premises of the recent investigations of bauxites in Croatia converged on geochemical variations detected in the bauxite deposits of the Lower Paleogene age (LPB) from the Croatian karst (Kovačević Galović et al., 2012). They employed statistical tools (discriminant function analysis), with special reference to the Istrian Peninsula because of its distinct geodynamic evolution through Cretaceous to Paleogene times (Peh and Kovačević Galović, 2014) and its relations to the rest of the ADCP in light of the ergodic hypothesis (swapping spatial for temporal variability) *via* comparison between two statistical (discriminant) models (Peh and Kovačević Galović, 2016). The latest study addressed the issues of the bauxite formation during the Miocene climatic optimum, based mostly on high-precision zircon geochronology (Brlek et al., 2021). The main idea behind the present work revolves around explication of the typical patterns of bauxite formation grounded in the development of discriminant function models based on the Compositional Data (CoDa) analysis of bauxite geochemical data. This method provides solid ground for the separation of the various *a priori* defined bauxite groups deposited in the changing, subaerially exposed, ADCP paleoenvironments from the earliest (Upper Triassic) to the latest (Miocene) periods of bauxite formation in accordance with their geochemical signature. In a sense, this study is a continuation of earlier investigations performed more locally with focus on the single (K/Pg) unconformity at the same platform (Kovačević Galović et al., 2012; Peh and Kovačević Galović 2014; Peh and Kovačević Galović 2016) which have been launched with the purpose of initiating the regional correlation studies within the entire area of the Croatian Karst Dinarides. This study presents a step further, trying to elucidate the patterns of bauxite formation through time as defined by eight successive regional unconformities ranging from Triassic to Neogene times.

The whole rock geochemical data analyzed here are of compositional nature (represented in wt% and mg/kg), providing information about relative magnitudes (as proportions of the whole). Thus, their statistical treatment is necessarily focused on the log-ratio approach introduced by Aitchison, 1982; Aitchison, 1986 and disseminated by contemporary proponents of compositional data analysis (e.g., Aitchison and Egozcue, 2005; Tolosana-Delgado et al., 2005; Buccianti et al., 2006; Reimann et al., 2012; Buccianti, 2013).

Geological setting

Croatian bauxites belong to the karst type typical for the Circum-Mediterranean region. They are emplaced in the carbonate succession of the Croatian Karst (External or Outer) Dinarides, in places more than 8,000 m thick, whose deposits have a stratigraphic range from the Middle Permian (or even Upper Carboniferous) to the Eocene (Vlahović et al., 2002). Evolution of the area of Karst Dinarides started on a spacious epeiric carbonate platform along the northern Gondwana margin with the deposition of siliciclastic material in the Carboniferous, mixed clastic-carbonate sediments in the Permian and carbonate and mixed siliciclastic-carbonate deposits during the Early Triassic. Intense tectonic activity in the Middle Triassic led to the separation of the Adria Microplate characterized by a locally significant volcanoclastic input in the thick sequence of shallow-water carbonates. The Middle/Late Triassic boundary is marked mainly by a relatively long emersion phase with common bauxite occurrences, followed by the formation of the Southern Tethyan Megaplatform (Vlahović et al., 2005), a huge isolated

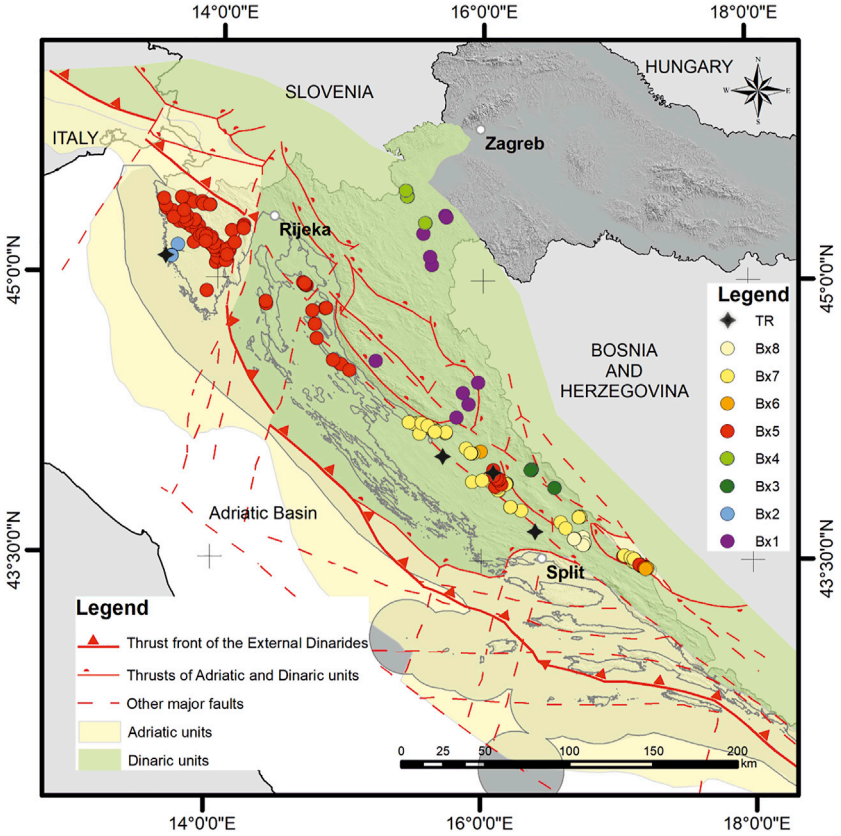

FIGURE 1
Geographical position of the study area showing locations of the sampled bauxites (BX1-BX8) and soils (TR).

intraoceanic platform represented by shallow-water carbonate deposits such as the Late Triassic Hauptdolomite and the Dachstein limestone. Segmentation of the huge platform into smaller carbonate platforms took place in the Late Lias resulting with the formation of the Adriatic Basin, with the Adriatic Carbonate Platform along its eastern side. Unresolved issues concerning the development of the Karst Dinarides at this stage of its development still remain (Vlahović et al., 2005, and references therein; Korbar, 2009, and references therein). Disagreements are exposed in different models of paleogeography and tectonostratigraphic constraints, particularly concerning Upper Cretaceous to Paleogene carbonates. The models in question assume the existence of a single (e.g., Vlahović et al., 2005), in contrast with the two carbonate platforms (e.g., Korbar, 2009) of characteristic two-domain Adriatic-Dinaric labelling (ADCP), each with different tectonostratigraphic constraints, that originated from disintegration of the Adriatic microplate (Adria) during the Upper Triassic—Lower Jurassic times and in later events at its plate boundaries (e.g., Vlahović et al., 2005; Schmid et al., 2008; Schmid et al., 2020; Korbar, 2009; Sisciani and Calamita, 2009; Márton, et al., 2010; Ustaszewski et al., 2010; Šumanovac, 2010; Márton, et al., 2011; Nocquet, 2012; Hinsbergen et al., 2014). The first ("Dinaric") includes the recent External Dinarides region, a highly deformed fold-and-thrust belt of Alpine origins created by the collision of Adria with the Austroalpine and Tisia domains while the second ("Adriatic") represents the Adriatic foreland, a more stable portion of Adria distinguished by normal faults and gentle compressional late-orogenic deformations, both studded with numerous bauxite deposits (Figure 1).

Gradual subsidence of the platform basement in the Late Jurassic and Cretaceous enabled a profuse production of predominantly shallow-marine carbonates. However, the interaction of eustatic sea-level changes and synsedimentary tectonics resulted in frequent local or regional emersions of variable duration characterized by the deposition of bauxites. In the Late Cretaceous, a gradual disintegration of the platform started as a result of collisional processes, causing differentiation of sedimentary environments and culminating with the formation of flysch basins. At the transition from the Cretaceous to the Paleogene a general emersion of variable duration took place on the ADCP and the Paleogene transgression occurred mostly during the Eocene (Vlahović et al., 2005). Renewed carbonate sedimentation in the

Palaeogene was largely controlled by intense tectonics with carbonate deposition continuing on carbonate ramps while areas of primary carbonate production were increasingly overwhelmed by clastic deposition (Vlahović et al., 2002). Lower Paleogene Liburnian formation (including the Kozina beds) and Eocene foraminiferal limestones are followed by transitional beds and flysch (Korbar, 2009). Tectonic contraction of the platform area in the Oligocene-Miocene resulted in the uplift and formation of the present Dinarides (Vlahović et al., 2002).

Bauxites

Karst bauxites in Europe, both those formed in the plate-interior settings such as bauxites in Croatia (Karst Dinarides), Italy (Southern Apennines), Hungary (Villány region) and Greece (Parnassus, Ghiona and Helicon mountains), as well as those developed in plate-margin environments including Hungarian bauxites (Transdanubian Central Range), are thoroughly discussed in numerous works (e.g., Bardossy, 1982; Mindszenty et al., 1995; Mindszenty et al., 2000; Mondillo et al., 2011; Sakač and Šinkovec, 1991; Šinkovec and Sakač, 1982; and others). More recently, the emphasis is put on geochemical and mineralogical issues concerning parental affinities, weathering processes as well as climatic and tectonostratigraphic constraints during bauxite formation either in single deposits or in regional settings focused more often on a specific bauxite-bearing horizon (e.g. Mondillo et al., 2022; Abedini et al., 2018; Abedini and Khosravi, 2020; Boni et al., 2012; Boni et al., 2013; Brlek et al., 2021; Kelemen et al., 2022; Mongelli et al., 2014; Mongelli, 2002; Peh and Kovačević Galović 2014; Peh and Kovačević Galović 2016; Putzolu et al., 2018; Sinisi, 2018; Zhao et al., 2021; and others). Lately, bauxite research has particularly focused on the potential for REE and associated critical metals (e.g. Radusinović et al., 2016; Papadopoulos et al., 2019; Radusinović and Papadopoulos, 2021; Mondillo et al., 2019; Mongelli et al., 2017; Tomašić et al., 2021; Yang et al., 2019; and others). Widely identified as regional markers of global events, bauxites occurred in distinctive periods in the geological history with warm and humid climates conjoined with tectonically controlled subaerial exposure of the carbonate platform (D'Argenio and Mindszenty, 1992; D'Argenio and Mindszenty, 1995). As a result, the karst bauxites exhibit unique geochemical signature that may help explain specific issues with regard to their genesis. Both a general consent and wide disagreement occur in the geological community, firstly regarding their polygenetic nature—inferring karstification prior to deposition and transformation of the soil-derived proto-bauxitic material (terra rossa) (Durn et al., 1999; Durn et al., 2007)—and, secondly, concerning the ultimate source of the precursor material for the incipient bauxite-type soils. Dispute about their residual or detrital origin was recently given the new impetus by virtue of the novel conception of isovolumetric interaction between the carbonate bedrock and airborne material (aeolian dust and volcanic ash), advanced by Merino and Banerjee (2008) and later expanded by Banerjee and Merino (2011). In this light the process of calcite substitution by clay prompts the origin of authigenic red claystone which subsequently undergoes pedogenesis. Combining the terra rossa as the proto-bauxitic material with processes of karst weathering occurring at its base presents the major paradigm shift in the genesis of karst bauxites. In this pattern the bauxite parent material is treated as paleosol derived from the interaction between the carbonate rock and airborne siliciclastic material—eolian and/or volcanic dust—or even terrestrial material such as loess or flysch (Durn et al., 1999; Durn 2003), as well as possible detritus from the neighboring ophiolitic complex replacing the older, residual, for new, detrital theory of bauxite origin.

Bauxites occur in various stratigraphic positions in the Croatian karst region, from the Triassic to the Miocene, with fundamental differences in chemical composition, mode of occurrence, and deposit type (Sakač and Šinkovec, 1991). According to their defined stratigraphic relationship to the basement and cover layers as well as the specific geotectonic position of a broad geographic scope, eight stratigraphic horizons of bauxite deposits were previously determined (Šinkovec and Sakač, 1991) (Figure 2) and are used in this study: 1) Upper Triassic (Carnian, BX1), 2) Upper Jurassic (Malmian, BX2), 3) Lower Cretaceous (Valanginian-Hauterivian, BX3), 4) Upper Cretaceous (Senonian, BX4), 5) Lower Paleogene (Paleocene, BX5), 6) Middle Eocene (BX6), 7) Upper Eocene (BX7), and 8) Miocene (BX8) (Figures 3A–E).

Materials and methods

Sampling, sample preparation and chemical analysis

Sampling was carefully designed to include the entire study area, comprising all investigated bauxite horizons bounded by regional unconformities, and carried out during several campaigns. A total of 219 samples (215 bauxite + 4 terra rossa samples) were collected at various sites from 8 previously determined bauxite horizons in the Croatian part of the ADCP. A single sample represents each site following the idea that bauxites from any single regional unconformity (from the Upper Triassic to the Miocene) should represent a bulk geochemical composition regardless of their particular positions within the ore body (e.g., at the contact with the related paleokarst or with its immediate cover), i.e., a composite sample. Following the results of previous investigations focused primarily on LPBs, it is tacitly accepted in the present work that multivariate analysis carried out on the bulk geochemistry of a number of cases is capable of identifying the most important geochemical processes addressing the bauxite autochthony-allochthony issues as well as those concerning vadose-phreatic depositional-diagenetic environments (D'Argenio and

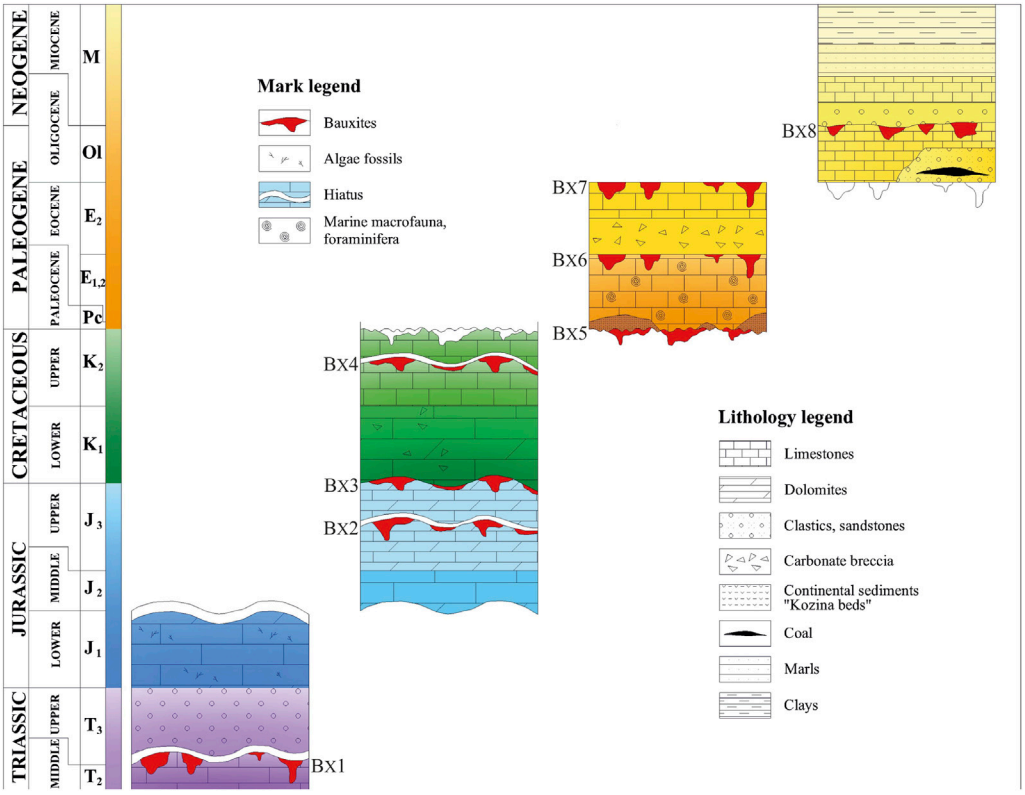

FIGURE 2
Stratigraphic position of bauxite-bearing horizons in the Croatian karst Dinarides: BX1 Upper Triassic, BX2 Upper Jurassic, BX3 Lower Cretaceous, BX4 Upper Cretaceous, BX5 Lower Paleogene (Paleocene), BX6 Middle Eocene, BX7 Upper Eocene, and BX8 Miocene.

Mindszenty, 1995; Bardossy, 1982) simply by reducing all details along the vertical profile to a few mathematical functions.

Bauxite samples weighing about 3 kg in total were crushed by hand, split into fractions by quartering, and finally ground in a tungsten carbide pestle mortar mill (Retsch Lab Equipment) and sieved to .063 mm (all work done in Croatian Geological Survey laboratories) in preparation for the analytical work. Chemical analysis was performed at the Bureau Veritas laboratory (former ACME Analytical Laboratories Ltd.) in Vancouver, Canada, applying the Lithogeochemical Whole Rock Major and Trace Element analytical method. Total abundances of the major oxides and a few minor elements were reported on a .2 g sample analyzed by ICP emission spectrometry following a Lithium metaborate/tetraborate fusion and dilute nitric digestion. Total trace elements were analyzed by ICP mass spectrometry—refractory elements went through the same decomposition as the major elements (additional .2 g sample) while the rest were digested in hot Aqua Regia and analyzed by ICP MS (.5 g sample). Analytical work was subjected to the strictest quality control in the ACME Labs, with blanks, duplicates and standard reference materials (STD SO-18) included in the CQ report, together with a certificate of analysis, as a measure of background noise, accuracy and precision. For the purpose of this work, the procedure for handling the data below the analytical detection limit (left-censored data) was accepted from Tarvainen et al. (2005) as the substitution method of assigning one-half of the detection limit value to censored data. This method is predominantly in use in geochemical and environmental studies (as per Antweiler and Taylor, 2008) developed from earlier works on analytical chemistry (e.g., Analytical Methods Committee, 1987).

Bulk mineralogy was determined by X-ray diffraction (XRD) analysis. XRD analysis was performed at the Croatian Geological Survey, on randomly oriented whole-rock powders using an X'Pert Powder X-ray diffractometer (Cu-Kα radiation, 45 kV, and 40 mA) at 2θ angles of 5°–66° and a step size of .02°. Mineral phases were identified from the XRD patterns using the ICDD PDF-4/Minerals database and the HighScorePlus software package.

Statistical analysis

Compositional data and log-ratio analysis

The bauxite data contain the set of 32-part geochemical compositions consisting of 10 major elements (represented as total

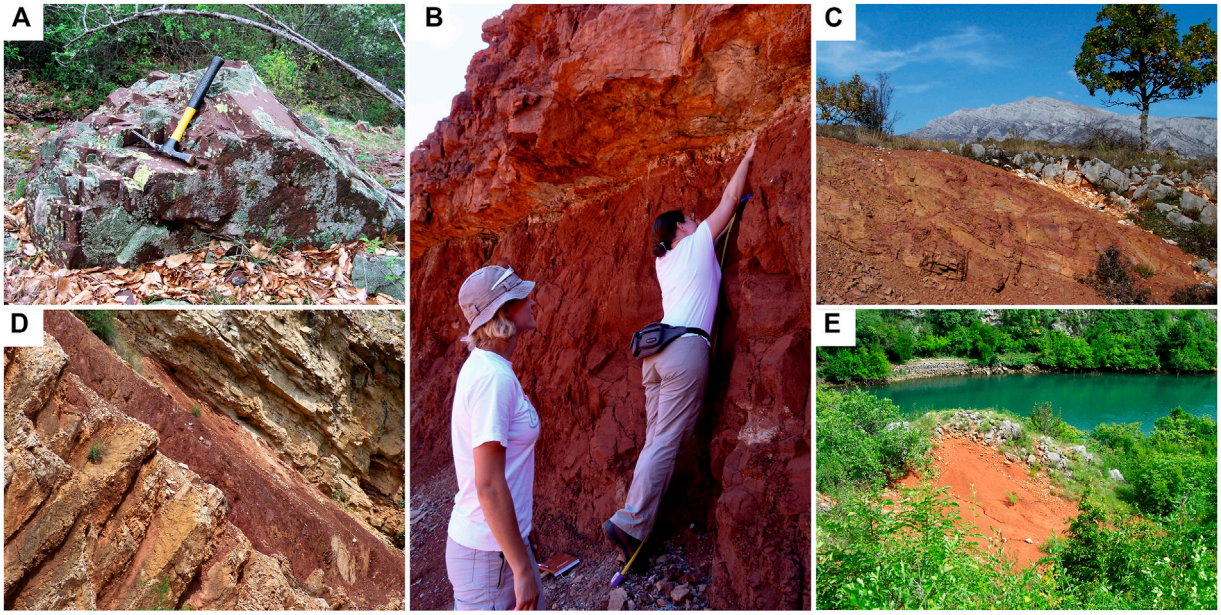

FIGURE 3
Field photographs of the typical bauxite-bearing horizons: **(A)** Upper Triassic bauxite (BX1) from Vrace deposit in the region of Lika. **(B)**. Sampling of the active Mondelako bauxite deposit near Rovinj (Istria), Upper Jurassic (Malmian) (BX2). **(C)** Outcrop of a typical small Lower Cretaceous bauxite deposit (BX3). Dinara Mt. is in the background. **(D)** Bauxite at the Upper Cretaceous (foraminiferal limestone)–Upper Eocene ("Promina beds") contact in the Northern Dalmatia (BX7). Underlying limestone beds show intense karstification. **(E)** Small outcrop of Miocene bauxite (BX8) at the bank of the Cetina River (Central Dalmatia).

abundances of major oxides) and 20 trace elements (Cr represented as Cr_2O_3) plus two rare-earth element groups summarized as light- and heavy rare earth elements (LREE = La+Ce+Pr+Nd+Sm; and HREE= Eu+Gd+Tb+Dy+Ho+Er+Tm+Yb+Lu) which were selected as predictor variables in building the original discriminant function model (DFM). The analyzed database includes 215 bauxite samples collected from bauxite deposits and occurrences over the entire Croatian part of ADCP, *a priori* separated in eight groups in accordance with their age (the age of hanging-wall rock formations). These comprise previously described horizons designated as the BX1—BX8 succession, from the lowest (Upper Triassic, BX1) to the highest (Miocene, BX8). Also, four samples of terra rossa soils (chromic luvisols) were included into the dataset as a control group (TR) keeping in mind that most karst bauxites have most probably originated by transformation of the soil-derived proto-bauxitic source material (terra rossa) as described earlier. These samples were selected as the most representative from the rich database collected during the multiyear regional geochemical survey based on the low-density topsoil sampling campaign over the karst region of Croatia (Halamić and Miko, 2009; Halamić et al., 2012; Hasan et al., 2020).

The whole rock composition of bauxite samples represents the classic example of compositional data (CoDa) in ore and environmental geochemistry. The nature of CoDa implies a mathematical property that all variables (compositions or component parts) in the analyzed sample are always positive values that must sum to a constant (unit value), usually expressed in percentages or mg/kg. As a result, all geochemical, mineralogical, and other datasets in the geoscience world are heavily plagued by the constant-sum constraint (CSC). This problem interferes with procedures of traditional statistics since individual variables are represented only as parts of some whole, or fractions of a constant sum, and cannot fluctuate independently (closed data) causing the presence of spurious correlations. Formally, CoDa cannot be represented in their raw form as points in the open, Euclidean space, where the scale is absolute, not relative. They refer to a restricted sample space known as simplex (simplicial complex) consisting of D parts or compositions (e.g., geochemical variables). Thus, a D-part composition (S^D) is really a subset of D-dimensional real space (R^D) and can be represented by the following expression (Pawlowsky-Glahn and Egozcue, 2007; Buccianti, 2013):

$$S^D = \left\{ (x_1, x_2, x_3, ..., x_D):\ x_i > 0\,(i = 1, 2, 3, ..., D), \sum_{i=1}^{D} x_i = \kappa \right\} \quad (1)$$

where κ is a constraint-sum constant, $x_1, x_2, x_3, \ldots x_D$ are components of the composition x, and 1, 2, 3, ..., D are parts of the composition x.

Simplex can "inflate" into the Euclidean vector space structure only after the proper transformation is applied to its components. From an array of transformations introduced in the literature the centered log-ratio transformation (clr) of raw (compositional) data, originally proposed by Aitchison (1986) is used in this work. The application of the centered log-ratio is deemed essential for processing CoDa in the multivariate statistical methods such as discriminant function analysis since it preserves original distances between corresponding compositions allowing them to be handled straightforwardly (Egozcue and Pawlowsky-Glahn, 2006; Tolosana-Delgado, 2012). The singularity problem inherent to a clr-transformed covariance matrix could be circumvented if MDA operates on its reduced form, which is, not relying on a full rank of covariance (Daunis-i-Estadela et al., 2011). Since clr-transformed data represent unbounded real vectors in real space, in this case Mahalanobis distances (MD) stay invariant regardless of which component may be removed from the analysis (Barceló-Vidal and Pawlowsky-Glahn, 1999). Non-essential clr-transformed variables may be amalgamated ("other") and removed from further analysis.

Clr-coefficients can be computed from the following expression:

$$clr(x) = \left(\log\frac{x_1}{g(x)}, \log\frac{x_2}{g(x)}, \log\frac{x_3}{g(x)}, \ldots, \log\frac{x_D}{g(x)}\right) \quad (2)$$

where $x_1, x_2, x_3, \ldots x_D$ represent parts (compositions), and $g(x)$ represents the geometric mean of the parts.

However, as the compositional nature of geochemical data is expressed either in wt%, or in ppm, affecting the scale, all measurements are converted into ppm before transformation by multiplying wt% by 10^4.

Discriminant function analysis—building a predictive discriminant model (DFM)

Multiple (multi-group) discrimination analysis (MDA) is one of the traditional multivariate statistical techniques, which is particularly useful in building the predictive model of a multiple-group discrimination based on the set of independent (predictor) variables. In many of its practical considerations in geosciences MDA is frequently applied when geological reasoning asks for the use of some independent criterion for separation with respect to the variables in the analyzed dataset. It is a capable tool in manipulating a great number of numeric attributes alleviating problems with organization, distinction, or comparison of the vast body of data down to the scale providing a clearer insight into the underlying geological, geochemical or environmental controls. Also, the data processed in this way can develop a mapping property capable of further elucidating the intrinsic relationship among the original variables. As a statistical method it is effective in pursuing the major sources of between-group differences such as, in this case, tracking down the differences in the whole rock composition of Croatian ADCP bauxites emplaced in diverse paleogeographical/paleotectonic settings during the Upper Triassic to Miocene times. Each bauxite horizon reflects a unique set of depositional platform dynamics making a regional marker of global events occurring at specific intervals in the stratigraphic record, a criterion autonomous with regards to the chemistry of hosted bauxite deposits. Objectives and principles of DA are described comprehensively in many statistical textbooks (e.g., Dillon and Goldstein, 1984; Davis, 1986; Rock, 1988; Reimann et al., 2008) and they were also regularly expounded by the same authors in various geochemical, environmental, sedimentological, bauxite and other studies (e.g., Peh et al., 2008; Kovačić et al., 2009; Peh and Halamić, 2010; Kovačević Galović et al., 2012; Peh and Kovačević Galović, 2014; Galović and Peh, 2016; Peh and Kovačević Galović, 2016; Grizelj et al., 2017; Šorša et al., 2018; Brunović et al., 2019; Hasan et al., 2020; Razum et al., 2020a; b, Razum et al., 2021). In this instance, MDA is envisaged to maximize the between-group variance in comparison to the variance within each group, classifying each individual sample into one of the *a priori* defined groups with minimum error rate (proportion of misclassified objects). Statistically, a hypothesis is tested that all observed groups have the same multivariate mean against the alternative that at least one multivariate mean is different (Rock, 1988). Provided that alternative hypothesis is accepted, the original suite of data is recalculated by MDA into a number of discriminant scores allocating each object or group (the latter represented by its mean) along one or more lines—linear discriminant functions. In this way the multivariate problem is reduced into a fewer-dimension solution, one less than the number of groups (K-1), or equal to the number of variables (p), whichever is smaller.

Consequently, the scope of this study revolves around building a predictive discriminant function model (DFM) with maximum classification efficiency which is based on eight *a priori* defined groups of ADCP bauxites (BX1—BX8) + one soil group (TR) and 32 log-ratio transformed CoDa geochemical variables (whole rock chemical analysis). For that purpose, a discriminant analysis from the statistical software package of STATISTICA, Release 7.1 (StatSoft, Inc., 2006) was used in order to achieve the best separation between the groups and explain the possible geological causes for the structure of input data by a single discriminant model. In the final analysis, this procedure implies the most effective transfer of mathematical (structure) model into a functional (geochemical) one, explaining post-hoc the analyzed dataset that is organized beforehand upon predictions.

Results

Weathering intensity in relation to mineralogical and geochemical characteristics

Mineralogical analysis based on XRD data revealed that the main oxy-hydroxides recorded in the most of the analyzed karst

TABLE 1 Mineralogical composition of characteristic bauxite samples from each analyzed karst bauxite group.

Group	Age	Sample	Locality	Major minerals	Minor minerals
BX1	Upper Triassic	LI-5	Baške Oštarije (Lika)	Kaolinite	Böhmite, hematite, anatase
BX2	Upper Jurassic	ISTJ-1	Bralić (Istra)	Böhmite	Kaolinite, hematite, goethite, anatase
BX3	Lower Cretaceous	VRDK-1	Vrlika (N Dalmatia)	Böhmite	Kaolinite, hematite, goethite, anatase
BX4	Upper Cretaceous	KOR-3	Kordun (Banovina)	Böhmite	Goethite, anatase
BX5	Paleocene/Lower Eocene	IPC-53	Motovun (Istra)	Böhmite	Gibbsite, hematite, goethite, kaolinite, anatase
BX6	Middle Eocene	COS 2–1	Ćosići (Imotski)	Gibbsite	Hematite, goethite, böhmite, kaolinite, anatase
BX7	Upper Eocene	MB-4	Mamutovo brdo (Imotski)	Gibbsite, böhmite	Hematite, goethite, anatase, kaolinite
BX8	Miocene	SNG-7	Sinj (C Dalmatia)	Gibbsite, kaolinite	Anatase, 2:1 clay minerals

bauxite samples are böhmite and/or gibbsite, hematite, goethite and anatase (Table 1). Böhmite is the major mineral phase mainly in the samples from the oldest horizons (BX2-BX5), whereas gibbsite occur in younger bauxite horizons (BX5-BX8), sometimes associated with böhmite. In some bauxite samples calcite and/or quartz occur. The ubiquitous clay mineral is kaolinite, which occurs dominantly in the Upper Triassic (BX1) and Miocene (BX8) horizons. Additionally, some of the Upper Jurassic (BX2) and Miocene (BX8) bauxites contain other clay minerals belonging to the 2:1 clay minerals group, which were not analyzed in detail. In the samples from the youngest Miocene bauxite horizons (BX8), the böhmite mineral phase is absent or is present in small amounts. It was also determined in the study of Miocene bauxite deposit of Crveni Klanac in Dalmatia. Additionally, the Authors gave evidence of the 2:1 clay minerals presence in this bauxite ore of Miocene age (Brlek et al., 2021).

Whole-rock chemical analyses gather information on the concentrations of major (wt%), minor and trace elements (mg/kg) in bauxites and soils. As expected, Al_2O_3 and Fe_2O_3 contents are high in all bauxite samples (on average 47.06% and 22.32%, respectively), while SiO_2 and TiO_2 have average values of 7.51% and 2.56%, respectively. The higher CaO concentrations in several bauxite samples from Lower Paleogene (BX5), Upper Eocene (BX7) and Miocene (BX8) correspond to the samples in which the calcite is observed. The highest Al_2O_3 concentrations are evident in Upper Cretaceous bauxites (BX4) (67.57–70.58%), while for most of the horizons it ranges between ~30% and 60% (Upper Triassic–BX1, Upper Jurassic–BX2, Lower Cretaceous–BX3, Middle and Upper Eocene–BX6 and BX7). The bauxites from the Miocene–BX8 show the lowest values (22.57–39.73%), while the Lower Paleogene bauxites–BX5 have the highest oscillation between a minimum value of 4.52% and a maximum of 58.58%. Terra rossa/red soil samples, which are marked as group TR, show the lowest detected Al_2O_3 values between 14.07% and 19.02%. In contrast, their concentrations of SiO_2 are the highest, between 45.64% and 60.09%. Among bauxite horizons, the samples from Miocene bauxites–BX8 have the highest content of SiO_2 (from 20.46% to 29.92%). Considerably high values of SiO_2 are evident in bauxites from Upper Triassic–BX1 (18.42–41.33%), Upper Jurassic–BX2 (14.04–22.69%) and Lower Cretaceous–BX3 (7.03–36.92%), while the Lower Paleogene–BX5, Middle and Upper Eocene–BX6 and BX7 bauxites oscillate between the minimum and maximum values of .91–36.91% (BX5), .37–17.46% and .51–17.48% (BX7), respectively. The lowest contents of SiO_2 are detected in the Upper Cretaceous bauxites–BX4 (1.61–3.75%). The ternary diagram Al_2O_3-Fe_2O_3-SiO_2 (Figure 4, after Aleva, 1994) classified the analyzed bauxites as ferritic, especially the bauxite horizons of Lower Paleogene (BX5), Middle and Upper Eocene (BX6 and BX7). The Upper Cretaceous bauxites (BX4) are distinguished from the rest of the bauxite samples, as the ones with the highest Al_2O_3 and lowest Fe_2O_3 content. The terra rossa/red soils are characterized by the similar lower content of iron, with similar values of Fe_2O_3 as the Upper Cretaceous bauxites. The Upper Jurassic (BX2) and Lower Cretaceous (BX3), as well as part of the Upper Eocene (BX7), Miocene (BX8) and Upper Triassic (BX1) bauxites moved towards SiO_2 and kaolinite angle, implying moderate lateritization, but still belonging to bauxites and laterites, in contrast to kaolinite and bauxitic kaolinite classification of terra rossa/red soils (TR), which underwent weak lateritization. The chemical index of alteration (CIA; $[Al_2O_3/Al_2O_3+CaO+Na_2O+K_2O] \times 100$) values of all bauxite samples range between 90.83 and 99.90, with the lowest values in bauxite samples with increased CaO content that are detected in several bauxite samples from Upper Jurassic (BX2) and Upper Eocene (BX7) horizons. In general, CIA values show low variability for all bauxite horizons (>90) and indicate a significant chemical weathering during bauxitization (Nesbitt and Young, 1982). Terra rossa/red soil samples (TR) have values between 75.16 and 86.89, which reflects a lower degree of weathering where only kaolinitization occurred without the formation of bauxite mineral gibbsite.

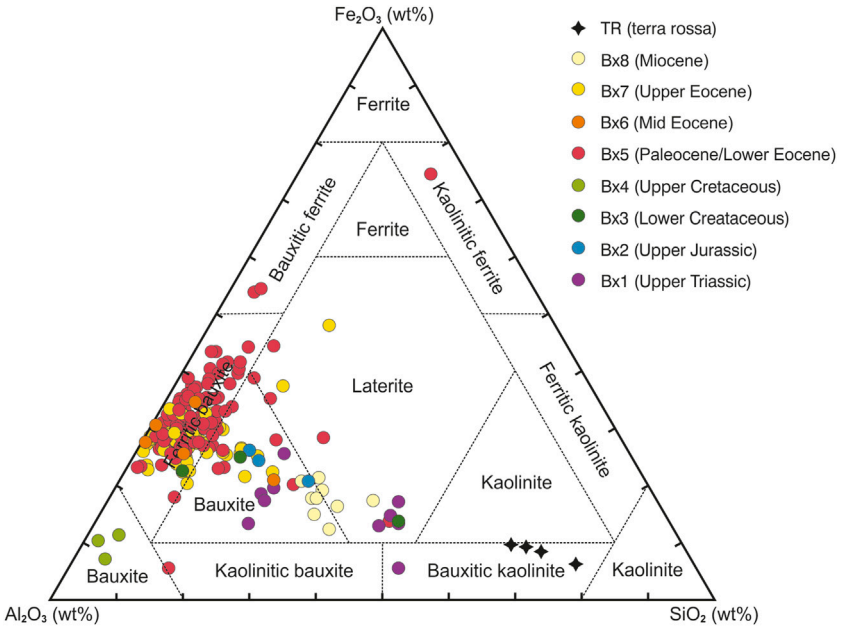

FIGURE 4
Ternary diagram Al_2O_3-Fe_2O_3-SiO_2, showing the mineralogical classification of all analyzed bauxite samples and the soil group (TR) (after Aleva, 1994).

Discrimination of bauxite horizons

Descriptive statistics for the whole data set prior to data transformation and subsequent multivariate statistical procedure is summarized in Figure 5 containing the categorized box-and-whisker plots (boxplots by group) that represent univariate statistics of geochemical data (descriptor variables—Min-Max; Median; 1st and 3rd Quartile) for each bauxite horizon. Additionally, results of the MDA are briefly recapitulated in Table 2 containing: a) the multivariate test for the overall significance of discrimination and; b) the tests of residual roots (discriminant functions). The Wilks'λ statistical test, employed routinely in the analysis, shows the vanishingly low probability (p<.000) confirming that all bauxite groups have the same multivariate mean—a precondition required to safely proceed with computing discriminant functions (DFs). Since the number of groups in the studied case amounts to nine (including the group of four topsoil samples) (K=9) the between-group variation is completely explained by the eight discriminant functions (K–1). However, despite the high statistical significance of the variation between the observed groups (p-level in Table 2), only a smaller number of DFs is used in further analysis to explain the natural between-group variation. In fact, statistical significance is often of little use if the geological explanation, supported by the high '*a posteriori*' classification rates, given in the initial assignments, is not readily available (Rock, 1988). Accordingly, labeling discriminant functions in terms of processes is an essential part of the analysis because it provides the geologically meaningful interpretation of the entire discrimination scheme. This procedure allows the underlying mathematical structure of the analyzed geochemical observations to be disclosed to the investigator. Discriminant loadings (simple correlations of variables with respective DFs) are particularly useful in clarifying individual contribution of each descriptor variable (chemical element) to the overall discrimination, highlighting the geologic processes thought to be fundamentally responsible for the pattern of the functional, that is, a mathematically expressed geologic model. When constructing the optimal discriminating design, a number of variables with small discriminant loadings can be discarded from the model. To this purpose the variable diagrams (Figure 6A) provide the quickest and most informative insight into the structure of the discriminant space suggesting which variables (descriptors) would be retained to explain the meaning of the discriminant functions, as well as which subset of variables most clearly separates the previously defined groups. Further, the association among descriptor variables and related groups can be best displayed geometrically, considering DFs as axes in the reduced discriminant space. However, in this work the clr-transformed variable and groups are displayed on scatterplots instead of bi-plots as their multivariate analogs because the origin of the bi-plot can no longer correspond to the geometric mean of the dataset after omitting the amalgamated variable ("other") in

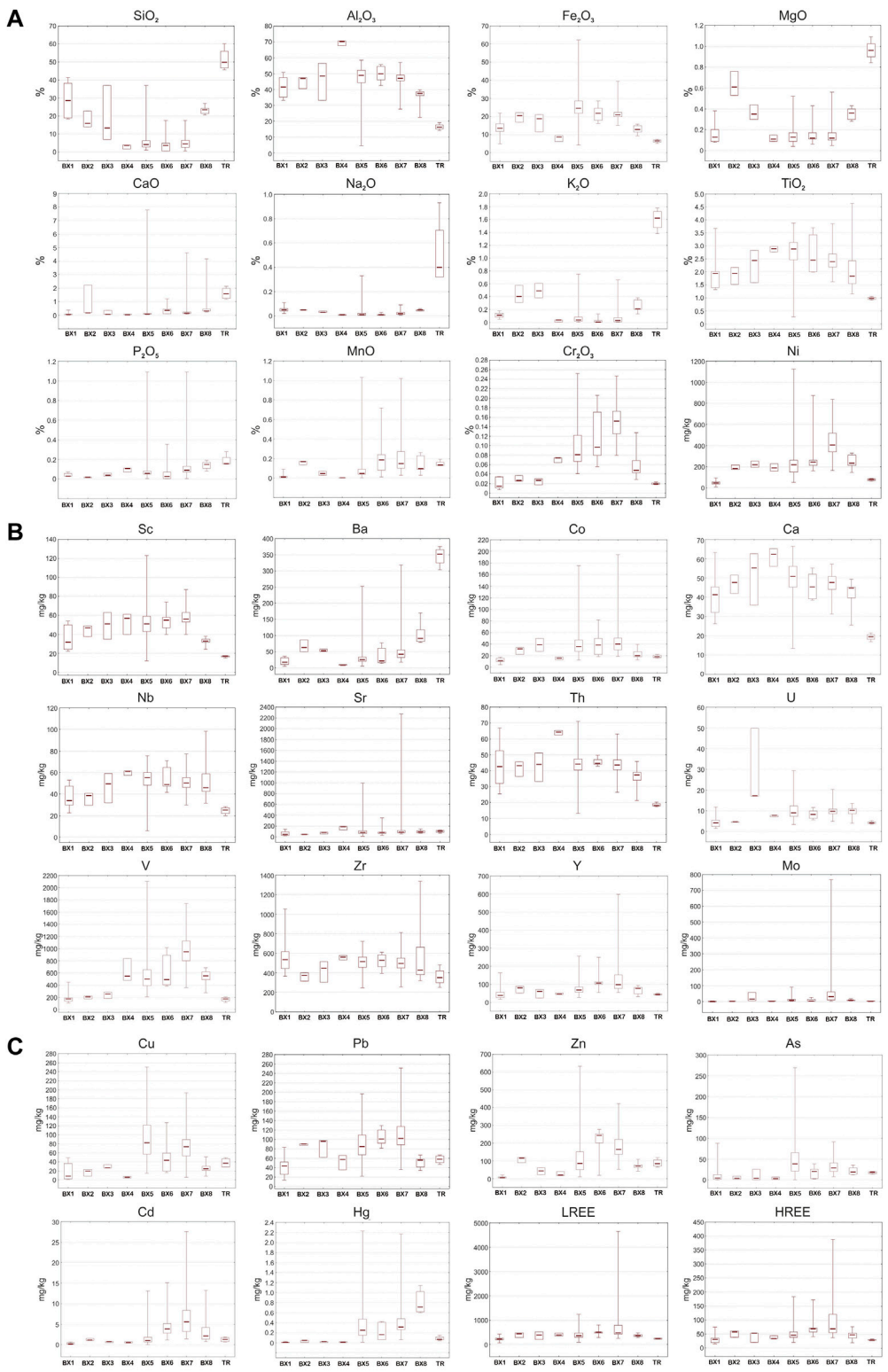

FIGURE 5
Box-and-whisker plots by groups, which represent univariate statistics of geochemical data (descriptor variables—min-max; median; and first and third quartile values) for each karst bauxite horizon (BX1-BX8) and soils (TR): **(A)** The abundances of major elements (expressed in %) and Ni (expressed in mg/kg). **(B)** The abundances of trace elements (expressed in mg/kg): Sc, Ba, Co, Ga, Nb, Sr, Th, U, V, Zr, V, Mo. **(C)** The abundances of trace elements (expressed in mg/kg): Cu, Pb, Zn, As, Cd, Hg, and LREE and HREE.

TABLE 2 Multivariate test for overall significance of discrimination (a) and tests of residual roots (b).

a)	
No. Of variables	32
Wilks' lambda	.0005
Approximate F ratio	9.052
Degrees of freedom	[256; 1,409]
p-level	$p < .000$

b)

DF	Eigen value	Eigen (%)	Eigen cum	Canon. R	Wilks' λ	Chi^2	df	p-level
1	8.504	45.37	45.37	.946	.001	1493.9	256	.000
2	4.763	25.41	70.78	.909	.005	1049.2	217	.000
3	1.909	10.18	80.96	.810	.028	703.3	180	.000
4	1.625	8.67	89.63	.787	.083	492.4	145	.000
5	.759	4.05	93.68	.657	.217	301.8	112	.000
6	.633	3.38	97.06	.622	.382	190.2	81	.000
7	.425	2.27	99.33	.546	.623	93.4	52	.000
8	.126	.67	100.00	.335	.888	23.5	25	.547

order to compensate for matrix ill-conditioning. The scatterplot of variable loadings (Figure 6A) represents discriminant axes as normalized vectors, while the scatterplot of individual objects (Figure 6B) defines the same as discriminant score vectors. Affiliation between variables and groups is examined using their corresponding position along the relevant axis which is vital for overall separation of groups and subsequent transfiguration of functional (structural) into a process model. Each DF contributes to a single geologic process responsible for the separation while the variables participate in this structure-process conversion as the building blocks assuming the role of process descriptors. In bipolar instances, though, where variables are united in negative relationship caution is required in the model assessment since the interpretation of variable-group interplay may not always be straightforward.

Discussion

Bauxites as provenance, climate and tectonics indicators

Labelling discriminant space (defined by K-1 DFs) is of paramount importance in MDA since it opens the way to recognition of the unseen relationships between the grouped data. Thus, the natural processes can be deduced, underlying the mathematical structure of geochemical observations. In this case, the first three discriminant functions (DF1-DF3) deserve the closer inspection since, collectively, they account for more than 80% of the total between-group difference in the computed model (Table 2). As seen from the scatterplot of variable loadings (Figure 6A), all considered DFs are bipolar owing to their key variables mutually polarized on respective diagrams, although the importance of some groups is not equally emphasized (Figure 6B). In the case of DF1 explaining almost half of the total variability (over 45%), it can be readily interpreted as an image of the inverse relationship between the suite of elements representing the building blocks of clay minerals—major elements SiO_2, Al_2O_3, MgO, K_2O, Na_2O, followed by Fe_2O_3, TiO_2, Zr, Th, Sc and others—against another suite of elements represented by trace elements, heavy metals in particular, including Cr_2O_3, Ni, Zn, Mo, Hg and others. Inspection into the scatterplots (Figures 6A, B) reveals a characteristic transition from former to the latter suite directly related to the ADCP environmental changes from the Late Triassic to the Miocene times. This pattern is in sharp contradistinction to earlier investigations focused only on Lower Paleogene bauxites (Kovačević Galović et al., 2012; Peh and Kovačević Galović, 2014; Peh and Kovačević Galović, 2016), where major elements did not contribute appreciably in the model configuration. It was suggested that within a particular bauxite-formation period observed *per se*, such as the Early

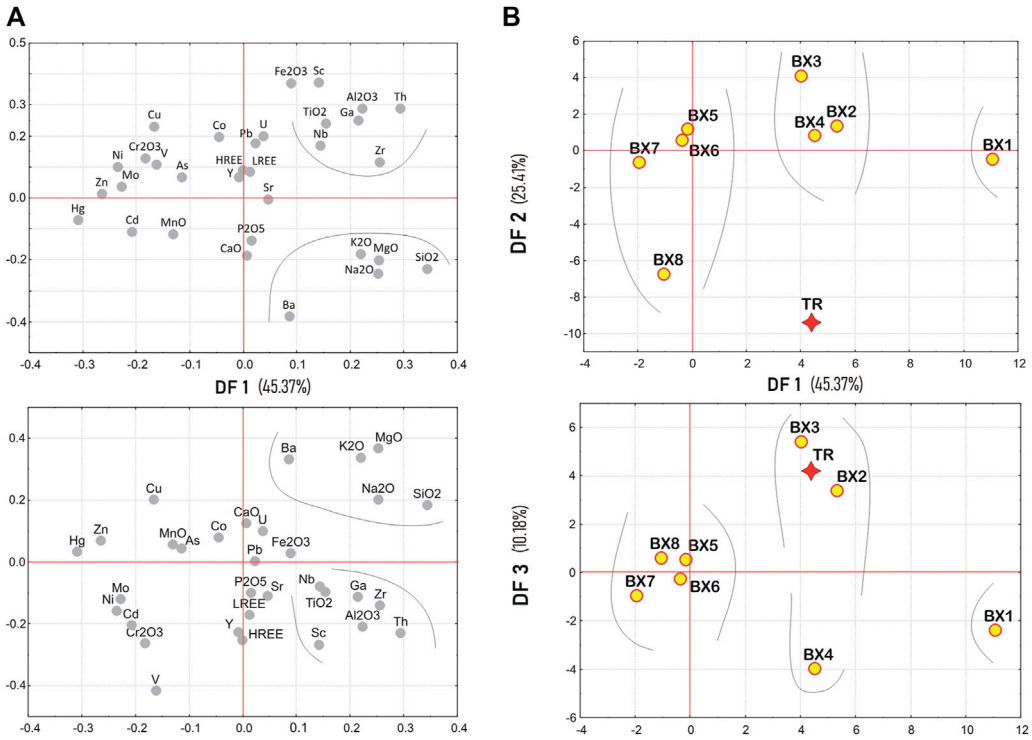

FIGURE 6
Comparison between variables and groups in the discriminant function model (DFM) of the clr-transformed data: scatterplots of **(A)** variable loadings and **(B)** bauxite groups in the reduced discriminant space of the first three discriminant functions (DF1–DF2 and DF1-DF3).

Paleogene, major elements performed a key role in all processes operating during sedimentary cycle (from weathering to burial to diagenesis) while minor and trace elements typically indicated a particular section of a cycle. Here, a temporal axis is involved into the tectonostratigraphic scheme indicating changing paleogeography and depositional dynamics on the evolving ADCP through the Upper Triassic—Miocene times. It is obvious from the variable-group scatterplots (Figures 6A, B) that bauxite groups make distinct clusters of which the Upper Triassic bauxites (BX1) forms a standalone unit characterized by an excessive amount of basic clay-mineral components, SiO_2 in particular. The cluster in the middle, encompassing Jurassic to Upper Cretaceous groups (BX2—BX4), shows the transition from "extreme" to "normal" bauxite geochemical composition represented by elements clustering around the central axis (CaO, P_2O_5, Y, LREE, HREE), as well as those slightly deviating in both directions (Sr, Pb, U, Co and others) thus signifying the "average" geochemistry of ADCP bauxites. The latter is characteristic of the youngest bauxite groups (BX5—BX8) formed from the Early Paleogene to the Miocene. In process terms, it may be assumed that DF1, along the BX1→BX8 time arrow, confronts the products of strong weathering precipitated in vadose (well-oxygenated) environments (BX1) with the bulk of trace elements present only in small quantities with respect to younger bauxite horizons (set on the opposite pole of the variable diagram) (Figure 5; Figure 6A). To this may be added that Nb, Zr, and Ga in particular, straightforwardly indicate hydrous conditions where bases were effectively leached in primary (proto) bauxite material (from right to left pole of DF1, Figure 6A). Otherwise said, durability of hiatuses, input of different material (detrital or residual) and changing environmental conditions (e.g., discontinued leaching as a result of changing climate or drainage conditions) (Kovačević Galović et al., 2012) together with later burial and diagenetic processes may have affected different bauxite horizons geochemically exactly as observed in the computed model—through the process of leaching being increasingly less effective in time (BX1→BX8). Another implication arising, following from DF1 structure is the inference of the precursor rock types as the bauxite parent material. A sharply polarized relationship between the two abovementioned sets of elements loaded on DF1 speaks strongly in favor of changing provenance of the source material, shifting steadily from felsic to mafic/ultramafic from the Upper Triassic to Miocene times. Also, potential precursor rock types can be easily deduced from the ternary diagram contrasting the Cr, Zr and Ga concentration values (compositions) of all bauxite groups (Figure 7) (Özlü, 1983). Chromium is typically enriched in ultramafic and mafic rocks and its elevated values in bauxites

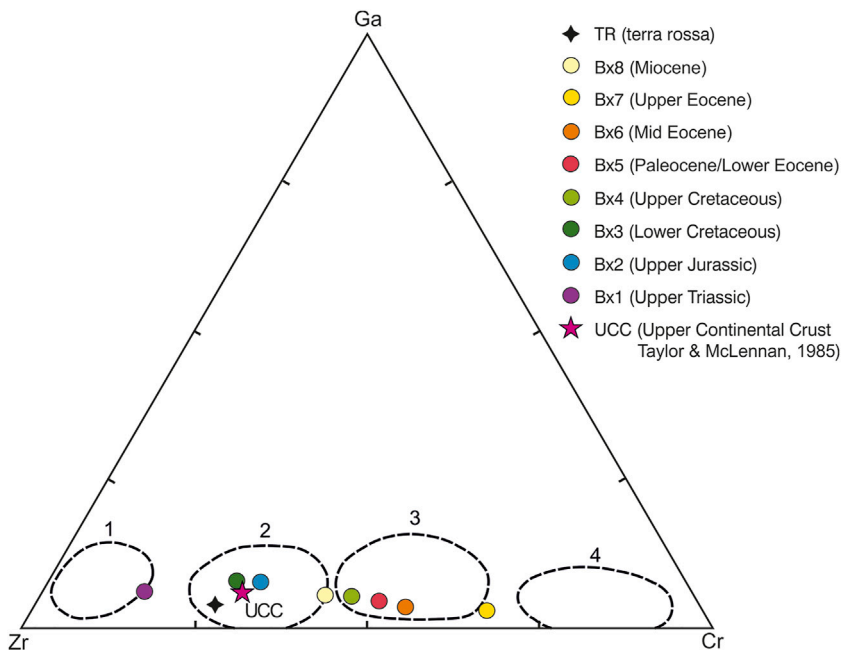

FIGURE 7
Ternary diagram for Zr, Cr and Ga concentrations in the samples of the eight investigated groups of bauxites in Croatia (BX1-BX8), including the soil group (TR), represented by their median (compositional) values; the numbered circles represent the area of influence of felsic (1), intermediate (2), mafic (3) and ultramafic (4) rocks indicated as probable parent material in genesis of the Mediterranean karst bauxites (after Özlü, 1983); UCC = average Zr-Cr-Ga content in the upper continental crust (modified after Taylor & McLennan, 1985).

suggest ophiolitic complexes containing ultramafics and related rocks as a parent material (DeVos et al., 2006). Together with other trace elements, such as Ga and Zr in particular (indicative, though, for felsic and intermediate rocks), which are considered immobile during weathering and hydrothermal alteration processes (MacLean and Barret, 1993), the ratios that Cr forms in bauxites do not differ greatly from those in parent rocks (Valeton et al., 1987) and therefore can be applied in bivariate or ternary diagrams for the determination of the parent rocks. Thus, the ternary diagram of Zr-Cr-Ga concentrations of Croatian ADCP karst bauxites (Figure 7) indicate that Upper Triassic (BX1) bauxite parent material could be traced to felsic or intermediate rocks, while Upper Jurassic (BX2) and Lower Cretaceous (BX3) bauxites that closely conform to average upper continental crust (UCC) are probably derived from intermediate rocks. Parent material for the Upper Cretaceous (BX4), Lower Paleogene (BX5), and Middle Eocene (BX6) were possibly mafic rocks, while Upper Eocene (BX7) bauxites show a shifting towards ultramafic values for chromium. Exception is, however, the youngest, Miocene bauxite (BX8), being placed on the verge of the intermediate rock cluster (Figure 7), indicating a provenance signature more typical for intermediate rocks. Note also that the oldest, Upper Triassic bauxites indicate an affinity of the precursor material with felsic (estimated from both weighted averages of surface samples and studies of shales and loess, as per Rudnick and Gao, 2013), rather than mafic rocks in the incipient stages of the ADCP development. Thus, the ternary diagram stands in support of the provenance issues indicated by the presence of still other "conservative" elements such as Nb and Th in the original MDA model attending SiO_2–Al_2O_3–Fe_2O_3 elemental cluster (Figure 6A).

Soils (terra rossa), included in the analysis as a control group (TR) due to the widely accepted idea that they represent detritally- or residually-derived proto-bauxitic material subsequently transformed, are clearly separated from other bauxite groups. Their proper nature, however, is decidedly explained only after the examination of DF2.

Most of the residual variation left after eliminating DF1 from further analysis is carried by the second discriminant function DF2 (over 25%) whose distinct property is separation of BX8 and TR groups from the rest, especially BX3, implying that Miocene bauxites are most different geochemically from all other bauxite groups, notably the Lower Cretaceous ones. The particularity of DF2 is that it highlights the TR group (the red soils) as the supposed proto-bauxite material formed in the incipient stage of subaerial exposure and interaction between karstified carbonate bedrock and airborne material (aeolian dust or volcanic ash) (Merino and Banerjee, 2008; Šušteršič et al., 2009; Banerjee and Merino, 2011), in a sheer contradistinction

TABLE 3 Classification matrix.

Groups	BX1	BX2	BX3	BX4	BX5	BX6	BX7	BX8	TR	% correct
BX1	10	0	0	0	0	0	0	0	0	100.00
BX2	0	3	0	0	0	0	0	0	0	100.00
BX3	0	0	3	0	0	0	0	0	0	100.00
BX4	0	0	0	3	0	0	0	0	0	100.00
BX5	0	0	0	0	101	1	7	0	0	92.66
BX6	0	0	0	0	1	3	1	0	0	60.00
BX7	0	0	0	0	1	1	71	0	0	97.26
BX8	0	0	0	0	0	0	0	9	0	100.00
TR	0	0	0	0	0	0	0	0	4	100.00
Total	10	3	3	3	103	5	79	9	4	94.52

Rows: Observed classifications (samples lost to other groups).
Columns: Predicted classifications (samples obtained from other groups).

TABLE 4 Squared Mahalanobis distances (SMD) between the bauxite groups (BX1—BX8) and soil (TR).

	BX1	BX2	BX3	BX4	BX5	BX6	BX7	BX8	TR
BX1	.00	107.30	193.58	125.27	139.04	148.56	174.84	205.49	187.01
BX2	107.30	.00	76.90	124.17	74.61	69.01	101.24	156.29	166.10
BX3	193.58	76.90	.00	149.63	112.31	121.91	142.58	221.12	262.47
BX4	125.27	124.17	149.63	.00	102.43	97.82	106.91	169.44	234.10
BX5	139.04	74.62	112.31	102.43	.00	11.52	11.65	72.11	160.14
BX6	148.56	69.01	121.91	97.82	11.52	.00	13.18	71.86	167.67
BX7	174.84	101.24	142.58	106.91	11.65	13.18	.00	53.21	156.85
BX8	205.49	156.29	221.12	169.44	72.11	71.66	53.27	.00	94.27
TR	187.01	166.10	262.47	234.10	160.14	167.67	156.85	94.27	.00

to all bauxite groups except BX8 (Miocene). This contrast is based on the strong presence of alkali and alkaline earth elements as building blocks of clay minerals—SiO_2, K_2O, Na_2O and MgO in modern terra rossa soils still intact by the process of bauxitization. Here, Ba is highlighted owing to its sorption behavior on clay minerals, probably a characteristic of regional soils in the Dinaric region, mostly soils derived from siliciclastic material and developed in mountainous/sub-mountainous areas (Halamić and Miko, 2009; Halamić et al., 2012; Hasan et al., 2020). In this sense the Miocene bauxites (BX8), as the latest products of bauxitization in the Croatian karst Dinarides, depart only slightly geochemically from modern soils. On the other side of the scale are all the other groups characterized by a higher content of alumina and associated elements (Fe_2O_3, TiO_2, Sc, Th, Ga . . .), while being more or less depleted in clay components prevalent in BX8 and TR groups. In process terms, DF2 can be easily described as the function of ferralitization, or, more typically desilication which includes removal of silica from primary silicates and even from quartz, and leaving the protobauxite material enriched with accumulated (hydr) oxides of Fe and Al (van Breemen and Buurman, 1988), involving also the noticeable depletion of basic cations. Mark, however, that positive values of discriminant coefficients (canonical means) keep all bauxite groups except BX8 close to the zero line implicating the "unfinished" process of chemical weathering during short, punctuated episodes of subaerial exposure.

Above said, it is exactly DF3, explaining the residual 10% of total variance (Table 2), that underscores a more complete loss of alkali and alkaline earth cations and SiO_2 by desilication, during intense weathering and subsequent

transformation of protobauxite material. As an inverse image of DF2, it highlights the Upper Cretaceous bauxites (BX4) as aluminum-rich bauxite with over 70% of Al_2O_3 (Figure 5), together with increased quantities of Th, Sc, Cr_2O_3, V, as well as Y and HREE, LREE. Similarly to DF2, DF3 can be interpreted as an indicator of extensive leaching of silica under extreme weathering conditions in hot and wet climate, analogous to those observed in the modern tropics and sub-tropics. However, it also involves the process of deferralitization since, unlike DF2, Fe2O3 is not the part of the Al_2O_3–Fe_2O_3–TiO_2–Th– . . . cluster, setting close to the zero line without any discriminatory potential (Figure 6). This process occurs in acidolytic environments, due to organic accumulation in weathering profiles in well-drained areas in a cool and humid climates, where all cations tend to be removed from the minerals (Chamley, 1989). Reducing conditions cause the dissolution of Fe oxides and Fe depletion in such environments (Do Nascimento et al., 2008). As the process of deferralitization in modern soils usually occurs through the production of soluble organic or inorganic complexes in extremely humid and well drained regions of the world, it may be assumed as the potential mechanism of iron leaching from protobauxites during weathering (e.g., Thiffault, 2019). Though kaolinite and bauxite deposits are considered to have been formed under humid tropical and subtropical conditions, kaolinite can form in cool temperate climates under moderate rainfall. For appreciable thickness to form, long periods of leaching are required. Less time is required in warmer regions, which is probably why the larger kaolin and bauxite deposits are restricted to the warmer climates. Additionally, it is necessary to have a relatively smooth terrain and quiet tectonic conditions so that chemical weathering can be more effective than erosion (Weaver, 1989), which corresponds to long-lasting emersion during the Upper Cretaceous, with a low-developed karst paleorelief where small Upper Cretaceous bauxite deposits occur in the Croatian part AdCP. DF3 discriminates the Upper Cretaceous (Senonian) as the only time period (epoch) having experienced the optimum bauxitiferous conditions in the Croatian part of ADCP, albeit resulting with small and rare deposits (Šinkovec et al., 1985).

Classification issues

Concerning the integrity of investigated groups, it is once again the classification efficiency that demonstrated its usefulness in the process of discrimination. In this regard, classification rates of *a priori* defined bauxite groups can be readily inspected by comparing the mathematically "predicted" (computed) and original ("natural") group membership of individual samples. Table 3 reveals that the discriminant model is organized with an extremely high efficiency of almost 95%. Setting aside Upper Triassic bauxites (BX1) that are literally "miles away" geochemically from any of the remaining bauxite groups, a fact obvious from the very high values of squared Mahalanobis distance (SMD) ranging from 107.30 for Jurassic (BX2) up to 205.49 for Miocene bauxites (Table 4), there is a great affinity between the three Paleogene groups—BX5, BX6 and BX7. Their SMD values range between 11.65 and 13.18 revealing similar climatic and tectonostratigraphic constrains during the punctuated episodes of Paleogene subaerial exposure over the entire Croatian part of ADCP. Three groups form a characteristic cluster mentioned before, and there is only a slight mingling of their members that may call for closer inspection into the age of hanging-wall formations, especially in the case of the Middle Eocene group (BX6). All other groups are correctly classified (100%) with notable distances among the groups forming the Jurassic-Cretaceous cluster ranging in SMD from minimally 76.90 (BX2/BX3) to maximum of 149.63 (BX3/BX4). As expected, the soils (TR) are the most distant of all bauxite groups representing an entity *per se*. Unsurprisingly, however, some affinity with Miocene bauxites (BX8), as indicated by DF3 (Figures 6A, B), is strongly validated by SMD values standing halfway to all other groups (BX1-BX7) (Table 4), mostly due to the high contents of silica and base cations ineffectively leached during bauxitization (Table 1).

Conclusion

In this study, a discriminant function model was built with the aim of distinguishing geochemically between the eight bauxite horizons ranging from the Upper Triassic to the Miocene and sampled from the various corners of the Croatian part of ADCP. Having derived their origin from various regional unconformities bauxites were supposed to have experienced different formation settings as regards both regional (volcanism and tectonics), and global (eustasy and climate), controls during the periods of subaerial exposure of the platform. From this perspective, their emplacement on carbonate platforms such as ADCP represents a rich data repository of valuable information on predicting depositional and diagenetic facies during geological history. Leaving aside possible rearrangements of control factors that may have generated variations as regards some specific bauxite horizon (horizontal, or within-period, causality) most notably articulated in flexural uplift and progressive formation of the forebulge unconformity in Istria during Lower Paleogene times, the focus of this research was given to changes in time (vertical causality) presumed to be of major importance in setting down the bauxite geochemical signature. Accordingly, although investigations presented in this work are targeted locally in spatial sense (Croatian part ADCP) results of MDA are pursued over the considerable timespan, that is, if oxymoron is apt in this case, non-locally in time, which may touch upon a sort of uniqueness in the bauxite studies. The results can be briefly summarized as follows:

1) Almost complete separation between the eight groups (horizons) of Croatian karst bauxites from various parts of ADCP (Inner

and Outer Karst) is accomplished by applying MDA on the set of 32-part geochemical compositions. Typically, only the Paleogene cluster (BX5–BX6–BX7) exhibits certain inconsistencies identified in mutual replacement of their members, notably between the Lower Paleogene and Upper Eocene groups. These, however, may well be elicited by the geochemical affinity between the groups in cases where the hanging wall sediments have been removed and relative age-dating by geological mapping was only inferential. Emplacement of older (BX1–BX4) and younger (BX8) bauxite horizons on ADCP left their geochemical imprint entirely individualized during the platform depositional history, most probably due to characteristic tectonostratigraphic controls predominant at each particular regional unconformity.

2) Three discriminant functions comprising over 80% of total variability are interpreted in terms of typical bauxite-forming processes on the ADCP subaerial exposure surfaces. DF1 is by far predominant (over 45%) signaling change in the bauxite geochemical record since the Upper Triassic (BX1) to Miocene (BX8) times caused by the complex interplay of changeable vadose–phreatic bauxite-forming karst paleo-environments and a progressively more emphasized input of mafic precursor material into the composition of deposited proto-bauxites. The other two discriminant functions (DF2-DF3) comprising further 25% and 10%, respectively, of the total model variance portray the processes of progressive ferralitization (DF2) and, finally, desilication (DF3) leaving ultimately Upper Cretaceous bauxites (BX4) as the most thoroughly "developed" bauxites with very high content of alumina (Med=70.29%) and very low content of silica (Med=3.66%), the latter on a par only with Paleogene bauxites (BX5-BX7). The geochemical signal of the modern soils (TR) corroborates the idea of their role in the genesis of karst bauxites as witnessed by the close ("half-way") relationship with the youngest bauxite group BX8 on DF2.

Data availability statement

The raw data supporting the conclusions of this article will be made available by the authors, without undue reservation.

Author contributions

All authors listed have made a substantial, direct, and intellectual contribution to the work and approved it for publication.

Funding

This study was supported by the Ministry of Science and Education, Republic of Croatia—Scientific Project: The Geological Maps of the Republic of Croatia and by EIT Raw Materials (European Institute of Innovation and Technology), Horizon 2020 project REEBAUX—Prospects of REE recovery from bauxite and bauxite residue in the ESEE region (project number 17089).

Acknowledgments

The authors are greatly indebted to and other reviewers whose comprehensive appraisal helped to clarify the authors' ideas and substantially improved this manuscript. Many thanks also to all who contributed to the execution of this research work.

Conflict of interest

The authors declare that the research was conducted in the absence of any commercial or financial relationships that could be construed as a potential conflict of interest.

Publisher's note

All claims expressed in this article are solely those of the authors and do not necessarily represent those of their affiliated organizations, or those of the publisher, the editors and the reviewers. Any product that may be evaluated in this article, or claim that may be made by its manufacturer, is not guaranteed or endorsed by the publisher.

References

Abedini, A., Khosravi, M., and Calagari, A. A. (2018). Geochemical characteristics of the Arbanos karst-type bauxite deposit, NW Iran: Implications for parental affinity and factors controlling the distribution of elements. *J. Geochem Explor* 200, 249–265. doi:10.1016/j.gexplo.2018.09.004

Abedini, A., and Khosravi, M. (2020). Geochemical constraints on the Triassic–Jurassic Amir-Abad karst-type bauxite deposit, NW Iran. *J. Geochem Explor* 211, 106489. doi:10.1016/j.gexplo.2020.106489

Aitchison, J., and Egozcue, J. J. (2005). Compositional data analysis: Where are we and where should we be heading? *Math. Geol.* 37, 829–850. doi:10.1007/s11004-005-7383-7

Aitchison, J. (1982). The statistical analysis of compositional data. *J. Roy. Stat. Soc. Ser. B* 44, 139–160. doi:10.1111/j.2517-6161.1982.tb01195.x

Aitchison, J. (1986). *The statistical analysis of compositional data.* London-New York: Chapman & Hall. doi:10.1002/bimj.4710300705

Aleva, G. J. J. (1994). *Laterites: Concepts, Geology, morphology and chemistry.* The Netherlands, Wageningen: International Soil Reference and Information Center.

Analytical methods committee (1987). Recommendations for the definition, estimation and use of the detection limit. *Analyst* 112, 199–204. doi:10.1039/an9871200199

Antweiler, R. C., and Taylor, H. E. (2008). Evaluation of statistical treatments of left-censored environmental data using coincident uncensored data sets: I. Summary statistics. *Environ. Sci. Technol.* 42, 3732–3738. doi:10.1021/es071301c

Banerjee, A., and Merino, E. (2011). Terra rossa Genesis by replacement of limestone by kaolinite. III. Dynamic quantitative model. *J. Geol.* 119, 259–274. doi:10.1086/659146

Barceló-Vidal, C., and Pawlowsky-Glahn, V. (1999). Letter to the editor: Comment on "singularity and nonnormality in the classification of compositional data" by Bohling GC, Davis JC, Olea RA, Harff J. *Math. Geol.* 31, 581–585.

Bardossy, G. (1982). *Karst bauxites: Bauxite deposits on carbonate rocks*. Budapest: Akadémiai Kiadó.

Blašković, I., Dragičević, I., and Pokrajčić, I. (1989). *Tectonic control of the origin of the paleorelief of bauxite deposits in the Western Herzegovina, Yugoslavia*, 19/22. Travaux ICSOBA, 231–238.

Boni, M., Reddy, S., Mondillo, N., Balassone, G., and Taylor, R. (2012). A distant magmatic source for Cretaceous karst bauxites of Southern Apennines (Italy), revealed through SHRIMP zircon age dating. *Terra nova.* 24, 326–332. doi:10.1111/j.1365-3121.2012.01068.x

Boni, M., Rollinson, G., Mondillo, N., Balassone, G., and Santoro, L. (2013). Quantitative mineralogical characterization of karst bauxite deposits in the southern Apennines, Italy. *Econ. Geol.* 108, 813–833. doi:10.2113/econgeo.108.4.813

Brlek, M., Gaynor, S. P., Mongelli, G., Bauluz, B., Sinisi, R., Brčić, V., et al. (2021). Karst bauxite formation during Miocene climatic optimum (central Dalmatia, Croatia): Mineralogical, compositional and geochronological perspectives. *Int. J. Earth. Sci.* 110, 2899–2922. doi:10.1007/s00531-021-02091-z

Brlek, M., Korbar, T., Košir, A., Glumac, B., Grizelj, A., and Otoničar, B. (2014). Discontinuity surfaces in Upper Cretaceous to Paleogene carbonates of central Dalmatia (Croatia): Glossifungites ichnofacies, biogenic calcretes, and stratigraphic implications. *Facies* 60, 467–487. doi:10.1007/s10347-013-0378-9

Brunović, D., Miko, S., Ilijanić, N., Peh, Z., Hasan, O., Kolar, T., et al. (2019). Holocene foraminiferal and geochemical records in the coastal karst dolines of Cres Island, Croatia. *Geol. Croat.* 72 (1), 19–42. doi:10.4154/gc.2019.02

Buccianti, A. (2013). Is compositional data analysis a way to see beyond the illusion? *Comp. Geosci.* 50, 165–173. doi:10.1016/j.cageo.2012.06.012

Buccianti, A., Mateu-Figueras, G., and Pawlowsky-Glahn, V. (Editors) (2006). *Compositional data analysis in the geosciences: From theory to practice* (London: Geol. Soc. Spec. Publ.), 264.

Chamley, H. (1989). *Clay sedimentology*. Berlin: Springer.

Crampton, S. L., and Allen, P. A. (1995). Recognition of forebulge unconformities associated with early stage foreland basin development; example from the North Alpine foreland basin. *AAPG Bull.* 79, 1495–1514.

D'Argenio, B., and Mindszenty, A. (1995). Bauxites and related palaeokarst: Tectonic and climatic event markers at regional unconformities. *Eclogae Geol. Helv.* 88, 453.

D'Argenio, B., and Mindszenty, A. (1992). Tectonic and climatic controls on paleokarst and bauxites. *Giorn. Geol.* 54 (1), 207.

Daunis-i-Estadella, J., Thió-Henestrosa, S., and Mateu-Figueras, G. (2011). "Two more things about compositional biplots: Quality of projection and inclusion of supplementary elements," in *Proceedings of the 4th international workshop on compositional data analysis (CoDaWork 2011)*. Editors J. J. Egozcue, R. Tolosana-Delgado, and M. I. Ortego (Girona, Spain: Universitat de Girona), 1–14.

Davis, J. C. (1986). *Statistics and data analysis in Geology*. 2nd ed. New York: John Wiley & Sons.

De Vos, W., Tarvainen, T., Salminen, R., Reeder, S., De Vivo, B., Demetriades, A., et al. (Editors) (2006). "Geochemical atlas of Europe," *Part 2 – interpretation of geochemical Maps, additional tables, figures, Maps, and related publications* (Espoo: Geological Survey of Finland).

Dillon, W. R., and Goldstein, M. (1984). *Multivariate analysis: Methods and applications*. New York: John Wiley & Sons.

Do Nascimento, N. R., Fritsch, E., Bueno, G. T., Bardy, M., Grimaldi, C., and Melfi, A. J. (2008). Podzolization as a deferralitization process: Dynamics and chemistry of ground and surface waters in an acrisol – podzol sequence of the upper Amazon Basin. *Eur. J. Soil Sci.* 59 (5), 911–924. doi:10.1111/j.1365-2389.2008.01049.x

Durn, G., Aljinović, D., Crnjaković, M., and Lugović, B. (2007). "Heavy and light mineral fractions indicate polygenesis of extensive terra rossa soils in Istria, Croatia," in *Developments in sedimentology, Heavy minerals in use*. Editors M. A. Mange and D. T. Wright (Amsterdam: Elsevier), 701–737. doi:10.1016/S0070-4571(07)58026-3

Durn, G., Ottner, F., and Slovenec, D. (1999). Mineralogical and geochemical indicators of the polygenetic nature of terra rossa in Istria, Croatia. *Geoderma* 91, 125–150. doi:10.1016/S0016-7061(98)00130-X

Durn, G. and Faculty of Mining Geology and Petroleum Engineering, University of Zagreb, Croatia (2003). Terra rossa in the Mediterranean region: Parent materials, composition and origin. *Geol. Croat.* 56/1, 83–100. doi:10.4154/GC.2003.06

Egozcue, J. J., and Pawlowsky-Glahn, V. (2006). "Simplicial geometry for compositional data," in *Compositional data analysis in the geosciences: From theory to practice*. Editors A. Buccianti, G. Mateu-Figueras, and V. Pawlowsky-Glahn (London: Geol. Soc. Spec. Publ.), 264, 145.

Galović, L., and Peh, Z. (2016). Mineralogical discrimination of the Pleistocene loess/paleosol sections in Srijem and Baranja, Croatia. *Aeolian Res.* 21, 151–162. doi:10.1016/j.aeolia.2016.04.006

Grizelj, A., Peh, Z., Tibljaš, D., Kovačić, M., and Kurečić, T. (2017). Mineralogical and geochemical characteristics of Miocene pelitic sedimentary rocks from the south-western part of the Pannonian Basin System (Croatia): Implications for provenance studies. *Geosci. Front.* 8 (1), 65–80. doi:10.1016/j.gsf.2015.11.009

Halamić, J. and Miko, S. (Editors) (2009). *Geochemical atlas of the Republic of Croatia* (Zagreb: Croatian Geological Survey).

Halamić, J., Peh, Z., Miko, S., Galović, L., and Šorša, A. (2012). Geochemical atlas of Croatia: Environmental implications and geodynamical thread. *J. Geochem Explor* 115, 36–46. doi:10.1016/j.gexplo.2012.02.006

Hasan, O., Miko, S., Ilijanić, N., Brunović, D., Dedić, Ž., Šparica Miko, M., et al. (2020). Discrimination of topsoil environments in a karst landscape: An outcome of a geochemical mapping campaign. *Geochem Trans.* 21, 1. doi:10.1186/s12932-019-0065-z

Hinsbergen, D. J. J., Mensink, M., Langereis, C. G., Maffione, M., Spalluto, L., Tropeano, M., et al. (2014). Did Adria rotate relative to Africa? *Solid earth.* 5, 611–629. doi:10.5194/se-5-611-2014

Kelemen, P., Dunkl, I., Csillag, G., Mindszenty, A., Józsa, S., Fodor, L., et al. (2022). Origin, timing and paleogeographic implications of Paleogene karst bauxites in the northern Transdanubian range, Hungary. *Int. J. Earth. Sci.*, 1–22. doi:10.1007/s00531-022-02249-3

Korbar, T. (2009). Orogenic evolution of the external Dinarides in the NE Adriatic region; a model constrained by tectonostratigraphy of Upper Cretaceous to Paleogene carbonates. *Earth-Sci. Rev.* 96, 296–312. doi:10.1016/j.earscirev.2009.07.004

Kovačević Galović, E., Ilijanić, N., Peh, Z., Miko, S., and Hasan, O. (2012). Geochemical discrimination of early Palaeogene bauxites in Croatia. *Geol. Croat.* 65 (1), 53–65. doi:10.4154/GC.2012.04

Kovačić, M., Peh, Z., and Grizelj, A. (2009). Discriminant function analysis of upper Miocene and Pliocene sands from the southwestern part of the Pannonian Basin system, Croatia. *Geol. Croat.* 62 (3), 189–200. doi:10.4154/GC.2009.12

MacLean, W. H., and Barrett, T. J. (1993). Lithogeochemical techniques using immobile elements. *J. Geochem. Explor.* 48, 109–133. doi:10.1016/0375-6742(93)90002-4

Márton, E., Zampieri, D., Grandesso, P., Ćosović, V., and Moro, A. (2010). New Cretaceous paleomagnetic results from the foreland of the Southern Alps and the refined apparent polar wander path for stable Adria. *Tectonophysics* 480, 57–72. doi:10.1016/j.tecto.2009.09.003

Márton, E., Zampieri, D., Kázmér, M., Dunkl, I., and Frisch, W. (2011). New Paleocene–Eocene paleomagnetic results from the foreland of the Southern Alps confirm decoupling of stable Adria from the African plate. *Tectonophysics* 504, 89–99. doi:10.1016/j.tecto.2011.03.006

Merino, E., and Banerjee, A. (2008). Terra rossa genesis, implications for karst, and eolian dust: A geodynamic thread. *J. Geol.* 116, 62–75. doi:10.1086/524675

Mindszenty, A., Csoma, A., Török, Á., Hips, K., and Hertelendi, E. (2000). Flexura jellegű előtéri deformációhoz köthető karsztbauxitszintek a Dunántúli-középhegységben (Rudistid limestones, bauxites, paleokarst and geodynamics. The case of the Cretaceous of the Transdanubian Range). *Bull. Geol. Soc. Hung.* 131, 107–152. (in Hungarian with ext. English abstract).

Mindszenty, A., D'Argenio, B., and Aiello, G. (1995). Lithospheric bulges recorded by regional unconformities. The case of mesozoic-tertiary Apulia. *Tectonophysics* 252, 137–161. doi:10.1016/0040-1951(95)00091-7

Mondillo, N., Balassone, G., Boni, M., Chelle-Michou, C., Cretella, S., Mormone, A., et al. (2019). Rare earth elements (REE) in Al- and Fe-(Oxy)-Hydroxides in bauxites of Provence and Languedoc (southern France): Implications for the potential recovery of REEs as by-products of bauxite mining. *Minerals* 9, 504. doi:10.3390/min9090504

Mondillo, N., Balassone, G., Boni, M., and Rollinson, G. (2011). Karst bauxites in the Campania Apennines (southern Italy): A new approach. *Period. Mineral.* 80, 407–432. doi:10.2451/2011PM0028

Mondillo, N., Nuzzo, M., Kalaitzidis, S., Boni, M., Santoro, L., and Balassone, G. (2022). Petrographic and geochemical features of the B3 bauxite horizon (Cenomanian-Turonian) in the Parnassos-Ghiona area: A contribution towards the genesis of the Greek karst bauxites. *Ore Geol. Rev.* 143, 104759. doi:10.1016/j.oregeorev.2022.104759

Mongelli, G., Boni, M., Buccione, R., and Sinisi, Rosa. (2014). Geochemistry of the Apulian karst bauxites (southern Italy): Chemical fractionation and parental affinities. *Ore Geol. Rev.* 63, 9–21. doi:10.1016/j.oregeorev.2014.04.012

Mongelli, G., Boni, M., Oggiano, G., Mameli, P., Sinisi, R., Buccione, R., et al. (2017). Critical metals distribution in Tethyan karst bauxite: The cretaceous Italian ores. *Ore Geol. Rev.* 86, 526–536. doi:10.1016/j.oregeorev.2017.03.017

Mongelli, G. (2002). Growth of hematite and boehmite in concretions from ancient karst bauxite: Clue for past climate. *Catena* 50, 43–51. doi:10.1016/S0341-8162(02)00067-X

Nesbitt, H. W., and Young, G. M. (1982). Early Proterozoic climates and plate motions inferred from major element chemistry of lutites. *Nature* 299, 715–717. doi:10.1038/299715a0

Nocquet, J.-M. (2012). Present-day kinematics of the mediterranean: A comprehensive overview of GPS results. *Tectonophysics* 579, 220–242. doi:10.1016/j.tecto.2012.03.037

Özlü, N. (1983). Trace element contents of karst bauxites and their parent rocks in the Mediterranean belt. *Min. Deposita* 18 (3), 469–476. doi:10.1007/BF00204491

Papadopoulos, A., Tzifas, I., and Tsikos, H. (2019). The potential for REE and associated critical metals in coastal sand (placer) deposits of Greece: A review. *Minerals* 9, 469. doi:10.3390/min9080469

Pawlowsky-Glahn, V., Egozcue, J. J., and Tolosana-Delgado, R. (2007). Lecture notes on compositional data analysis. Available at: https://www.researchgate.net/publication/37814008_Lecture_Notes_on_Compositional_Data_Analysis (Accessed November 20, 2022).

Peh, Z., and Halamić, J. (2010). Discriminant function model as a tool for classification of stratigraphically undefined radiolarian cherts in ophiolite zones. *J. Geochem. Explor.* 107, 30–38. doi:10.1016/j.gexplo.2010.06.003

Peh, Z., and Kovačević Galović, E. (2014). Geochemistry of Istrian Lower Palaeogene bauxites – is it relevant to the extent of subaerial exposure during Cretaceous times? *Ore Geol. Rev.* 63, 296–306. doi:10.1016/j.oregeorev.2014.05.020

Peh, Z., and Kovačević Galović, E. (2016). Geochemistry of Lower Palaeogene bauxites – unique signature of the tectonostratigraphic evolution of a part of the Croatian Karst. *Geol. Croat.* 69 (2), 269–279. doi:10.4154/gc.2016.24

Peh, Z., Šajn, R., Halamić, J., and Galović, L. (2008). Multiple discriminant analysis of the Drava River alluvial plain sediments. *Environ. Geol.* 55, 1519–1535. doi:10.1007/s00254-007-1102-2

Putzolu, F., Papa, A., Mondillo, N., Boni, M., Balassone, G., and Mormone, A. (2018). Geochemical characterization of bauxite deposits from the Abruzzi mining district (Italy). *Minerals* 8, 298. doi:10.3390/min8070298

Radusinović, S., Jelenkovic, R., Pačevski, A., Simić, V., Božović, D., Holclajtner-Antunović, I., et al. (2016). Content and mode of occurrences of rare earth elements in the Zagrad karstic bauxite deposit (Nikšić area, Montenegro). *Ore Geol. Rev.* 80, 406–428. doi:10.1016/j.oregeorev.2016.05.026

Radusinović, S., and Papadopoulos, A. (2021). The potential for REE and associated critical metals in karstic bauxites and bauxite residue of Montenegro. *Minerals* 11, 975. doi:10.3390/min11090975

Razum, I., Bajo, P., Brunović, D., Ilijanić, N., Hasan, O., Röhl, U., et al. (2021). Past climate variations recorded in needle-like aragonites correlate with organic carbon burial efficiency as revealed by lake sediments in Croatia. *Sci. Rep.* 11, 7568. doi:10.1038/s41598-021-87166-2

Razum, I., Miko, S., Ilijanić, N., Hasan, O., Šparica Miko, M., Brunović, D., et al. (2020a). A compositional approach to the reconstruction of geochemical processes involved in the evolution of Holocene marine flooded coastal karst basins (Mljet Island, Croatia). *Appl. Geochem.* 116, 104574. doi:10.1016/j.apgeochem.2020.104574

Razum, I., Miko, S., Ilijanić, N., Petrelli, M., Röhl, U., Hasan, O., et al. (2020b). Holocene tephra record of Lake Veliko jezero, Croatia: Implications for the central mediterranean tephrostratigraphy and sea level rise. *Boreas* 49 (3), 653–673. doi:10.1111/bor.12446

Reimann, C., Filzmoser, P., Fabian, K., Hron, K., Birke, M., Demetriades, A., et al. (2012). The concept of compositional data analysis in practice – total major element concentrations in agricultural and grazing land soils of Europe. *Sci. Total. Environ.* 426, 196–210. doi:10.1016/j.scitotenv.2012.02.032

Reimann, C., Filzmoser, P., Garrett, R. G., and Dutter, R. (2008). *Statistical data analysis explained: Applied environmental statistics with R*. New York: John Wiley & Sons.

Rock, N. M. S. (1988). *Lecture notes in earth Sciences, 18: Numerical Geology*. Berlin: Springer-Verlag.

Rudnick, R., and Gao, S. (2013). Composition of the continental crust. *Treatise Geochem.* 3, 1–51. doi:10.1016/B978-0-08-095975-7.00301-6

Sakač, K., and Šinkovec, B. (1991). The bauxites of the Dinarides. *Trav. ICSOBA* 21, 1–11.

Schmid, S., Fügenschuh, B., Kounov, A., Matenco, L., Nievergelt, P., Oberhänsli, R., et al. (2020). Tectonic units of the Alpine collision zone between Eastern Alps and western Turkey. *Gondwana Res.* 78, 308–374. doi:10.1016/j.gr.2019.07.005

Schmid, S. M., Bernoulli, D., Fügenschuh, B., Matenco, L., Schefer, S., Schuster, R., et al. (2008). The Alpine-Carpathian-Dinaridic orogenic system: Correlation and evolution of tectonic units. *Swiss J. Geosci.* 101, 139–183. doi:10.1007/s00015-008-1247-3

Scisciani, V., and Calamita, F. (2009). Active intraplate deformation within Adria: Examples from the Adriatic region. *Tectonophysics* 476, 57–72. doi:10.1016/j.tecto.2008.10.030

Sinisi, R. (2018). Mineralogical and geochemical features of Cretaceous bauxite from San Giovanni Rotondo (Apulia, southern Italy): A provenance tool. *Minerals* 8, 567. doi:10.3390/min8120567

Šinkovec, B., and Sakač, K. (1991). Bauxite deposits of Yugoslavia — The state of the art. *Acta Geol. hung.* 34/4, 307–315.

Šinkovec, B., and Sakač, K. (1982). The Paleogene bauxites of Dalmatia. *Trav. ICSOBA* 12, 293–331.

Šinkovec, B., Šušnjara, A., and Sakač, K. (1985). Boksiti Korduna i susjednih područja. *Geol. Vjesn.* 38, 215–233.

Šorša, A., Peh, Z., and Halamić, J. (2018). Geochemical mapping the urban and industrial legacy of Sisak, Croatia, using discriminant function analysis of topsoil chemical data. *J. Geochem. Explor.* 187, 155–167. doi:10.1016/j.gexplo.2017.07.014

StatSoft, Inc. (2006). STATISTICA (data analysis software system). Available at: www.statsoft.com2006.

Šumanovac, F. (2010). Lithosphere structure at the contact of the Adriatic microplate and the Pannonian segment based on the gravity modelling. *Tectonophysics* 485, 94–106. doi:10.1016/j.tecto.2009.12.005

Šušteršič, F., Rejšek, K., Mišič, M., and Eichler, F. (2009). The role of loamy sediment (terra rossa) in the context of steady state karst surface lowering. *Geomorphology* 106, 35–45. doi:10.1016/j.geomorph.2008.09.024

Tarvainen, T., Reeder, S., and Albanese, S. (2005). "Database management and map production," in *Geochemical atlas of Europe, Part 1, background information, methodology and Maps*. Editors R. Salminen, M. J. Batista, M. Bidovec, A. Demetriades, B. De Vivo, W. De Vos, et al. (Geological Survey of Finland, Espoo).

Thiffault, E. (2019). "Boreal forests and soils," in *Developments in soil science 36 global change and forest soils*. Editors M. Busse, C. P. Giardina, D. M. Morris, and D. S. Page-Dumroese (Amsterdam: Elsevier), 59–82. doi:10.1016/B978-0-444-63998-1.00005-7

Tolosana-Delgado, R., Otero, N., and Pawlowsky-Glahn, V. (2005). Some basic concepts of compositional geometry. *Math. Geol.* 37, 673–680. doi:10.1007/s11004-005-7374-8

Tolosana-Delgado, R. (2012). Uses and misuses of compositional data in sedimentology. *Sediment. Geol.* 280, 60–79. doi:10.1016/j.sedgeo.2012.05.005

Tomašić, N., Čobić, A., Bedeković, M., Miko, S., Ilijanić, N., Gizdavec, N., et al. (2021). Rare earth elements enrichment in the upper Eocene Tošići-Dujići bauxite deposit, Croatia, and relation to REE mineralogy, parent material and weathering pattern. *Minerals* 11, 1260. doi:10.3390/min11111260

Ustaszewski, K., Kounov, A., Schmid, S., Schaltegger, U., Krenn, E., Frank, W., et al. (2010). Evolution of the Adria-Europe plate boundary in the northern

Dinarides: From continent-continent collision to back-arc extension. *Tectonics* 29. doi:10.1029/2010TC002668

Valeton, I., Biermann, M., Reche, R., and Rosenberg, F. (1987). Genesis of nickel laterites and bauxites in Greece during the Jurassic and Cretaceous, and their relation to ultrabasic parent rocks. *Ore Geol. Rev.* 2, 359–404. doi:10.1016/0169-1368(87)90011-4

van Breemen, N., and Buurman, P. (1998). *Ferralitization in soil formation*. Wagenigen, The Netherlands: Kluwer Academic Publishers, 291–312.

Vlahović, I., Tišljar, J., Velić, I., and Matičec, D. (2005). Evolution of the Adriatic carbonate platform: Palaeogeography, main events and depositional dynamics. *Palaeogeogr. Palaeoclimat. Palaeoecol.* 220, 333–360. doi:10.1016/j.palaeo.2005.01.011

Vlahović, I., Tišljar, J., Velić, I., Matičec, D., and Maticec, D. (2002). The karst Dinarides are composed of relics of a single Mesozoic platform: Facts and consequences. *Geol. Croat.* 55/2, 171–183. doi:10.4154/GC.2002.15

Weaver, C. E. (1989). *Clays, muds, and shales*. Amsterdam: Elsevier.

Yang, S., Qingfei, W., Deng, J., Wang, Y., Kang, W., Liu, X., et al. (2019). Genesis of karst bauxite-bearing sequences in Baofeng, Henan (China), and the distribution of critical metals. *Ore Geol. Rev.* 115, 103161. doi:10.1016/j.oregeorev.2019.103161

Zhao, L., Liu, X., Yang, S., Ma, X., Liu, L., and Sun, X. (2021). Regional multi-sources of Carboniferous karstic bauxite deposits in North China Craton: Insights from multi-proxy provenance systems. *Sediment. Geol.* 421, 105958. doi:10.1016/j.sedgeo.2021.105958

6.2. Geochemical insights and mineral resource potential of rare earth elements (REE) in the Croatian karst bauxites

By Kovačević Galović, E., Ilijanić, N.*, Gizdavec, N., Miko, S., Peh, Z.

Published in Minerals 2025, 15(2), 192.

DOI: https://doi.org/10.3390/min15020192

This paper investigates the distribution and enrichment of rare earth elements (REE) in Croatian karst bauxites across eight bauxite-bearing horizons of the Adriatic–Dinaric Carbonate Platform, ranging from the Upper Triassic to the Neogene. Geochemical and statistical analyses were used to evaluate the controls on REE distribution and fractionation at the regional scale. The results reveal systematic differences in REE concentrations between horizons, with the highest enrichment recorded in the Middle and Upper Eocene bauxites. Variations in REE content primarily reflect differences in the geochemical characteristics of the source material, paleogeographic evolution, and physicochemical conditions during weathering and bauxitization. The study further indicates that REE distribution is influenced by specific mineral hosts and secondary geochemical processes. The obtained results provide the regional framework for understanding REE behavior in Croatian karst bauxites and establish the basis for assessing their resource potential as alternative sources of critical raw materials.

minerals

MDPI

Article

Geochemical Insights and Mineral Resource Potential of Rare Earth Elements (REE) in the Croatian Karst Bauxites

Erli Kovačević Galović, Nikolina Ilijanić *, Nikola Gizdavec, Slobodan Miko and Zoran Peh

Croatian Geological Survey, Sachsova 2, 10000 Zagreb, Croatia; ekovacevic@hgi-cgs.hr (E.K.G.); ngizdavec@hgi-cgs.hr (N.G.); smiko@hgi-cgs.hr (S.M.); zpeh@hgi-cgs.hr (Z.P.)
* Correspondence: nilijanic@hgi-cgs.hr

Abstract: Karst bauxites are valuable terrestrial records of paleoclimate and tectonic evolution formed under tropical to subtropical conditions during the subaerial exposure of carbonate platforms. This study explores Croatian bauxite deposits within the Adriatic–Dinaric Carbonate Platform (ADCP), with a focus on the distribution and enrichment of rare earth elements (REE) across eight bauxite horizons from the Triassic to Neogene periods. The research applies statistical analyses of geochemical data, as well as developed models, to assess the factors influencing REE distribution and fractionation. The study found that variations in parent material, along with changes in paleogeographical and paleotectonic settings, significantly affected the REE content. The median REE concentrations in the analyzed bauxite horizons range from approximately 250 to 570 mg/kg. Notable REE enrichment was observed in the Late Paleogene, particularly in the Middle and Upper Eocene horizons. The analysis highlights the importance of physicochemical conditions, such as Eh and pH, during the weathering processes that lead to bauxite formation. The results suggest that the presence of REE-bearing minerals, rather than clay minerals, could possibly contribute to elevated concentrations of heavy REE (HREE). These findings indicate that Croatian bauxites, enriched in REE and associated trace elements, are significant not only as geological markers of past climatic and tectonic events but also as potential sources of critical raw materials. This study underscores the potential for the economic exploitation of these deposits in the context of modern technological demands.

Keywords: karst bauxites; geochemical data; rare earth elements; critical raw materials; Adriatic–Dinaric Carbonate Platform; bauxite horizons; geodynamic evolution

check for updates

Academic Editors: Roberto Buccione, Farhad Ahmadnejad, Kunyue Ling and Batoul Taghipour

Received: 24 January 2025
Revised: 14 February 2025
Accepted: 17 February 2025
Published: 19 February 2025

Citation: Kovačević Galović, E.; Ilijanić, N.; Gizdavec, N.; Miko, S.; Peh, Z. Geochemical Insights and Mineral Resource Potential of Rare Earth Elements (REE) in the Croatian Karst Bauxites. *Minerals* **2025**, *15*, 192. https://doi.org/10.3390/min15020192

Copyright: © 2025 by the authors. Licensee MDPI, Basel, Switzerland. This article is an open access article distributed under the terms and conditions of the Creative Commons Attribution (CC BY) license (https://creativecommons.org/licenses/by/4.0/).

1. Introduction

Karst bauxites are residual deposits formed by intense chemical weathering in hot and humid tropical or subtropical climates. These deposits are enriched in aluminum hydroxides (gibbsite and boehmite) with subordinate amounts of kaolinite, iron oxides, hydroxides, and titanium oxides [1,2]. Karst bauxites serve as significant terrestrial paleoclimate indicators because of their ability to record low-frequency climatic changes [3,4]. Their genesis involves complex interactions between atmospheric, biospheric, and lithospheric factors, often under greenhouse conditions and tectonically controlled subaerial exposure of carbonate platforms [5].

Karst bauxites in Europe, including those formed in plate-interior settings such as Croatia (karst Dinarides), Italy (Southern Apennines), Hungary (Villány region), and Greece (Parnassus, Ghiona, and Helicon mountains), as well as plate-margin environments like the Transdanubian Central Range in Hungary, have been extensively studied (e.g., [1,6–9] and

others). They are recognized as regional markers of global events tied to specific intervals in the geological record, characterized by warm and humid climates coupled with tectonically driven subaerial exposure of carbonate platforms [5,10].

The genesis of Mediterranean karst bauxites, including those in Croatia, has historically been debated, with early studies focusing on paleoclimate-related geochemical and mineralogical processes [6,11–13] and local tectonics [14]. More recent investigations have integrated these findings into larger tectonostratigraphic frameworks, linking bauxitization events to orogenic processes and stratigraphic gaps in the Adriatic–Dinaric Carbonate Platform (ADCP) [15–22]. These studies emphasize the role of global climatic events, such as the Paleocene–Eocene Thermal Maximum and other greenhouse episodes, in creating the conditions necessary for widespread bauxitization [23]. Such events often coincide with massive volcanic eruptions, high-temperature and precipitation periods, elevated atmospheric CO_2 levels, the release of methane hydrates from the oceans, and oceanic anoxia, highlighting the interconnectedness of bauxite formation with global environmental change [4,23].

Historically, bauxite deposits have been explored as valuable sources of aluminum. The exploitation of bauxite has been widespread across Europe, particularly in the Mediterranean region. In Croatia, pyritized bauxite deposits in the Mirna River valley (Minjera deposit) in Istria were exploited as early as the 16th century [24], making them the first bauxites to be analyzed and mined in the world, while their genesis was studied more recently [25]. The period from 1914 to 1990 marked the peak of bauxite exploitation in Croatia, with an estimated 27.5 million tons extracted [26]. Bauxite mining in Croatia was primarily concentrated in the Dalmatian and Istrian regions, where deposits were of the highest quality. Consequently, most of these deposits have now been depleted. Currently, only two bauxite exploitation fields remain active [27]. The ongoing implementation of the "Map of Mineral Resources of the Republic of Croatia" at the Croatian Geological Survey (HGI-CGS) systematizes data on primary and secondary deposits and occurrences of mineral resources, maintaining them in a database. The database contains spatial data for approximately 700 bauxite deposits and occurrences, although a significant number of these represent clusters of deposits, indicating that the actual number of distinct bauxite deposits is even higher.

Recent studies have increasingly focused on the geochemical and mineralogical characteristics of karst bauxites, examining their parental affinities, weathering processes, and the climatic and tectonostratigraphic constraints that shaped their formation, often focusing on specific bauxite-bearing horizons (e.g., [21,22,28–30]). Furthermore, recent research has highlighted the potential for rare earth elements (REE) and other associated critical metals in bauxite deposits, underscoring the importance of these deposits in both geological and economic contexts (e.g., [31–38] and others). This growing interest in critical raw materials (CRMs) is driven by concerns over their long-term availability because modern technology depends on nearly all stable elements in the periodic table. The European Union (EU) assesses the economic importance of metals based on their criticality, considering supply risks and economic value. Despite increasing demand, the EU relies heavily on imports from suppliers with near-monopolistic control, prompting the Commission to propose the Critical Raw Materials Act in March 2023 [39] to secure a diversified, sustainable supply. With REE playing a crucial role in technology, especially in magnets, lighting, and batteries, mining remains the primary source of these materials, as recycling efforts are insufficient. China currently dominates the global REE market, producing nearly 90%, whereas the EU continues to depend on imports. The European Commission has identified REE, particularly heavy REE (HREE), as critical materials with significant supply risk. While deposits in Greenland and the Fennoscandian shield have been identified, further exploration is

needed to discover additional primary resources in Europe, including alternative mineral sources where REE can be exploited as by-products [40,41].

Ongoing research focuses on the geochemical aspects of karst bauxites, with the aim of refining the understanding of their genesis, paleoclimate implications, and potential for economic exploitation. This study builds significantly on prior research into the geochemical records of Croatian karst bauxite horizons [42]. However, the REE geochemistry of these deposits has not yet been systematically investigated. The primary objective of this research is to present entirely new findings on the REE geochemistry of Croatian karst-type bauxite horizons compared with other relevant karst-type bauxite deposits in the region. This work represents the first attempt to advance the future exploration of REE-rich Croatian karst bauxites, emphasizing their potential contribution to meeting sustainable REE demands. The integration of regional studies within frameworks such as the Adriatic–Dinaric Carbonate Platform further enhances their significance as markers of tectonic and climatic evolution in the geological record.

2. Geological Setting

Croatian karst bauxites are incorporated into a thick carbonate succession of Croatian karst Dinarides (Figure 1a) that extends from the Middle Permian, or potentially the Upper Carboniferous, to the Eocene. This succession, with thicknesses exceeding 8000 m in certain areas, represents the remnants of multiple vertically stacked stratigraphic units formed within the ADCP under varying geological and tectonic conditions [43,44]. The geology of Croatian karst Dinarides has been described in numerous studies (e.g., [15–17,42,44]).

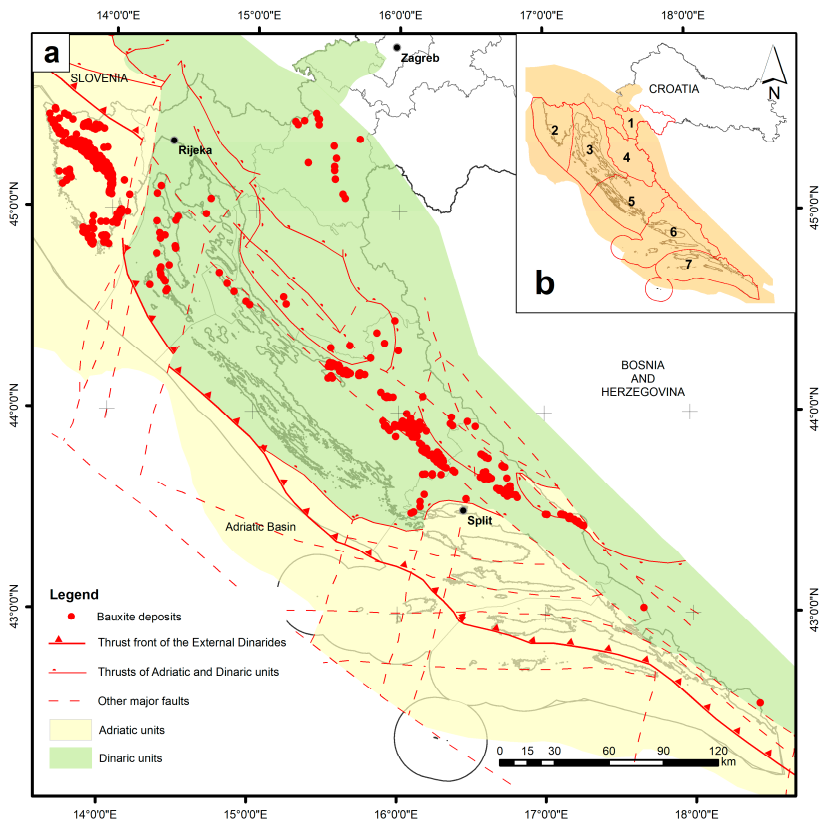

Figure 1. (**a**) Deposits and occurrences of bauxites in Croatia (red dots; source: Map of Mineral Resources of the Republic of Croatia, Croatian Geological Survey) [45] within Adriatic (yellow area) and Dinaric (green area) units in Croatian karst Dinarides. (**b**) Geographical position of External Dinarides in the Republic of Croatia (orange area). The numbers represent seven subregions of the Republic of Croatia: 1. Banovina and Kordun, 2. Istrian peninsula, 3. Kvarner coast and Velebit foothill, 4. Lika, 5. Northern Dalmatia, 6. Central Dalmatia, and 7. Southern Dalmatia.

Because of various geodynamic movements in the Dinarides during their evolution, dry land surfaces of variable duration came into existence, resulting in the development of paleokarst and bauxitization processes. Bauxites occur in various stratigraphic positions in the Croatian Dinaric karst region from the Triassic to the Miocene, with fundamental differences in chemical composition, mode of occurrence, and deposit type [6]. According to their stratigraphic relationship with the basement and cover layers and the specific geotectonic position of a wide geographic scope, eight stratigraphic horizons (Figure 2) of bauxite deposits were determined [13] and used in this study: (1) Upper Triassic; (2) Upper Jurassic; (3) Lower Cretaceous; (4) Upper Cretaceous; (5) Paleocene; (6) Middle Eocene; (7) Upper Eocene; and (8) Miocene.

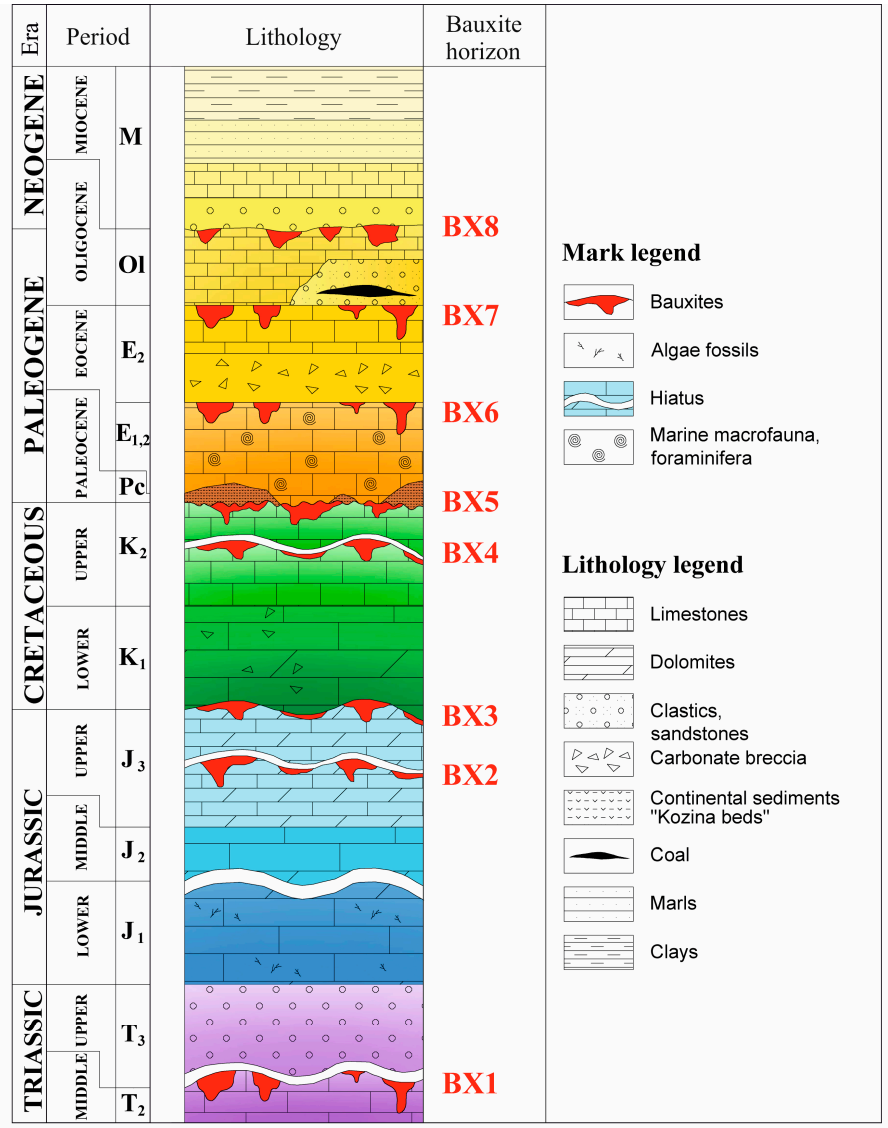

Figure 2. Stratigraphic positions of bauxite-bearing horizons in the schematic representation of the Croatian karst Dinarides: BX1 Upper Triassic, BX2 Upper Jurassic, BX3 Lower Cretaceous, BX4 Upper Cretaceous, BX5 Paleocene, BX6 Middle Eocene, BX7 Upper Eocene, and BX8 Miocene. Modified from [42].

The geological evolution of the karst Dinarides began during the Carboniferous era as an extensive epeiric carbonate platform located along the northern margin of Gondwana. Middle Triassic tectonic activity led to the separation of the Adria microplate [46,47] and the accumulation of a substantial sequence of shallow-water carbonates locally influenced by volcanic activity. The Middle to Upper Triassic transition is marked by a prolonged

emergence period, leading to the deposition of bauxite deposits and signaling the isolation of an intraoceanic carbonate platform from continental influences [15]. The Upper Triassic bauxite horizon (BX1) is associated with the onset of Alpine orogeny and is primarily located in Lika, Kordun, and northern Dalmatia [48]. These deposits likely originated from the weathering of Ladinian clastics and pyroclastics, which accumulated in relief depressions within Middle Triassic carbonates. The deposits vary in size, ranging from small eroded remnants to significant outcrops. Classified predominantly as clayey bauxites, they are often interbedded with bauxitic and kaolinitic clays. Owing to their low quality, only a few tens of thousands of tons have been exploited, while the remaining reserves are estimated at several million tons [26].

During the Late Jurassic, the extensive carbonate platform fragmented into smaller platforms, forming the Adriatic Basin and the ADCP along its eastern margin. The development of the karst Dinarides remains debated, with models proposing either a single platform ([15], and references therein) or two distinct domains in the Adriatic–Dinaric region ([16], and references therein), shaped by the disintegration of the Adriatic microplate. Gradual subsidence during the Late Jurassic and Cretaceous sustained shallow marine carbonate production. Periodic emergence due to tectonics and sea-level fluctuations led to the formation of bauxites. The Upper Jurassic bauxites (BX2 horizon), formed on Malmian carbonates from carbonate substrates and aeolian material, are primarily located on the Istrian Peninsula [25,48]. Although the distribution is limited, the five identified deposits are substantial, with total reserves exceeding 5 million tons. Because of their high silica content, these bauxites were not considered economically viable for exploitation [26]. One of the two currently active bauxite exploitation fields in Croatia is ″Rovinj-1″, where Jurassic bauxite is exploited and used as a corrective material in cement production [27]. The Lower Cretaceous (BX3) bauxite occurrences and small deposits are found in Central Dalmatia [6]. Underlain by Upper Jurassic limestones, these deposits are characterized as clayey bauxites and likely formed through incomplete bauxitization of kaolinitic clays [26]. Owing to their low alumina content and limited potential, they have never been exploited. Upper Cretaceous (BX4) bauxite deposits are located in the Kordun region [6] with Cenomanian limestone bedrock. Although research indicates that these bauxites have a high aluminum content, bauxite ore typically occurs in small lenses, limiting their economic value. Only one deposit (″Frketići″) is known to have been exploited historically [26].

The Cretaceous–Paleogene boundary marks a significant tectonic and paleogeographic shift driven by the collision of the Adria microplate with the European plate. This event initiated the uplift and emergence of the ADCP leading to widespread karstification and bauxite formation [18,49,50]. Deposits on the ADCP were tectonically dissected during the Paleogene into several small sedimentary basins characterized by ramp-type carbonate deposition along their margins [15]. The subsequent Early Eocene transgression re-established sedimentation, beginning with the deposition of the Kozina deposits, which comprised palustrine and marginal marine carbonates that filled karstified depressions on the platform surface [51]. Tectonic deformation during the Early Eocene further transformed the ADCP into a carbonate ramp environment, facilitating the deposition of foraminiferal limestone facies [15,52]. The termination of carbonate deposition in the Middle Eocene was marked by transitional beds and flysch sedimentation.

The Cretaceous to Eocene interval is considered to be the most favorable for bauxitization [1]. Most bauxite deposits in Croatian karst Dinarides formed during the early to late Paleogene [13] and are associated with three distinct stratigraphic discontinuities.

The Paleocene bauxites (BX5 horizon) are widespread in Istria, the northern Adriatic islands, and Dalmatia. They formed during the emersion phase following the Laramian orogeny, deposited on the paleorelief of Upper Cretaceous limestones, and bounded by

transgressive Kozina formations [6]. With a high alumina content, these bauxites were among the most economically significant bauxites in Croatia during the 20th century. While most deposits in Istria were small (50 to 25,000 tons of ore), by 1976 around 10,000 deposits had been identified, most of which, as well as those on the northern Adriatic islands, are now exhausted [25]. In Dalmatia, Paleocene bauxites are even smaller and less numerous, with the largest deposits also having been depleted.

The Middle Eocene bauxites (BX6) occur as small deposits in northern and central Dalmatia [13], deposited between Upper Cretaceous limestones or Eocene foraminiferal limestones and the Jelar carbonate breccias. Although many deposits have been depleted, tens of thousands of tons of ore are estimated to remain [26].

The Upper Eocene (BX7) bauxite horizon is found in northern and central Dalmatia. Their formation is linked to the emersion caused by the Pyrenean orogeny in the Middle Eocene, with accumulation in the paleorelief of Upper Cretaceous or older Paleogene limestones, and less commonly in the Kozina or Jelar deposits, overlain by transgressive Promina deposits. These high-quality deposits are large, with high aluminum content, and were historically the most economically significant. In 2012, over 5 million tons of exploitable reserves had been confirmed in Dalmatia [27]. One of the two currently active bauxite exploitation fields in Croatia is ″Kruševo″, where high-quality Upper Eocene bauxite is being extracted [27].

During the Oligocene–Miocene, platform contraction led to the uplift of the Dinarides and marked the last significant period of bauxite formation. Numerous deposits of Miocene clayey bauxites (BX8 horizon) are located in central Dalmatia and Kordun [13]. In the form of large, irregular lenses formed in situ from diverse parent materials [21], they are underlain by karstified Cretaceous limestones and overlain by Miocene clastic deposits. Owing to their high clay content, they were exploited on a limited scale for use in the brick industry [26].

3. Materials and Methods

3.1. Sampling, Sample Preparation, and Geochemical Analysis

The bauxite outcrops examined in this study are located along approximately 400 km of Croatian karst Dinarides. The sampling methodology was designed to comprehensively cover the entire study area, including all the bauxite horizons defined by regional unconformities, and was implemented through multiple field campaigns. Systematic sampling was conducted at 215 locations across eight previously identified bauxite horizons within Croatian karst Dinarides (Figure 3). Each site was represented by a single composite sample, adhering to the principle that bauxites associated with a specific regional unconformity (spanning from the Upper Triassic to the Miocene) should capture an integrated geochemical composition. This method ensures a representative characterization of bulk geochemistry, regardless of the precise spatial position of the bauxite within the ore body, such as at the interface with the paleokarst surface or its immediate overlying deposits. Building on the findings of previous studies [17,19,20,42], the present work operates on the implicit assumption that multivariate analysis of bulk geochemical data from multiple cases can effectively elucidate the key geochemical processes relevant to bauxite autochthony and allochthony, as well as the conditions of vadose and phreatic depositional–diagenetic environments [1,5]. This approach simplifies the complexities of vertical profile details by condensing them into a limited set of mathematical functions.

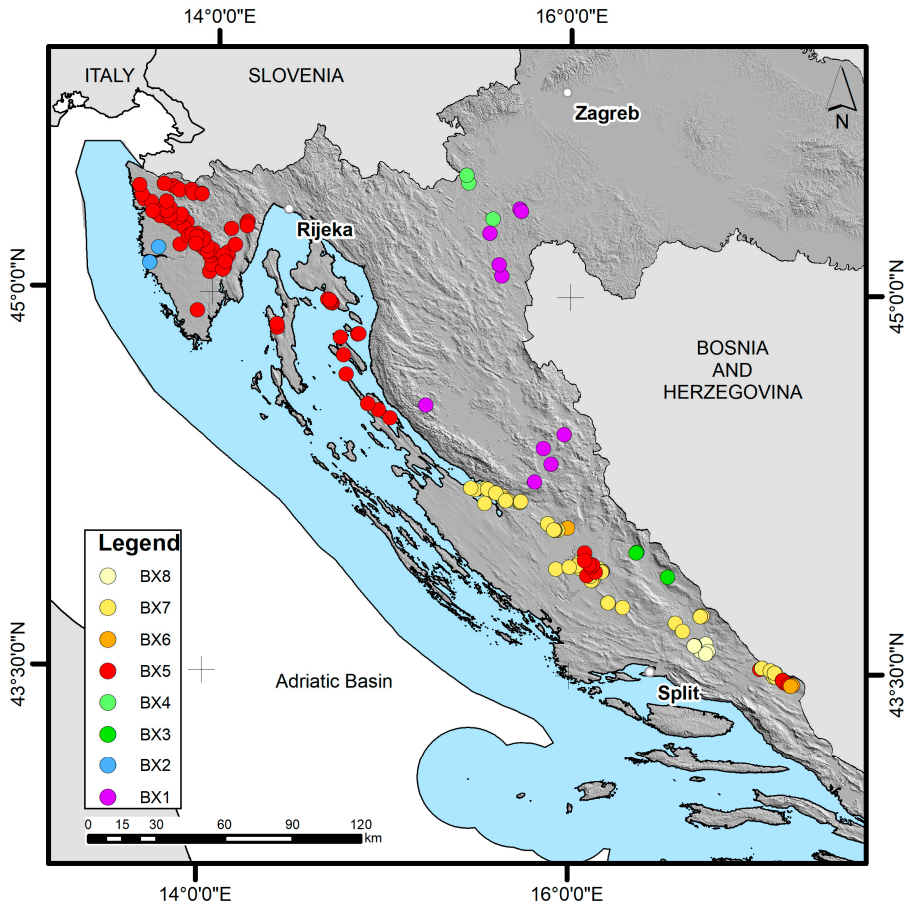

Figure 3. Locations of the sampled bauxite deposits from eight bauxite-bearing horizons from the Upper Triassic to the Miocene (BX1–BX8) in the study area (Croatian karst Dinarides).

Approximately 3 kg of each bauxite sample were manually crushed, divided into fractions using the quartering method, and subsequently ground using a tungsten carbide pestle and mortar mill (Retsch Lab Equipment). The ground material was sieved to a particle size of <0.063 mm. All sample preparation was conducted in the laboratories of the Croatian Geological Survey for subsequent analytical procedures.

Geochemical analyses were conducted at the Bureau Veritas laboratory (formerly ACME Analytical Laboratories Ltd.) in Vancouver, Canada, using the Lithogeochemical Whole Rock Major and Trace Element analytical method. Major oxides and select minor elements were quantified on 0.2 g of sample via inductively coupled plasma emission spectroscopy (ICP-AES) after lithium metaborate/tetraborate fusion and dissolution in dilute nitric acid. Trace elements, including refractory elements, were analyzed using inductively coupled plasma mass spectrometry (ICP-MS). Refractory elements underwent the same digestion as major elements (0.2 g of sample), while other elements, including rare earth elements (REE), were measured after modified hot aqua regia digestion (0.5 g of sample). Analytical quality control included blanks, duplicates, and standard reference materials (STD SO-18) to ensure accuracy and precision, with the results documented in a certified quality (CQ) report. To handle data below the detection limit, the substitution method proposed in [53] was applied, assigning half the detection limit value to censored data, which is a widely used approach in geochemical and environmental studies, as outlined in [54].

The rare earth element concentrations were normalized to chondrite [55]. The Ce and Eu anomalies were calculated as $Ce/Ce^* = Ce_N/\sqrt{(La_N \times Pr_N)}$ and $Eu/Eu^* = Eu_N/\sqrt{(Sm_N \times Gd_N)}$, respectively [56], where the subscript "N" refers to values normalized to chondrite.

3.2. Statistical Analysis and Modelling

The geochemical data were statistically processed to elucidate the variations in REE elements between the considered bauxite horizons. Both univariate and multivariate analyses were used in this study. The latter was deemed appropriate in the case of Paleogene bauxite groups that showed increased concentrations of REE compared with other investigated horizons. Thus, discriminant function analysis (DFA) was applied to the BX5, BX6, and BX7 groups to build a model combining REE (including Sc and Y) and major elements and to define possible affiliation of REE with certain elements that would imply possible hosting minerals. For this purpose, the Paleocene group (BX5) was divided into two separate divisions—Dalmatia (BX5D) and Istria together with north Adriatic islands (BX5A), respectively—on the grounds of conceivably different provenances of protobauxite material due to different paleogeographic and paleotectonic settings. The principles of DFA, together with the behavior of compositional data (geochemical data characterized with a constant-sum constraint), are described elsewhere in detail (e.g., [19,20,42,57,58]) and will not be discussed at length here.

4. Results

4.1. Trace and Rare Earth Elements

Elements considered relatively immobile during sedimentary processes, such as REE, Nb, certain transition trace elements (Sc, Co, Cr, and Ni), Al, Ti, and Th, are invaluable for discriminating source area compositions. The geochemical analysis and the mineralogical characteristics of Croatian karst bauxite samples have been comprehensively presented and discussed in a previous publication, which successfully discriminated among eight horizons using multiple discrimination analysis (MDA) [42]. The Upper Cretaceous bauxites (BX4) are aluminum-rich (median values (med.) ~70%) and associated with elevated levels of TiO_2, Sc, Th, and Ga, while being relatively depleted in Fe_2O_3 and SiO_2 and other clay components, which are more prevalent in the Upper Triassic (BX1) and Miocene bauxites (BX8) [42]. The Paleogene bauxites (BX5–BX7), classified as ferritic bauxites, are also characterized by low SiO_2 content and are mineralogically associated with böhmite, gibbsite, hematite, goethite, anatase, and kaolinite [42]. Previous findings indicate that Nb, Ga, Zr, and Th are closely associated with the SiO_2–Al_2O_3–Fe_2O_3 elemental cluster, which is related to enrichment in the Upper Jurassic (BX2) and Lower and Upper Cretaceous (BX3 and BX4) bauxites. Nb concentrations are the highest in the Upper Cretaceous (BX4) bauxites (med. ~60 mg/kg) and the lowest in the Upper Triassic (BX1) and Upper Jurassic (BX2) bauxites (med. ~35–40 mg/kg), with median values of ~50 mg/kg in all bauxite horizons. Ga and Th exhibit similar behavior and vary between 41 and 62 mg/kg and 37 and 64 mg/kg in bauxite horizons, respectively, with the highest values in Upper Cretaceous bauxites (BX4). Zr levels are relatively consistent across all bauxite horizons (med. ~500 mg/kg), with the lowest median value (~370 mg/kg) in the Upper Jurassic bauxites (BX2). Among trace elements, Ni is most enriched in the Upper Eocene (BX7) bauxites (med. ~400 mg/kg), followed by the Lower Cretaceous (BX3), Paleocene (BX5), Middle Eocene (BX6), and Miocene (BX8) bauxites (med. ~200 mg/kg). Cr shows the highest concentrations in the Middle and Upper Eocene (BX6 and BX7) (med. 0.1–0.15%), followed by the Upper Cretaceous (BX4) and Paleocene (BX5) bauxites (med. 0.7–0.8%), with the lowest values in the Upper Triassic (BX1), Upper Jurassic (BX2), Lower Cretaceous (BX3), and Miocene (BX8) horizons. Higher V content is observed in the Upper Cretaceous (BX4) to Miocene bauxite (BX8) horizons (med. ~500 mg/kg), peaking in the Upper Eocene (BX7) bauxites (>900 mg/kg). Co shows similar enrichment (~35–40 mg/kg), except in the Upper Triassic (BX1), Upper Cretaceous (BX4), and Miocene (BX8) bauxites (~10–20 mg/kg). Sc is the most abundant from the Upper Jurassic (BX2) to the Upper Eocene (BX7) horizons (med.

~53 mg/kg), but exhibits significant variability in the Paleocene (BX5) bauxite deposits, while it is the lowest in Upper Triassic (BX1) and Miocene (BX8) bauxites (med. ~30 mg/kg). Y is the most enriched in the Middle Eocene (BX6) and Upper Eocene (BX7) bauxites (med. 98–106 mg/kg); higher values are identified also in the Upper Jurassic (BX2) and Miocene (BX8) bauxites (76–80 mg/kg), while the lowest values occur in the Upper Triassic (BX1) and Upper Cretaceous (BX4) bauxites (38–45 mg/kg).

However, this study places emphasis on REE. The bauxite horizons in Croatia exhibit varying REE contents (Figures 4–6). The quantified concentrations of light rare earth elements (ΣLREE La–Sm) [59], heavy rare earth elements (ΣHREE Eu–Lu), and total rare earth elements (ΣREE La–Lu) in the eight horizons range as follows: ΣLREE from 70 to 4657 mg/kg (with median values between 219 and 506 mg/kg), ΣHREE from 15 to 388 mg/kg (med. 31–70 mg/kg), and ΣREE from 83 to 5045 mg/kg (med. 250–575 mg/kg), respectively (Table 1, Figure 4).

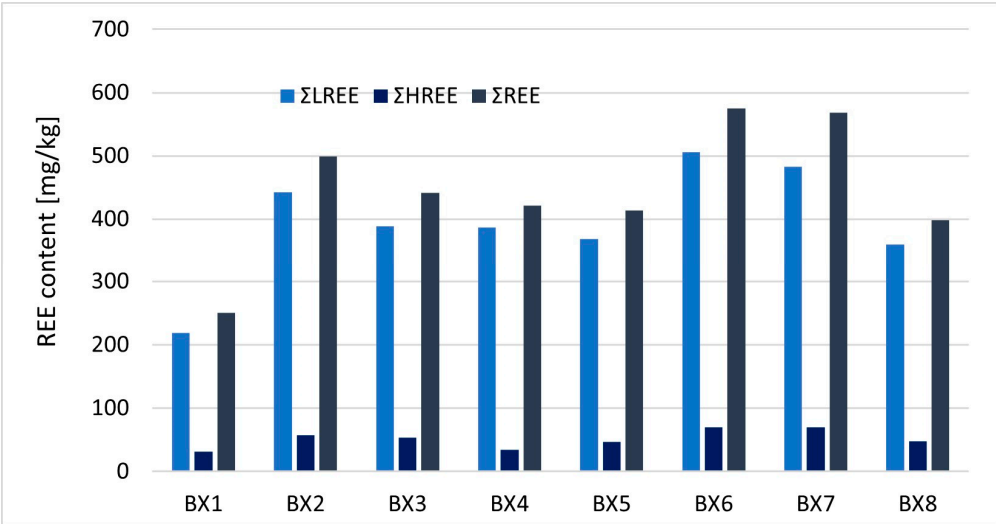

Figure 4. Diagram showing median values of ΣLREE, ΣHREE, and ΣREE in the Croatian karst bauxite horizons (BX1–BX8).

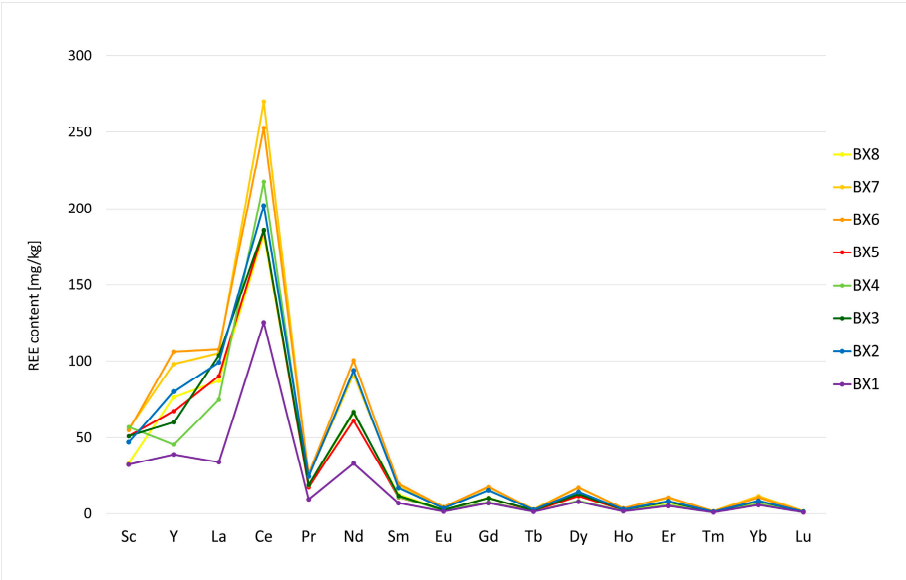

Figure 5. Median REE values (including Sc and Y) in the Croatian karst bauxite horizons (BX1–BX8).

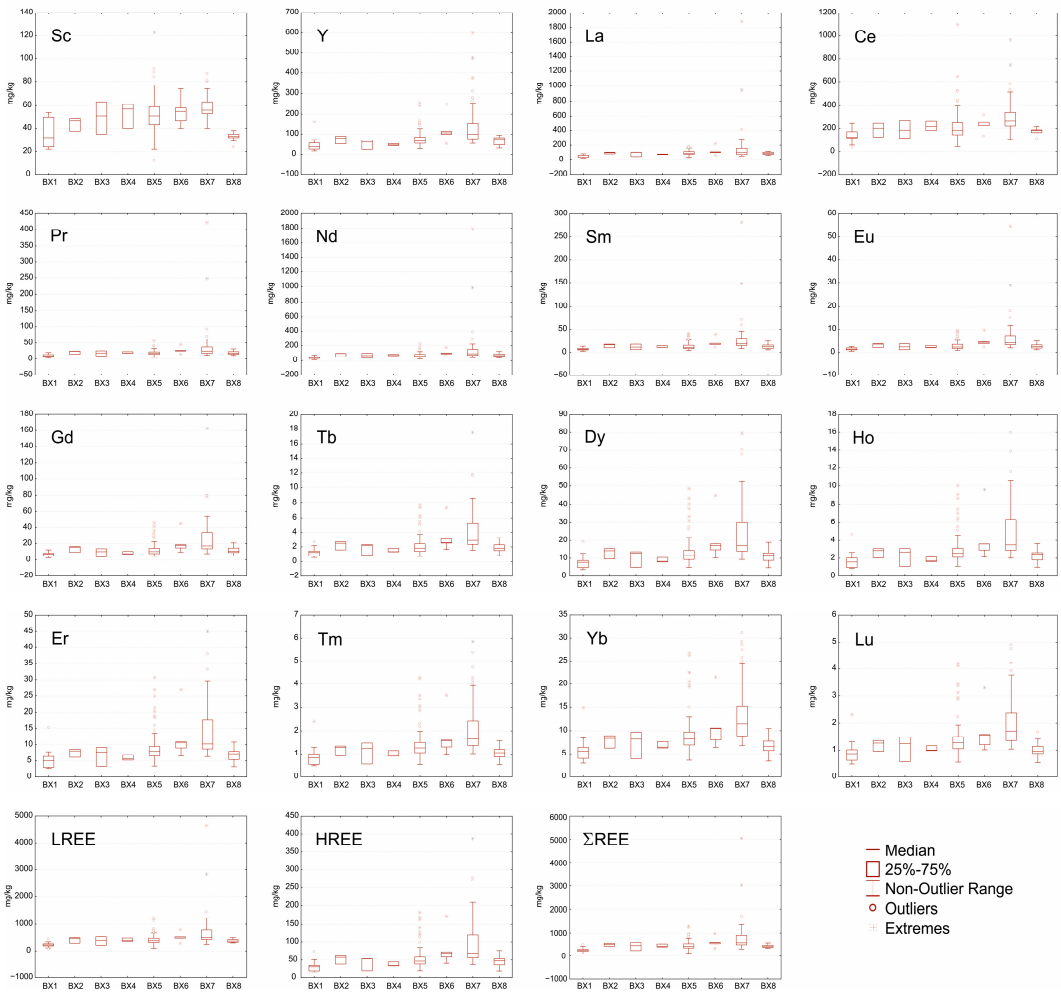

Figure 6. Box-and-whisker plots showing abundances of REE elements (including Sc and Y), LREE, HREE, and ΣREE (displayed in mg/kg) in the Croatian karst bauxite horizons. The plots represent univariate statistics of geochemical data (descriptor variables min–max, median, and first and third quartile values) for each bauxite horizon (BX1–BX8).

Among the bauxite horizons, the highest ΣREE contents were observed in the Middle Eocene (BX6) and Upper Eocene (BX7) bauxites, which exhibited median values of 575 and 568 mg/kg, respectively (Figure 6). This indicates a significant enrichment of REE during these geological periods, calling for more scrutiny of their appearance and distribution, especially by means of distinctive statistical models, as mentioned before. Conversely, bauxites from the Upper Jurassic (BX2), Lower Cretaceous (BX3), Upper Cretaceous (BX4), Paleocene (BX5), and Neogene (BX8) deposits exhibited similar median ΣREE contents, with values of 500, 441, 421, 414, and 398 mg/kg, respectively. The Upper Triassic (BX1) bauxites presented the lowest median ΣREE content of 250 mg/kg. These findings suggest that the geological period significantly influences the REE content in bauxite deposits, with Eocene bauxites showing notable enrichment compared with other periods. Furthermore, all analyzed bauxite samples contain higher concentrations of LREE compared with HREE. The most abundant REE is Ce in all Croatian karst bauxite horizons (med. 120–260 mg/kg). Cerium (Ce) exhibits the highest concentration in samples across all horizons (Figure 6), except for two Upper Eocene deposits (BX6 and BX7), which display significantly elevated concentrations of lanthanum (La) and neodymium (Nd).

Normalized REE patterns offer significant information when evaluated using different reference materials. Chondrite normalization highlights that REE distribution and enrichment are primarily influenced by the bauxite's parent material, whereas normalization to

the upper continental crust can elucidate the role of bauxitization processes in shaping REE distribution within a bauxite profile [37]. The chondrite-normalized REE distribution patterns reveal both shared characteristics and notable distinctions among the analyzed bauxite horizons (Figure 7a). While all groups exhibit typical LREE enrichment with negatively sloping patterns, relatively flat HREE, and consistent negative Eu anomalies, subtle yet significant differences emerge. The absence of a positive Ce anomaly in the Upper Jurassic (BX2) bauxites, which contrasts with its presence in other horizons, may reflect unique redox conditions during their formation. Furthermore, the extent of REE enrichment relative to chondrite varies across groups. The Upper Triassic (BX1) horizon displays comparatively lower enrichment levels, particularly for LREE, while horizons such as the Middle Eocene (BX6) and Upper Eocene (BX7) demonstrate pronounced LREE enrichment, with enrichment factors exceeding several hundred times. These variations likely reflect differences in the geochemical composition of the parent material and the environmental or diagenetic conditions that governed bauxitization. Normalization to the upper continental crust (Figure 7b) highlights significant differences among the bauxite horizons, particularly in the degree of HREE enrichment and the presence of subtle anomalies. The Upper Triassic horizon (BX1) consistently displays the lowest REE concentrations across the spectrum compared with the other horizons, reflecting either a weaker influence of bauxitization processes or compositional differences in its precursor material. Middle Eocene (BX6) and Upper Eocene (BX7) bauxites stand out with enhanced overall REE enrichment, which may reflect localized geochemical processes or microenvironmental conditions that favored the retention or concentration of heavier REEs.

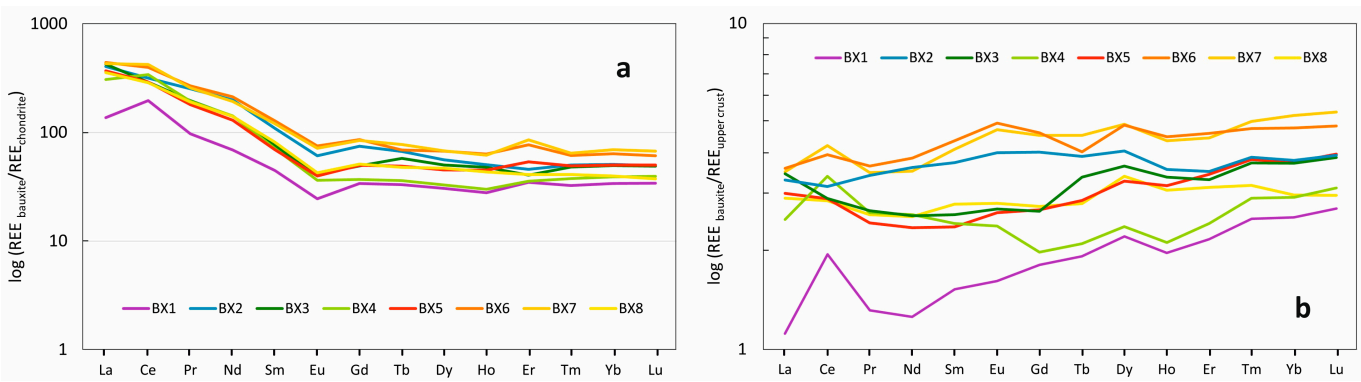

Figure 7. REE patterns for median values from the Croatian karst bauxite horizons (BX1–BX8) normalized to (**a**) chondrite and (**b**) upper continental crust. The normalization factors are from [55] (chondrite) and [60] (UCC).

The median values for ΣLREE/ΣHREE, $(La/Yb)_N$, $(La/Sm)_N$, and $(Gd/Yb)_N$ ratios in the Croatian karst bauxite samples are as follows: ΣLREE/ΣHREE from 6.78 to 10.49, $(La/Yb)_N$ from 4.17 to 9.44, $(La/Sm)_N$ from 3.4 to 5.23, and $(Gd/Yb)_N$ from 0.84 to 1.5 (Table 1). The median values of the La/Y ratios range from 0.93 to 1.72. Ce and Eu anomalies are evident in all bauxite groups. These anomalies are indicated by the Ce/Ce* and Eu/Eu* ratios. The Ce/Ce* index varies among the studied groups, with values ranging between 0.96 and 1.43. Higher values are associated with the Upper Triassic (BX1), Lower Cretaceous (BX3) and Upper Cretaceous (BX4) bauxites, while a slightly negative anomaly is present in the bauxites of the Upper Jurassic (BX2). Europium produces constant negative anomalies in all samples, with Eu/Eu* ratios comprised between 0.62 and 0.72.

Table 1. Geochemical parameters of REE and selected ratios in the Croatian karst bauxite horizons. The subscript "N" refers to values normalized to chondrite.

Horizon		ΣREE	ΣLREE	ΣHREE	ΣLREE/ ΣHREE	La/Y	Sm/Nd	Eu/Eu*	Ce/Ce*	$(La/Yb)_N$	$(La/Sm)_N$	$(Gd/Yb)_N$
BX1	min	83.14	67.90	15.24	3.12	0.39	0.18	0.56	0.97	2.28	2.20	0.59
	max	484.44	433.18	74.67	10.40	1.92	0.27	0.72	2.33	8.84	5.20	1.20
	mean	262.66	228.62	34.04	7.11	1.00	0.21	0.63	1.60	4.73	3.51	0.94
	med	250.09	218.68	31.20	7.75	0.93	0.20	0.62	1.43	4.17	3.49	0.91
	st. dev	116.71	103.75	17.57	2.43	0.49	0.03	0.05	0.49	1.89	0.93	0.20
BX2	min	322.56	283.82	38.74	7.33	1.11	0.18	0.66	0.87	7.50	3.49	1.19
	max	543.00	481.39	61.61	7.81	1.60	0.20	0.67	1.19	8.92	5.13	1.49
	mean	455.05	402.49	52.56	7.62	1.34	0.19	0.66	1.01	8.31	4.19	1.39
	med	499.60	442.27	57.33	7.71	1.31	0.19	0.66	0.96	8.51	3.94	1.48
	st. dev	116.78	104.62	12.16	0.26	0.25	0.01	0.01	0.16	0.73	0.85	0.17
BX3	min	230.23	209.88	20.35	7.32	1.49	0.17	0.67	1.00	7.34	3.64	0.82
	max	570.92	517.45	53.47	10.31	1.84	0.19	0.72	1.36	8.56	5.69	1.35
	mean	414.18	371.89	42.30	9.10	1.68	0.18	0.70	1.22	7.85	4.68	1.00
	med	441.40	388.33	53.07	9.68	1.72	0.18	0.72	1.28	7.64	4.71	0.84
	st. dev	171.97	154.44	19.01	1.58	0.18	0.01	0.03	0.19	0.63	1.03	0.30
BX4	min	386.60	352.09	33.89	10.20	1.53	0.16	0.69	1.19	7.11	3.48	0.90
	max	512.83	468.19	44.64	11.42	1.74	0.18	0.74	1.51	8.10	4.33	1.09
	mean	440.16	402.48	37.68	10.70	1.63	0.17	0.71	1.36	7.64	4.01	0.99
	med	421.05	387.16	34.51	10.49	1.62	0.17	0.71	1.40	7.70	4.23	0.97
	st. dev	65.25	59.55	6.04	0.64	0.11	0.01	0.03	0.16	0.50	0.47	0.10
BX5	min	114.36	94.03	20.33	3.92	0.63	0.12	0.57	0.63	2.77	1.73	0.40
	max	1295.34	1233.11	183.37	19.82	2.20	0.30	0.77	10.19	13.84	13.33	2.17
	mean	467.62	412.74	54.89	7.88	1.33	0.19	0.70	1.28	7.40	5.34	1.09
	med	413.85	368.67	46.78	7.75	1.33	0.18	0.70	1.05	7.39	5.23	1.06
	st. dev	200.69	179.57	29.04	2.11	0.34	0.03	0.04	0.96	1.94	2.25	0.35
BX6	min	327.25	286.20	41.05	4.68	0.89	0.19	0.70	0.77	6.42	3.23	1.23
	max	980.22	807.78	172.44	7.98	1.31	0.22	0.73	1.22	9.19	4.08	1.70
	mean	597.48	514.73	82.76	6.79	1.04	0.20	0.72	1.03	7.37	3.66	1.44
	med	575.18	505.76	69.42	7.01	0.95	0.20	0.72	1.02	6.93	3.54	1.44
	st. dev	237.61	187.57	51.63	1.24	0.17	0.01	0.01	0.17	1.07	0.38	0.17
BX7	min	299.35	243.54	37.70	3.60	0.43	0.15	0.67	0.07	3.64	2.09	0.90
	max	5044.76	4656.72	388.04	15.70	12.20	0.26	0.82	4.46	48.19	5.00	4.82
	mean	769.29	671.77	97.52	7.05	1.23	0.21	0.72	1.31	7.48	3.43	1.48
	med	568.63	482.94	69.57	6.78	1.00	0.20	0.72	1.14	6.07	3.40	1.37
	st. dev	643.13	591.93	62.82	2.00	1.54	0.02	0.03	0.64	6.74	0.65	0.61
BX8	min	325.17	292.17	19.95	6.24	0.92	0.16	0.63	0.62	5.60	2.94	0.81
	max	557.05	480.77	76.28	15.60	2.46	0.20	0.67	1.53	15.06	8.48	1.90
	mean	416.25	370.59	45.66	8.86	1.49	0.18	0.65	1.09	9.35	4.83	1.36
	med	397.88	359.41	47.91	8.52	1.41	0.18	0.66	1.03	9.44	4.58	1.50
	st. dev	79.15	66.48	16.03	2.92	0.51	0.01	0.01	0.32	2.69	1.58	0.33

4.2. Statistical Analysis Applied to the Paleogene Bauxite Horizon

Lower Paleogene bauxites in Croatia have been investigated extensively in many earlier studies, especially those addressing the orogenic evolution of the External Dinarides in the NE Adriatic and SW Dinaric regions of the ADCP [sensu 16]. However, in this case, we deal with issues perceived from a particular angle, which is the question of the occurrence of REE and the provenance of proto-bauxitic material in general in the early phases of bauxite genesis. As said earlier, DFA serves as an exceptionally advantageous tool in elucidating these matters. Selected bauxite groups represent the grouping criterion, which is independent of the analyzed variables (geochemical composition) and thus determines the strategy of analysis. The latter is conceptually centered on the construction of a characteristic discriminant function model (DFM), and, to this end, a discriminant analysis panel from the STATISTICA statistical software package, version 7.1 [61], was applied. In this process, the statistical package (linear discriminant function) automatically determines the best combination of variables so that the computed discriminant functions (DFs) provide optimal contributions to multi-group discrimination. Superfluous overlapping and possible

misapprehension of group memberships in the computed model are thus avoided, at any rate, to the extent that analysis is used for confirmatory purposes. The results presented in this work are summarized briefly in Table 2, which contains the multivariate test for the overall significance of discrimination together with the tests of residual roots (DFs). The Wilks' λ statistical test, used regularly in DFA, indicates an extremely low probability ($p < 0.05$), which is required to proceed smoothly in computing discriminant functions (DFs) and to select the number of functions that explain the maximum variation within groups. Based on these assumptions, it is obvious that the third discriminant function (DF3) can be omitted from further inspection because of both the probability issue ($p > 0.05$) and low variability (only 2.8% of the total variance).

Table 2. (**a**) Multivariate test for the overall significance of discrimination and (**b**) tests of residual roots.

(a)	
No. of variables	32
Wilks' lambda	0.0481
Approximate F ratio	8.341
Degrees of freedom	[96; 455]
p-level	$p < 0.000$

(**b**)

DF	Eigen value	Eigen (%)	Eigen cum (%)	Canon. R	Wilks' λ	Chi^2	df	*p*-level
1	7.224	84.94	84.94	0.937	0.048	509.9	96	0.000
2	1.036	12.24	97.18	0.713	0.395	155.9	62	0.000
3	0.242	2.82	100.00	0.805	0.905	36.4	30	0.194

5. Discussion

5.1. The Variation of Trace Elements and REE in Different Bauxite Horizons

The geochemical imprint of Croatian karst bauxite horizons has demonstrated that the temporal axis plays a significant role in their differentiation, indicating varying conditions during the evolution of the ADCP from the Late Triassic to the Miocene [42]. The lowest REE concentrations (med. 250 mg/kg) are observed in the Upper Triassic (BX1) bauxites. In contrast, the Middle Eocene (BX6) and Upper Eocene (BX7) bauxites are enriched in REE content, with median values slightly exceeding 550 mg/kg. Similar trends have been identified in Croatian karst bauxites in Dalmatia [22,37,62]. These findings align with the typical total REE concentrations in karst bauxites, which range from 100 to 500 mg/kg [31]. The results of the geochemical analyses of Croatian karst bauxites indicate that the geological period significantly influences the REE content in bauxite deposits. This is particularly evident in the notable enrichment observed in the Eocene deposits, with the Middle Eocene (BX6) and Upper Eocene (BX7) horizons exhibiting higher ΣREE concentrations (Figure 4).

Concerning Ga, a valuable critical metal whose exploration in bauxites has attracted global attention in recent years [63], the concentrations in Croatian karst bauxites (med. 41–62 mg/kg) align with the typical trend observed in karstic bauxites (avg. 59 mg/kg) [63]. The highest enrichment (med. 62 mg/kg) is observed in Upper Cretaceous aluminum-rich bauxites (BX4), and the lowest in the Upper Triassic (BX1) and Miocene (BX8) bauxites (41–44 mg/kg).

The distribution and fractionation of REE in bauxites are influenced by factors such as the parent rock composition, soil pH, organic and inorganic ligands, ionization potential, microbial activity, and stability of REE-bearing minerals [28,56,64]. Water–rock interactions, including sedimentation, chemical weathering, and diagenesis under varying Eh and pH conditions, also play a key role [65,66]. The pH of the depositional environment is a critical factor governing the enrichment and fractionation of REE in bauxite. Under acidic

conditions, REE exhibit increased mobility, with HREE preferentially leached due to their tendency to form aqueous complexes, resulting in a relative enrichment of LREE through adsorption onto mineral surfaces. Conversely, in neutral to alkaline environments, HREE precipitate, leading to distinct fractionation patterns between LREE and HREE ([67], and references therein). ΣLREE/ΣHREE ratios of 6.78 to 10.49 indicate a moderate fractionation of LREE from HREE, with higher values suggesting a greater degree of enrichment of LREE relative to HREE (Table 1, Figure 8).

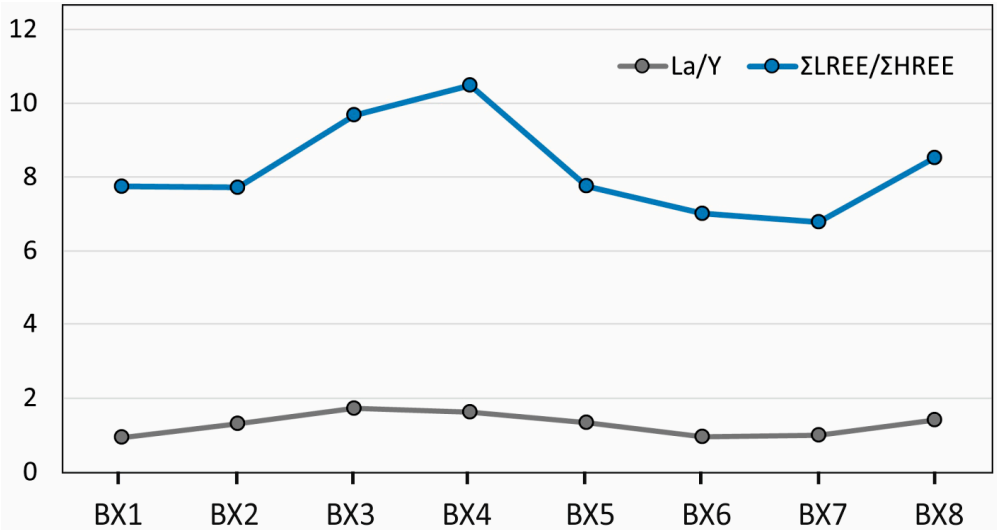

Figure 8. Comparison of La/Y and ΣLREE/ΣHREE value curves for median values in the Croatian karst bauxite horizons.

$(La/Yb)_N$, $(La/Sm)_N$, and $(Gd/Yb)_N$ ratios are widely used to assess the fractionation of LREE from HREE in karst bauxite deposits. The $(La/Yb)_N$ ratios, ranging from 4.17 to 9.44, similar to the ΣLREE/ΣHREE ratios, reflect the preferential enrichment of lighter over heavier rare earth elements in Croatian karst bauxites (Figure 9). The $(La/Yb)_N$ ratio in karst-type bauxites is governed by pH variations in the soil solution [56]. The $(La/Sm)_N$ ratios, which oscillate from 3.4 to 5.23, indicate that the enrichment of LREE relative to mid-range REE (MREE) is less pronounced than the enrichment of LREE relative to HREE in analyzed bauxites. The $(Gd/Yb)_N$ ratios provide insight into the relative behavior of mid-range REE compared with heavier REE. Ranging from 0.84 to 1.5, they demonstrate only slight fractionation between MREE and HREE in the bauxite horizons. Upper Jurassic (BX2) and Miocene (BX8) bauxites exhibit the highest fractionation ratios, in contrast to Upper Triassic (BX1) and Upper Eocene (BX7) bauxites, where fractionation is the least pronounced. Using chondrite-normalized $(La/Yb)_N$ (9.2), $(La/Sm)_N$ (4.2), and $(Gd/Yb)_N$ (1.4) ratios of the Upper Continental Crust (UCC) composition [60], it is apparent that the fractionation between LREE and MREE, as well as between MREE and HREE, are closely aligned with those observed in the studied bauxite groups. Conversely, the $(La/Yb)_N$ ratio, which exhibits the greatest variability among the groups, is generally lower than that of the UCC, with the exception of the Upper Jurassic (BX2) and Miocene (BX8) bauxites. This pattern is further corroborated by the UCC-normalized spider diagram of REE distribution within the groups (Figure 7b), which reveals a relative enrichment of HREE over LREE compared with the UCC. The diagram clearly illustrates that HREE are more abundant than LREE in the groups exhibiting a lower $(La/Yb)_N$ ratio.

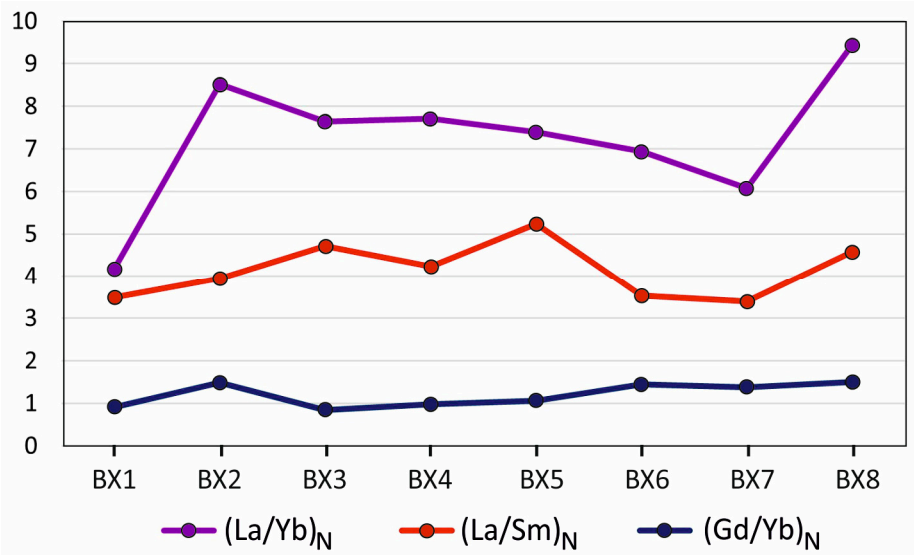

Figure 9. Median REE fractionation ratios for the Croatian karst bauxite horizons (BX1–BX8).

The behavior of REE in bauxite deposits is controlled by the physicochemical conditions, particularly Eh and pH, of the environment during weathering processes that lead to their formation [68]. The La/Y ratios were calculated to help interpret the REE distributions in the bauxite horizons and determine the pH conditions during the bauxitization process. Variations in La/Y in bauxites reflect changes in the pH during bauxitization [33,62,69]. Specifically, La/Y values less than 1 indicate acidic conditions, as observed in the Upper Triassic (BX1) and Middle Eocene (BX6) bauxites, whereas values greater than 1 indicate basic conditions, as observed in other horizons (Figure 10). According to Crnički [70], weathering under basic conditions leads to the enrichment of LREE, while under acidic conditions, their concentration, in relation to HREE, decreases. A comparison of the ΣLREE/ΣHREE value curves with those for the La/Y ratio for the bauxite groups (Figure 8) reveals a similar trend, confirming that the bauxitization processes for the Upper Triassic (BX1) and Middle Eocene (BX6) bauxites likely occurred in an acidic environment, whereas basic conditions prevailed for the other groups.

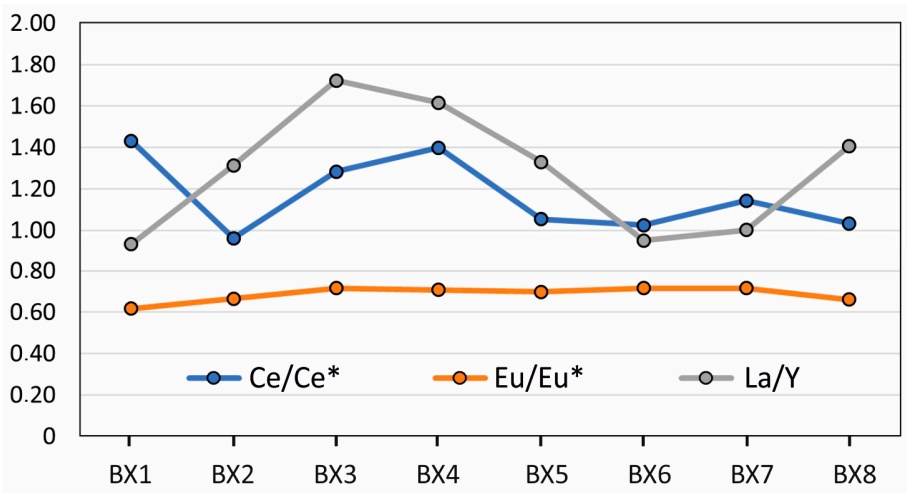

Figure 10. Variation in Ce-anomalies, Eu-anomalies, and La/Y ratios for the Croatian karst bauxite horizons (BX1–BX8). The values represent the median values for a particular horizon.

The range of the median Eu and Ce anomalies in the bauxite horizons adds further detail to the REE distribution patterns. As reported in the literature, the strongly oxidizing environment characteristic of the bauxitization process leads to unique behavior for cerium

(Ce), which transitions from the 3^+ to 4^+ valence states and commonly precipitates as Ce^{4+} oxides or is incorporated into Fe-hydroxides, while other REE remain in solution [30,69]. The values of the median Ce/Ce* ratios, ranging from 0.96 to 1.43, suggest that the bauxite deposits were subject to variable geochemical processes that differently fractionate Ce from other REE (Figure 10). The predominantly positive Ce anomalies observed in the bauxite horizons signify persistent oxidizing conditions throughout the alteration process. These conditions have resulted in varying degrees of Ce enrichment, which are influenced by local environmental factors. In contrast, the Eu/Eu* ratio consistently remains below 1, indicating persistent negative Eu anomalies in chondrite-normalized patterns. The stable nature of the Eu/Eu* ratio across the groups, with values ranging from 0.62 to 0.72, underscores its independence from weathering processes, aligning with observations from numerous studies on other bauxite deposits [30]. Additionally, no correlation exists between Eu/Eu* and Ce/Ce* (Figure 10), confirming that the Eu/Eu* values were not influenced by the pH conditions of the bauxitization process. Consequently, the Eu anomaly serves as a reliable proxy for identifying bauxite source rocks. Among the several proxies used to determine the parent rock(s) of karst bauxites, the Eu anomaly—defined as an index of chemical differentiation minimally affected by minor fractionation during intense weathering—proves particularly useful for elucidating the parent material of these deposits (e.g., [29,56,71,72]). While karst bauxite deposits are typically hosted within carbonate successions, the dissolution of carbonate bedrock alone is insufficient to explain their formation. Instead, it is likely that a diverse range of protoliths contributed the material necessary for bauxitization [1,3,29]. Although Eu/Eu* ratios generally correlate with magma oxidation states and oxygen fugacity, literature reports that in the context of bauxite deposits, negative Eu anomalies are indicative of felsic parental rocks. Conversely, the presence of positive or absent Eu anomalies may suggest the involvement of mafic material in bauxite formation [30,32,73]. The Eu/Eu* ratio in the bauxite horizons is relatively close to that of the Upper Continental Crust (Eu/Eu* = 0.66 [60]). Lower median values of the Eu anomaly in the Upper Triassic (BX1) suggest felsic influence, whereas higher values in the Upper Cretaceous (BX4), Mid-Eocene (BX6), and Upper Eocene (BX7) are more "mafic" than the UCC.

Al and Ti, with low water/upper crust partition coefficients and residence times, are key in tracing sedimentary rock parent material [73]. Previous studies have used TiO_2/Al_2O_3 ratios to identify bauxite protoliths, considering it a sensitive index of parental affinity, which records the composition of the protolith when both elements exhibit conservative behavior [28,56,73]. The correlation between the Al_2O_3 and TiO_2 contents in the studied samples yields a correlation coefficient (R2) of ~0.5, suggesting that the TiO_2/Al_2O_3 ratio remained mostly unchanged during bauxitization, making it representative of the parent rock. Discriminant analysis of the Paleogene bauxite horizons plots these two elements near each other, confirming their positive correlation (more is elaborated further in the text). As previously mentioned, Eu anomalies indicate chemical differentiation and often retain values closer to those of the protolith than other provenance proxies [56]. As shown in Figure 11a, the TiO_2/Al_2O_3 and Eu/Eu* ratios for all groups plot near the UCC, with the bauxites of the Lower Cretaceous (BX3), Paleocene (BX5), Lower Eocene (BX6), Upper Eocene (BX7), and Miocene (BX8) horizons shifting more toward the basalt values. Sm/Nd ratios, like Eu/Eu* values, reflect chemical differentiation and a decrease in value during magmatic fractional crystallization [56] and exhibit only minor fractionation during intense tropical weathering [74]. Thus, they have been effectively used to identify parent rocks of bauxites [28,56]. In the Eu/Eu* vs. Sm/Nd binary diagram (Figure 11b), all bauxite groups are positioned near the fields representing Post-Archean Australian Shales (PAAS) and cratonic sandstones. Specifically, the Lower Cretaceous (BX3), Lower Eocene (BX5), Middle

Eocene (BX6), and Miocene (BX8) align closely with or fall within two distinct mixing curves: one between cratonic sandstones and basaltic andesites, and the other between PAAS and basaltic andesites. The presence of andesite, a characteristic product of explosive volcanism, as an end member in both mixing curves suggests a distant magmatic origin for the parental material(s) in the Croatian karst bauxite horizons.

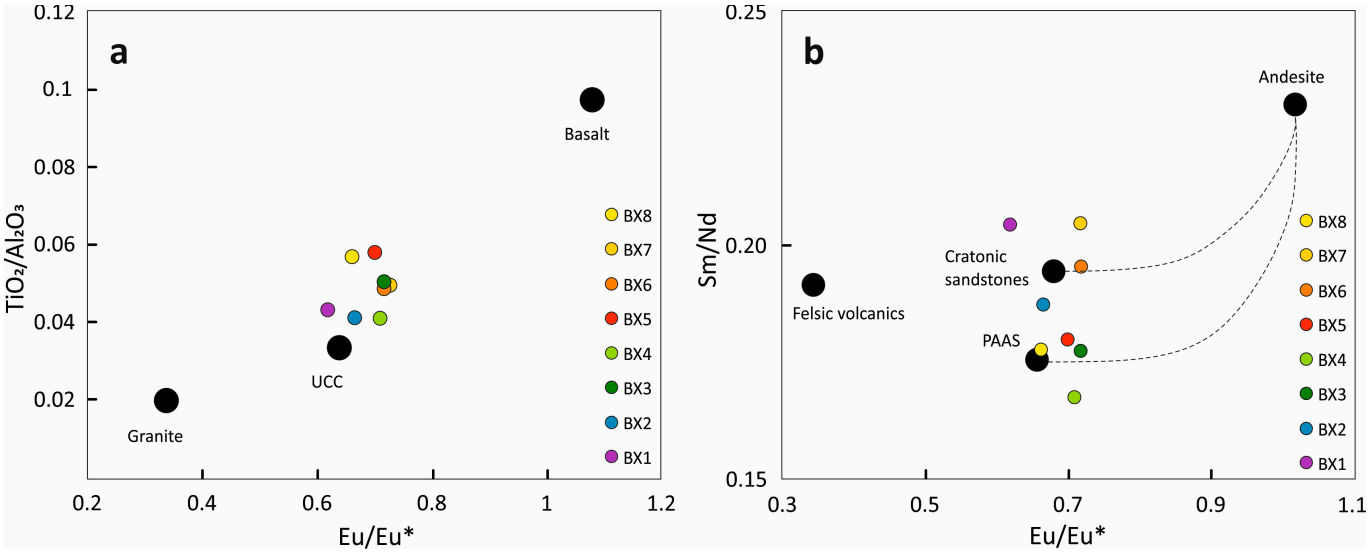

Figure 11. (**a**) Eu/Eu* and TiO_2/Al_2O_3 binary diagram (modified after [28]). (**b**) Eu/Eu* vs. Sm/Nd binary diagram showing mixing lines between average standard lithologies. Modified after [56]. Colored circles represent the median values of the Croatian karst bauxite horizons (BX1–BX8).

Nickel (Ni) is readily soluble as Ni^{2+} ions under intense weathering conditions, facilitating its mobilization within the weathering profile. However, in bauxite deposits, Ni concentrations can be significantly influenced by the adsorption processes associated with the presence of iron oxyhydroxides, which are commonly abundant in these environments. Such adsorption can alter the Ni/Cr ratios, thereby reducing their reliability as direct indicators of protoliths. Consequently, these ratios must be interpreted with caution, considering the potential impact of secondary processes [56]. The composition of the bauxite groups in the Cr vs. Ni diagram was compared with that of other Mediterranean karst bauxites (Figure 12). Croatian karst bauxites of all horizons show similarities to bauxites from Campania, Sardinia, Turkey, and the Zagros Simply Fold Belt (ZSFB) in southwest Iran. The Upper Triassic (BX1) group exhibits the lowest Cr and Ni values, whereas the Upper Eocene (BX7) group is closest to the values observed in Apulia and Greece. A notable similarity can also be observed with the Montenegrin bauxites [36] of the same age, indicating potential parallels in the geochemical characteristics and formation processes of these deposits.

Bivariate plots of the Cr and Ni concentrations were used to identify the precursor rock(s) of the eight Croatian karst bauxite horizons (Figure 13). In the diagram, they fit well into the karst bauxite field, with the exception of the Upper Triassic bauxites (BX1) that plot near shale and slate, and the Upper Jurassic (BX2) and Lower Cretaceous (BX3), which are positioned closer to basalt. A progressive shift from felsic to ultrabasic rocks can be observed in progressively younger Croatian karst bauxite horizons. These results are consistent with the findings of the previous study [42].

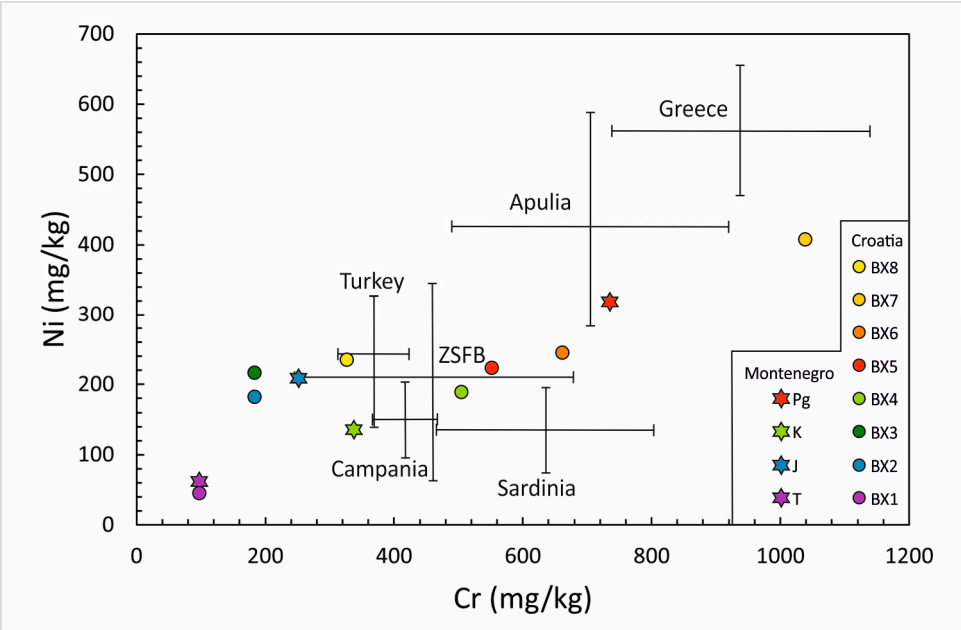

Figure 12. Binary diagram of Cr vs. Ni showing the median composition of the bauxite horizons relative to other Mediterranean karst bauxite deposits represented as average values and standard deviations. Colored circles represent the median values of the Croatian karst bauxite horizons (BX1–BX8). Colored stars represent median values of Montenegrin bauxite from four stratigraphic horizons [36] (modified after [28]).

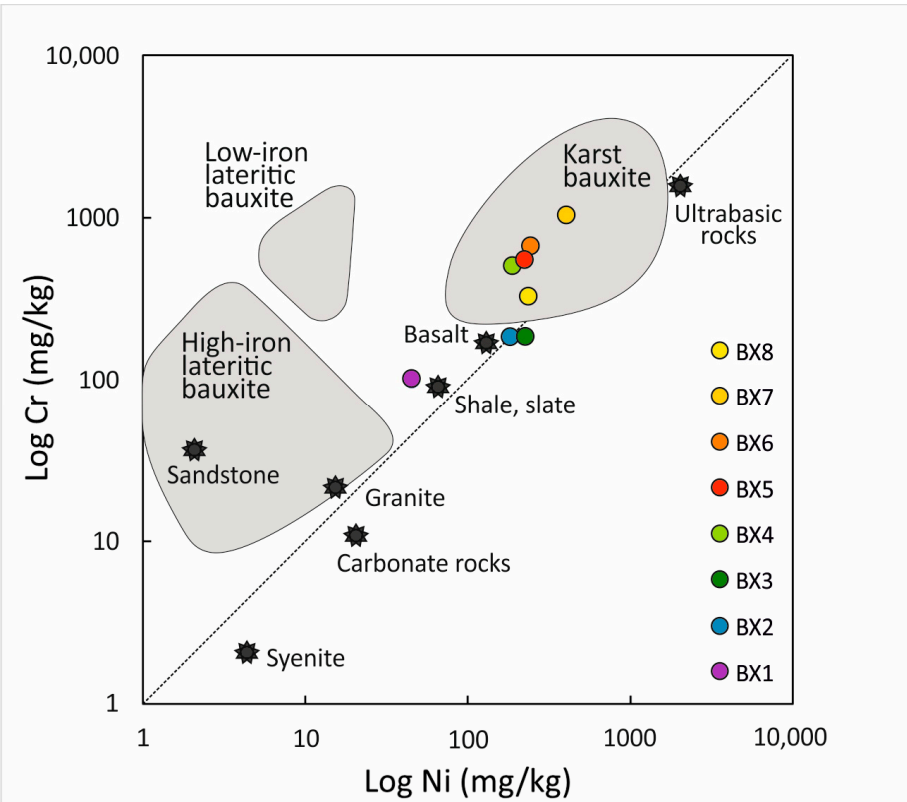

Figure 13. Binary diagram showing the concentration of Cr vs. Ni in laterite- and karst-type bauxites and potential precursor rocks. Colored circles represent median values of the Croatian karst bauxite horizons (BX1–BX8) (modified after [75]).

5.2. Discrimination of the Paleogene Bauxite Horizons

An essential step in DFA is the labeling of selected DFs, as ascribing an appropriate geological significance to the selection of qualities (geochemical variables) is of prime importance to the process of discrimination. It is essential to comment that the labeling of each selected DF is fundamentally the conversion of a statistical (structural) model into a geological (process) model. In the current analysis, simple scatterplots (variable loadings vs. group means, Figure 14a,b) built on the first two DFs (DF1–DF2) represent the solid basis for constructing the geological DFM. As can be seen from the model, the over-important DF1 (accounting for 85% of total variability) is all about variables indicating the discrimination between groups based on provenance issues. This division can be understood as revealing an inverse relationship between the opposing variables, geochemical elements strongly separating the BX5A group from the rest. By this discrimination, even bauxites of the same age but belonging to different paleogeography and tectonic settings—Paleocene bauxites from the Dinaric (BX5D) and Adriatic (BX5A) regions—are dissimilar. As seen from the adjacent diagrams (Figure 14a,b), BX5A (Adriatic cluster—Istria and North Adriatic Islands) is associated with elements forming the building blocks of various aluminosilicate minerals, typically clays (SiO_2, Al_2O_3, K_2O, and Na_2O) together with Fe_2O_3, TiO_2, etc., which, together with the former, also represent abundant compounds of proto-bauxitic source materials. On the other side, there are three remaining groups (the Dinaric cluster—BX5D, BX6, and BX7), whose elemental association (MnO, Cr_2O_3, P_2O_5, CaO, Ni, V, etc.) indicates mineral deposits related to precursor mafic and ultramafic rocks. To the latter also gravitate REE and some trace elements such as Cd, Zn, and Mo. Therefore, DF1 can be easily recognized as a function of provenance (felsic vs. mafic/ultramafic) controlling the REE distribution. DF2 is of minor importance (12%), indicating variations in some other elements, particularly the increase in Fe_2O_3, Pb, Co, and others in the BX5D group, together with a slight increase in Hg and Sr in the BX7 group, and vice versa.

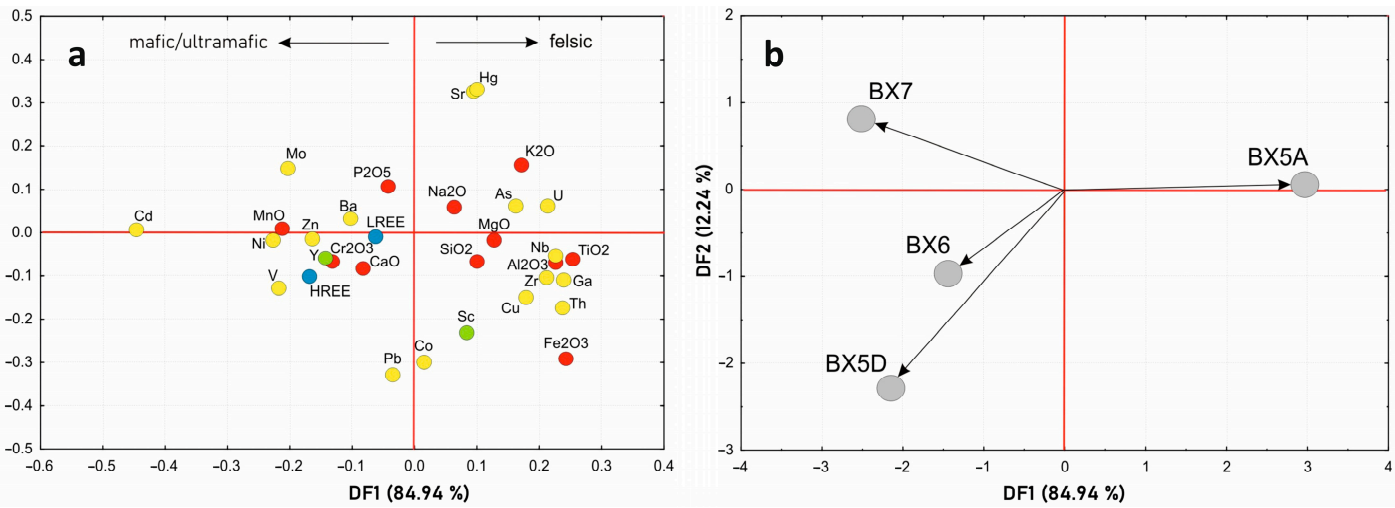

Figure 14. Comparison between variables and Croatian karst bauxite horizons in the discriminant function model (DFM) of the clr-transformed data: scatterplots of (**a**) variable loadings and (**b**) bauxite horizons in the reduced discriminant space of the first two discriminant functions (DF1–DF2).

Considering everything, an overarching account of the origin and emplacement of a part of the Paleogene bauxite deposits on the ADCP (Lower Paleogene bauxites) with respect to the dynamic tectonostratigraphic scheme and changing paleoenvironment is thoroughly elucidated by multivariate statistical models exposed in earlier works [17,19,20].

However, in order to provide more clarity about the REE enrichment in younger horizons (BX5–BX7), the latter needs to be scrutinized geochemically using the same tools

as in the case of the entire geological history of ADCP [42]. In contrast to the earlier model highlighting the geochemical differences in successive geological periods (from Triassic to Miocene), in this case, the focus is on the geochemical variations affecting geographical emplacement within the same period (the Paleogene). As defined by the constructed discriminant function model (DFM) for Paleogene horizons (Figure 14), DF1 is all about the provenance of the proto-bauxite material, in which the position of REE (more prominently HREE) shows affinity to a group of elements (both major and trace) characteristic of mafic and ultramafic rocks. To avoid repeating what is explained earlier, it is of importance whence the precursor materials rich in REE came that have later deposited on ADCP to form bauxites of the Paleogene age. As indicated in earlier studies [17,20], BX5A, BX6, and BX7 have been depositories for the ingress of REE from a source external to ADCP, most probably from the Dinaridic ophiolite belt with ultramafic massifs and genetically associated sedimentary formations (e.g., [76]) east of the study area. As seen in the variable diagrams, REE are associated with major (CaO, P_2O_5) and trace element (MnO, Cr_2O_3) oxides at the negative pole of DF1, indicating a possible mineral assemblage in the Dinaric cluster enriched in REE (Figure 14). It is suggested that the REE in karst bauxites are adsorbed mainly on the surface of clay-sized constituents or by detrital and authigenic REE-bearing minerals [31]. REE–fluoro–carbonates of the bastnäsite group are the most frequent REE minerals in karst bauxites [73] and are associated with detrital zircon and REE phosphates (monazite and xenotime), such as Apulian and Abruzzi karst bauxites [77,78]. In Montenegrin karst bauxites, phosphates with REE (monazite and xenotime), REE carbonates–Ce, and Nd are detected [33,36]. In Croatian karst bauxites of the Upper Eocene age in Dalmatia, monazite-(Ce) and xenotime-(Y) were identified as detrital REE minerals as well as authigenic florencite-(Ce) [37], who reported that the absence of REE fluorcarbonates could be related to unfavorable pH conditions (lower pH values). Our study reveals that REE are associated with the CaO component and P_2O_5, which points to an assemblage that indicates the possible presence of REE–phosphates. The P_2O_5 content is also related to MnO, suggesting the possible scavenging role of Mn–oxyhydroxides as a proxy channel for the accumulation of phosphorus in the Dinaric cluster. In the latter case, the Fe_2O_3 component is completely excluded from the process, leaving the main role to Mn. It is widely understood that phosphate adsorption by goethite and other Fe oxyhydroxides strongly influences its concentration in soils and strongly oxidized aquatic environments [79], a process that is important for controlling phosphate concentration in the bauxite-forming paleoenvironment. As for the obvious depletion of ferric constituents in the BX5D-BX6-BX7 cluster, some investigations show that Zn may substitute for Fe in Fe oxy-hydroxides (goethite) based on the fact that Zn has been detected to increase with the MnO content in bauxite [80]. Zn is very close to MnO in the variable scatterplot (Figure 14a). However, the mineralogical nature of the Zn and Mn components and their relation to REE in bauxite deposits still remain to be better understood in future investigations.

The opposite pole of the function occupies a single BX5A group, referred to as the Adriatic cluster, characterized by bauxite more enriched in aluminum and related compounds (Al_2O_3, Fe_2O_3, TiO_2, Ga, and Nb) as well as other "conservative" (that is, relatively immobile) elements, such as Th, Zr, and U). This leaves the isolated BX5A group as clayey in general (SiO_2, K_2O, Na_2O, and MgO), indicating that the felsic rocks were the primary origin of the precursor material (Figure 14a,b), possibly from the Alpine region. As a rule, this elemental assemblage is significantly depleted with regard to REE content.

5.3. Croatian REE Resource Potential of Karst Bauxites

The assessment of REE potential in Croatian karst bauxites generally depends on their geological mode of occurrence. In Figure 15, bauxite deposits, occurrences, and exploited

areas are marked as medium groups of bauxite deposits. The small groups of bauxite deposits refer to very small surface occurrences of bauxite. Traditionally, deposits in the Croatian karst region have been classified based on the mode of exploitation as either open-pit mining or underground mining [81]. In Šibenik-Knin County, part of Central Dalmatia (Figures 1b and 6), which serves as an example of areas containing medium and small groups of bauxite deposits (Figure 15), most proven reserves suitable for open-pit mining account for less than 17% of the total proven reserves [82]. Open-pit exploitation was successfully practiced until the late 1980s on small bauxite ore deposits, whose densities in the Istria Peninsula (Figures 1b and 2) averaged between 40 and 45 deposits per km^2, with the total exploited reserves reaching 150,000 t [81]. In the aforementioned region, more than 7.500 deposits and bauxite occurrences have been discovered (Map of Mineral Resources of the Republic of Croatia). Generally, individual bauxite bodies in Northern, Central, and Southern Dalmatia (Figures 1b, 5, 6 and 7) were larger, ranging from 500 to 20,000 t. In Šibenik-Knin County (Figure 15), more than 700 deposits with proven reserves totaling 3,247,052 t of exploitable bauxite ore have been identified, of which 85% are unsuitable for open-pit mining [82]. According to available data from the Croatian Mining Directorate [27], the proven reserves of minable karst bauxite amount to approximately 6,500,000 t (data from 2011, when the exploitation of bauxite ceased owing to unfavorable market conditions), of which 85% was suitable for underground exploitation. It is estimated that the total potential exploitable reserves in Croatia could reach 12,000,000 t [83], dispersed across several hundred ore deposits. Although Croatia had a significant tradition of combined open-pit and underground bauxite mining during the 1980s, exemplified by one of the largest mines, Kalun (located in the city of Drniš, Figure 15) in Central Dalmatia, exploitation was abandoned by 1990 owing to market and technological constraints. Currently, the underground bauxite mining industry successfully employs longwall shearers for ore extraction [84]. The Mining Strategy of the Republic of Croatia [83] predicted that the annual bauxite production in Croatia could reach 1,500,000 t. The mineral potential of the Croatian karst bauxite region in Dalmatia with regard to REE was recognized by [40] and supported by the data obtained in this study. The total REE content in the Croatian bauxites ranges from 83 to 5045 mg/kg, with the majority of the remaining identified reserves located in the Dalmatian region. These deposits are primarily of Upper Eocene age (BX7) and have the highest total REE concentrations (med. 570 mg/kg). The results of a leaching study of Greek bauxite samples [85] indicate that up to 47% of the REE in bauxite are easily leachable. According to the same study, Greek bauxite deposits contain average REE concentrations in the range of 400–500 mg/kg of REE, which is slightly lower than those observed in Dalmatian bauxites. The leachability of REE is a function of the REE mineralogy [35]. There are only a few studies on REE mineralogy in Dalmatian bauxite ores [37,42], which would be essential for determining possible metallurgical processing. Studies have been conducted on ores from the Mamutovac deposit [86], which has potential for open-pit mining. Despite the significant potential of Croatian bauxite reserves, current technical and economic conditions render their exploitation economically unviable.

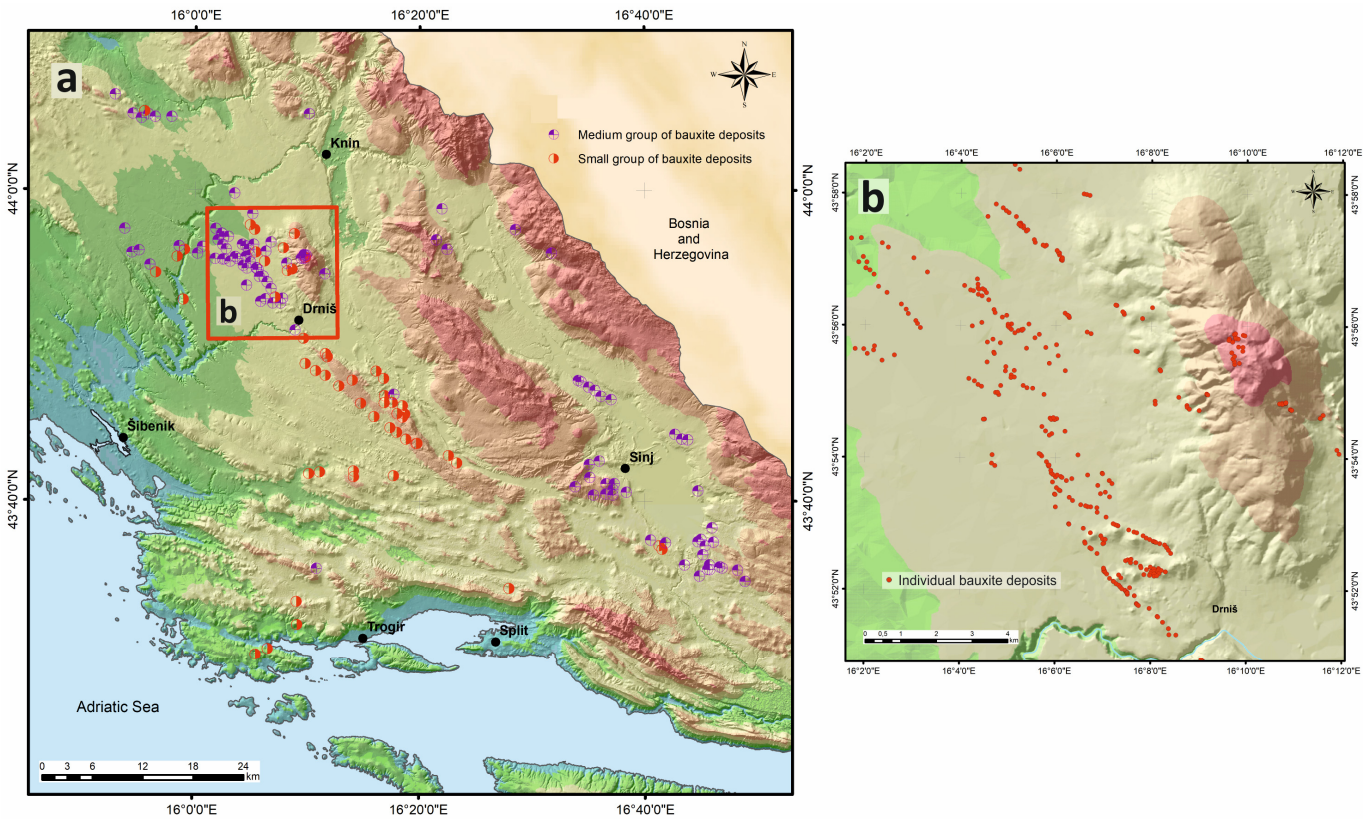

Figure 15. (**a**) Distribution of bauxite deposit groups in Central Dalmatia, (**b**) detailed density of individual deposits (source: Map of Mineral Resources of the Republic of Croatia, Croatian Geological Survey) [45].

6. Conclusions

The investigations performed in this study show that varying parent material as well as changing paleogeographical/paleotectonic settings from Triassic to Neogene times significantly affect the REE content in bauxite deposits, with noticeable enrichment in the Late Paleogene, which is particularly evident in the higher ΣREE contents of the Middle Eocene (BX6) and Upper Eocene (BX7) bauxite horizons. Generally, it has been shown that the performance of REE in bauxite deposits is contingent on physicochemical conditions, particularly Eh and pH, in the paleoenvironment during weathering processes that led to their formation. Various indices, REE fractionation ratios and patterns, as well as results of univariate and multivariate statistics (DFA) and developed models (DFM), were employed to scan the factors controlling the distribution and fractionation of REE in eight bauxite horizons emplaced in the Croatian part of the ADCP and to consider their possible extraction. These indicate prevailingly mafic/ultramafic precursor rocks (most probably from the Dinaridic ophiolite belt) as provenances of the original protobauxite material deposited on the ADCP during a series of more or less prolonged emersion phases and adhering climatic, tectonic, and volcanic events. The results show that, more often than not, this material is enriched in REE, particularly in the context of younger Paleogene bauxite horizons—from BX5, excluding the westernmost part of the ADCP (Istria and North Adriatic islands) to BX7. In this regard, the DFA performed on a particular set of bauxite groups—those of the Paleogene period—showed analogous results. Intentionally divided into four distinct groups (BX5 separated into Adriatic and Dinaric clusters, BX5A and BX5D), instead of originally three (BX5, BX6, BX7), Paleogene bauxites exhibited the typical pattern of felsic (BX5A) vs. mafic/ultramafic provenance of protobauxite material. The latter is enriched in REE (HREE in particular) together with accompanying trace assemblages (Cr_2O_3, Ni, V, etc.)

and major oxides (P_2O_5, CaO, and MnO), indicating the possible presence of the typical bauxite REE minerals such as phosphates in the aforementioned bauxites. Regarding Croatia's rare earth element resource potential, karst Dinarides bauxites exhibit a wide variety of deposit sizes, predominantly within the medium to small range. Historically, these deposits have been classified based on their extraction methods, either open-pit or underground mining. In Šibenik-Knin County, located in Central Dalmatia, open-pit mining once held significance but accounted for less than 17% of the total proven reserves, with the majority of economically viable deposits being more suited for underground extraction. Despite a strong legacy of bauxite mining, market challenges and technological constraints led to the near-complete cessation of activities by 1990. However, modern advancements, such as the adoption of longwall shearers in underground operations, indicate the potential for more efficient resource recovery. This highlights the need for further geological evaluations and could revive interest in the exploitation of both bauxites and rare earth elements within the Croatian Karst Dinarides.

Author Contributions: Conceptualization, E.K.G. and N.I.; methodology, Z.P. and S.M.; software, Z.P.; formal analysis, E.K.G. and Z.P.; resources, S.M. and N.I.; writing—original draft preparation, E.K.G. and Z.P.; writing—review and editing, N.I., N.G. and S.M.; visualization, E.K.G., N.I., Z.P., S.M. and N.G.; supervision, N.I.; project administration, Z.P.; funding acquisition, S.M. and N.I. All authors have read and agreed to the published version of the manuscript.

Funding: The research was funded by the Horizon 2020 EIT Raw Materials (European Institute of Innovation and Technology) project REEBAUX—Prospects of REE recovery from bauxite and bauxite residue in the ESEE region (project number 17089) and by the Ministry of Science, Education and Youth scientific project "Map of Mineral Resources of the Republic of Croatia" (project number MZOS-181-1811096-1104; in Croatian: Karta mineralnih sirovina Republike Hrvatske).

Data Availability Statement: The original contributions presented in this study are included in the article. Further inquiries can be directed to the corresponding author.

Acknowledgments: This work was supported by the Croatian Geological Survey (HGI-CGS) and the Ministry of Science, Education and Youth of the Republic of Croatia through the financing of the national research project "Map of Minerals Resources of the Republic of Croatia". The authors are grateful to the reviewers for their valuable feedback, which helped improve this manuscript. We also thank everyone who contributed to this research.

Conflicts of Interest: The authors declare no conflicts of interest.

References

1. Bárdossy, G. *Karst Bauxites: Bauxite Deposits on Carbonate Rocks*; Elsevier Scientific Publication: Amsterdam, The Netherlands, 1982; p. 441.
2. Schellmann, W. Geochemical differentiation in laterite and bauxite formation. *Catena* **1994**, *21*, 131–143. [CrossRef]
3. Bárdossy, G.; Combes, P.J. Karst bauxites: Interfingering of deposition and palaeoweathering. *Spec. Publ. Int. Assoc. Sedimentol.* **1999**, *27*, 189–206.
4. Retallack, G.J. Lateritization and bauxitization events. *Econ. Geol.* **2010**, *105*, 655–667. [CrossRef]
5. D'Argenio, B.; Mindszenty, A. Bauxites and related paleokarst: Tectonic and climatic event markers at regional unconformities. *Eclog. Geol. Helv.* **1995**, *88*, 453–499.
6. Sakač, K.; Šinkovec, B. The bauxites of the Dinarides. *Trav. ICSOBA* **1991**, *20–21*, 1–12.
7. Mindszenty, A.; Csoma, A.; Török, Á.; Hips, K.; Hertelendi, E. Flexura jellegű előtéri deformációhoz köthető karsztbauxitszintek a Dunántúli-középhegységben (Rudistid limestones, bauxites, paleokarst and geodynamics. The case of the Cretaceous of the Transdanubian Range). *Bull. Geol. Soc. Hung.* **2000**, *131*, 107–152. (In Hungarian with Extended English Abstract)
8. Laskou, M.; Economou-Eliopoulos, M. The role of microorganisms on the mineralogical and geochemical characteristics of the Parnassos-Ghiona bauxite deposits, Greece. *J. Geochem. Explor.* **2007**, *93*, 67–77. [CrossRef]
9. Mondillo, N.; Boni, M.; Balassone, G.; Rollinson, G. Karst bauxites in the Campania Apennines (southern Italy): A new approach. *Period. Mineral.* **2011**, *80*, 407–432.

10. D'Argenio, B.; Mindszenty, A. Tectonic and climatic control on paleokarst and bauxites. *G. Geol.* **1992**, *54*, 207–218.
11. Šinkovec, B. The Origin of Early Palaeogene Bauxites of Istria, Yugoslavia. In Proceedings of the 3rd International Congress of ICSOBA, Nice, France, 6–8 June 1973; ICSOBA: Nice, France, 1973; Volume 3, pp. 151–164.
12. Šinkovec, B.; Sakač, K. The Paleogene Bauxites of Dalmatia. *Trav. ICSOBA* **1982**, *12*, 294–331.
13. Šinkovec, B.; Sakač, K. Bauxite Deposits of Yugoslavia—The State of the Art. *Acta Geol. Hung.* **1991**, *34/4*, 307–315.
14. Blašković, I.; Dragičević, I.; Pokrajčić, I. Tectonic control of the origin of the paleorelief for bauxite deposits in western Herzegovina, Yugoslavia. *Trav. ICSOBA* **1989**, *19*, 230–238.
15. Vlahović, I.; Tišljar, J.; Velić, I.; Matičec, D. Evolution of the Adriatic Carbonate Platform: Palaeogeography, Main Events and Depositional Dynamics. *Palaeogeogr. Palaeoclimatol. Palaeoecol.* **2005**, *220*, 333–360. [CrossRef]
16. Korbar, T. Orogenic evolution of the external Dinarides in the NE Adriatic region: A model constrained by tectonostratigraphy of Upper Cretaceous to Paleogene carbonates. *Earth-Sci. Rev.* **2009**, *96*, 296–312. [CrossRef]
17. Kovačević Galović, E.; Ilijanić, N.; Peh, Z.; Miko, S.; Hasan, O. Geochemical discrimination of early Palaeogene bauxites in Croatia. *Geol. Croat.* **2012**, *65*, 53–65. [CrossRef]
18. Brlek, M.; Korbar, T.; Košir, A.; Glumac, B.; Grizelj, A.; Otoničar, B. Discontinuity surfaces in Upper Cretaceous to Paleogene carbonates of central Dalmatia (Croatia): Glossifungites ichnofacies, biogenic calcretes, and stratigraphic implications. *Facies* **2014**, *60*, 467–487. [CrossRef]
19. Peh, Z.; Kovačević Galović, E. Geochemistry of Istrian Lower Palaeogene bauxites—Is it relevant to the extent of subaerial exposure during Cretaceous times? *Ore Geol. Rev.* **2014**, *63*, 296–306. [CrossRef]
20. Peh, Z.; Kovačević Galović, E. Geochemistry of Lower Palaeogene bauxites—Unique signature of the tectonostratigraphic evolution of a part of the Croatian Karst. *Geol. Croat.* **2016**, *69*, 269–279. [CrossRef]
21. Brlek, M.; Gaynor, S.P.; Mongelli, G.; Bauluz, B.; Sinisi, R.; Brčić, V. Karst bauxite formation during Miocene climatic optimum (Central Dalmatia, Croatia): Mineralogical, compositional and geochronological perspectives. *Int. J. Earth Sci.* **2021**, *110*, 2899–2922. [CrossRef]
22. Brčić, V.; Dunkl, I.; Mindszenty, A.; Brlek, M.; Trinajstić, N.; Bajo, P.; Bauluz, B.; Mišur, I.; Karius, V.; Šuica, S.; et al. A time-space window between Eocene karst bauxite genesis and the first molasse deposition in the Dinaric Foreland Basin in North Dalmatia, Croatia. *Front. Earth Sci.* **2023**, *11*, 1224164. [CrossRef]
23. Retallack, G.J. Greenhouse crises of the past 300 million years. *Geol. Soc. Am. Bull.* **2009**, *121*, 1441–1455. [CrossRef]
24. Šinkovec, B.; Sakač, K.; Durn, G. Pyritized bauxites from Minjera, Istria, Croatia. *Nat. Croat.* **1994**, *3*, 41–65.
25. Perković, I.; Martinuš, M.; Cvetko Tešović, B.; Vlahović, I.; Matešić, D.; Newton, R.J.; He, T.; Šoufek, M.; Razum, I.; Durn, G. Tracing the evolution of the world's first mined bauxite from palaeotopography to pyritization: Insights from Minjera deposits, Istria, Croatia. *Geol. Croat.* **2024**, *77*, 159–178. [CrossRef]
26. Marković, S. *Hrvatske Mineralne Sirovine (Croatian Mineral Raw Materials)*; Institut za Geološka Istraživanja, Zavod za Geologiju: Zagreb, Croatia, 2002; p. 544. (In Croatian)
27. JISMS "Unique Information System of Mineral Resources" ("Jedinstveni Informacijski Sustav Mineralnih Sirovina" in Croatian)—WebGis Portal. Available online: https://mingo.gov.hr/o-ministarstvu-1065/djelokrug/uprava-za-industriju-i-rudarstvo/rudarstvo/jisms-rh/6980?impaired=0 (accessed on 27 December 2024).
28. Ahmadnejad, F.; Zamanian, H.; Taghipour, B.; Zarasvandi, A.; Buccione, R.; Ellahi, S.S. Mineralogical and geochemical evolution of the Bidgol bauxite deposit, Zagros Mountain Belt, Iran: Implications for ore genesis, rare earth elements fractionation and parental affinity. *Ore Geol. Rev.* **2017**, *86*, 755–783. [CrossRef]
29. Abedini, A.; Khosravi, M. Geochemical constraints on the Triassic–Jurassic Amir-Abad karst-type bauxite deposit, NW Iran. *J. Geochem. Explor.* **2020**, *11*, 106489. [CrossRef]
30. Mondillo, N.; Di Nuzzo, M.; Kalaitzidis, S.; Boni, M.; Santoro, L.; Balassone, G. Petrographic and geochemical features of the B3 bauxite horizon (Cenomanian–Turonian) in the Parnassos-Ghiona area: A contribution towards the genesis of the Greek karst bauxites. *Ore Geol. Rev.* **2022**, *143*, 104759. [CrossRef]
31. Deady, D.; Mochos, E.; Goodenough, K.; Williamson, B.; Wall, F. Rare earth elements in karst-bauxites: A novel untapped European resource? In Proceedings of the ERES2014: 1st European Rare Earth Resources Conference, Milos, Greece, 4–7 September 2014; pp. 1–12.
32. Mongelli, G.; Boni, M.; Oggiano, G.; Mameli, P.; Sinisi, R.; Buccione, R. Critical metals distribution in Tethyan karst bauxite: The Cretaceous Italian ores. *Ore Geol. Rev.* **2017**, *86*, 526–536. [CrossRef]
33. Radusinović, S.; Jelenković, R.; Pačevski, A.; Simić, V.; Božović, D.; Holclajtner-Antunović, I.; Životić, D. Content and mode of occurrences of rare earth elements in the Zagrad karstic bauxite deposit (Nikšić area, Montenegro). *Ore Geol. Rev.* **2017**, *80*, 406–428. [CrossRef]
34. Gamaletsos, P.N.; Godelitsas, A.; Filippidis, A.; Pontikes, Y. The Rare Earth Elements Potential of Greek Bauxite Active Mines in the Light of a Sustainable REE Demand. *J. Sustain. Met.* **2019**, *5*, 20–47. [CrossRef]

35. Mondillo, N.; Balassone, G.; Boni, M.; Chelle-Michou, C.; Cretella, S.; Mormone, A. Rare earth elements (REE) in Al- and Fe-(oxy)-hydroxides in bauxites of Provence and Languedoc (southern France): Implications for the potential recovery of REEs as by-products of bauxite mining. *Minerals* **2019**, *9*, 504. [CrossRef]
36. Radusinović, S.; Papadopoulos, A. The potential for REE and associated critical metals in karstic bauxites and bauxite residue of Montenegro. *Minerals* **2021**, *11*, 975. [CrossRef]
37. Tomašić, N.; Čobić, A.; Bedeković, M.; Miko, S.; Ilijanić, N.; Gizdavec, N.; Matošević, M. Rare Earth Elements Enrichment in the Upper Eocene Tošići-Dujići Bauxite Deposit, Croatia, and Relation to REE Mineralogy, Parent Material and Weathering Pattern. *Minerals* **2021**, *11*, 1260. [CrossRef]
38. Zhang, S.; Zhao, F.; Liu, D.; Zhao, L.; Zhang, X.; Lin, J.; Dong, H.; Zhao, S.; Liu, X.; Zan, M. Modes of Occurrence of Critical Metal Elements (Li, REEs, and Other Critical Elements) in Low-Grade Bauxite from Southern Shanxi Province, China. *Minerals* **2022**, *12*, 990. [CrossRef]
39. European Commission. Regulation of the European Parliament and of the Council Establishing a Framework for Ensuring a Secure and Sustainable Supply of Critical Raw Materials and Amending Regulations (EU) 168/2013, (EU) 2018/858, 2018/1724 and (EU) 2019/1020, Brussels, 16.3.2023, COM(2023) 160 Final, 2023/0079 (COD). Available online: https://single-market-economy.ec.europa.eu/publications/european-critical-raw-materials-act_en (accessed on 18 October 2024).
40. Goodenough, K.M.; Schilling, J.; Jonsson, E.; Kalvig, P.; Charles, N.; Tuduri, J.; Deady, E.A.; Sadeghi, M.; Schiellerup, H.; Müller, A.; et al. Europe's rare earth element resource potential: An overview of REE metallogenetic provinces and their geodynamic setting. *Ore Geol. Rev.* **2016**, *72*, 838–856. [CrossRef]
41. Goodenough, K.M.; Wall, F.; Merriman, D. The Rare Earth Elements: Demand, Global Resources, and Challenges for Resourcing Future Generations. *Nat. Resour. Res.* **2018**, *27*, 201–216. [CrossRef]
42. Ilijanić, N.; Kovačević Galović, E.; Gizdavec, N.; Ivkić Filipović, I.; Miko, S.; Peh, Z. Geochemical records in subaerial exposure environments in Croatia using discriminant function analysis of bauxite data. *Front. Earth Sci.* **2023**, *10*, 1055435. [CrossRef]
43. Tišljar, J.; Vlahović, I.; Velić, I.; Sokač, B. Carbonate Platform Megafacies of the Jurassic and Cretaceous Deposits of the Karst Dinarides. *Geol. Croat.* **2002**, *55*, 139–170. [CrossRef]
44. Vlahović, I.; Tišljar, J.; Velić, I.; Matičec, D. The Karst Dinarides Are Composed of Relics of a Single Mesozoic Platform: Facts and Consequences. *Geol. Croat.* **2002**, *55*, 171–183. [CrossRef]
45. Map of Mineral Resources of the Republic of Croatia, Croatian Geological Survey. Available online: https://www.hgi-cgs.hr/karta-mineralnih-sirovina-republike-hrvatske-1200-000/ (accessed on 27 December 2024).
46. Márton, E.; Zampieri, D.; Kázmér, M.; Dunkl, I.; Frisch, W. New Paleocene–Eocene paleomagnetic results from the foreland of the Southern Alps confirm decoupling of stable Adria from the African plate. *Tectonophysics* **2011**, *504*, 89–99. [CrossRef]
47. Nocquet, J.-M. Present-day kinematics of the Mediterranean: A comprehensive overview of GPS results. *Tectonophysics* **2012**, *579*, 220–242. [CrossRef]
48. Šinkovec, B.; Sušnjara, A.; Sakač, K. Boksiti Korduna i susjednih područja (Bauxites of Kordun and neighboring areas). *Geol. Vjesn.* **1985**, *38*, 215–233. (In Croatian)
49. Matičec, D.; Vlahović, I.; Velić, I.; Tišljar, J. Eocene limestones overlying Lower Cretaceous deposits of western Istria (Croatia): Did some parts of present Istria form land during the Cretaceous? *Geol. Croat.* **1996**, *49*, 117–127.
50. Durn, G. Terra rossa in the Mediterranean region: Parent materials, composition and origin. *Geol. Croat.* **2003**, *56*, 83–100. [CrossRef]
51. Španiček, J.; Ćosović, V.; Mrinjek, E.; Vlahović, I. Early Eocene Evolution of Carbonate Depositional Environments Recorded in the Čikola Canyon (North Dalmatian Foreland Basin, Croatia). *Geol. Croat.* **2017**, *70*, 11–25. [CrossRef]
52. Ćosović, V.; Mrinjek, E.; Nemec, W.; Španiček, J.; Terzić, K. Development of transient carbonate ramps in an evolving foreland basin. *Basin Res.* **2018**, *30*, 746–765. [CrossRef]
53. Tarvainen, T.; Reeder, S.; Albanese, S. Database Management and Map Production. In *Geochemical Atlas of Europe: Part 1, Background Information, Methodology and Maps*; Salminen, R., Batista, M.J., Bidovec, M., Demetriades, A., De Vivo, B., De Vos, W., Duris, M., Gilucis, A., Gregotauskiene, V., Halamić, J., et al., Eds.; Geological Survey of Finland: Espoo, Finland, 2005; p. 526.
54. Antweiler, R.C.; Taylor, H.E. Evaluation of statistical treatments of left-censored environmental data using coincident uncensored data sets: I. Summary statistics. *Environ. Sci. Technol.* **2008**, *42*, 3732–3738. [CrossRef]
55. Evensen, N.M.; Hamilton, P.J.; O'Nions, R.K. Rare-earth abundances in chondritic meteorites. *Geochim. Cosmochim. Acta* **1978**, *42*, 1199–1212. [CrossRef]
56. Mongelli, G.; Boni, M.; Buccione, R.; Sinisi, R. Geochemistry of the Apulian karst bauxites (southern Italy): Chemical fractionation and parental affinities. *Ore Geol. Rev.* **2014**, *63*, 9–21. [CrossRef]
57. Hasan, O.; Miko, S.; Ilijanić, N.; Brunović, D.; Dedić, Ž.; Šparica Miko, M.; Peh, Z. Discrimination of topsoil environments in a karst landscape: An outcome of a geochemical mapping campaign. *Geochem. Trans.* **2020**, *21*, 1. [CrossRef] [PubMed]
58. Galović, L.; Šorša, A.; Peh, Z. Modelling the paleopedological development of loess/palaeosol sections using discriminant function analysis of compositional geoscience data, case study in Eastern Croatia. *J. Geochem. Explor.* **2024**, *262*, 107473. [CrossRef]

59. Mongelli, G.; Mameli, P.; Sinisi, R.; Buccione, R.; Oggiano, R.; Rees, G. Critical raw materials in Cretaceous Mediterranean-type bauxite: The case of the Sardinian ore (Italy). *Ore Geol. Rev.* **2021**, *139*, 104559. [CrossRef]
60. Taylor, R.S.; McLennan, S.M. *Planetary Crusts: Their Composition, Origin and Evolution*; Cambridge University Press: Cambridge, UK, 2009; p. 378.
61. StatSoft Inc. *STATISTICA (Data Analysis Software System)*, Version 7.1; StatSoft Inc.: Tulsa, Oklahoma, 2006.
62. Crnički, J.; Jurković, I. Rare earth elements in Triassic bauxites of Croatia, Yugoslavia. *Trav. ICSOBA* **1990**, *19*, 239–248.
63. Qi, H.; Gong, N.; Zhang, S.-Q.; Li, J.; Yuan, G.-L.; Liu, X.-F. Research Progress on the Enrichment of Gallium in Bauxite. *Ore Geol. Rev.* **2023**, *160*, 105609. [CrossRef]
64. Abedini, A.; Khosravi, M.; Calagari, A.A. Geochemical characteristics of the Arbanos karst-type bauxite deposit, NW Iran: Implications for parental affinity and factors controlling the distribution of elements. *J. Geochem. Explor.* **2019**, *200*, 249–265. [CrossRef]
65. Nesbitt, H.W. Mobility and fractionation of rare earth elements during weathering of a granodiorite. *Nature* **1979**, *279*, 206–210. [CrossRef]
66. Ling, K.Y.; Zhu, X.Q.; Tang, H.S.; Du, S.J.; Gu, J. Geology and geochemistry of the Xiaoshanba bauxite deposit, Central Guizhou Province, SW China: Implications for the behavior of trace and rare earth elements. *J. Geochem. Explor.* **2018**, *190*, 170–186. [CrossRef]
67. Reinhardt, N.; Proenza, J.; Villanova-de-Benavent, C.; Aiglsperger, T.; Bover-Arnal, T.; Torró, L. Geochemistry and mineralogy of rare earth elements (REE) in bauxitic ores of the Catalan Coastal Range, NE Spain. *Minerals* **2018**, *8*, 562. [CrossRef]
68. Abedini, A.; Khosravi, M. Geochemical Characteristics of Aluminum-Bearing Iron Ores: A Case Study from the Kolijan Karst-Type Bauxite Deposit, Northwestern Iran. *Minerals* **2024**, *14*, 151. [CrossRef]
69. Maksimović, Z.; Pantó, G. Contribution to the Geochemistry of the rare earth elements in the karst–bauxite deposits of Yugoslavia and Greece. *Geoderma* **1991**, *51*, 93–109. [CrossRef]
70. Crnički, J. Raspodjela lantanida u boksitima Hrvatske i njihovo značenje za genezu boksita (Distribution of Lanthanides in Bauxites of Croatia and Their Significance for the Genesis of Bauxites). Ph.D. Thesis, University of Zagreb, Zagreb, Croatia, 1987. (In Croatian)
71. Khosravi, M.; Abedini, A.; Alipour, S.; Mongelli, G. The Darzi-Vali bauxite deposit, West-Azarbaidjan Province, Iran: Critical metals distribution and parental affinities. *J. Afr. Earth Sci.* **2017**, *129*, 960–972. [CrossRef]
72. Sinisi, R. Mineralogical and geochemical features of Cretaceous bauxite from San Giovanni Rotondo (Apulia, Southern Italy): A provenance tool. *Minerals* **2018**, *8*, 567. [CrossRef]
73. Mameli, P.; Mongelli, G.; Oggiano, G.; Dinelli, E. Geological, geochemical and mineralogical features of some bauxite deposits from Nurra (Western Sardinia, Italy): Insights on conditions of formation and parental affinity. *Int. J. Earth Sci.* **2007**, *96*, 887–902. [CrossRef]
74. Viers, J.; Wasserburg, G.J. Behavior of Sm and Nd in a Lateritic Soil Profile. *Geochim. Cosmochim. Acta* **2004**, *68*, 2043–2054. [CrossRef]
75. Schroll, E.; Sauer, D. Beitrag zur Geochemie von Titan, Chrom, Nikel, Cobalt, Vanadium und Molibdan in bauxitischen gestermen und problem der stofflichen herkunft des Aluminiums (Contribution to the geochemistry of titanium, chromium, nickel, cobalt, vanadium, and molybdenum in bauxitic rocks and the problem of the material origin of aluminum). *Trav. ICSOBA* **1968**, *5*, 83–96. (In German)
76. Pamić, J.; Balen, D.; Herak, M. Origin and geodynamic evolution of Late Paleogene magmatic associations along the Periadriatic-Sava-Vardar magmatic belt. *Geodin. Acta* **2002**, *15*, 209–231. [CrossRef]
77. Mongelli, G. Ce-anomalies in the textura components of Upper Cretaceous karst bauxites from the Apulian carbonate platform (southern Italy). *Chem. Geol.* **1997**, *14*, 69–79. [CrossRef]
78. Putzolu, F.; Papa, A.; Mondillo, N.; Boni, M.; Balassone, G.; Mormone, A. Geochemical characterization of bauxite deposits from the Abruzzi mining district (Italy). *Minerals* **2018**, *8*, 298. [CrossRef]
79. Torrent, J.; Schwertmann, U.; Barrón, V. Fast and Slow Phosphate Sorption by Goethite-Rich Natural Materials. *Clays Clay Miner.* **1992**, *40*, 14–21. [CrossRef]
80. Feret, F.; See, J. Occurrence and characterization of Zn and Mn in bauxite. *TMS Light Metals* **2006**, *41*, 111–116.
81. Vujec, S.; Marušić, R.; Sakač, K. Underground Bauxite Exploitation in the Western Dinarids Essential Facts and Comments. *Rud.-Geol.-Naft. Zb.* **1994**, *6*, 71–94.
82. Lukšić, B.; Miko, S.; Pencinger, V.; Dedić, Ž. *Rudarsko-Geološka Studija Šibensko-Kninske Županije (Mining and Geological Study of the Šibenik-Knin County)*; Documentation fund Croatian Geological Survey 115/06; Hrvatski Geološki Institut: Zagreb, Croatia, 2006; p. 270. (In Croatian)
83. Živković, S.A.; Krasić, D.; Dekanić, I.; Golub, I.; Nuić, J.; Rajković, D.; Saftić, B. *Strategija Gospodarenja Mineralnim Sirovinama Republike Hrvatske (Strategy for the Management of Mineral Resources of the Republic of Croatia)*; Faculty of Mining, Geology, and Petroleum Engineering: Zagreb, Croatia, 2008; p. 301. (In Croatian)

84. Wang, S.; Li, X. Fully Mechanized Longwall Mining in an Underground Bauxite Deposit: A Case Study. *Geotech. Geol. Eng.* **2018**, *36*, 1231–1248. [CrossRef]
85. Mouchos, E.; Wall, F.; Williamson, B.J.; Palumbo-Roe, B. Easily leachable rare earth element phases in the Parnassus-Giona bauxite deposits, Greece. *Bull. Geol. Soc. Greece* **2016**, *50*, 1952–1958. [CrossRef]
86. Tomašić, N. (Ed.) *Bauxite and Bauxite Residue as a Potential Resource of REE in the ESEE Region*; University of Zagreb Faculty of Science: Zagreb, Croatia, 2020; p. 86.

Disclaimer/Publisher's Note: The statements, opinions and data contained in all publications are solely those of the individual author(s) and contributor(s) and not of MDPI and/or the editor(s). MDPI and/or the editor(s) disclaim responsibility for any injury to people or property resulting from any ideas, methods, instructions or products referred to in the content.

6.3. Mineralogical and geochemical variability of the Mamutovac-1a Upper Eocene karst bauxite deposit (Croatian Dinarides) and its CRM potential

By Kovačević Galović, E., Ilijanić, N., Fajković, H.*, Miko, S., Tomašić, N., Peh, Z., Ivkić Filipović, I., Gizdavec, N., Teskera, D.

Published in Minerals 2026, 16(5), 547.

DOI: https://doi.org/10.3390/min16050547

This paper presents a detailed mineralogical, petrographic, and geochemical investigation of the Upper Eocene Mamutovac-1a bauxite deposit in the Croatian Dinarides. A multi-proxy approach combining drill-core logging, X-ray diffraction, magnetic susceptibility measurements, whole-rock geochemistry, and aqua regia extractions was applied to evaluate the processes controlling deposit evolution and the distribution of rare earth elements (REE). The results reveal pronounced vertical facies, mineralogical, and geochemical zonation, reflecting a polygenetic history involving in-situ bauxitization, reworking, redeposition, and fluid-mediated redistribution. REE concentrations increase toward the deeper parts of the profile, with geochemical evidence suggesting that phosphate minerals likely represent one of the principal REE hosts, while clay minerals play a subordinate role. The study demonstrates that local physicochemical conditions play an important role in controlling deposit-scale variability and the vertical redistribution of mineral phases and elements. The observed mineralogical and geochemical zonation, particularly the increasing abundance of clay minerals toward the lower part of the profile, provides the basis for testing the second hypothesis of this doctoral dissertation. Elevated concentrations of REE and other critical elements further support the resource potential of the deposit as a potential alternative source of critical raw materials.

minerals

MDPI

Article

Mineralogical and Geochemical Variability of the Mamutovac-1a Upper Eocene Karst Bauxite Deposit (Croatian Dinarides) and Its CRM Potential

Erli Kovačević Galović [1], Nikolina Ilijanić [1], Hana Fajković [2,*], Slobodan Miko [1], Nenad Tomašić [2], Ivona Ivkić Filipović [1], Nikola Gizdavec [1], Zoran Peh [1] and Dominik Teskera [2]

1 Department of Mineral Resources and Marine Geology, Croatian Geological Survey, 10000 Zagreb, Croatia; ekovacevic@hgi-cgs.hr (E.K.G.); nilijanic@hgi-cgs.hr (N.I.); smiko@hgi-cgs.hr (S.M.); iivkic@hgi-cgs.hr (I.I.F.); ngizdavec@hgi-cgs.hr (N.G.); zpeh@hgi-cgs.hr (Z.P.)
2 Department of Geology, Faculty of Science, University of Zagreb, Horvatovac 102a, 10000 Zagreb, Croatia; ntomasic@geol.pmf.unizg.hr (N.T.); dominik44tes@gmail.com (D.T.)
* Correspondence: hanaf@geol.pmf.unizg.hr

Abstract

Karst bauxites represent important archives of paleoenvironmental conditions and potential sources of REE and other critical raw materials (CRMs). This study presents a multiproxy investigation of the Upper Eocene Mamutovac-1a bauxite deposit (Croatian Dinarides), integrating petrography, X-ray diffraction (XRD), magnetic susceptibility, whole-rock geochemistry, and aqua regia extractions along a 25.1 m drill core. The deposit shows clear vertical variability defined by four facies-based zones, accompanied by systematic mineralogical and geochemical changes. The bauxite is dominated by böhmite, gibbsite, hematite, and anatase, with subordinate goethite and clay minerals. ΣREE concentrations range from 276 to 670 mg/kg and increase toward the deeper zones, with consistent LREE enrichment relative to HREE, negative Eu anomalies, and variable Ce anomalies. Correlations suggest that REE are likely associated with phosphate phases, with a possible secondary contribution from clay minerals. The integrated dataset indicates a polygenetic, multi-stage evolution involving both in situ bauxitization and episodic reworking and redeposition, controlled by variable redox conditions and fluid–rock interaction. Geochemical signatures suggest a mixed provenance with contributions from intermediate to ultramafic sources. The elevated concentrations and enhanced extractability of selected elements (La, Sc, Ga, V) indicate that the deposit may represent a potential secondary source of CRMs.

Keywords: karst bauxite; geochemical data; rare earth elements; critical raw materials; paleoenvironment

Check for updates

Academic Editor: Giovanni Grieco

Received: 20 March 2026
Revised: 2 May 2026
Accepted: 14 May 2026
Published: 19 May 2026

Copyright: © 2026 by the authors. Licensee MDPI, Basel, Switzerland. This article is an open access article distributed under the terms and conditions of the Creative Commons Attribution (CC BY) license.

1. Introduction

Karst bauxites are residual deposits formed by intense chemical weathering of aluminosilicate material under warm and humid climatic conditions [1–5]. Together with lateritic and Tikhvin-type bauxites, karst bauxites represent one of the three principal genetic types of bauxite deposits [1]. They typically develop on subaerially exposed carbonate platforms where karstification creates morphological traps such as depressions, fissures, and paleokarst cavities suitable for the accumulation of bauxitic material [1,6,7]. Mineralogically, karst bauxites are predominantly composed of aluminum hydroxides (gibbsite and/or böhmite) accompanied by varying proportions of clay minerals, iron oxides and hydroxides,

and titanium oxides [1,3,4,6,8–12]. In addition to in situ weathering, external inputs such as aeolian or volcaniclastic material may have contributed aluminosilicate components, further influencing the mineralogical and geochemical composition of the resulting bauxite bodies ([1,4,13,14] and references therein). Consequently, many karst bauxite deposits may display complex polygenetic characteristics and pronounced vertical variability in their mineralogical and geochemical properties [4,10,15,16]. Karst bauxites in Europe are predominantly distributed within the Mediterranean Bauxite Belt, which represents one of the most important global provinces of karst bauxite formation [1,17]. This belt extends along the northern margin of the Mediterranean region, from southern France through the Dinarides and Greece to Turkey and is considered the classical region for karst bauxite development [1]. Bauxite formation within this belt spans a wide geological time range, from the Permian to the Miocene, with the most significant accumulation occurring during the Upper Cretaceous [1].

In the Mediterranean region, karst bauxites are closely associated with carbonate platforms that experienced periods of tectonically induced emergence and prolonged subaerial exposure [1]. Their formation is commonly linked to regional stratigraphic discontinuities marking interruptions in marine sedimentation, during which karstification and intense weathering processes allowed the accumulation of residual aluminous material [4,6,18]. In recent years, karst bauxites have attracted increasing scientific interest not only as indicators of paleoenvironmental and tectonic evolution but also as potential sources of critical metals, particularly light rare earth elements (LREE) ([11,19–29] and others). The distribution and fractionation of REE within bauxite deposits are controlled by multiple factors, including the composition of the precursor materials, the intensity of chemical weathering, pH and redox conditions, and post-depositional redistribution processes within the weathering profile [9,14,30–32]. These factors can cause selective enrichment or depletion of specific REE, resulting in distinct vertical geochemical trends within individual bauxite bodies [9,14,33]. Consequently, detailed geochemical investigations of well-preserved bauxite deposits provide valuable insights into the genetic mechanisms and processes controlling element mobility, mineralogical hosts of REE, and the evolution of the weathering system (e.g., [9–11,34–38]).

Within the Croatian Karst Dinarides, numerous bauxite deposits formed on the Adriatic–Dinaric Carbonate Platform (ADCP), where repeated phases of uplift, karstification, and erosion created favorable conditions for bauxitization [17,39–45]. These deposits occur within eight stratigraphically defined horizons [46,47] that reflect major emersion phases of the platform and are therefore important markers of regional tectonostratigraphic evolution and continental weathering episodes [48,49]. In the Croatian Karst Dinarides, the Upper Eocene represents one of the most significant periods of bauxite formation, as constrained by biostratigraphic data and regional stratigraphic correlations [46,47,50]. Previous studies show that Upper Eocene bauxites, together with Upper Paleocene and Middle Eocene horizons, exhibit the highest ΣREE contents among bauxite-bearing horizons in Croatia. Median ΣREE values for the Upper Eocene horizon are 568.63 mg/kg, with individual deposits reaching up to 5044.76 mg/kg, reflecting pronounced REE enrichment [48,49].

However, despite extensive research on bauxites in Croatia, integrated investigations of individual deposits that combine petrographic, mineralogical, magnetic, and detailed REE geochemical data along vertical profiles remain relatively limited. Such studies are essential for understanding the internal structure of bauxite bodies, the processes responsible for element redistribution during bauxitization, and the relationship between primary weathering processes and later diagenetic modifications. The present study focuses on the Mamutovac-1a bauxite deposit located in the Promina area of the External Dinarides in

Croatia. Based on its stratigraphic position, the deposit belongs to the Upper Eocene bauxite horizon developed on the Adriatic–Dinaric Carbonate Platform. In the Promina area, these bauxites typically occur within karstified Upper Cretaceous carbonate successions and are overlain by Upper Eocene–Oligocene Promina deposits [17,51,52]. Using drill-core material obtained during exploration of the deposit, this study investigates the vertical variability of mineralogical, textural, magnetic susceptibility, and geochemical characteristics within the bauxite deposit. Particular emphasis is placed on the distribution and fractionation of rare earth elements to constrain the processes governing their mobility and enrichment during bauxitization and subsequent post-depositional modification. In addition, the study aims to characterize the physicochemical, elemental, and mineralogical composition of the dominant (fine) fraction of bauxite and to assess the readily extractable critical raw materials (CRMs) (La, Sc, Ga and V). The results contribute to a better understanding of the internal structure and polygenetic development of karst bauxites in the Dinarides and provide new insights into REE behavior in Mediterranean-type bauxite systems.

2. Geological Setting

The Mamutovac-1a bauxite deposit is situated within the Municipality of Promina in Šibenik–Knin County, Croatia, southwest of the village of Oklaj (Figure 1a). Structurally, the area belongs to the Croatian karst Dinarides, forming part of the high-karst thrust sheet of the Dinaric orogen [53,54]. The deposit is exposed in a shallow syncline, part of a system of NW–SE–trending anticlines and synclines typical of the External Dinarides [40]. The limbs and hinge zones of these folds acted as natural traps for bauxite accumulation, while tectonic activity promoted partial redeposition of previously formed bauxite [55,56].

The regional stratigraphy is dominated by carbonates of the Adriatic Carbonate Platform (AdCP), ranging from the Toarcian to the Eocene (details in [39,40,57,58]) (Figure 1a,b). In the Mamutovac area, Upper Cretaceous rudist limestones form the base, overlain by Paleogene Kozina deposits and foraminiferal limestones [39,56,59–61]. These limestones were deposited in shallow marine environments and later subjected to subaerial exposure and intense karstification, forming a paleorelief with depressions, fractures, and fissures suitable for bauxite accumulation [1,15,16].

The wider Dinaric region experienced several phases of bauxite formation related to Late Cretaceous uplift and emergence of the Adriatic Carbonate Platform [41,43,44,62,63], and bauxite occurrences in the wider Promina Municipality area, associated with periods of emersion, occur within three stratigraphic horizons [46,47] (Figure 1b). Considering its stratigraphic position and its relationship to the overlying strata, the Mamutovac-1a bauxite deposit belongs to the Upper Eocene (BX7) bauxite horizon of the Croatian karst bauxites [48,49]. During the Middle to Late Eocene (Lutetian to Priabonian), warm and humid subtropical conditions favored intense chemical weathering and bauxitization of exposed carbonate and volcaniclastic material [46,47]. At the same time, intensified orogenic uplift and thrust propagation resulted in widespread erosion, renewed karstification, and the development of a regional erosional unconformity, which acted as the principal control on the formation and spatial distribution of the Upper Eocene bauxite deposits in the Promina area [52,64]. Aeolian and fluvial input of volcanic ash, derived from contemporaneous Eocene magmatism in the wider region, contributed to the formation of aluminous precursor material, as confirmed by a recent study of a different deposit within the same exploitation field [17,45].

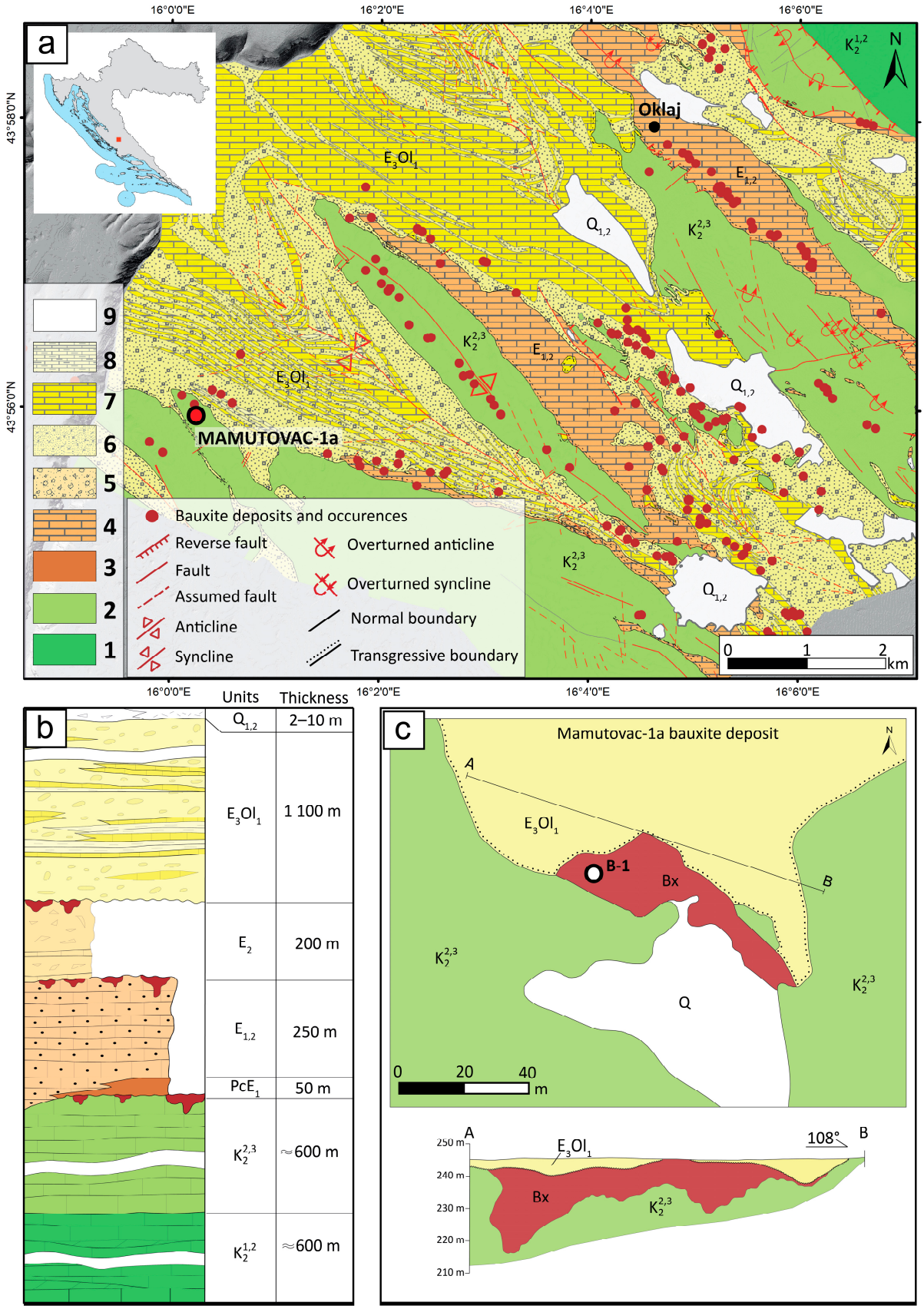

Figure 1. (**a**) Geological map of the Promina Municipality in Šibenik-Knin County, modified after [52], showing numerous bauxite deposits and occurrences, including the location of the Mamutovac-1a deposit. The geological units on the map (as well as on (**b**,**c**)) are as follows: 1—Upper Cretaceous (Cenomanian–Turonian) limestones with dolomite intercalations ($K_2^{1,2}$), 2—Upper Cretaceous (Turonian–Coniacian) rudist limestones ($K_2^{2,3}$), 3—Paleogene Kozina beds (PcE_1), 4—Paleogene for-

aminiferal limestones ($E_{1,2}$), 5—Paleogene Jelar deposits–limestone breccias (E_2), 6—Paleogene Promina beds–conglomerates, breccias, limestones, calcareous marls (E_3Ol_1), 7—Paleogene Promina beds–limestones (E_3Ol_1), 8—Paleogene Promina beds–marly limestone (E_3Ol_1), 9—Quaternary–terra rossa with rock fragments ($Q_{1,2}$). The inset map shows the location of the studied area in Croatia; (**b**) Geological column of the studied area with bauxite-bearing horizons. Modified after [52]. Bauxite occurrences in the wider region are associated with periods of emersion and occur within three stratigraphic horizons, while the studied Mamutovac-1a deposit is genetically linked to the Upper Eocene emersion phase. Note that the thickness of the geological units is not to scale; (**c**) Detailed geological map and geological profile of the Mamutovac-1a bauxite deposit. The location of borehole B-1 is marked with the black and white dot in the detailed geological map. Modified after [51].

Tectonic activity associated with the Dinaric orogeny reshaped the paleorelief and controlled the distribution of bauxite [39]. Folded and faulted structures created anticline hinges and synclinal depressions that served as traps for redeposited bauxite [17]. The semi-lithified bauxite fragments, along with pisolitic clasts, accumulated in synclinal areas, while the more uplifted limbs contributed material through local erosion and redeposition [17]. These processes continued until the Eocene–Oligocene transition, when deposition of Promina molasse covered the entire area [65]. The overlying Promina Formation, composed of alternating conglomerates, breccias, limestones, and marls, reflects sedimentation in deltaic to shallow-marine environments with frequent lateral and vertical facies changes, representing the transition from emergence to renewed sedimentation under variable depositional conditions. These deposits covered the bauxite deposits, protecting them from further erosion and preserving the thin, widely distributed, and partially redeposited bodies observed today [56]. Quaternary sediments in the area are limited to minor alluvial deposits along the Krka River [52,65].

Geological and Resource Characteristics of the Mamutovac-1a Bauxite Deposits

The Mamutovac-1a deposit is part of the non-active exploitation field Mamutovac [66]. The exploitation field, located in the north-western part of the Promina plateau, comprises ten bauxite deposits, several of which have already been fully exploited. The deposits occur within a relatively narrow elevation range of approximately 244–256 m a.s.l. and typically form irregular, lens-shaped bodies with lateral dimensions of up to about 100 m and an average thickness of around 4 m [51]. Previous studies of the Mamutovac exploitation field indicate that deposit morphology is strongly controlled by the underlying paleokarst relief, resulting in uneven basal contacts and frequent occurrences of pinnacled limestone protrusions that locally penetrate and segment the ore bodies [51]. This is consistent with the general characteristics of karst bauxite deposits developed on karstified carbonate substrates [4]. The basal contacts are often irregular and infill depressions in the karstified substrate, whereas the upper contacts with overlying sediments are relatively planar [51]. The Mamutovac-1a deposit is formed on Upper Cretaceous rudist limestones. The outcrop of the deposit measures approximately 80 × 10–25 m, while the ore body extends a further 30–80 m beneath the Promina cover towards the northeast. It forms an elongated trough, reaching up to ~30 m in thickness in its central part and thinning towards both ends. The overlying Promina deposits are well stratified, dominated by conglomerates with subordinate marls and limestones. In the southeastern part, the succession is locally covered by a thin layer of Quaternary terra rossa [51] (Figure 1c).

The bauxites are predominantly of böhmitic or mixed böhmitic–gibbsite composition [51]. However, their quality modulus generally ranges between 2 and 4, indicating relatively low ore quality, and a substantial proportion of the material has therefore been classified as off-balance ore in previous resource assessments [51]. Exploration of the Ma-

mutovac exploitation field has a long history, beginning prior to the First World War and continuing through several major exploration campaigns during the second half of the twentieth century and the early twenty-first century, which included trenching, shallow pits, and extensive drilling programs. Among the identified deposits, Mamutovac-1a represents the most economically significant body, with estimated reserves of ~112 kt, within a total of ~291 kt of remaining exploitable bauxite in the Mamutovac exploitation field [51,52].

3. Materials and Methods

To investigate the vertical variability of the Mamutovac-1a bauxite deposit, exploratory drilling was carried out at a representative location selected based on previous investigations [51]. The selected site corresponds to a thicker part of the ore body, where it is exposed at the surface and not covered by overlying Promina deposits or terra rossa. Drilling was performed vertically. Drill core B-1, obtained at this location (coordinates: E: 460,164.5 m, N: 486,6035.2 m), had a diameter of 101 mm and was recovered in a partially compact and locally fragmented condition. The borehole reached a total depth of 26.4 m, of which 25.1 m of core was retrieved. Core loss occurred at the contact with the limestone basement, which is more permeable than the overlying bauxite. During drilling, water inflow at this contact led to washing out and loss of the lowermost part of the core. As a result, the lowermost 1.3 m of the core was not recovered.

The extracted core was systematically placed into plastic PVC core boxes, transported, and securely stored in the laboratories of the Croatian Geological Survey. The bauxite core was initially subjected to macroscopic description, with color characterization performed for all depth intervals using the Munsell Soil Color Charts [67]. Based on macroscopic observations, specific 5 cm thick intervals from various depths were selected for sampling and further analysis. The collected samples were dried to a constant weight in a drying oven. Once dried, they were finely ground using an agate mortar and pestle, rendering them suitable for subsequent analytical procedures.

For the determination of textural properties, thin sections were prepared from 11 bauxite samples collected along the core at representative intervals (Figure 2). Samples were selected to cover the entire core length, with preference given to sufficiently compact material suitable for thin section preparation, and were examined using a polarizing optical microscope (Olympus BX51TF, Olympus Corporation, Tokyo, Japan).

The measurement of magnetic susceptibility in 42 pulverized and homogenized samples from various depth intervals of the bauxite drill core was conducted using a Bartington MS2 device with a dual-frequency MS2B sensor (Bartington Instruments Ltd., Witney, UK) in the laboratories of the Croatian Geological Survey. Samples were packed into plastic containers with a volume of 10 cm^3, weighed, and subsequently measured first at a low frequency (0.465 kHz) and then at a high frequency (4.65 kHz). The obtained results were used to determine mass-specific magnetic susceptibility values at low frequency χ_{lf}, as well as the frequency-dependent magnetic susceptibility χ_{fd}, expressed as percentages.

The mineral composition of the selected bauxite samples was determined through qualitative mineralogical analysis using X-ray powder diffraction (XRD) on a PANalytical X'Pert Powder diffractometer (Malvern Panalytical, Almelo, The Netherlands) at the Croatian Geological Survey. It is equipped with a Cu ceramic X-ray tube (CuKα radiation, λ = 1.5406 Å), a vertical goniometer of θ-θ geometry, a graphite monochromator, and a PIXcel detector. Measurements were performed at 45 kV and 40 mA, with a step size of 0.02°2θ, and a counting time of 100 s per step, over the 5–66°2θ range. The obtained diffraction patterns were analyzed using the X'Pert HighScore Plus software package (ver. 4.5; PANalytical B.V., Almelo, The Netherlands), which is linked to the ICDD PDF-4/Minerals database containing reference data for all known mineral species. The bulk mineralogical

analysis involved examining a total of 42 finely ground bauxite samples. Powdered samples were crushed using an agate mortar and pestle, and subsequently prepared as random mounts on Al holders using the back-loading method. Oriented aggregates were prepared from approximately 10 g of seven selected bauxite samples across the core to provide detailed insight into the mineralogy of clay minerals. The clay mineral fraction (<2 μm) was separated by centrifugation, and the suspension was eyedropped onto glass slides and allowed to air-dry at room temperature to obtain oriented mounts. A series of standard treatments were then applied [68], including ethylene glycol solvation (overnight) and heating at 400 °C and 550 °C (>0.5 h). X-ray diffraction measurements were subsequently performed in the 4–30° 2θ range. These diagnostic tests facilitated the identification of clay minerals with overlapping basal reflections.

Geochemical analyses of bauxites were performed utilizing the whole rock major and trace element analytical method at the Bureau Veritas laboratory (formerly ACME Analytical Laboratories Ltd.) in Vancouver, BC, Canada. They were conducted on 23 bauxite core samples (~5 g of samples ground in an agate mortar and pestle), collected at approximately one-meter intervals, to assess chemical composition variations along the core. Major oxides and minor elements were quantified using inductively coupled plasma atomic emission spectroscopy (ICP-AES) on 0.2 g of sample following lithium borate fusion and dissolution in dilute nitric acid. Trace and rare earth elements (REE) underwent the same digestion process as major elements (0.2 g of sample) and were analyzed via inductively coupled plasma mass spectrometry (ICP-MS). To ensure analytical accuracy and precision, quality control measures included blanks, duplicates, and standard reference materials (STD SO-19), with results documented in a certified quality (CQ) report. Analytical uncertainties were <5%, except for elements at concentrations lower than 10 mg/kg, for which uncertainties were 5% to 15%. Recoveries of the standard reference material (STD SO-19) were within 95–105%.

Additionally, eight subsamples of bauxite were also analyzed using ICP-ES/MS after treatment with a modified aqua regia digestion (1:1:1 HNO_3:HCl:H_2O) at the Bureau Veritas laboratory to complement the overall geochemical dataset. At the Croatian Geological Survey, the aqua regia digestion (HCl:HNO_3, 1:3 ratio) was performed on two selected samples with a solid-to-liquid ratio of 1:20 in a hot block digestion system at 90 °C. After digestion, the solutions were dried and powdered for mineralogical detection of the resulting bauxite residue using X-ray diffraction (XRD) and compared with the untreated bauxite samples.

4. Results

4.1. Mineralogy and Texture

4.1.1. Macroscopic Description of the Core

Macroscopic observations reveal systematic variations in color, texture, and degree of consolidation along the core (Figure 2a). The color of the bauxite falls within the red–yellow (YR) range of the Munsell Soil Color Charts [67], with a general shift from darker red hues (2.5 YR) in the upper part of the core (0–14 m) to more brownish tones (5–7.5 YR) at greater depths (14–25 m) (Figure 2a). Core solidity varies from well-consolidated to poorly consolidated material that locally disintegrated during drilling (Figure 2a). The uppermost 0–0.5 m of the core consists of a disturbed, poorly consolidated bauxite interval containing abundant limestone fragments and showing clear signs of limestone disintegration. From 0.5 to 11 m, the core is predominantly well consolidated and characterized by a red groundmass with abundant ooids and occasional larger grains (up to 1 cm), typically lighter in color than the surrounding material. Bleaching features and occasional black coatings are present (Figure 2b–g). Within this interval, local sections of weaker consolidation occur (e.g., ~6.8–8.2 m), where the material becomes more friable and disaggregated. A distinct change

is observed between 11 and 14 m, where the bauxite becomes finer-grained, with a reduced abundance of ooids and generally poorer consolidation. Bleaching features are common in this part of the core. Between 14 and 15.5 m, the material becomes more consolidated again and is characterized by red to dark red bauxite with abundant light-colored ooids (up to 1 mm). Irregular to subrounded darker aggregates (up to ~5 mm) occur locally, together with bleaching zones (Figure 2h). Below 15.5 m, the core is dominated by red to brown, fine-grained bauxite with a general decrease in ooid abundance. Bleaching features are frequent in the upper part of this interval but diminish with depth and are absent in the lowermost part. Black coatings are abundant, and the material is generally moderately consolidated (Figure 2i–l).

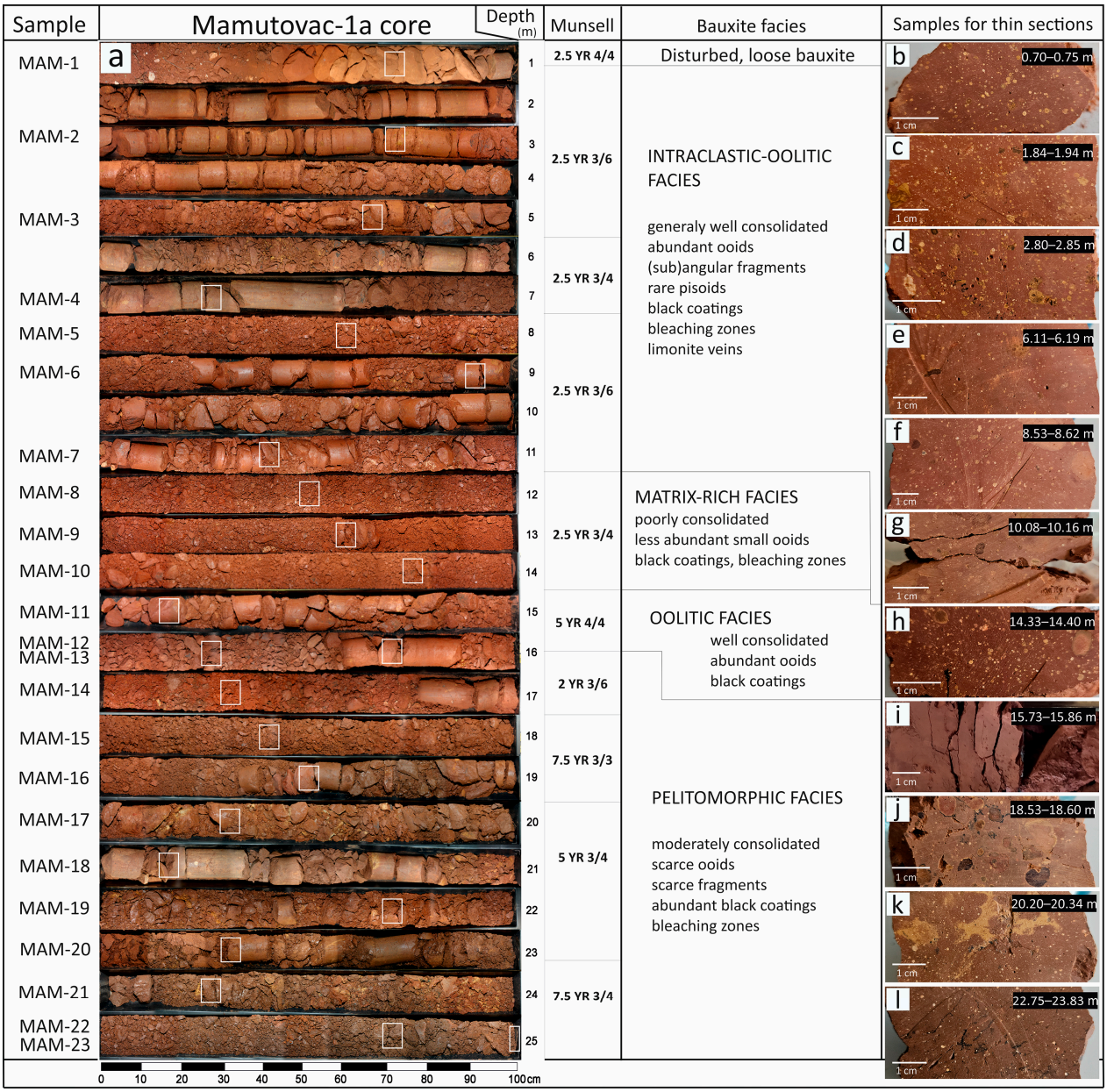

Figure 2. (**a**) Photographic overview of the Mamutovac-1a drill core with depth indicated in meters (0–25 m). White rectangles indicate the exact positions of intervals sampled for geochemical analyses, corresponding to the samples listed on the left. The adjacent column shows the dominant Munsell color codes for zones defined based on bauxite facies, together with a brief macroscopic description of their characteristics. (**b**–**l**) Hand-specimen photographs of the samples used for preparation of thin sections, with the corresponding depth ranges indicated.

4.1.2. Textural and Mineralogical Properties

Thin-section observations reveal a dominantly dark red to reddish-brown, pelitomorphic to microclastic matrix rich in Fe oxi-hydroxides across all samples. Based on variations in petrographic characteristics, four main facies types are distinguished (Figures 2 and 3a–h), following approaches commonly applied to karst bauxites (e.g., [69]). The intraclastic–oolitic facies is characterized by abundant ooids and frequent intraclasts embedded in a fine-grained ferruginous matrix. Ooids are typically well-rounded to subrounded and display concentric internal structures. Locally, ooids exhibit composite internal structures and partially disrupted concentric laminae. They are commonly lighter in color than the surrounding matrix, with outer laminae locally showing partial to complete iron depletion. Intraclasts are angular to subangular and exhibit variable internal textures, locally showing iron depletion. They also display internal heterogeneity and irregular boundaries. Iron-rich coatings and impregnations are common, forming discontinuous rims around clasts and filling small voids (Figure 3a–d). In contrast, the matrix-rich, poorly consolidated facies is dominated by fine-grained material with reduced ooid abundance and weak cementation. No thin sections were prepared from this interval due to the poorly consolidated nature of the material. The oolitic facies is characterized by abundant ooids embedded in a fine-grained red matrix. Ooids are mostly light-colored and typically up to 1 mm in size. Minor intraclasts are present, and iron-rich coatings and impregnations occur locally (Figure 3e). The pelitomorphic facies is dominated by a fine-grained matrix with only rare ooids. Small intraclasts (up to 1 mm) are locally present. Ferruginous impregnations are abundant in this zone and occur both as diffuse concentrations within the matrix and as irregular coatings and infillings (Figure 3f–h).

The vertical distribution of these facies defines four zones along the core. Zone I (0.5–11 m) is dominated by the intraclastic–oolitic facies; however, a distinct interval between ~6.8 and 8.2 m is characterized by the occurrence of matrix-rich, poorly consolidated facies. Zone II (11–14 m) is dominated by matrix-rich, poorly consolidated facies. Zone III (14–15.5 m) corresponds to the oolitic facies. Zone IV (15.5–25 m) is dominated by pelitomorphic facies.

XRD analysis identified böhmite, gibbsite, hematite, and anatase as the major mineral phases, while goethite, kaolinite, and rutile occur as minor phases (Figures 4–6; Table S1 in the Supplementary Material). The interpretation of mineral abundances is based on relative peak intensities rather than quantitative phase analysis. The mineralogical composition varies systematically between facies types, which largely correspond to the defined zones along the core. The intraclastic–oolitic facies (Zone I; 0.5–11 m) is dominated by böhmite, with gibbsite as a subordinate phase. Hematite is consistently present and more abundant than goethite, which occurs in lower proportions. Anatase is present in minor amounts, while clay minerals are scarce. Detailed XRD analysis following diagnostic tests on oriented clay mounts of two selected bauxite samples from this zone allowed identification of kaolinite (1:1 type clay mineral) (Figure 5a). It appears as poorly crystallized (disordered) kaolinite. The chlorite/vermiculite mixed-layer mineral is identified as a 2:1 clay mineral. The matrix-rich, poorly consolidated facies (Zone II; 11–14 m) retains böhmite as the dominant phase, accompanied by an increase in gibbsite. Hematite reaches a relative maximum in this zone, whereas goethite is absent or negligible. Anatase and kaolinite also show higher relative abundances compared to Zone I, with minor contributions of chlorite/vermiculite mixed-layer mineral. The oolitic facies (Zone III; 14–15.5 m) remains dominated by böhmite. Compared to the overlying matrix-rich facies, this zone shows a decrease in gibbsite and kaolinite, while the chlorite/vermiculite mixed-layer mineral is present in small amounts. Hematite is present but less pronounced than in Zone II, while goethite reappears and remains less abundant than hematite. Anatase persists in minor and relatively stable amounts. The pelitomorphic facies (Zone IV; 15.5–25 m) is

characterized by an increase in gibbsite, which locally exceeds böhmite. Böhmite remains present but is less dominant than in the overlying facies. Presence of diaspore has also been identified in several samples from Zone IV. Hematite decreases, becoming very low in the lowermost part of the core (between 19 and 25 m), whereas goethite increases and generally occurs in higher proportions than hematite. Clay minerals are more abundant, with kaolinite showing a general increase in relative abundance with depth within this zone. Well-crystallized (ordered) kaolinite was identified in the two selected samples at depths of 19.30 m and 21.7 m. The chlorite/vermiculite mixed-layer mineral (Figure 5b) is also more prominent in this zone compared to the others. Anatase is relatively more abundant compared to all other zones. Rutile appears exclusively within this lowermost facies (specifically between 18 and 23 m), although only in minor amounts.

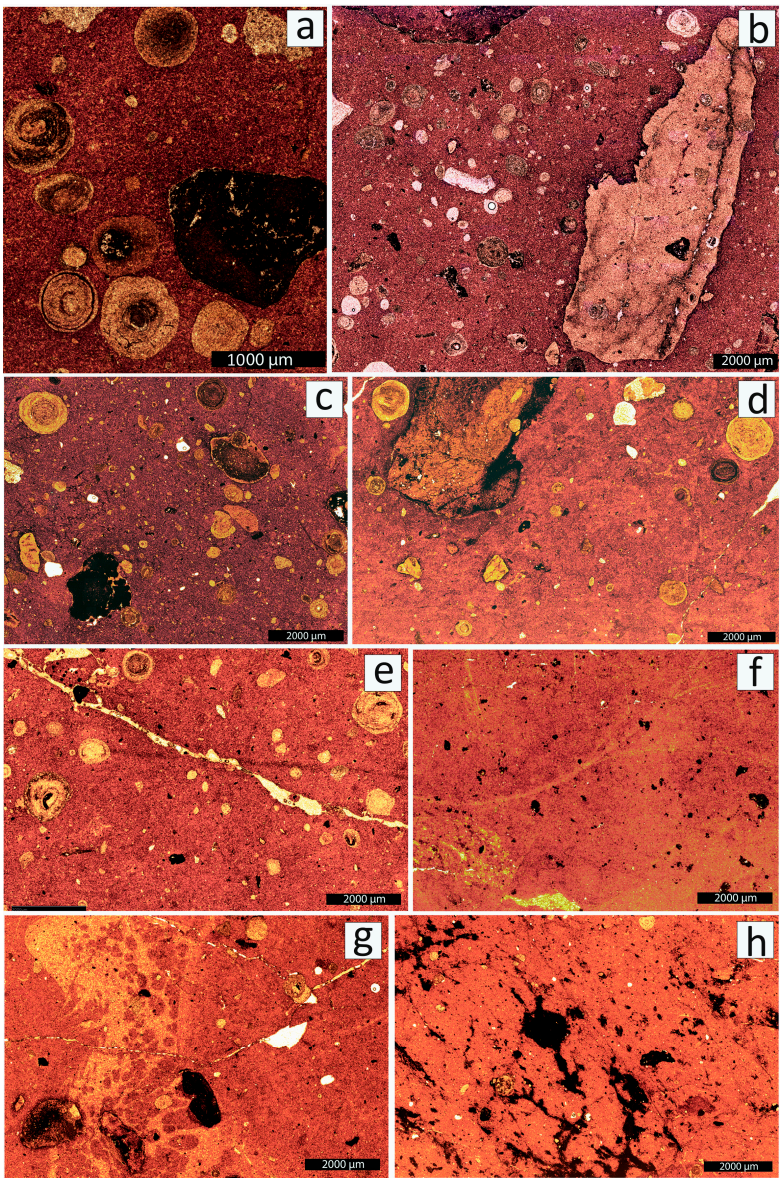

Figure 3. Thin-section photomicrographs of selected bauxite samples from the Mamutovac-1a core: (**a**) 0.70 m, (**b**) 1.84 m, (**c**) 2.80 m, (**d**) 8.53 m, (**e**) 14.33 m, (**f**) 15.73 m, (**g**) 18.53 and (**h**) 22.67 m. (**a**–**d**) Samples from the upper part of the core (Zone I; intraclastic–oolitic facies), characterized by abundant, well-developed ooids and intraclasts embedded in a fine-grained ferruginous matrix. (**e**) Sample from the oolitic facies (Zone III), showing abundant light-colored ooids and a relatively grain-rich texture. (**f**–**h**) Samples from the lower part of the core (Zone IV; pelitomorphic facies), dominated by a fine-grained matrix with sparse to rare ooids and abundant ferruginous impregnations.

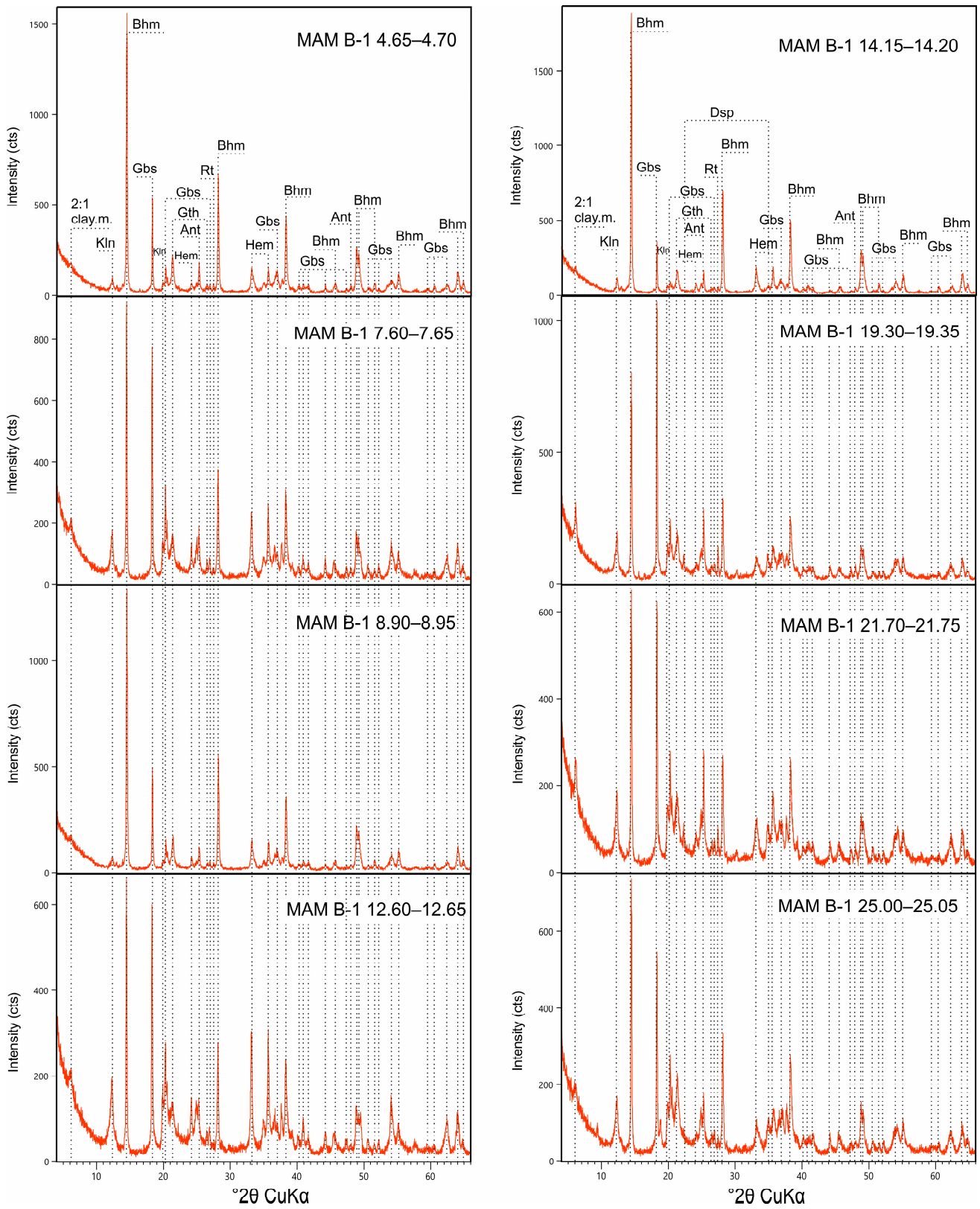

Figure 4. XRD patterns of selected bauxite samples from the Mamutovac-1a deposit. Mineral abbreviations [70]: Bhm: böhmite, Gbs: gibbsite, Hem: hematite, Gth: goethite, Ant: anatase, Kln: kaolinite, Dsp: diaspore, Rt: rutile.

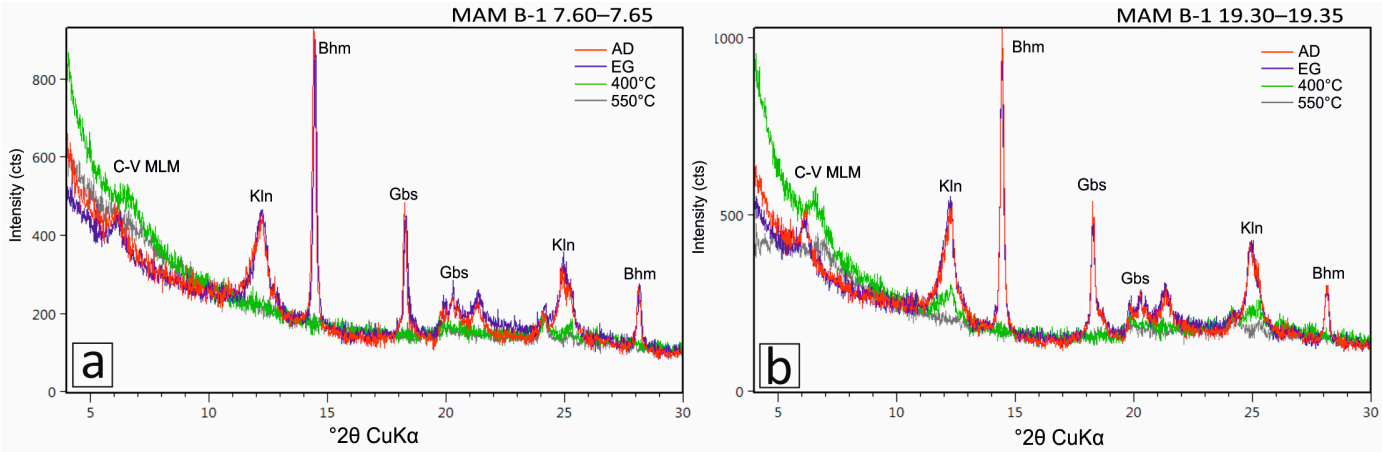

Figure 5. XRD patterns obtained from oriented mounts of the clay fraction of two selected bauxite samples from the Mamutovac-1a deposit; (**a**) sample from 7.60–7.65 m depth; (**b**) sample from 19.30–19.35 m depth. AD: air-dried, EG: ethylene-glycolated, 400 °C and 550 °C, heated. Mineral abbreviations [70]: Bhm: böhmite, Gbs: gibbsite, Kln: kaolinite. C-V MLM refers to chlorite–vermiculite mixed-layer mineral.

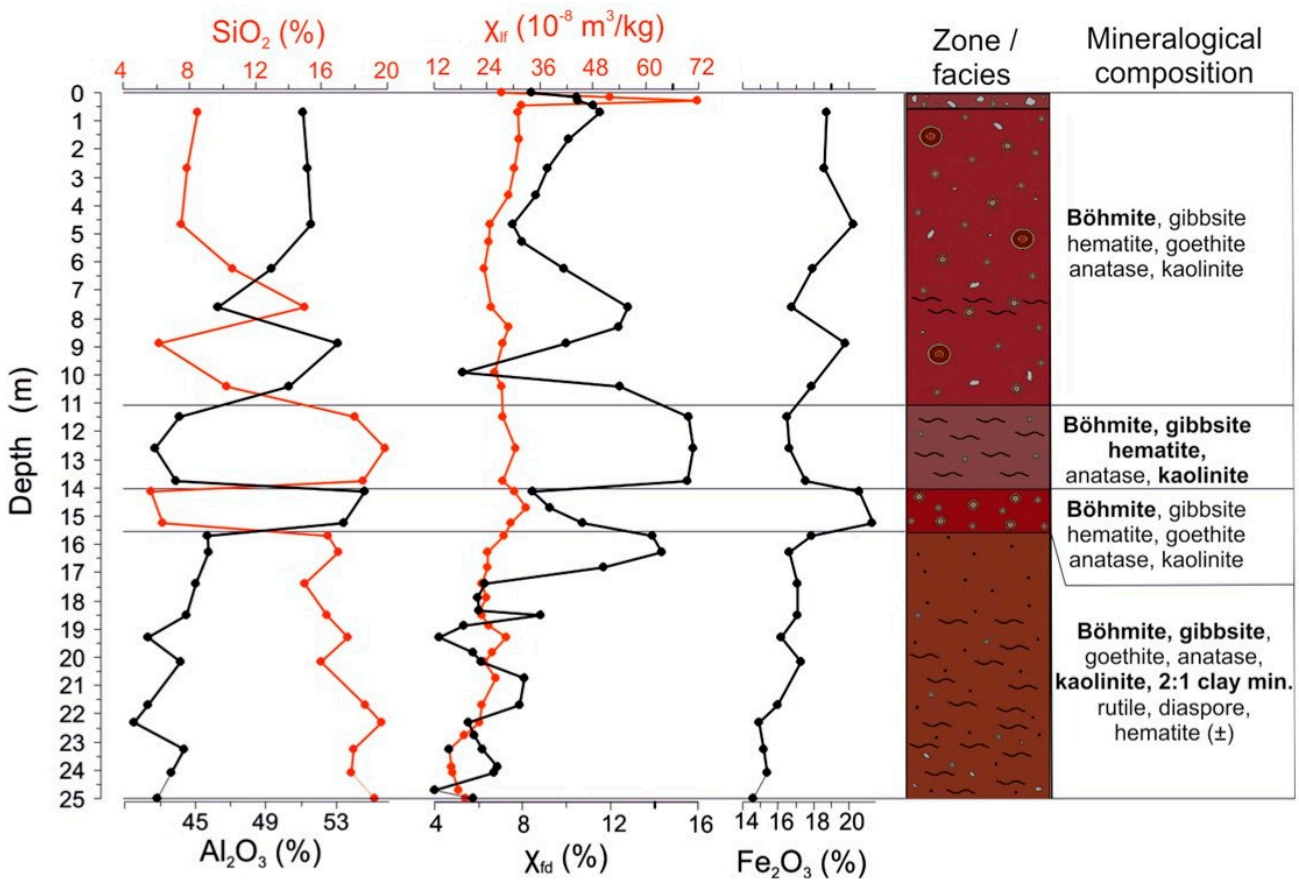

Figure 6. Variation of mass magnetic susceptibility (χ_{lf}) and frequency-dependent magnetic susceptibility (χ_{fd}) with depth in the Mamutovac-1a core, shown alongside SiO_2, Al_2O_3, and Fe_2O_3 contents and mineralogical composition. The combined major oxide, magnetic susceptibility and mineralogical data support the subdivision of the core into four facies-based zones defined by petrographic characteristics (from top to bottom: Zone I—intraclastic–oolitic facies, Zone II—matrix-rich facies, Zone III—oolitic facies, and Zone IV—pelitomorphic facies).

4.1.3. Magnetic Susceptibility

The mass magnetic susceptibility (χ_{lf}) ranges from 15.49 to 71.69 × 10^{-8} m^3/kg (Figure 6), with the highest values in the uppermost part of the profile and the lowest values in the lowermost interval (Zone IV). A general decrease in χ_{lf} with depth is observed, with higher average values in Zones I–III compared to Zone IV. Frequency-dependent susceptibility (χ_{fd}) follows a similar trend, showing higher values in the upper part of the core.

4.2. Geochemistry

Major, trace, and rare earth element compositions of 23 representative samples from the Mamutovac-1a core are summarized in Table 1. Total REE (ΣREE) as well as ΣLREE and ΣHREE values are provided in Table 2. Concentrations are reported in mg/kg, which is numerically equivalent to ppm. Sample positions along the core are shown in Figure 2a.

Table 1. Geochemical composition of the 23 bauxite samples from the Mamutovac-1a core.

Sample	MAM-1	MAM-2	MAM-3	MAM-4	MAM-5	MAM-6	MAM-7	MAM-8	MAM-9	MAM-10	MAM-11	MAM-12
Depth (m)	0.7–0.75	2.70–2.75	4.65–4.70	6.25–6.30	7.60–7.65	8.90–8.95	10.40–10.45	11.50–11.55	12.60–12.65	13.75–13.80	14.15–14.20	15.25–15.30
(%)												
SiO_2	8.51	7.86	7.52	10.61	15.03	6.19	10.26	18.02	19.88	18.49	5.69	6.37
Al_2O_3	50.65	50.97	51.16	48.86	45.83	52.69	49.89	43.66	42.3	43.46	54.19	52.99
Fe_2O_3	18.25	18.13	19.72	17.45	16.29	19.28	17.37	16	16.12	17.04	20.07	20.85
MgO	0.22	0.25	0.19	0.24	0.29	0.16	0.24	0.35	0.4	0.38	0.21	0.22
CaO	0.15	0.12	0.11	0.13	0.17	0.1	0.13	0.19	0.2	0.2	0.09	0.09
Na_2O	0.07	0.06	0.08	0.07	0.08	<0.01	0.03	0.04	0.05	0.06	0.04	0.06
K_2O	0.06	0.05	0.03	0.05	0.06	0.02	0.05	0.09	0.12	0.11	0.06	0.09
TiO_2	2.62	4.04	2.93	2.72	2.53	2.74	2.44	1.62	1.33	1.36	2.81	2.45
P_2O_5	0.04	0.09	0.07	0.06	0.05	0.04	0.04	0.03	0.03	0.03	0.03	0.04
MnO	0.1	0.09	0.14	0.16	0.11	0.12	0.11	0.07	0.05	0.1	0.12	0.16
Cr_2O_3	0.146	0.174	0.142	0.127	0.117	0.147	0.144	0.138	0.147	0.168	0.173	0.184
LOI	18.7	17.6	17.4	19	18.9	18	18.8	19.3	18.9	18.1	16	15.9
Total	99.55	99.47	99.5	99.53	99.53	99.53	99.55	99.58	99.6	99.56	99.53	99.5
(mg/kg)												
Ba	30	36	26	31	36	22	27	35	35	36	31	37
Ni	322	324	390	379	390	357	382	444	480	550	464	511
Sc	49	48	50	44	41	49	42	40	43	51	57	57
Be	6	5	6	2	4	5	5	4	4	2	6	8
Co	34.7	40.4	45.4	44.5	40.3	42.3	37.1	30.4	30.4	44.7	36.5	50.2
Cs	1.9	2.1	1.1	1.8	2.2	1.2	1.9	2.6	3.1	2.7	2.5	3.1
Ga	59.1	57.1	56.4	56.8	56.3	57.2	53.4	51.4	51.9	52.8	57.4	58.2
Hf	13.3	21	15.6	13.9	13.2	13.8	12.1	8.4	6.9	6.6	14.1	12.5
Nb	51	77.1	55.9	53	50.5	54.6	47.8	32.1	26.8	28	53.2	49.3
Rb	4.7	4.2	2.1	3.1	4.1	1.7	3.2	5.9	7.7	6.6	4.8	6.6
Sn	11	12	10	10	9	11	9	7	7	8	11	11
Sr	146.3	278.4	132.5	149.5	176.2	94.2	103.4	98.7	84.1	74	66.8	65.1
Ta	3.6	5.5	4.3	3.7	3.8	3.9	3.6	2.4	2	1.9	3.6	3.1
Th	44.6	53.1	45.4	43.1	39.5	43.6	38.8	32.9	31.5	31.9	44.6	44.7
U	18.6	21.5	16.4	15.7	14.9	15.1	12.6	12.2	11.5	11.7	13.5	12.6
V	1204	1248	1309	1216	1260	1195	1191	1308	1291	1387	1192	1293
W	6	9	7.2	6.3	6.5	6.7	6.3	4	4.2	4.6	7.1	6.3
Zr	499.5	780.5	553.4	497.1	475.2	537.2	439.6	283.9	231.2	237.8	511.8	450.3
Y	54.5	72.3	68.4	58.6	53.3	60.6	48.4	35.5	33.2	38.1	62.5	78.4
(mg/kg)												
La	84.7	102.2	84.4	77.9	74.3	75.5	61.5	50	46.6	51	85.3	102
Ce	207.8	224.5	245	193.5	211.6	200.1	253.6	149.3	163.8	203.2	264.9	190.7
Pr	15.4	18.3	15.5	14.55	14.75	14.28	12.09	9.41	8.95	10.39	17.52	25.72
Nd	56.5	66.7	58.7	55.2	54	55.3	46.2	33.8	32.2	38.9	66.2	104.8
Sm	10.61	12.9	13.54	11.63	11.18	12.71	9.91	7.02	6.29	8.54	15.69	28.48
Eu	2.24	2.71	2.96	2.55	2.36	2.8	2.15	1.5	1.38	1.92	3.54	6.74
Gd	9.42	11.45	11.93	9.78	9.17	10.78	8.68	6.07	5.76	7.08	12.97	25.31
Tb	1.5	1.97	2.07	1.71	1.57	1.86	1.47	1.02	0.96	1.25	2.42	4.46
Dy	9.32	12.87	13.28	10.53	9.8	11.43	9.33	6.26	5.93	7.67	14.97	25.53
Ho	1.96	2.67	2.75	2.27	2	2.38	1.96	1.36	1.27	1.62	2.87	4.76
Er	6.06	8.13	8.85	6.98	6.55	7.29	6.24	4.4	4.27	5.19	9.44	13.64
Tm	0.93	1.29	1.35	1.14	1.02	1.2	0.99	0.67	0.65	0.86	1.58	2.04
Yb	6.35	8.62	9.37	7.82	7.36	7.76	6.6	4.81	4.39	6.04	10.99	13.05
Lu	0.97	1.33	1.43	1.14	1.11	1.22	1.04	0.72	0.68	0.92	1.71	1.99

Table 1. *Cont.*

Sample	MAM-13	MAM-14	MAM-15	MAM-16	MAM-17	MAM-18	MAM-19	MAM-20	MAM-21	MAM-22	MAM-23
Depth (m)	15.70–15.75	16.30–16.35	17.40–17.45	18.50–18.54	19.30–19.35	20.15–20.20	21.70–21.75	22.30–22.35	23.25–23.30	24.10–24.15	25.00–25.10
(%)											
SiO_2	16.41	17.03	15	16.34	17.6	15.97	18.67	19.68	17.99	17.84	19.2
Al_2O_3	45.28	45.32	44.6	44.07	41.92	43.71	41.9	41.08	43.94	43.21	42.39
Fe_2O_3	17.37	16.1	16.57	16.57	15.68	16.78	15.46	14.4	14.66	14.91	14.11
MgO	0.42	0.44	0.43	0.47	0.73	0.57	0.72	0.73	0.47	0.49	0.64
CaO	0.19	0.19	0.18	0.19	0.21	0.19	0.23	0.24	0.22	0.23	0.24
Na_2O	0.07	0.05	0.06	0.06	0.11	0.08	0.13	0.13	0.09	0.09	0.1
K_2O	0.12	0.12	0.11	0.12	0.13	0.1	0.14	0.16	0.12	0.12	0.16
TiO_2	1.56	1.63	2.78	2.75	4.71	3.95	3.84	3.93	1.95	2.04	3.06
P_2O_5	0.07	0.08	0.07	0.08	0.15	0.13	0.13	0.13	0.05	0.06	0.1
MnO	0.14	0.14	0.4	0.22	0.21	0.23	0.25	0.78	0.81	1.28	0.91
Cr_2O_3	0.127	0.107	0.123	0.12	0.108	0.106	0.101	0.088	0.101	0.099	0.086
LOI	17.7	18.3	19.1	18.4	17.7	17.5	17.8	17.9	19	19	18.3
Total	99.54	99.55	99.46	99.48	99.34	99.39	99.42	99.38	99.5	99.46	99.43
(mg/kg)											
Ba	48	42	54	47	65	46	64	82	55	72	70
Ni	580	584	592	560	419	415	429	588	571	780	591
Sc	44	39	41	42	41	42	39	39	40	42	40
Be	8	7	4	5	7	8	6	6	8	6	5
Co	53.1	60.7	44.5	35.5	46	44.7	63.4	113.6	69	89	77.3
Cs	3.8	4.6	6.4	6.5	7.3	5	7.1	8	5.5	5.9	8
Ga	51.2	51.3	50.4	48.8	47.6	50.7	46.8	46.7	48.6	49.9	49.2
Hf	7.8	8	15	14.2	25.8	21.4	20.5	20.4	9.4	10.5	15.5
Nb	31	33.3	53.5	52.7	89.3	74.8	71.3	71.2	38.4	39.4	57
Rb	9.1	9.4	9.6	10.7	12.1	8.4	14	15.4	10.1	10.9	14.9
Sn	8	8	9	9	10	10	9	8	8	7	8
Sr	103.7	142.8	203.4	233.4	680.9	448.3	616.9	625.7	198.3	213.9	443.3
Ta	1.9	2.1	3.7	3.7	5.8	5.4	5.2	5	2.8	2.9	3.9
Th	34.7	34.3	42.3	38.9	46.8	45	44.4	43.9	34.4	34.8	39.2
U	12.5	13.4	16	15.7	22.3	20.4	22.6	20.3	15.3	15	18.8
V	1284	1107	1202	1196	1248	1362	1161	1135	1313	1360	1152
W	4.5	4.8	6.2	6.4	15.3	9.4	9.4	8.9	5.5	5.6	7.7
Zr	275.8	276.2	555.8	537.1	963.3	795.1	757.9	757.4	347.5	359.9	561.3
Y	65	70.3	101.6	99.6	98.4	85.4	76.8	79	63	73	83.3
(mg/kg)											
La	120.7	176.8	147.8	145.4	161.8	123.9	114.4	115.2	87.4	96.2	109.6
Ce	156.1	180.9	296.7	183.7	206.7	152.7	178.4	301.7	254.3	247.1	285.7
Pr	26.64	42.06	30.22	30.31	27.31	23.35	21.71	23.41	18.08	21.28	23.72
Nd	102.9	153	110.4	114.8	96.4	83.6	75.8	85.3	67.2	80.5	86.9
Sm	26.06	27.49	18.85	21.51	15.97	14.49	13.08	14.78	13.19	17.43	16.98
Eu	6.29	6.05	4.12	4.89	3.32	2.95	2.66	3.1	3.02	3.75	3.61
Gd	23.88	23.98	19.33	22.11	15.26	13.38	11.69	13.33	12.67	15.23	15.37
Tb	4.21	3.55	2.7	3.21	2.44	2.19	1.92	2.17	2.02	2.55	2.52
Dy	23.48	19.34	15.8	18.36	15.32	13.74	12.5	13.49	11.97	15.34	15.09
Ho	4.29	3.51	3.32	3.73	3.34	2.96	2.63	2.93	2.44	3.13	3.16
Er	11.85	9.64	9.73	10.97	9.98	9.07	8.11	8.67	7.61	9.37	9.44
Tm	1.7	1.29	1.34	1.42	1.46	1.32	1.23	1.28	1.09	1.38	1.42
Yb	10.66	8.01	8.61	8.69	9.91	8.6	8.13	8.72	7.29	9.12	9.32
Lu	1.59	1.17	1.33	1.36	1.53	1.39	1.24	1.32	1.11	1.38	1.43

4.2.1. Major Element Geochemistry

The sampled intervals are characterized by Al_2O_3 as the dominant oxide (41.08–54.19 wt%), followed by Fe_2O_3 (14.11–20.85 wt%), while SiO_2 (5.69–19.88 wt%) and TiO_2 (1.33–4.71 wt%) show more variable concentrations (Table 1, Figure 7a).

The mass fractions of Al_2O_3, Fe_2O_3, SiO_2, and TiO_2 show distinct variations across the defined facies (Figure 7a). Al_2O_3 is highest in the intraclastic–oolitic facies (Zone I), decreases in the matrix-rich facies (Zone II), and shows a local increase in the oolitic facies (Zone III), followed by a general decline in the pelitomorphic facies (Zone IV). Fe_2O_3 displays a broadly similar distribution, with higher values in Zone I, a decrease in Zone II, and a local maximum in Zone III, followed by decreasing values toward Zone IV. SiO_2 content varies significantly and generally shows an opposite trend to Al_2O_3 and Fe_2O_3 (Figure 7a), with elevated values in the matrix-rich facies (Zone II) and in the deeper pelitomorphic facies (Zone IV), as well as locally within Zone I (e.g., ~8 m). Al_2O_3 and Fe_2O_3 show a broadly positive covariation (Figure 8a), whereas SiO_2 exhibits a pronounced inverse relationship with both Al_2O_3 and Fe_2O_3 (Figure 8b,c). Overall, Al_2O_3 and Fe_2O_3 show a general decrease with depth, whereas SiO_2 tends to increase toward the lower part of the profile.

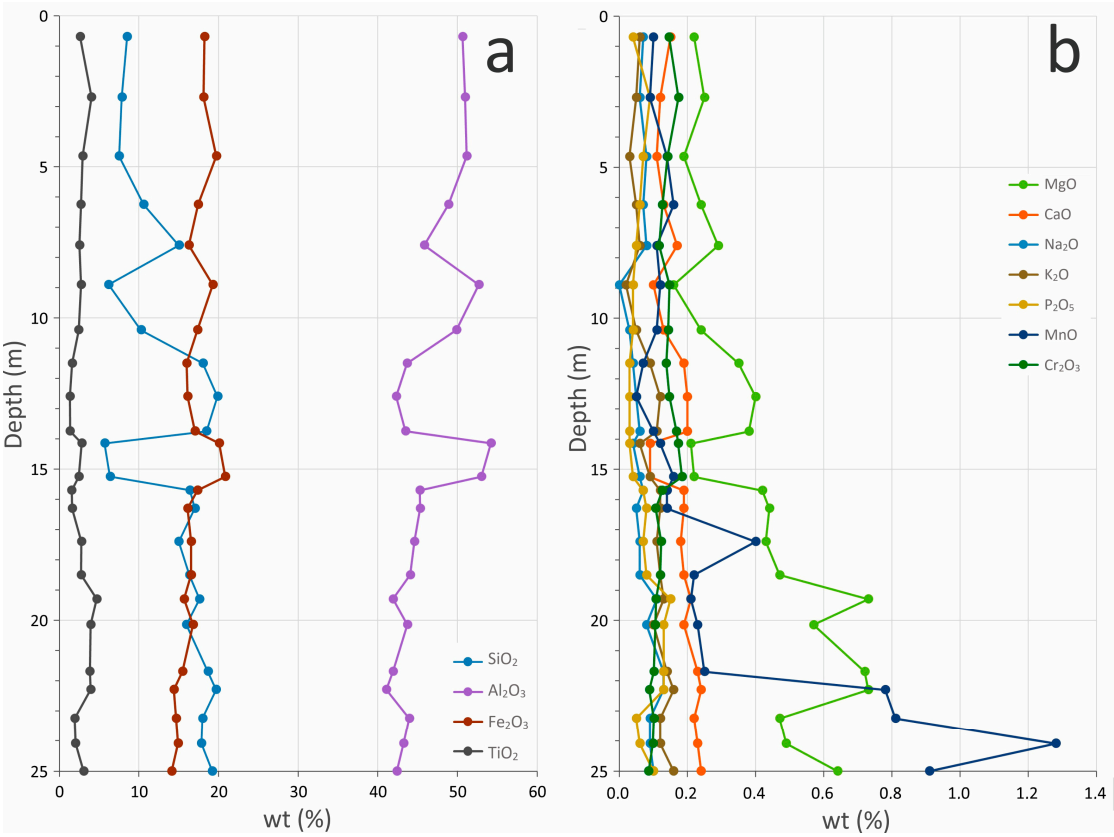

Figure 7. Diagram showing the distribution of (**a**) major and (**b**) other oxides in the 23 Mamutovac-1a core samples and their variation with depth.

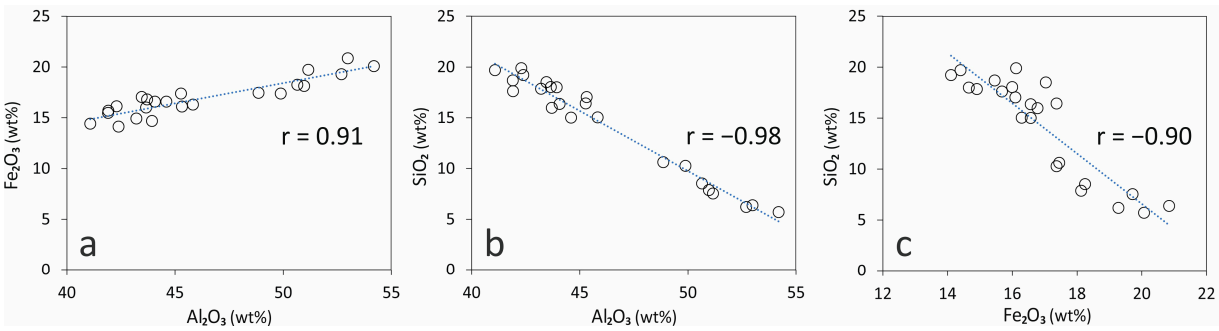

Figure 8. Bivariate plots of (**a**) Al_2O_3–Fe_2O_3, (**b**) Al_2O_3–SiO_2, and (**c**) Fe_2O_3–SiO_2 showing positive correlations between Al_2O_3 and Fe_2O_3, and their negative correlations with SiO_2.

TiO_2 exhibits moderate variability, with a slight decrease from Zone I to Zone II, followed by a local increase in the oolitic facies (Zone III), and fluctuating values, with a tendency toward slightly higher concentrations in the pelitomorphic facies (Zone IV).

In addition to the major oxides, oxides exhibiting mass fractions ranging from 0.01 wt% to 1 wt% were also detected, specifically MgO (0.16–0.73 wt%), CaO (0.09–0.24 wt%), Na_2O (0.03–0.13 wt%), K_2O (0.02–0.16 wt%), P_2O_5 (0.03–0.15 wt%), MnO (0.05–1.28 wt%), and Cr_2O_3 (0.09–0.18 wt%) (Table 1, Figure 7b). MgO, CaO, and K_2O show strong positive correlations with SiO_2 (r = 0.81, 0.96, and 0.85, respectively; Table S2 in the Supplementary Material) and therefore follow a similar distribution, including lower values in the oolitic facies (Zone III) and higher values in the pelitomorphic facies (Zone IV). P_2O_5 shows a similar distribution to TiO_2, correlating positively with it (r = 0.79; Table S2 in the Supplementary Material), with lower values in the upper facies (Zones I–III) and an increase in the pelitomorphic facies (Zone IV). In contrast, Cr_2O_3 shows an opposite trend,

with relatively higher values in the upper facies (Zones I–III), and correlates positively with Fe_2O_3 (r = 0.84; Table S2 in the Supplementary Material). MnO shows the most pronounced variation, with low values in the upper facies (average ~0.15 wt%) and a sharp increase in the pelitomorphic facies (Zone IV), reaching up to 0.95 wt%.

The observed geochemical variations broadly correspond to the mineralogical composition of the defined facies. The intraclastic–oolitic facies (Zone I) and oolitic facies (Zone III), characterized by the dominance of böhmite and hematite, show higher Al_2O_3 and Fe_2O_3 contents, reflecting the abundance of Al- and Fe-bearing mineral phases. In contrast, the matrix-rich facies (Zone II) and pelitomorphic facies (Zone IV), which contain higher proportions of clay minerals and gibbsite, show higher SiO_2 contents and selected minor oxides. In particular, elevated SiO_2, MgO, and K_2O contents are consistent with the increased contribution of clay minerals, whereas higher TiO_2 values reflect the presence of Ti-bearing phases such as anatase and rutile. Similarly, the distribution of P_2O_5 shows higher values in the pelitomorphic facies (Zone IV). The positive relationship between Cr_2O_3 and Fe_2O_3 suggests that Cr is at least partly associated with Fe-bearing phases, likely through adsorption or substitution in Fe oxi-hydroxides.

4.2.2. Trace Element Geochemistry

The most abundant trace elements in the core are V (1239 mg/kg), Cr (884.7 mg/kg), Zr (508 mg/kg), Ni (482 mg/kg), and Sr (234 mg/kg) (Table 1, Figure 9a–e). Vanadium ranges from 1107 to 1387 mg/kg, Zr from 231 to 963 mg/kg, and Ni from 322 to 780 mg/kg, while Sr ranges from 65 to 681 mg/kg. Cr concentrations range from 588.6 to 1259.4 mg/kg and broadly follow the vertical trend observed for Cr_2O_3.

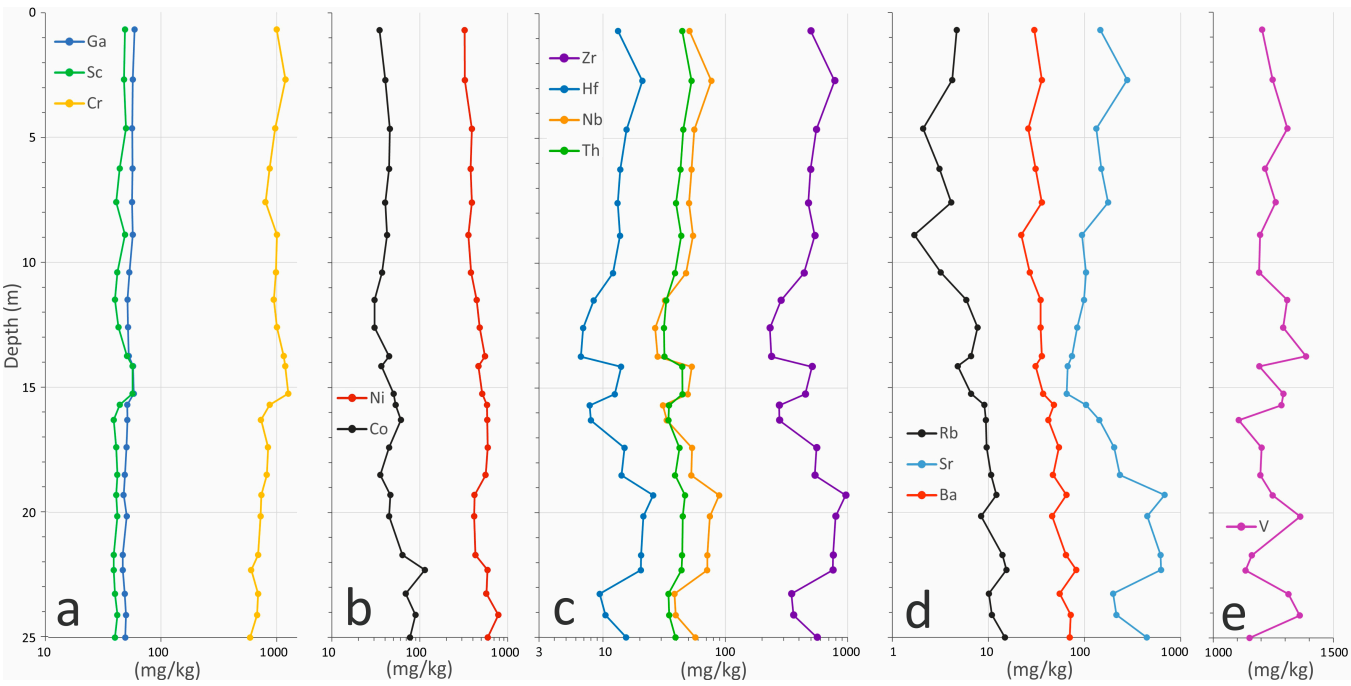

Figure 9. Depth-dependent variations of selected trace elements in the Mamutovac-1a bauxite core. Trace elements are grouped according to their correlations with major oxides: (**a**) Ga, Sc, and Cr, (**b**) Ni and Co, (**c**) Zr, Hf, Nb, and Th, (**d**) Rb, Sr, and Ba, and (**e**) V. Panels (**a**–**d**) are plotted on a logarithmic scale, whereas panel (**e**) is shown on a linear scale.

Sn and Sc show a decrease in Zone II, followed by a local increase toward Zone III and more variable values in Zone IV. In contrast, Cr shows a less systematic distribution, with no clearly defined facies-dependent trend, while Ga displays only minor variations

across the profile. All four elements display systematic relationships with Fe_2O_3, showing positive correlations (Cr r = 0.84, Ga r = 0.83, Sn r = 0.76, Sc r = 0.88), while Sn also correlates with TiO_2 (r = 0.55). The observed distribution of Cr, Ga, Sn, and Sc is consistent with their association with Fe oxi-hydroxides, which are most abundant in Zones I and III (Figure 9a). Ni and Co show a general increase from Zones I–II toward Zone IV, with some local variability (Figure 9b). Both elements show strong positive correlations with MnO (Ni r = 0.73; Co r = 0.82), along with negative to moderate correlations with Fe_2O_3 (Ni r = −0.49; Co r = −0.56). Zr, Hf, Nb, Ta, Th, U, and W follow a general pattern of decreasing values from Zone I to Zone II, a local maximum in Zone III, and more irregular variations in Zone IV (Figure 9c). These elements exhibit strong positive correlations with TiO_2 (Zr r = 0.99, Hf r = 0.99, Nb r = 0.99, Ta r = 0.98, Th r = 0.85, U r = 0.91, W r = 0.92; Table S2), as well as weaker and variable positive correlations with P_2O_5. A nearly perfect positive correlation between Zr and Hf (r = 0.99) is also observed. Rb, Cs, Sr, and Ba show a progressive increase from Zone I toward Zone IV (Figure 9d). These elements display generally positive correlations with K_2O, MgO, P_2O_5, CaO, Na_2O, and MnO, and negative correlations with Al_2O_3 and Fe_2O_3. The strongest correlations are observed between Rb and K_2O (r = 0.96), Cs and MgO (r = 0.93), and Sr and P_2O_5 (r = 0.93). Vanadium shows no clear facies-dependent trend and exhibits irregular variability throughout the profile, without significant correlations with major oxides (Figure 9e).

4.2.3. REE Geochemistry

The bauxite samples from the Mamutovac-1a core show variable REE contents (Table 1, Figure 10). The total REE content (ΣREE) ranges from 276 to 670 mg/kg. ΣREE values are lower in Zones I–II, reach a local minimum in Zone III, and increase again toward Zone IV, although individual samples show some variability. Similar distribution patterns are observed for both light REEs (ΣLREE; La–Sm) and heavy REEs (ΣHREE; Eu–Lu). ΣLREE ranges from 250 to 604 mg/kg and represents the dominant fraction of total REE content, whereas ΣHREE concentrations are significantly lower, ranging from 25 to 98 mg/kg. Variations are more pronounced in the ΣLREE fraction, while ΣHREE shows comparatively subdued variability.

The REE distribution is characterized by enrichment of LREE relative to HREE, as reflected in ΣLREE/ΣHREE ratios ranging from 4.63 to 10.20 (Table 2). These ratios show systematic vertical variations, with slightly higher values in the upper part of the profile (Zones I–II; average ~8.8) compared to deeper intervals (Zones III–IV; average ~7.6). A local minimum in ΣLREE/ΣHREE is observed at approximately 15–16 m, corresponding to the transition between Zones III and IV. The $(La/Yb)_N$ ratios range between 5.24 and 14.90, with generally lower and decreasing values from Zones I to III, followed by a sharp increase to a maximum at 16.30–16.35 m in Zone IV, and generally higher values in Zone IV, with a decreasing trend. The $(La/Sm)_N$ ratios range between 2.25 and 6.38, with decreasing values from Zones I to III and higher values in Zone IV, where a local maximum is observed at 19.30–19.35 m. The $(Gd/Yb)_N$ ratios range between 0.95 and 2.42 and remain relatively uniform across all zones, with slightly higher values in the upper part of Zone IV.

The La/Y ratio ranges from 1.23 to 2.51 and remains consistently above unity throughout the profile. Values are relatively uniform in Zones I–III, whereas higher and more variable values are observed in Zone IV, including a pronounced peak at 16.30–16.35 m.

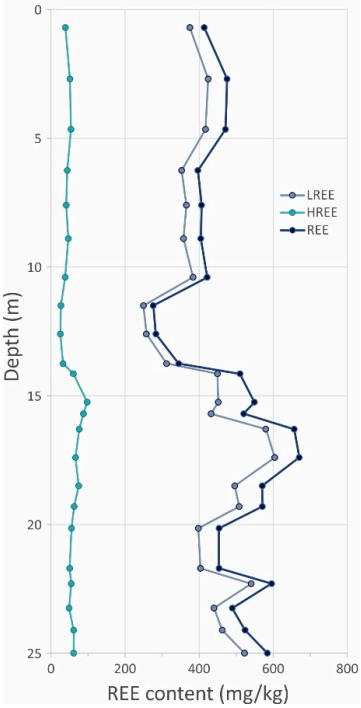

Figure 10. Diagram illustrating the absolute values of ΣLREE, ΣHREE, and ΣREE for the 23 Mamutovac-1a core samples and their variation with depth.

Table 2. Geochemical parameters of Rare Earth Elements and selected ratios for the 23 Mamutovac-1a core samples. The normalization factors for chondrite are from [71].

Sample	MAM-1	MAM-2	MAM-3	MAM-4	MAM-5	MAM-6	MAM-7	MAM-8	MAM-9	MAM-10	MAM-11	MAM-12
Depth (m)	0.7–0.75	2.70–2.75	4.65–4.70	6.25–6.30	7.60–7.65	8.90–8.95	10.40–10.45	11.50–11.55	12.60–12.65	13.75–13.80	14.15–14.20	15.25–15.30
ΣREE	413.76	475.64	471.13	396.70	406.77	404.61	421.76	276.34	283.13	344.58	510.10	549.22
ΣLREE	375.01	424.60	417.14	352.78	365.83	357.89	383.30	249.53	257.84	312.03	449.61	451.70
ΣHREE	38.75	51.04	53.99	43.92	40.94	46.72	38.46	26.81	25.29	32.55	60.49	97.52
ΣL/ΣH	9.68	8.32	7.73	8.03	8.94	7.66	9.97	9.31	10.20	9.59	7.43	4.63
$(La/Yb)_N$	9.00	8.00	6.08	6.72	6.81	6.57	6.29	7.02	7.16	5.70	5.24	5.28
$(La/Sm)_N$	5.03	4.99	3.92	4.22	4.18	3.74	3.91	4.48	4.66	3.76	3.42	2.25
$(Gd/Yb)_N$	1.20	1.07	1.03	1.01	1.01	1.12	1.06	1.02	1.06	0.95	0.95	1.57
La/Y	1.55	1.41	1.23	1.33	1.39	1.25	1.27	1.41	1.40	1.34	1.36	1.30
Sm/Nd	0.19	0.19	0.23	0.21	0.21	0.23	0.21	0.21	0.20	0.22	0.24	0.27
Eu/Eu*	0.68	0.68	0.71	0.73	0.71	0.73	0.71	0.70	0.70	0.75	0.76	0.77
Ce/Ce*	1.38	1.25	1.63	1.38	1.54	1.47	2.24	1.66	1.93	2.12	1.65	0.90

Sample	MAM-13	MAM-14	MAM-15	MAM-16	MAM-17	MAM-18	MAM-19	MAM-20	MAM-21	MAM-22	MAM-23
Depth (m)	15.70–15.75	16.30–16.35	17.40–17.45	18.50–18.54	19.30–19.35	20.15–20.20	21.70–21.75	22.30–22.35	23.25–23.30	24.10–24.15	25.00–25.10
ΣREE	520.35	656.79	670.25	570.46	570.74	453.64	453.50	595.40	489.39	523.76	584.26
ΣLREE	432.40	580.25	603.97	495.72	508.18	398.04	403.39	540.39	440.17	462.51	522.90
ΣHREE	87.95	76.54	66.28	74.74	62.56	55.60	50.11	55.01	49.22	61.25	61.36
ΣL/ΣH	4.92	7.58	9.11	6.63	8.12	7.16	8.05	9.82	8.94	7.55	8.52
$(La/Yb)_N$	7.64	14.90	11.59	11.29	11.02	9.72	9.50	8.92	8.09	7.12	7.94
$(La/Sm)_N$	2.92	4.05	4.94	4.26	6.38	5.38	5.51	4.91	4.17	3.47	4.06
$(Gd/Yb)_N$	1.81	2.42	1.81	2.06	1.24	1.26	1.16	1.24	1.40	1.35	1.33
La/Y	1.86	2.51	1.45	1.46	1.64	1.45	1.49	1.46	1.39	1.32	1.32
Sm/Nd	0.25	0.18	0.17	0.19	0.17	0.17	0.17	0.17	0.20	0.22	0.20
Eu/Eu*	0.77	0.72	0.66	0.69	0.65	0.65	0.66	0.68	0.71	0.70	0.68
Ce/Ce*	0.66	0.50	1.07	0.67	0.75	0.68	0.86	1.40	1.54	1.31	1.35

All samples exhibit clear Ce and Eu anomalies. The Ce/Ce* ratio ranges from 0.50 to 2.24, with predominantly positive anomalies in Zones I–III, followed by a shift toward negative values through Zone III and predominantly negative anomalies in the upper part of Zone IV. Positive Ce anomalies are again observed in the lowermost part of the core (22–25 m). Eu shows consistently negative anomalies throughout the core, with Eu/Eu* values ranging from 0.65 to 0.77, increasing slightly from Zones I to III and followed by lower values in Zone IV.

Most REEs show strong mutual positive correlations, whereas Ce displays distinct behavior compared to the other REEs (Table S3 in the Supplementary Material) and shows a moderate positive correlation with MnO (r = 0.57). None of the REEs show significant correlations with Al_2O_3 and Fe_2O_3, indicating no direct association with the main bauxitic components. In contrast, positive correlations are observed between ΣREE (excluding Ce) and P_2O_5, with the strongest relationships for La (r = 0.69), Y (r = 0.71), Pr (r = 0.53), and Nd (r = 0.47). Moderate correlations are also observed with K_2O (Pr r =0.48, La r = 0.45, Nd r = 0.45) and MgO (La r =0.52, Y r = 0.49, Pr r = 0.43), as well as with TiO_2 (Y r = 0.64, La r = 0.43, Lu r = 0.42), although their strength varies among individual elements.

4.2.4. Extraction with Aqua Regia

Bauxite deposits primarily serve as sources of aluminum, but they also contain a range of elements classified as critical raw materials (CRMs). The extraction of such elements from bauxite and red mud can be achieved through direct leaching processes using mineral acids (e.g., HNO_3, HCl, H_2SO_4, and aqua regia), which are considered highly effective [72]. These elements are commonly leached with other components, which may affect selectivity, particularly with respect to iron [72]. In this study, aqua regia extraction was applied to evaluate the leachability of selected elements from the Mamutovac bauxite.

The concentrations of selected CRMs (La, Ga, Sc and V) in the Mamutovac-1a deposit fall within the range reported for karst bauxite deposits worldwide (Ga; [73]), including those from southern Italy, Sardinia [11], and Montenegro [21]. The only exception is V, which shows elevated concentrations (approximately three times higher) compared to previously reported Mediterranean-type bauxites [11,21]. Total and aqua regia extractable concentrations are presented in Table 3.

Table 3. Statistical parameters for selected elements Fe, P (%), Sc, Ga, V and La (mg/kg) after the aqua regia (a.r.) extraction (% element amount extracted).

Element	Treatment	N	Mean	Minimum	Maximum	Std. Dev.
Fe (%)	total	8	11.68	9.87	12.76	0.92
P (%)	total	8	0.030	0.013	0.057	0.015
Sc (mg/kg)	total	8	44	39	51	4.2
Ga (mg/kg)	total	8	52.3	46.8	59.1	4.2
V (mg/kg)	total	8	1224	1152	1387	77
La (mg/kg)	total	8	95.7	51.0	145.4	32.2
Fe (%)	aqua regia	8	10.75	9.00	11.62	0.88
P (%)	aqua regia	8	0.009	0.004	0.013	0.003
Sc (mg/kg)	aqua regia	8	34.4	25.8	43.2	5.7
Ga (mg/kg)	aqua regia	8	22.5	18.9	24.9	2.0
V (mg/kg)	aqua regia	8	1063	969	1262	93
La (mg/kg)	aqua regia	8	29.0	16.9	55.6	13.1
Fe	% extracted	8	92.02	88.98	97.08	2.46
P	% extracted	8	33.57	22.91	45.83	8.22
Sc	% extracted	8	78.05	66.15	84.71	6.35
Ga	% extracted	8	43.36	36.55	49.80	5.39
V	% extracted	8	86.75	83.89	90.99	2.29
La	% extracted	8	30.28	18.01	38.24	6.60

XRD analysis of the residue after aqua regia extraction and dissolution of goethite and hematite (Figure 11) shows that the main mineralogical composition remains largely comparable to that of the untreated bauxite samples, with the notable removal of Fe oxi-hydroxides. This indicates that the acid treatment primarily affects Fe-bearing phases, while the general mineralogical framework is preserved.

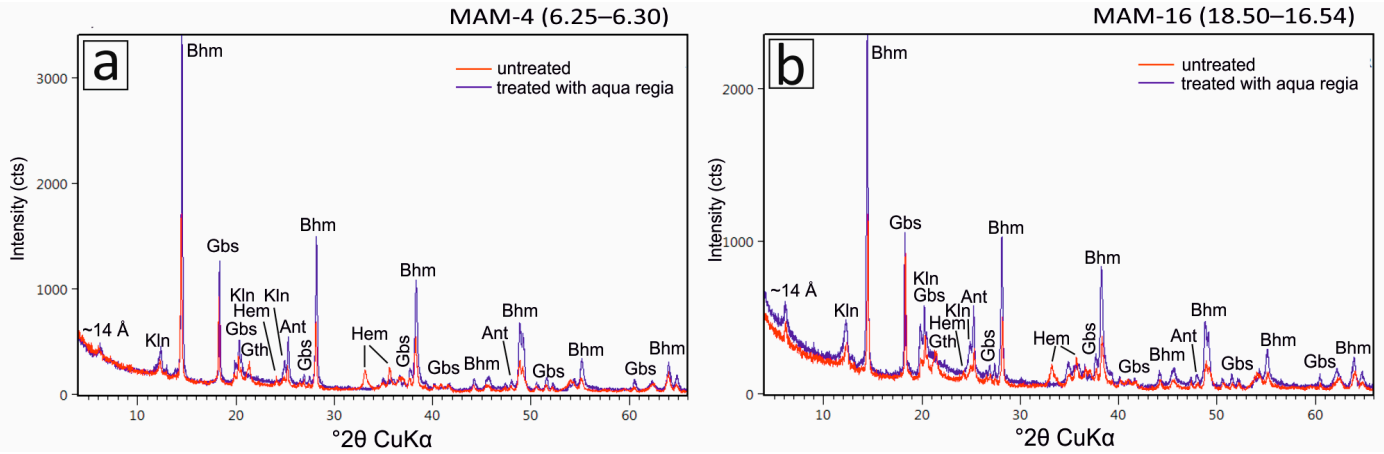

Figure 11. XRD patterns for bauxite samples (**a**) MAM-4 (6.25–6.30 m) and (**b**) MAM-16 (18.50–18.54 m), before and after aqua regia (a.r.) treatment. Mineral abbreviations [70]: Bhm: böhmite, Gbs: gibbsite, Hem: hematite, Gth: goethite, Ant: anatase, Kln: kaolinite.

5. Discussion

5.1. Facies Variability and Implications for Depositional Processes

The vertical variability of the Mamutovac-1a core is expressed through changes in facies distribution and associated textural features (Figures 2 and 3). The intraclastic–oolitic facies (Zone I) and oolitic facies (Zone III) are characterized by abundant ooids, intraclasts, and micro-pebbles embedded in a fine-grained matrix. Ooids are predominantly rounded to subrounded and commonly display concentric internal structures, locally showing composite features and partially disrupted laminae (Figure 3a–e). Intraclasts are irregular to subangular, with heterogeneous internal textures and irregular boundaries. These features indicate that a significant part of the material was redeposited after initial bauxitization [4,17,74]. In contrast, the matrix-rich facies (Zone II) shows a reduced abundance of coated grains and is dominated by fine-grained material, whereas the pelitomorphic facies (Zone IV) is composed of a homogeneous matrix with only rare ooids and small intraclasts (Figure 3f–h). The absence or scarcity of coated grains in these intervals indicates a lower degree of reworking compared to Zones I and III [1,4]. The vertical alternation of these facies suggests repeated redistribution of bauxitic material within the profile, rather than uniform accumulation. In this context, Zone II represents a transitional interval separating two horizons characterized by more intensive reworking (Zones I and III), marked by a reduced abundance of coated grains and a higher proportion of fine-grained material. According to Bárdossy [1], facies dominated by intraclasts and coated grains correspond to reworked (allothigenic) bauxite, whereas pelitomorphic textures are characteristic of authigenic formation. The observed distribution therefore indicates that reworked material predominates in Zones I and III, while Zone IV, and partly Zone II, reflect a greater contribution of authigenic material. The combined sedimentological and petrographic features indicate that the deposit formed through multi-stage accumulation involving both in situ bauxitization and episodic reworking and redeposition.

Post-depositional modification of the Mamutovac-1a ore body is reflected in variations in consolidation across the defined zones. Well-lithified intervals alternate with poorly con-

solidated material, indicating differences in cementation and compaction intensity within the profile. Color variations show a systematic vertical pattern. Dark red hues dominate Zone I, whereas Zones III–IV are characterized by 5 YR and 7.5 YR hues, indicating a shift toward yellowish-brown tones (Figure 2). Such variations are commonly associated with changes in iron mineralogy and hydration state during diagenesis [75]. Secondary coatings occur as discontinuous rims and infillings on clasts, with a more frequent occurrence in Zone IV (Figure 3f–h). Black coatings are associated with Mn- and/or Fe-oxide accumulations, whereas yellow coatings correspond to goethite-rich alteration products [2]. Their distribution indicates localized fluid circulation and secondary mineral precipitation following deposition. These post-depositional features are more pronounced in Zones III–IV, suggesting more extensive secondary modification in the lower part of the profile.

5.2. Mineralogical and Geochemical Variability in Response to Evolving Physico-Chemical Conditions

Böhmite is the dominant Al-bearing phase in Zones I–III, whereas gibbsite becomes relatively more abundant in Zone IV (Figures 4–6). Minor amounts of diaspore are also observed in Zone IV. This vertical distribution reflects differences in the degree of diagenetic modification across the profile. The dominance of böhmite in the upper and middle parts of the core (Zones I–III) indicates dehydration and transformation following initial bauxitization, as commonly observed in karst-hosted bauxite profiles [2,76,77]. Böhmite is widely interpreted as a secondary phase formed from gibbsite under near-surface conditions through water loss during compaction. The prevalence of this phase in Zones I and III, which are also characterized by abundant coated grains, is consistent with reworking of already transformed bauxitic material. The relative enrichment of gibbsite in Zone IV indicates a lower degree of transformation and greater preservation of earlier-formed phases, consistent with more stable or water-saturated conditions where dehydration is limited [1,78]. The presence of minor diaspore in this interval may reflect localized transformation of boehmite under specific physico-chemical conditions. Supergene diaspore is commonly formed under reducing and alkaline conditions [4,36]. Özlü [79] has also interpreted mineral assemblages containing syn-diagenetic diaspore as indicators of reducing, likely alkaline environments. Anatase occurs throughout the core, with a slight increase in Zones III–IV, while rutile is restricted to a narrow interval within Zone IV (18–23 m). The increased abundance of anatase in the lower part of the core may reflect changes in physico-chemical conditions, including variations in redox state. In karst bauxite systems, anatase has been linked to relatively reducing and lower pH conditions [79]. Similar mineral assemblages, characterized by böhmite as the dominant Al-bearing phase and anatase as the main Ti-bearing phase, have been reported from karst bauxites in other parts of the Mediterranean region, including southern Italy [9] and Montenegro [21]. The distribution of Fe oxi-hydroxides also varies systematically along the profile. Hematite dominates in Zones I–II and shows relatively stable proportions, with a local maximum in Zone II, whereas its abundance decreases toward Zone IV, where goethite becomes more prominent. This trend is consistent with a transition from relatively more oxidizing and dehydrated conditions in the upper part of the profile to more hydrated conditions in the lower zones. Fe oxi-hydroxides are sensitive to variations in redox conditions, fluid composition, and drainage within the weathering environment [80]. Hematite typically forms under strongly oxidizing conditions and may originate from the transformation of primary Fe-bearing minerals or through dehydration of goethite [2,77]. Kaolinite is present in all zones but becomes more abundant and better crystallized in Zone IV, whereas it occurs in lower amounts and with poorer crystallinity in the upper zones. The reduced abundance of clay minerals in the upper part of the profile is consistent with more intensive leaching, which promotes silica removal during advanced chemical weathering and favors the formation

of Al-rich phases such as gibbsite and böhmite. In contrast, the retention of kaolinite and the presence of chlorite/vermiculite mixed-layer mineral in the lower part of the profile suggest less intensive leaching, possibly related to slower drainage conditions or increased detrital input [81]. Similar occurrences of 2:1 clay minerals have been reported in bauxites of the Dinaric karst region, including hydroxy-interlayered vermiculite identified in the Crveni Klanac deposit [45]. Overall, the mineral assemblages suggest formation under variable physico-chemical conditions, ranging from relatively oxidizing and dehydrated, likely more acidic environments in the upper and middle parts of the bauxite body (Zones I–III) to more hydrated and locally reducing, possibly more alkaline conditions in the lowermost parts (Zone IV).

Mass magnetic susceptibility (χ_{lf}) decreases with depth, broadly following the distribution of Fe-bearing phases, particularly hematite, which are more abundant in the upper zones (Figure 6). Higher frequency-dependent susceptibility (χ_{fd}) values in the upper part of the profile indicate the presence of ultrafine superparamagnetic particles [82]. The limited development of pedogenic features suggests that these particles are more likely inherited from reworked material rather than formed in situ, supporting the interpretation of a polygenetic origin of the bauxite deposit.

Major element variability in the Mamutovac-1a core reflects differences in the degree of desilicification and Al and Fe redistribution across the defined facies (Figures 6 and 7a). The inverse relationship between SiO_2 and Al_2O_3–Fe_2O_3 (Figure 8) indicates that silica removal was a primary control on the chemical evolution of the deposit, consistent with the fundamental role of desilicification in bauxite formation [1,2]. Zones I and III, characterized by elevated Al_2O_3 and Fe_2O_3 contents, correspond to intervals where desilicification was more effective, leading to residual enrichment of Al and Fe. Such geochemical signatures are typical of advanced bauxitization stages, where silica is progressively removed and Al–Fe oxi-hydroxides become dominant [1,4]. The positive covariation between Al_2O_3 and Fe_2O_3 suggests largely parallel enrichment of these elements, a relationship commonly observed in lateritic and karst-hosted bauxites under conditions of limited element mobility [32]. In contrast, Zones II and IV show increased SiO_2 contents and lower Al_2O_3 and Fe_2O_3 values, indicating less efficient desilicification and a greater contribution of less altered material. According to Bárdossy [1], elevated silica in bauxitic profiles may reflect either incomplete leaching or the incorporation of detrital clay material, particularly in polygenetic karst systems. This interpretation is consistent with the higher abundance of clay minerals and gibbsite observed in these zones, suggesting a lower degree of bauxitization compared to Zones I and III. The vertical distribution of Fe_2O_3 further reflects changes in redox and hydration conditions during bauxitization and early diagenesis. Higher Fe_2O_3 contents in the upper part of the profile correspond to hematite-dominated assemblages, which typically form under more oxidizing and dehydrated conditions, whereas the relative increase in goethite in deeper intervals indicates more hydrated conditions [2,80]. This transition is consistent with progressive modification of Fe oxi-hydroxides controlled by changes in Eh–pH conditions within the paleokarst system.

The ternary diagrams (Figure 12) illustrate different aspects of bauxite composition and evolution: the first reflects compositional classification, the second highlights the degree of lateritization and Fe enrichment, and the third shows the relative contribution of clay- and Fe-rich components. The dispersed distribution of Zone I samples between the bauxite and ferritic bauxite fields indicates variable Fe participation and heterogeneous geochemical conditions, consistent with reworking and redistribution of bauxitic material in karst environments [4]. Samples from Zones II and IV cluster within the bauxite field and correspond to moderate to strong lateritization, reflecting more uniform but less advanced chemical differentiation. In contrast, Zone III samples plot within the ferritic bauxite field

and correspond to strong lateritization, indicating relatively enhanced Fe enrichment. In the clay–Fe ternary diagram, all samples fall within the argillo–ferruginous bauxite field, indicating a consistent contribution of both clay-related and Fe-rich components across the profile. The limited separation between zones suggests that, despite vertical variability in major element concentrations, the overall geochemical character of the deposit remains within the same compositional domain, typical of polygenetic karst bauxites [1].

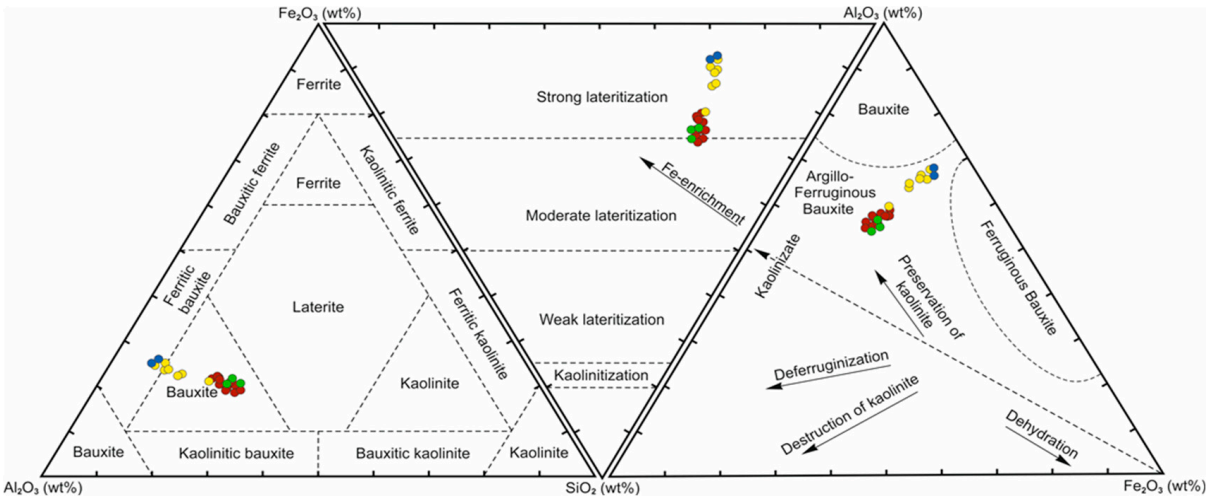

Figure 12. Al_2O_3–SiO_2–Fe_2O_3 ternary diagrams showing mineralogical classification, degree of lateritization, and bauxite classification. Modified after [32] and references therein. Sample points are color-coded according to the defined bauxite facies: yellow for Zone I (0.5–11 m), green for Zone II (11–14 m), blue for Zone III (14–15.5 m), and red for Zone IV (15.5–25 m).

TiO_2 shows variable distribution along the profile despite its general immobility during chemical weathering (Figure 7a). The lack of systematic correlation with Al_2O_3, Fe_2O_3, or SiO_2 indicates that Ti behaved largely independently of the main geochemical processes controlling bauxitization. Such behavior is typical for Ti in bauxite deposits, where it is commonly concentrated in resistant minerals and reflects residual enrichment or detrital input rather than in situ chemical redistribution [1,9,32]. The relative enrichment of TiO_2 in the lower part of the profile may therefore reflect localized accumulation of Ti-bearing detrital material or residual concentration under conditions of reduced leaching intensity.

The distribution of minor oxides reflects facies-dependent geochemical variability and differences in element behavior during bauxitization and subsequent diagenesis. MgO, CaO, and K_2O show a strong positive correlation with SiO_2, indicating their association with silicate phases and suggesting a link to detrital material or incomplete desilicification. Their enrichment in Zone IV, together with higher SiO_2 contents, points to reduced leaching efficiency and a greater contribution of less altered material in the lower part of the profile, whereas their lower concentrations in Zone III are consistent with more advanced bauxitization. P_2O_5 follows a similar vertical pattern, with higher values in Zone IV and lower values in Zones I–III. This distribution indicates that phosphorus is not directly linked to the main Al–Fe enrichment processes but is instead associated with specific mineral phases or localized accumulation in the lower part of the profile. Cr_2O_3 shows relatively higher values in Zones I–III and correlates positively with Fe_2O_3, indicating its association with Fe-bearing phases. This relationship suggests that chromium was incorporated into Fe oxi-hydroxides during bauxitization and was largely retained within Fe-bearing phases during subsequent diagenetic modification [2,80]. MnO exhibits the most pronounced variation, with low values in Zones I–III and a marked increase in Zone IV. This enrichment reflects the redox-sensitive behavior of manganese and its tendency for secondary

mobilization and reprecipitation, leading to enrichment in the lower part of the bauxite body [1,35]. The distribution of minor oxides therefore distinguishes between the upper part of the profile (Zones I–III), where more efficient leaching resulted in a chemically cleaner bauxitic assemblage, and the lower part (Zone IV), where higher contents of SiO_2, MnO, and alkali elements reflect reduced leaching efficiency and increased retention of clay-related components under less efficient drainage conditions, together with localized secondary redistribution processes. This interpretation is consistent with established models of bauxite evolution, where incomplete leaching leads to enrichment in silica and mobile elements [1,32].

Trace element distribution in the Mamutovac-1a core reflects variations in dominant geochemical controls and mineral hosts along the profile. High-field-strength elements (Zr, Hf, Nb, Ta, Th, U) show limited coupling with the main Al–Fe geochemical trends and are primarily controlled by their residence in resistant minerals such as zircon and Ti-bearing phases. Their distribution therefore largely reflects detrital inheritance and is only minimally affected by post-depositional processes [32,35]. In the upper part (Zones I–III), trace element distribution is largely controlled by Fe oxi-hydroxides, reflecting incorporation of Cr, Ga, Sn, and Sc into these phases during ferruginization under oxidizing conditions [14,80]. The decrease observed in Zone II and subsequent increase toward Zone III likely reflect variations in the abundance and redistribution of these Fe-bearing phases along the profile. Toward the lower part of the bauxite body (Zone IV), the distribution of trace elements indicates a shift in dominant geochemical hosts. The enrichment of Mn, Ni, and Co reflects changing redox conditions that enabled mobilization of Mn in solution and its subsequent reprecipitation as Mn oxides, which act as efficient scavengers for transition metals [83]. This pattern indicates redistribution of trace elements through percolating fluids and their accumulation in Mn-rich phases under more hydrated conditions [84]. In addition to Mn-bearing phases, the increased abundance of large-ion lithophile elements (Rb, Cs, Sr, Ba) in Zone IV indicates a stronger influence of clay-related components. This interpretation is supported by the strong correlations of Rb with K_2O and Cs with MgO, indicating their association with clay-related phases. Their incorporation into phyllosilicate phases reflects reduced leaching efficiency and retention of less altered material in the lower part of the profile [32,35]. These relationships indicate that trace element distribution is governed by a combination of detrital inheritance and secondary redistribution processes, with a clear transition from Fe-dominated to Mn- and clay-influenced geochemical environments along the profile. Such variability reflects changes in redox conditions, fluid circulation, and mineral stability within the paleokarst system [9,84]. Vanadium does not follow this general pattern and shows irregular distribution, suggesting that its behavior is controlled by local geochemical conditions rather than by a single dominant mineral host [80].

5.3. Parental Affinity and Source Characteristics of the Bauxite Material

Despite extensive geological and geochemical research, the identification of source rocks and the understanding of ore-forming processes in karst-type bauxites remain challenging. It is generally accepted that these deposits are derived from a combination of materials, including weathering products of various lithologies within the provenance area and, to a lesser extent, components associated with the underlying carbonate rocks subjected to karstification [1]. However, the dissolution of carbonate bedrock alone is insufficient to account for bauxite formation [9]. Unlike lateritic bauxites, which are commonly linked directly to their precursor rocks [2], karst bauxites typically originate from mixed and often distal sources. Proposed protoliths include fluvially transported detritus, aeolian input, volcanic material, and contributions from mafic and felsic basement rocks [1,9,33].

As a result of intense weathering, major, trace, and rare earth elements undergo significant fractionation, which complicates the reconstruction of parental relationships [9]. Consequently, the evaluation of source affinity in karst bauxites relies primarily on indirect geochemical approaches, including immobile element ratios, trace-element systematics, and REE patterns [14]. In this study, due to the lack of direct data from the underlying bedrock, interpretations are based on such indirect geochemical constraints.

To evaluate the parental affinity of the studied bauxite, it is essential to identify elements that behave conservatively during bauxitization. Alkali and alkaline earth elements are typically leached during intense weathering, whereas several trace elements (e.g., Zr, Nb, Ta, Ti, Hf, and Ga) are generally considered immobile [33,85,86]. Ratios of these immobile elements (e.g., Zr/Hf, Nb/Ta, Zr/Ti) are therefore widely used to constrain source characteristics, as they are less affected by weathering and diagenetic processes and tend to preserve the geochemical signature of the precursor material [14].

The behavior of immobile elements was first evaluated to assess the reliability of geochemical proxies. Zr and Ti are widely regarded as conservative elements during intense weathering and bauxitization, as they are primarily hosted in resistant mineral phases. The strong correlation between Zr and Ti confirms their immobile behavior in the studied system (Table S2 in the Supplementary Material). However, slight variations in Zr/Ti ratios with depth (Figure 13) suggest that the system was not derived from a single homogeneous source but rather reflects variable input and compositional heterogeneity of the source material.

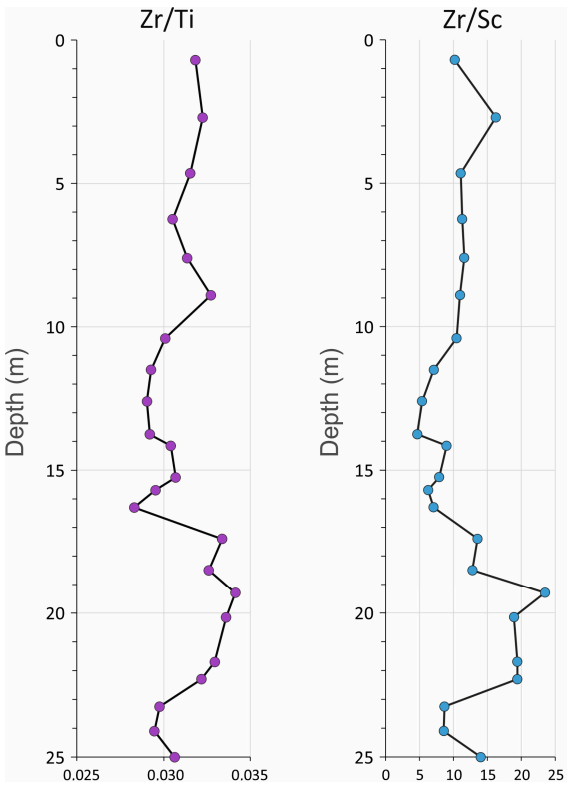

Figure 13. Depth-dependent variations of Zr/Ti and Zr/Sc ratios in the Mamutovac-1a bauxite core.

Zr/Sc ratios show a heterogeneous vertical distribution, decreasing from Zone I to Zone II, followed by a local maximum in Zone III, and reaching the highest but strongly fluctuating values in Zone IV (Figure 13). Th, Sc, and Zr are generally considered to be largely unaffected by late-stage diagenetic processes and primarily reflect the composition of their source rocks, with Zr being particularly resistant [9,87]. Zr is predominantly hosted in highly resistant zircon minerals, which are commonly reported in karst baux-

ites and have been documented in the Mamutovac area based on detrital zircon U–Pb geochronology [17]. It may become enriched through sediment recycling, whereas Sc typically preserves a provenance signal comparable to other REE [88]. Accordingly, the Zr/Sc ratio is widely used as a proxy for evaluating the extent of sediment recycling, with elevated values typically indicating progressive enrichment of zircon relative to Sc-bearing minerals. The observed variability suggests that the contribution of compositionally mature or recycled material was not uniform throughout the profile. The local maximum in Zone III indicates a temporary increase in zircon enrichment, while the highest and strongly fluctuating values in Zone IV point to a more heterogeneous input of compositionally mature material. Therefore, the vertical variation in Zr/Sc most likely reflects changes in the proportion of compositionally mature versus less evolved material rather than a simple, monotonic increase in sediment recycling. The relatively constant Zr/Hf ratios (r = 0.99) indicate a dominant detrital zircon control and suggest that recycling processes primarily concentrated zircon without significantly modifying its original source signature [89].

Trace elements such as Cr, Zr, and Ga, which are relatively immobile during weathering and diagenesis, are often used to constrain the provenance of karst bauxites and indicate contributions from felsic to ultramafic parent rocks [79]. The distribution of samples in the Zr–Cr–Ga ternary diagram (Figure 14) shows systematic variations when grouped according to the defined bauxite facies. Samples from the intraclastic–oolitic facies (Zone I) and the pelitomorphic facies (Zone IV) predominantly plot within the field corresponding to mafic parent rock compositions. In contrast, samples from the matrix-rich (Zone II) and oolitic facies (Zone III) show a slight shift towards the ultramafic field, reflecting a higher contribution of Cr-rich components. These variations indicate that the source material was not uniform but instead reflect contributions from compositionally diverse parent rocks. As noted by Özlü [79], such geochemical discrimination provides only a general indication of source rock affinity, as the detrital nature of karst bauxites may obscure direct relationships with specific parent lithologies. Accordingly, the results indicate a heterogeneous and mixed provenance, with contributions ranging from intermediate to ultramafic material. Bivariate plots of Cr and Ni (Ni/Cr ratios) place the Mamutovac-1a samples within the karst bauxite field (Figure 15).

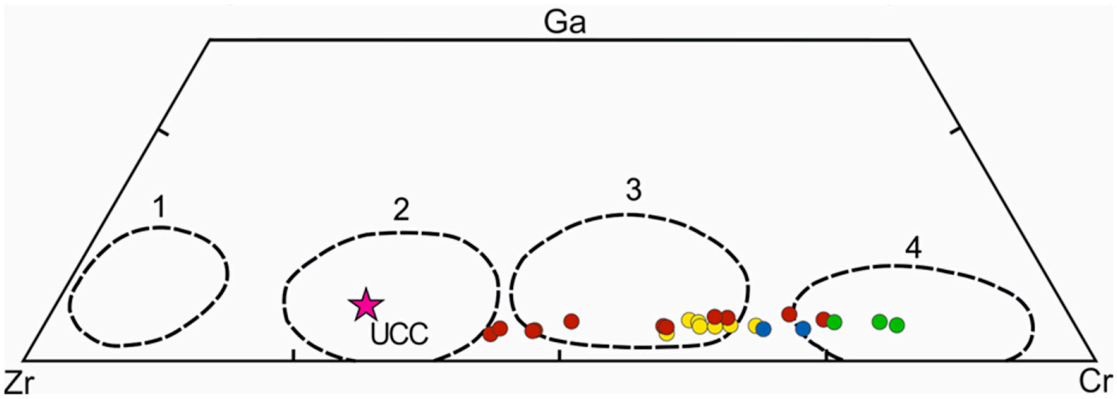

Figure 14. Ternary Zr–Cr–Ga diagram for the 23 samples from the Mamutovac-1a bauxite core. Numbered circles indicate the fields corresponding to felsic (1), intermediate (2), mafic (3), and ultramafic (4) rocks, representing probable parent materials in the genesis of Mediterranean karst bauxites. Modified after [79]. UCC denotes the average Zr–Cr–Ga composition of the upper continental crust and is modified after [87]. Sample points are color-coded according to the defined bauxite facies: yellow for Zone I (0.5–11 m), green for Zone II (11–14 m), blue for Zone III (14–15.5 m), and red for Zone IV (15.5–25 m).

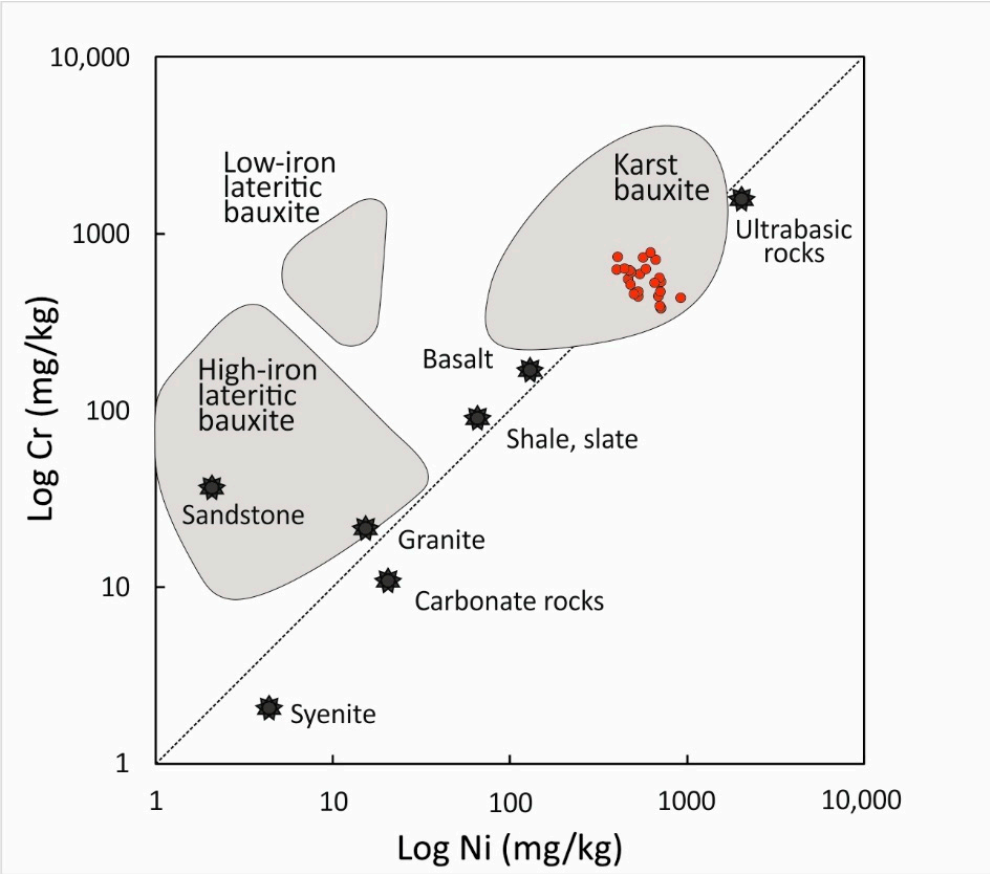

Figure 15. Binary diagram showing the concentrations of Cr vs. Ni in laterite- and karst-type bauxites and potential precursor rocks. Red dots represent the values of the 23 samples from the Mamutovac-1a bauxite core. Modified after [90].

Eu anomalies are indicators of chemical differentiation and thus represent a useful proxy in provenance studies of karst bauxites. They are commonly considered relatively conservative during bauxitization and intense weathering and therefore tend to retain values close to those of the precursor material more effectively than many other geochemical indicators [9,12,80,83,91]. The studied samples show Eu anomalies that are generally higher (Eu/Eu* = 0.65–0.77) than the Eu anomaly of the Upper Continental Crust (Eu/Eu* = 0.66; [87]), suggesting a shift towards more mafic-influenced source components relative to typical upper crustal compositions (Table 2). The TiO_2/Al_2O_3 ratio is often used as an indicator of parental affinity when both elements exhibit relatively conservative behavior [14,35]. The relationship between the Eu anomaly and TiO_2/Al_2O_3 shows a noticeable dispersion of TiO_2/Al_2O_3 values, indicating that the system is not compositionally homogeneous (Figure 16). This variability, together with the consistently elevated Eu/Eu* values, supports a heterogeneous and mixed source with contributions from less evolved components. Previous studies from the Promina area suggest that bauxitization involved both residual carbonate weathering and input of volcaniclastic material, including volcanic ash [17]. The geochemical data presented here, however, indicate a mixed provenance and do not constrain the specific nature of the primary source rocks.

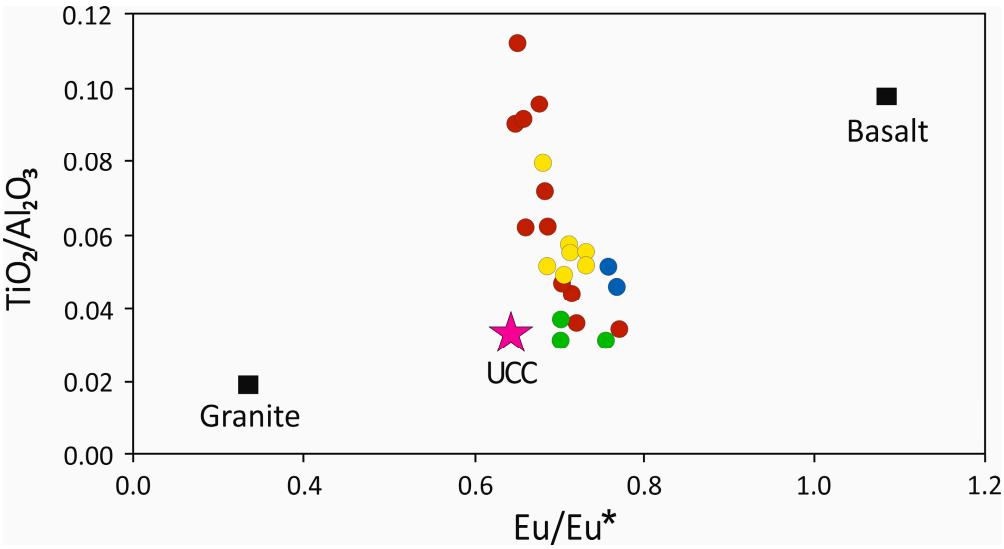

Figure 16. Eu anomaly vs. TiO_2/Al_2O_3 for the 23 samples from the Mamutovac-1a bauxite core. Eu/Eu* and TiO_2/Al_2O_3 depart from the average composition of upper crustal rocks [87] and point towards a more mafic composition. Sample points are color-coded according to the defined bauxite facies: yellow for Zone I (0.5–11 m), green for Zone II (11–14 m), blue for Zone III (14–15.5 m), and red for Zone IV (15.5–25 m).

5.4. Factors Controlling the Distribution and Fractionation of REE

The REE distribution along the studied core exhibits systematic vertical variations, reflecting a combination of inheritance from the parent material and subsequent redistribution during bauxitization and diagenetic processes. These variations are expressed through differences in total REE contents, fractionation patterns, and anomaly development across the defined zones.

REE patterns normalized to different reference compositions provide insight into both provenance and post-depositional evolution. Chondrite-normalized patterns primarily reflect the geochemical signature of the parent material, whereas normalization to the upper continental crust (UCC) highlights modifications related to bauxite formation and subsequent geochemical processes [26]. The chondrite-normalized diagram (Figure 17a,b) shows that all samples are characterized by enrichment of LREE relative to HREE, expressed by a general decrease from La to Lu, a relatively flat HREE segment, and a systematic negative Eu anomaly. Clear differences are observed between the defined zones. Samples from Zone II show the lowest REE concentrations and the weakest enrichment, whereas Zones III and IV exhibit higher abundances. Zone IV is characterized by the strongest LREE enrichment, while Zone III displays comparatively higher HREE levels, with Zone I showing intermediate characteristics. These variations reflect differences in weathering intensity, transport, and post-depositional redistribution processes. At the same time, the overall REE pattern partly preserves the parent material signature, as REE fractionation during bauxitization may be limited (e.g., [9,84,86]). Despite zonal differences, consistent LREE enrichment relative to HREE is evident, with LREE reaching several hundred times chondritic values, whereas HREE show only moderate enrichment [71]. In contrast to the relatively uniform negative Eu anomaly, Ce anomalies show marked variability between zones, indicating differences in redox conditions and fluid-mediated processes during post-depositional evolution.

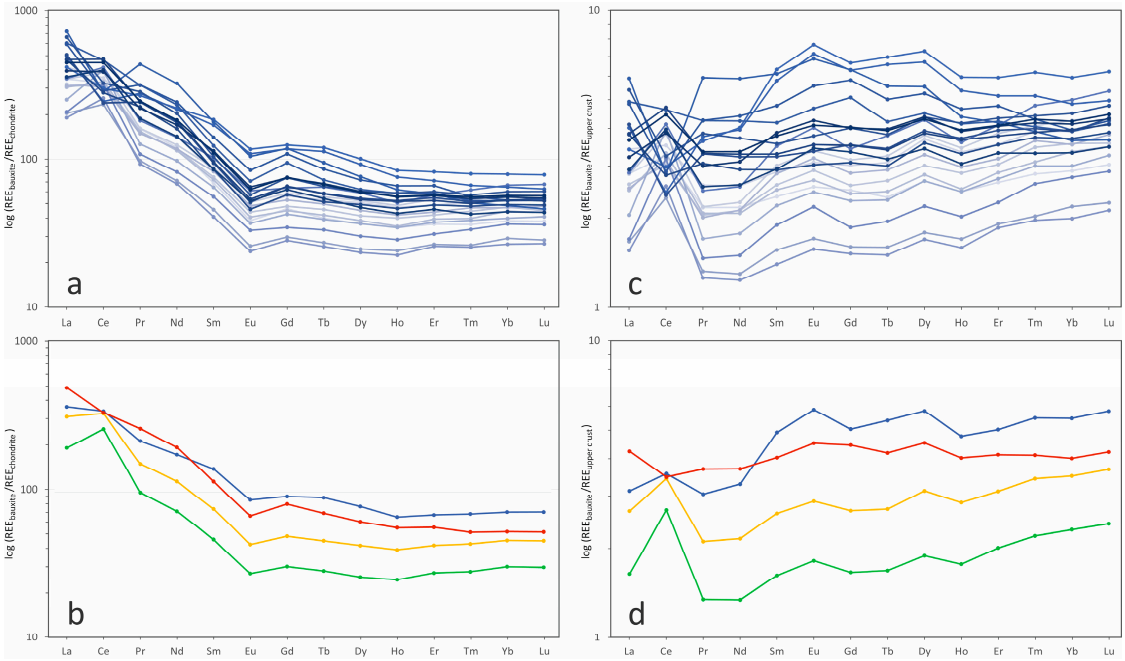

Figure 17. Spider diagrams of REE values for 23 samples from the Mamutovac-1a core, normalized to (**a**,**b**) chondrite and (**c**,**d**) upper continental crust (UCC). Panels (**a**,**c**) show all samples, whereas panels (**b**,**d**) present averaged patterns for individual facies-based zones. The normalization factors are from [71] for chondrite and [92] for UCC. Colors correspond to zones: Zone I (0.5–11 m, yellow), Zone II (11–14 m, green), Zone III (14–15.5 m, blue), and Zone IV (15.5–25 m, red).

Normalization to the UCC (Figure 17c,d) shows clear zonal variability, with the lowest values in Zone II and progressively higher abundances in Zones III and IV. Zone III is distinguished by pronounced MREE and HREE enrichment, reflected in an upward trend from Sm to Lu, whereas Zone IV exhibits a more uniform pattern with moderate enrichment across both LREE and HREE. Zone I shows intermediate characteristics between these end members. Compared to chondrite-normalized patterns, the Eu anomaly appears positive due to normalization to a crustal reference composition characterized by a negative Eu anomaly [92]. In contrast, Ce anomalies remain variable across the defined zones, with negative anomalies more evident in the deeper parts of the succession, suggesting localized redox-controlled redistribution.

REE fractionation is characterized by consistent enrichment of LREE relative to HREE. Zones I and II show relatively elevated and stable ΣLREE/ΣHREE ratios, indicating persistent LREE enrichment in the upper part of the succession (Figure 18a). A marked decrease in ΣLREE/ΣHREE is observed in Zone III, where the lowest values occur, pointing to reduced fractionation between LREE and HREE. In contrast, Zone IV is characterized by higher and more variable ratios, indicating renewed LREE enrichment under more heterogeneous geochemical conditions. These variations are commonly attributed to changes in REE mobility and retention during weathering and subsequent geochemical evolution, controlled by pH-dependent fractionation and adsorption processes [14,84]. Under acidic conditions, HREEs are preferentially mobilized due to stronger aqueous complexation, resulting in relative LREE enrichment through adsorption onto mineral surfaces. In contrast, under neutral to alkaline conditions, HREEs become less mobile and are more likely to precipitate ([9,84] and references therein). REE fractionation is also strongly influenced by the stability of REE–carbonate complexes, which preferentially stabilize HREEs in solution and enhance their mobility relative to LREEs (e.g., [14,93]). Accordingly, LREEs are preferentially retained through adsorption and incorporation into phosphate minerals, whereas HREEs remain more mobile in solution.

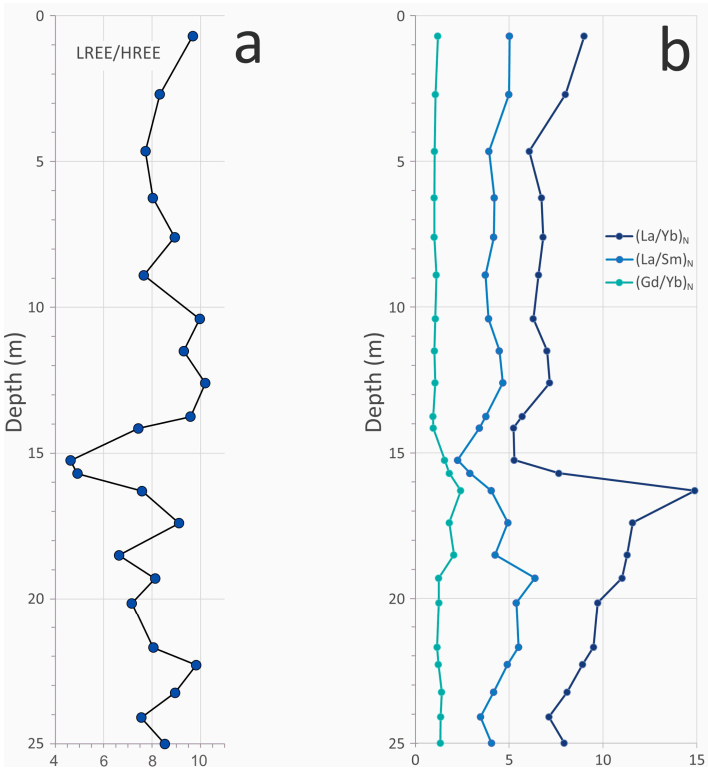

Figure 18. (**a**) Depth-dependent variations of ΣLREE/ΣHREE, (**b**) REE fractionation ratios along the Mamutovac-1a core.

Fractionation indices derived from chondrite-normalized ratios further constrain these trends. The $(La/Yb)_N$ and $(La/Sm)_N$ ratios decrease from Zones I to III, indicating reduced fractionation between LREE and both MREE and HREE (Figure 18b). In contrast, Zone IV is characterized by generally higher but variable values, reflecting enhanced LREE retention and more heterogeneous geochemical conditions. In contrast, $(Gd/Yb)_N$ ratios remain relatively uniform, indicating limited fractionation between MREE and HREE. In karst bauxite systems, $(La/Yb)_N$ ratios are primarily controlled by pH-dependent REE mobility [9], and the observed zonal variations therefore reflect changes in pH and fluid interaction during diagenesis.

La/Y values remain consistently above unity throughout the succession (Figure 19). Distinct zonal variations are observed, with relatively lower and more uniform values in Zones I–III and generally higher, more variable values in Zone IV, including a pronounced peak at its upper boundary. Yttrium (Y), although not a lanthanide, behaves geochemically similarly to heavy rare earth elements (HREE) and is therefore commonly used as their proxy in REE fractionation studies, particularly in assessing the relative mobility of LREE versus HREE during weathering and fluid–rock interaction. The La/Y ratio has often been used as an indicator of weathering conditions. Values lower than 1 are commonly associated with acidic environments, whereas values above 1 are generally interpreted to reflect more basic conditions [21,94–96]. Although La/Y ratios are commonly interpreted as indicators of pH conditions, they should be treated with caution, as they reflect the combined effects of pH-dependent processes, adsorption, complexation, and mineralogical controls, rather than pH alone [9]. In this context, the relatively moderate and uniform La/Y ratios in Zones I–III may reflect the influence of meteoric waters and vadose conditions, where fluctuating pH and fluid circulation promote more uniform REE fractionation. In contrast, the higher La/Y values observed in Zone IV suggest enhanced retention of LREE relative to Y, likely related to increased interaction with the carbonate basement and evolving pore-water chemistry, potentially under mildly alkaline conditions that favor adsorption processes.

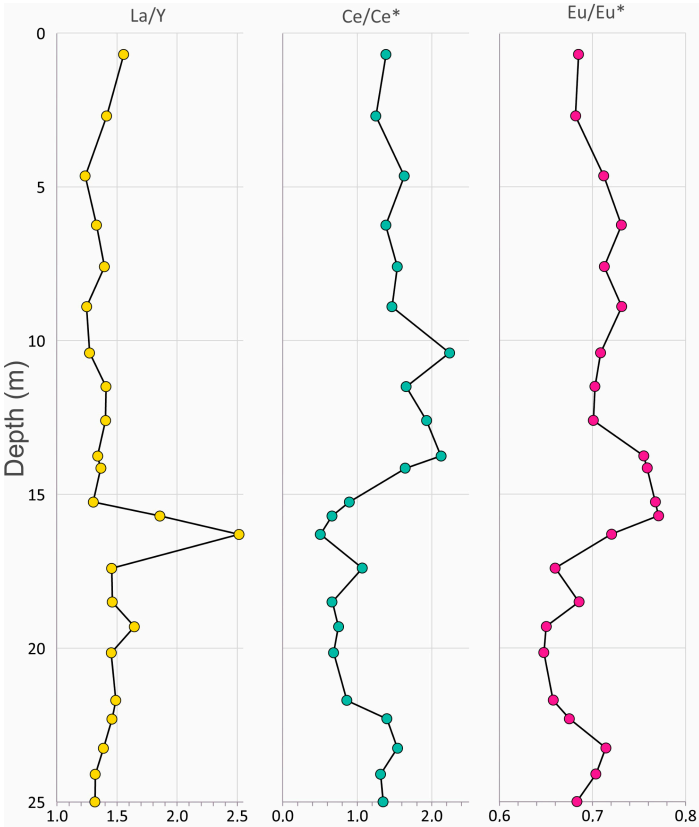

Figure 19. Depth-dependent variations of La/Y ratios and Ce and Eu anomalies in the Mamutovac-1a bauxite core.

Ce anomalies show clear vertical variations, with predominantly positive values in Zones I–III, followed by a transition toward negative anomalies through Zone III and predominantly negative values in the upper part of Zone IV (Figure 19). Positive Ce anomalies are again observed in the lowermost part of the succession. The transition from positive Ce anomalies in the upper zones to negative values at intermediate depths closely resembles patterns described in Mediterranean karst bauxites, where downward percolation of Ce-depleted solutions, following Ce^{4+} precipitation in oxidizing upper horizons, leads to the development of negative Ce anomalies at depth [9,83]. Under oxidizing conditions, Ce^{3+} is readily oxidized to Ce^{4+} and preferentially removed from solution through precipitation or adsorption onto Fe oxi-hydroxides, resulting in positive Ce anomalies, whereas negative anomalies reflect interaction with Ce-depleted percolating fluids [34,83,96]. Accordingly, positive anomalies in the upper part of the succession indicate oxidizing and likely more acidic conditions typical of vadose environments, while negative anomalies in the upper part of Zone IV reflect downward migration of Ce-depleted solutions under more reducing and possibly more alkaline conditions. Ahmadnejad et al. [14] reported from the Bidgol bauxite deposit that Ce exhibits positive anomalies in the upper parts of the profile, related to Ce^{4+} fixation under oxidizing conditions, followed by a transition to negative anomalies at depth, reflecting more reducing and likely alkaline conditions. The reappearance of positive anomalies in the lowermost part of the succession points to specific geochemical conditions near the contact with the carbonate basement. Similar features have been reported in Mediterranean bauxite deposits and are commonly attributed to the influence of carbonate bedrock, which may promote Ce fixation in carbonate-bearing REE minerals such as bastnäsite and parisite [86,97]. In the studied core, the proximity to carbonate bedrock likely provided an additional source of carbonate ions, facilitating Ce precipitation in the deepest part of the deposit.

Eu anomalies are consistently negative across all zones and show only minor variation (Figure 19). The limited variability of Eu/Eu* values and the lack of correlation with redox-sensitive REE such as Ce indicate that Eu was not substantially affected by post-depositional processes. The implications of Eu anomalies for parental affinity are discussed in Section 5.3.

Correlation patterns further constrain the controls on REE distribution (Table S3 in the Supplementary Material). The lack of correlation between REE and major bauxitic components such as Al_2O_3 and Fe_2O_3 indicates that REEs are not primarily associated with the main Al- and Fe-bearing phases (e.g., [84,96]) but rather suggests redistribution during bauxite formation and subsequent geochemical evolution. In contrast, the observed relationship with P_2O_5 suggests that phosphate minerals likely represent important hosts for REE [1,80]. Supporting evidence from other karst bauxite deposits indicates that REE are commonly hosted in phosphate minerals. Residual and authigenic monazite and xenotime reported from the Zagrad bauxites (Montenegro) indicate partial redeposition of REE minerals from primary sources [21]. The association between REE and P_2O_5 observed in the Mamutovac-1a core is consistent with findings from Spanish karst bauxites, where monazite-(Ce) and xenotime-(Y) of predominantly detrital origin were identified as the main REE-bearing minerals [84], as well as from the Tošići–Dujići Upper Eocene deposit in Croatia, where the same detrital REE phosphate minerals have been reported [26]. Similarly, residual and authigenic monazite and xenotime documented in the Zagrad deposit (Montenegro) indicate partial redistribution of REE during post-depositional processes [21]. Authigenic REE phosphates documented in Cretaceous bauxites from Campania [98] further support the role of phosphate phases in REE fixation. The coexistence of detrital and authigenic REE-bearing phases, as documented in the Zagrad deposit, suggests that REE distribution reflects both inherited and secondary processes, rather than a single-stage enrichment mechanism [21]. Moderate positive correlations with K_2O and MgO further suggest that clay minerals may also contribute to REE retention, most likely through adsorption processes. A recent study of bauxites from the Adriatic–Dinaric Carbonate Platform indicates that elevated concentrations of HREE are primarily associated with REE-bearing mineral phases rather than clay minerals (49), further supporting a subordinate role of clays in REE hosting. The distinct behavior of Ce, which shows no clear association with these phases, further indicates that its redistribution is primarily controlled by redox conditions rather than mineralogical hosts. Overall, the observed REE distribution reflects the combined influence of protolith inheritance and subsequent redistribution during bauxite formation under variable redox and pH conditions. The zonal variability and Ce anomalies indicate that REE mobility was largely controlled by fluid–rock interaction, with indications of an additional influence of the carbonate basement on pore-water chemistry.

5.5. Distribution and Extractability of Selected Critical Elements (La, Sc, Ga, V) in the Mamutovac-1a Deposit

Bauxite deposits are not only important for aluminum production but also contain a range of elements classified as critical metals, such as lithium, scandium, titanium, vanadium, gallium, zirconium, niobium, hafnium, tantalum, and rare earth elements. The distribution of these elements is primarily associated with aluminum, iron, and titanium oxi-hydroxides, as well as clay minerals, and to a lesser extent with detrital phases [11]. According to Yang et al. [99], lithium, boron, vanadium, chromium, and gallium in the Baofeng bauxites show a distribution pattern similar to K_2O and SiO_2, with higher concentrations in clay-rich layers than in bauxite horizons, indicating an association with clay minerals.

Gallium (Ga) and Vanadium (V) are elements commonly associated with bauxite systems and are known to be recovered from the byproducts of aluminum (Al) production.

Due to the similar ionic radii of Ga^{3+} (0.62 nm) and Al^{3+} (0.57 nm), they can easily form isomorphous substitutions, resulting in a strong correlation (r = 0.89) between Ga and Al across all samples (Table S2 in the Supplementary Material). This finding aligns with Mongelli et al. [10], who observed Ga in aluminum oxides such as böhmite, gibbsite, and diaspore within bauxite ore. Aqua regia extraction yielded an average Ga extraction rate of 43%. Vanadium in bauxite is commonly associated with titanium oxides [10,27], suggesting the potential for V to undergo isomorphous substitution of Ti due to similar ionic radii. In the studied deposit, V shows no clear correlation with other trace or major elements (Table S2 in the Supplementary Material). The average vanadium concentration in Mamutovac-1a is 1224 mg/kg (based on samples used for aqua regia extraction), with 86.9% of V being extracted, a value comparable to that of FE (Table 3), indicating that V is largely associated with Fe minerals in the bauxite. It is widely accepted that rare earth elements (REEs) are introduced into karst systems mainly as adsorbed ions on clay particle surfaces or as discrete REE minerals [9,10]. The aqua regia extraction of La (30.3%) is comparable to that of P (33.6%), suggesting that La is at least partially incorporated into phosphate mineral phases. La shows a strong correlation (r = 0.69) with P_2O_5 and lacks correlation with Ca, which is consistent with the interpretation by Tomašić et al. [26], who suggest that light REEs are linked with carbonate in the bauxite from the Tošići-Dujići deposit (Table S3 in the Supplementary Material). The aqua regia extraction of bauxite from the nearby Tošići–Dujići deposit yielded higher extraction rates of light REEs, ranging from 34% to 64% [26]. The extraction of critical raw materials (CRMs) from bauxite ore using aqua regia indicates that bauxite may represent a potential source of CRMs [99–101], in addition to bauxite residue or red mud [102,103].

6. Conclusions

The Mamutovac-1a core exhibits a vertically zoned bauxite body defined by four facies-based zones, accompanied by systematic mineralogical and geochemical variations, including a transition from böhmite-dominated to more gibbsite- and clay-rich assemblages with depth. Macroscopic observations and petrographic textures (ooids, intraclasts, and coated grains) indicate episodic transport and redeposition. Major and trace element data show consistent vertical trends, while REE concentrations increase with depth and display pronounced stratigraphic differentiation, including consistent LREE enrichment, stable negative Eu anomalies, and variable Ce anomalies. Magnetic susceptibility also varies along the core and likely reflects changes in the abundance and grain-size distribution of magnetic carriers, although it should be regarded as supporting rather than standalone genetic evidence.

The geochemical data indicate a heterogeneous and mixed provenance with contributions from compositionally diverse source materials ranging from intermediate to ultramafic components. In this context, the vertical zonation reflects differences in depositional and post-depositional processes, with the upper part showing evidence of repeated reworking, whereas the lowermost interval preserves a stronger in situ component. These features indicate a polygenetic, multi-stage evolution involving both in situ bauxitization and episodic reworking and redeposition. The observed REE distribution reflects a combination of inheritance from the parent material and subsequent redistribution during bauxite formation under variable redox and pH conditions, as reflected in the mineralogical zonation of the profile. The upper zones (I–III), dominated by boehmite and hematite and characterized by predominantly positive Ce anomalies, indicate more oxidizing and likely more acidic conditions, whereas the lowermost interval (Zone IV), marked by increased gibbsite, the presence of diaspore, and higher proportions of anatase (locally with rutile), and elevated Mn contents, corresponds to more reducing and likely more alkaline con-

ditions. Variations in REE fractionation are primarily controlled by changes in element mobility, with preferential retention of LREE and relative mobility of HREE. The association between REE and P_2O_5 indicates that phosphate minerals might be the main hosts for REE, whereas no clear relationship with Al- and Fe-bearing phases is observed. Moderate correlations with K_2O and MgO further suggest a secondary role of clay minerals in REE retention.

The integrated petrographic, mineralogical, and geochemical dataset provides new insight into the processes controlling the formation and evolution of karst-hosted Upper Eocene bauxite deposits in the Croatian karst Dinarides. Although the present study does not address the economic feasibility of REE extraction, these results indicate that karst-hosted bauxites may represent potential secondary sources of critical raw materials. The enhanced recovery of La, Sc, Ga, and V using aqua regia further emphasizes this potential, extending beyond conventional aluminum production.

Supplementary Materials: The following supporting information can be downloaded at: https://www.mdpi.com/article/10.3390/min16050547/s1, Table S1: Mineralogical composition of the bauxite samples from the Mamutovac-1a deposit; Table S2: Pearson correlation matrix of major and trace elements; Table S3: Pearson correlation matrix of major and rare earth elements.

Author Contributions: Conceptualization, E.K.G. and H.F.; methodology, Z.P. and S.M.; software, Z.P.; formal analysis, E.K.G. and N.T.; resources, S.M. and N.I.; writing—original draft preparation, E.K.G. and D.T.; writing—review and editing, N.I., I.I.F., H.F., N.G. and S.M.; visualization, E.K.G., H.F., N.I., Z.P., S.M. and N.G.; supervision, N.I. and N.T.; project administration, Z.P.; funding acquisition, S.M. and N.I. All authors have read and agreed to the published version of the manuscript.

Funding: This study was supported by the Croatian Geological Survey, Department of Mineral Resources and Marine Geology and by EIT Raw Materials (European Institute of Innovation and Technology), Horizon 2020 project REEBAUX—Prospects of REE recovery from bauxite and bauxite residue in the ESEE region (project number 17089). This work is part of the Master's Thesis of Dominik Teskera at the Geological Department, Faculty of Science, University of Zagreb.

Data Availability Statement: The original contributions presented in this study are included in the article. Further inquiries can be directed to the corresponding author.

Acknowledgments: This work was supported by the Croatian Geological Survey (HGI-CGS) and the Ministry of Science, Education and Youth of the Republic of Croatia through the financing of the national research project "Map of Minerals Resources of the Republic of Croatia". We would like to thank the Academic Editor and the reviewers for their valuable comments and constructive suggestions, which significantly improved the manuscript.

Conflicts of Interest: The authors declare no conflicts of interest.

References

1. Bárdossy, G. *Karst Bauxites: Bauxite Deposits on Carbonate Rocks*; Elsevier Scientific Publication: Amsterdam, The Netherlands, 1982; p. 441.
2. Bárdossy, G.; Aleva, G.J.J. *Lateritic Bauxites. Developments in Economic Geology*; Elsevier Scientific Publication: Amsterdam, The Netherlands, 1990; Volume 27, p. 624.
3. Schellmann, W. Geochemical differentiation in laterite and bauxite formation. *Catena* **1994**, *21*, 131–143. [CrossRef]
4. D'Argenio, B.; Mindszenty, A. Bauxites and related paleokarst: Tectonic and climatic event markers at regional unconformities. *Eclog. Geol. Helv.* **1995**, *88*, 453–499.
5. Mindszenty, A. Bauxites: Feedbacks of System Earth at Greenhouse times. *Geol. Croat.* **2016**, *69*, 79–87. [CrossRef]
6. Bárdossy, G.; Combes, P.J. Karst bauxites: Interfingering of deposition and palaeoweathering. *Spec. Publ. Int. Assoc. Sedimentol.* **1999**, *27*, 189–206.
7. Liu, X.F.; Wang, Q.F.; Zhang, Q.Z.; Feng, Y.W.; Cai, S.H. Mineralogical characteristics of the superlarge Quaternary bauxite deposits in Jingxi and Debao counties, western Guangxi, China. *J. Asian Earth Sci.* **2012**, *52*, 53–62. [CrossRef]
8. Retallack, G.J. Lateritization and bauxitization events. *Econ. Geol.* **2010**, *105*, 655–667. [CrossRef]

9. Mongelli, G.; Boni, M.; Buccione, R.; Sinisi, R. Geochemistry of the Apulian karst bauxites (southern Italy): Chemical fractionation and parental affinities. *Ore Geol. Rev.* **2014**, *63*, 9–21. [CrossRef]
10. Mongelli, G.; Buccione, R.; Gueguen, E.; Langone, A.; Sinisi, R. Geochemistry of the Apulian allochthonous karst bauxite, southern Italy: Distribution of critical elements and constraints on Late Cretaceous peri-Tethyan palaeogeography. *Ore Geol. Rev.* **2016**, *77*, 246–259. [CrossRef]
11. Mongelli, G.; Boni, M.; Oggiano, G.; Mameli, P.; Sinisi, R.; Buccione, R.; Mondillo, N. Critical metals distribution in Tethyan karst bauxite: The Cretaceous Italian ores. *Ore Geol. Rev.* **2017**, *86*, 526–536. [CrossRef]
12. Sinisi, R. Mineralogical and geochemical features of Cretaceous bauxite from San Giovanni Rotondo (Apulia, Southern Italy): A provenance tool. *Minerals* **2018**, *8*, 567. [CrossRef]
13. Boni, M.; Reddy, S.M.; Mondillo, N.; Balassone, G.; Taylor, R. A distant magmatic source for Cretaceous karst bauxites of Southern Apennines (Italy), revealed through SHRIMP zircon age dating. *Terra Nova* **2012**, *24*, 326–332. [CrossRef]
14. Ahmadnejad, F.; Zamanian, H.; Taghipour, B.; Zarasvandi, A.; Buccione, R.; Ellahi, S.S. Mineralogical and geochemical evolution of the Bidgol bauxite deposit, Zagros Mountain Belt, Iran: Implications for ore genesis, rare earth elements fractionation and parental affinity. *Ore Geol. Rev.* **2017**, *86*, 755–783. [CrossRef]
15. Valeton, I. Processes of allochthony and autochthony in bauxites of carbonate platforms of the Mediterranean area. *Miner. Wealth* **1991**, *71*, 13–28.
16. Valeton, I. Element concentration and formation of ore deposits by weathering. *Catena* **1994**, *21*, 99–129. [CrossRef]
17. Brčić, V.; Dunkl, I.; Mindszenty, A.; Brlek, M.; Trinajstić, N.; Bajo, P.; Bauluz, B.; Mišur, I.; Karius, V.; Šuica, S.; et al. A time-space window between Eocene karst bauxite genesis and the first molasse deposition in the Dinaric Foreland Basin in North Dalmatia, Croatia. *Front. Earth Sci.* **2023**, *11*, 1224164. [CrossRef]
18. D'Argenio, B.; Mindszenty, A. Tectonic and climatic control on paleokarst and bauxites. *G. Geol.* **1992**, *54*, 207–218.
19. Deady, D.; Mochos, E.; Goodenough, K.; Williamson, B.; Wall, F. Rare earth elements in karst-bauxites: A novel untapped European resource? In Proceedings of the ERES2014: 1st European Rare Earth Resources Conference, Milos, Greece, 4–7 September 2014; pp. 1–12.
20. Goodenough, K.M.; Schilling, J.; Jonsson, E.; Kalvig, P.; Charles, N.; Tuduri, J.; Deady, E.A.; Sadeghi, M.; Schiellerup, H.; Müller, A.; et al. Europe's rare earth element resource potential: An overview of REE metallogenetic provinces and their geodynamic setting. *Ore Geol. Rev.* **2016**, *72*, 838–856. [CrossRef]
21. Radusinović, S.; Jelenković, R.; Pačevski, A.; Simić, V.; Božović, D.; Holclajtner-Antunović, I.; Životić, D. Content and mode of occurrences of rare earth elements in the Zagrad karstic bauxite deposit (Nikšić area, Montenegro). *Ore Geol. Rev.* **2017**, *80*, 406–428. [CrossRef]
22. Goodenough, K.M.; Wall, F.; Merriman, D. The Rare Earth Elements: Demand, Global Resources, and Challenges for Resourcing Future Generations. *Nat. Resour. Res.* **2018**, *27*, 201–216. [CrossRef]
23. Gamaletsos, P.N.; Godelitsas, A.; Filippidis, A.; Pontikes, Y. The Rare Earth Elements Potential of Greek Bauxite Active Mines in the Light of a Sustainable REE Demand. *J. Sustain. Met.* **2019**, *5*, 20–47. [CrossRef]
24. Mondillo, N.; Balassone, G.; Boni, M.; Chelle-Michou, C.; Cretella, S.; Mormone, A. Rare earth elements (REE) in Al- and Fe-(oxy)-hydroxides in bauxites of Provence and Languedoc (southern France): Implications for the potential recovery of REEs as by-products of bauxite mining. *Minerals* **2019**, *9*, 504. [CrossRef]
25. Radusinović, S.; Papadopoulos, A. The potential for REE and associated critical metals in karstic bauxites and bauxite residue of Montenegro. *Minerals* **2021**, *11*, 975. [CrossRef]
26. Tomašić, N.; Čobić, A.; Bedeković, M.; Miko, S.; Ilijanić, N.; Gizdavec, N.; Matošević, M. Rare earth elements enrichment in the Upper Eocene Tošići-Dujići bauxite deposit, Croatia. *Minerals* **2021**, *11*, 1260. [CrossRef]
27. Zhang, S.; Zhao, F.; Liu, D.; Zhao, L.; Zhang, X.; Lin, J.; Dong, H.; Zhao, S.; Liu, X.; Zan, M. Modes of occurrence of critical metal elements in low-grade bauxite. *Minerals* **2022**, *12*, 990. [CrossRef]
28. Peytcheva, I.; Bilić, Š.; Georgiev, S.; Pavičić, I.; Šumanovac, F.; Hikov, A.; Holma, M.; Guillong, M.; Grubišić, I. Posušje bauxites in Bosnia and Herzegovina: A source of critical raw materials and a paleoclimatic marker. *Rev. Bulg. Geol. Soc.* **2023**, *84*, 133–136. [CrossRef]
29. Bilić, Š.; Peytcheva, I.; Georgiev, S.; Holma, M.; Hikov, A.; Pavičić, I.; Šumanovac, F.; Deljak, G.; Kurylo, S.; Guillong, M. Mineralogy, petrology, geochemistry and U-Pb zircon age of Upper Cretaceous bauxites from Jajce, Bosnia and Herzegovina. *Ore Geol. Rev.* **2025**, *184*, 106736. [CrossRef]
30. Nesbitt, H.W. Mobility and fractionation of rare earth elements during weathering of a granodiorite. *Nature* **1979**, *279*, 206–210. [CrossRef]
31. Ling, K.Y.; Zhu, X.Q.; Tang, H.S.; Du, S.J.; Gu, J. Geology and geochemistry of the Xiaoshanba bauxite deposit, Central Guizhou Province, SW China: Implications for the behavior of trace and rare earth elements. *J. Geochem. Explor.* **2018**, *190*, 170–186. [CrossRef]

32. Abedini, A.; Khosravi, M.; Calagari, A.A. Geochemical characteristics of the Arbanos karst-type bauxite deposit, NW Iran: Implications for parental affinity and factors controlling the distribution of elements. *J. Geochem. Explor.* **2019**, *200*, 249–265. [CrossRef]
33. Zamanian, H.; Ahmadnejad, F.; Zarasvandi, A. Mineralogical and geochemical investigations of the Mombi bauxite deposit, Zagros Mountains, Iran. *Chem. Erde* **2016**, *76*, 13–37. [CrossRef]
34. Mongelli, G. Ce-anomalies in the textural components of Upper Cretaceous karst bauxites from the Apulian carbonate platform (southern Italy). *Chem. Geol.* **1997**, *14*, 69–79. [CrossRef]
35. Mameli, P.; Mongelli, G.; Oggiano, G.; Dinelli, E. Geological, geochemical and mineralogical features of some bauxite deposits from Nurra (Western Sardinia, Italy): Insights on conditions of formation and parental affinity. *Int. J. Earth Sci.* **2007**, *96*, 887–902. [CrossRef]
36. Liu, X.F.; Wang, Q.F.; Feng, Y.W.; Li, Z.; Cai, S.H. Genesis of the Guangou karstic bauxite deposit in western Henan, China. *Ore Geol. Rev.* **2013**, *55*, 162–175. [CrossRef]
37. Buccione, R.; Mongelli, G.; Sinisi, R.; Boni, M. Relationship between geometric parameters and compositional data: A new approach to karst bauxites exploration. *J. Geochem. Explor.* **2016**, *169*, 192–201. [CrossRef]
38. Perković, I.; Martinuš, M.; Cvetko Tešović, B.; Vlahović, I.; Matešić, D.; Newton, R.J.; He, T.; Šoufek, M.; Razum, I.; Durn, G. Tracing the evolution of the world's first mined bauxite from palaeotopography to pyritization: Insights from Minjera deposits, Istria, Croatia. *Geol. Croat.* **2024**, *77*, 159–178. [CrossRef]
39. Vlahović, I.; Tišljar, J.; Velić, I.; Matičec, D. Evolution of the Adriatic Carbonate Platform. *Palaeogeogr. Palaeoclimatol. Palaeoecol.* **2005**, *220*, 333–360. [CrossRef]
40. Korbar, T. Orogenic evolution of the external Dinarides in the NE Adriatic region: A model constrained by tectonostratigraphy of Upper Cretaceous to Paleogene carbonates. *Earth-Sci. Rev.* **2009**, *96*, 296–312. [CrossRef]
41. Kovačević Galović, E.; Ilijanić, N.; Peh, Z.; Miko, S.; Hasan, O. Geochemical discrimination of early Palaeogene bauxites in Croatia. *Geol. Croat.* **2012**, *65*, 53–65. [CrossRef]
42. Brlek, M.; Korbar, T.; Košir, A.; Glumac, B.; Grizelj, A.; Otoničar, B. Discontinuity surfaces in Upper Cretaceous to Paleogene carbonates of central Dalmatia (Croatia): Glossifungites ichnofacies, biogenic calcretes, and stratigraphic implications. *Facies* **2014**, *60*, 467–487. [CrossRef]
43. Peh, Z.; Kovačević Galović, E. Geochemistry of Istrian Lower Palaeogene bauxites—Is it relevant to the extent of subaerial exposure during Cretaceous times? *Ore Geol. Rev.* **2014**, *63*, 296–306. [CrossRef]
44. Peh, Z.; Kovačević Galović, E. Geochemistry of Lower Palaeogene bauxites—Unique signature of the tectonostratigraphic evolution of a part of the Croatian Karst. *Geol. Croat.* **2016**, *69*, 269–279. [CrossRef]
45. Brlek, M.; Gaynor, S.P.; Mongelli, G.; Bauluz, B.; Sinisi, R.; Brčić, V. Karst bauxite formation during Miocene climatic optimum (Central Dalmatia, Croatia): Mineralogical, compositional and geochronological perspectives. *Int. J. Earth Sci.* **2021**, *110*, 2899–2922. [CrossRef]
46. Sakač, K.; Šinkovec, B. The bauxites of the Dinarides. *Trav. ICSOBA* **1991**, *20–21*, 1–12.
47. Šinkovec, B.; Sakač, K. Bauxite Deposits of Yugoslavia—The State of the Art. *Acta Geol. Hung.* **1991**, *34*, 307–315.
48. Ilijanić, N.; Kovačević Galović, E.; Gizdavec, N.; Ivkić Filipović, I.; Miko, S.; Peh, Z. Geochemical records in subaerial exposure environments in Croatia using discriminant function analysis of bauxite data. *Front. Earth Sci.* **2023**, *10*, 1055435. [CrossRef]
49. Kovačević Galović, E.; Ilijanić, N.; Gizdavec, N.; Miko, S.; Peh, Z. Geochemical insights and mineral resource potential of rare earth elements (REE) in the Croatian karst bauxites. *Minerals* **2025**, *15*, 192. [CrossRef]
50. Šinkovec, B.; Sakač, K. The Paleogene bauxites of Dalmatia. *Trav. ICSOBA* **1982**, *12*, 294–331.
51. Lukšić, B.; Pencinger, V.; Jurić, A.; Jurić, J. *Elaborat o Rezervama Boksita u Eksploatacijskom Polju Mamutovac [Elaboration on the Bauxite Reserves in the Mamutovac Exploitation Field—In Croatian]*; Fund of Professional Documents 032/04: Unpublished report; Croatian Geological Survey: Zagreb, Croatia, 2004; p. 24.
52. Kruk, B.; Dedić, Ž.; Kovačević-Galović, E.; Kruk, L. *Osnove Gospodarenja Mineralnim Sirovinama na Području Općine Promina u Šibensko-Kninskoj Županiji [Basics of Mineral Resource Management in the Promina Municipality, Šibenik-Knin County—In Croatian]*; Fund of Professional Documents 050/14: Unpublished report; Croatian Geological Survey: Zagreb, Croatia, 2014; p. 124.
53. Schmid, S.M.; Bernoulli, D.; Fügenschuh, B.; Matenco, L.; Schefer, S.; Schuster, R.; Tischler, M.; Ustaszewski, K. The Alpine-Carpathian-Dinaridic orogenic system: Correlation and evolution of tectonic units. *Swiss J. Geosci.* **2008**, *101*, 139–183. [CrossRef]
54. Schmid, S.M.; Fügenschuh, B.; Kounov, M.; Matenco, L.; Nievergelt, P.; Oberhänsli, R.; Pleuger, J.; Schefer, S.; Schuster, R.; Tomljenović, B.; et al. Tectonic units of the Alpine collision zone between Eastern Alps and western Turkey. *Gondwana Res.* **2020**, *78*, 308–374. [CrossRef]
55. Babić, L.J.; Zupanič, J. Laterally variable development of a basin-wide transgressive unit of the North Dalmatian foreland basin (Eocene, Dinarides, Croatia). *Geol. Croat.* **2012**, *65*, 1–27. [CrossRef]
56. Ćosović, V.; Mrinjek, E.; Nemec, W.; Španiček, J.; Terzić, K. Development of transient carbonate ramps in an evolving foreland basin. *Basin Res.* **2018**, *30*, 746–765. [CrossRef]

57. Tišljar, J.; Vlahović, I.; Velić, I.; Sokač, B. Carbonate platform megafacies of the Jurassic and Cretaceous deposits of the Karst Dinarides. *Geol. Croat.* **2002**, *55*, 139–170. [CrossRef]
58. Velić, I.; Vlahović, I.; Matičec, D. Depositional sequences and palaeogeography of the Adriatic carbonate platform. *Mem. Soc. Geol. It.* **2002**, *57*, 141–151.
59. Velić, I.; Vlahović, I. *Explanatory Text for Geologic Map of Croatia 1:300,000*; Croatian Geological Survey: Zagreb, Croatia, 2009.
60. Španiček, J.; Ćosović, V.; Mrinjek, E.; Vlahović, I. Early Eocene evolution of carbonate depositional environments recorded in the Čikola Canyon (North Dalmatian Foreland Basin, Croatia). *Geol. Croat.* **2017**, *70*, 11–25. [CrossRef]
61. Babić, L.J.; Zupanič, J. The youngest stage in the evolution of the Dinaric carbonate platform: The upper nummulitic limestones in the North Dalmatian foreland, middle Eocene, Croatia. *Nat. Croat.* **2016**, *25*, 55–71. [CrossRef]
62. Sakač, K. A new survey of stratigraphic position of bauxite-bearing horizons in Croatia (Yugoslavia). *Bull. Sci. Cons. Acad. Yougosl.* **1972**, *17*, 221–223.
63. Sakač, K.; Šinkovec, B.; Durn, G.; Benić, J. The bauxites and Jelar beds. *Rud.-Geol.-Naft. Zb.* **1993**, *5*, 59–64.
64. Marković, S. *Hrvatske Mineralne Sirovine (Croatian Mineral Raw Materials—In Croatian)*; Institut za geološka istraživanja, Zavod za geologiju: Zagreb, Croatia, 2002; p. 544.
65. Babić, L.J.; Zupanić, J.; Kurtanjek, D. Sharply-topped alluvial gravel sheets in the Palaeogene Promina basin (Dinarides, Croatia). *Geol. Croat.* **1995**, *48*, 33–48.
66. JISMS "Unique Information System of Mineral Resources" ("Jedinstveni Informacijski sustav Mineralnih Sirovina" in Croatian)—WebGis Portal. Available online: https://jisms.gospodarstvo.gov.hr/#/maps (accessed on 27 January 2026).
67. Munsell Color Company. *Munsell Soil Color Charts*; Munsell Color Company: Baltimore, MD, USA, 1994; p. 12.
68. Moore, D.M.; Reynolds, R.C., Jr. *X-Ray Diffraction and the Identification and Analysis of Clay Minerals*, 2nd ed.; Oxford University Press: New York, NY, USA, 1998; p. 378.
69. Gürsu, S.; Kiraz, E.; Bozkaya, G.; Bozkaya, Ö.; Yiğmatepe, M. Petrogenetic Characteristics of Karstic Meta-Bauxite Deposits in Milas Area, SW Türkiye: Insights on Chemical Fractionations and Parental Affinities. *J. Afr. Earth Sci.* **2026**, *234*, 105893. [CrossRef]
70. Warr, L.N. IMA–CNMNC approved mineral symbols. *Miner. Mag.* **2021**, *85*, 291–320. [CrossRef]
71. Evensen, N.M.; Hamilton, P.J.; O'Nions, R.K. Rare-earth abundances in chondritic meteorites. *Geochim. Cosmochim. Acta* **1978**, *42*, 1199–1212. [CrossRef]
72. Tsakanika, L.A.; Panagiotatos, G.; Lymperopoulou, T.; Chatzitheodoridis, E.; Ochsenkühn, K.; Ochsenkühn-Petropoulou, M. Direct phosphoric acid leaching of bauxite residue for selective scandium extraction. *Metals* **2022**, *12*, 228. [CrossRef]
73. Schulte, R.F.; Foley, N.K. *Compilation of Gallium Resource Data for Bauxite Deposits*; Open-File Report 2013-1272; U.S. Geological Survey, U.S. Department of the Interior: Reston, VA, USA, 2013; p. 14.
74. Abedini, A.; Khosravi, M. Geochemical characteristics of aluminum-bearing iron ores: A case study from the Kolijan karst-type bauxite deposit, northwestern Iran. *Minerals* **2024**, *14*, 151. [CrossRef]
75. Economou-Eliopoulos, M.; Kontou, M.; Megremi, I. Biogeochemical redox processes controlling the element cycling: Insights from karst-type bauxite, Greece. *Minerals* **2022**, *12*, 446. [CrossRef]
76. Valeton, I. *Bauxites*; Elsevier Scientific Publishing: Amsterdam, The Netherlands, 1972; p. 226.
77. Temur, S.; Kansun, G. Geology and petrography of the Masatdagi diasporic bauxites, Alanya, Antalya, Turkey. *J. Asian Earth Sci.* **2006**, *27*, 512–522. [CrossRef]
78. Mamedov, V.; Boeva, N.; Makarova, M.; Shipilova, E.; Melnikov, P. The problem of the formation of boehmite and gibbsite in bauxite-bearing lateritic profiles. *Minerals* **2022**, *12*, 389. [CrossRef]
79. Özlü, N. Trace-element content of "karst bauxites" and their parent rocks in the Mediterranean Belt. *Miner. Depos.* **1983**, *18*, 469–476. [CrossRef]
80. Abedini, A.; Khosravi, M. Geochemical constraints on the Triassic–Jurassic Amir-Abad karst-type bauxite deposit, NW Iran. *J. Geochem. Explor.* **2020**, *11*, 106489. [CrossRef]
81. Velde, B.; Meunier, A. *The Origin of Clay Minerals in Soils and Weathered Rocks*; Springer: Berlin/Heidelberg, Germany, 2008. [CrossRef]
82. Dearing, J.A.; Dann, R.J.L.; Hay, K.; Lees, J.A.; Loveland, P.J.; Maher, B.A.; O'Grady, K. Frequency-dependent susceptibility measurements of environmental materials. *Geophys. J. Int.* **1996**, *124*, 228–240. [CrossRef]
83. Mondillo, N.; Di Nuzzo, M.; Kalaitzidis, S.; Boni, M.; Santoro, L.; Balassone, G. Petrographic and geochemical features of the B3 bauxite horizon (Cenomanian–Turonian) in the Parnassos-Ghiona area: A contribution towards the genesis of the Greek karst bauxites. *Ore Geol. Rev.* **2022**, *143*, 104759. [CrossRef]
84. Reinhardt, N.; Proenza, J.; Villanova-de-Benavent, C.; Aiglsperger, T.; Bover-Arnal, T.; Torró, L. Geochemistry and mineralogy of rare earth elements (REE) in bauxitic ores of the Catalan Coastal Range, NE Spain. *Minerals* **2018**, *8*, 562. [CrossRef]
85. Calagari, A.A.; Abedini, A. Geochemical investigations on Permo–Triassic bauxite deposit at Kanisheeteh, east of Bukan, Iran. *J. Geochem. Explor.* **2007**, *94*, 1–18. [CrossRef]

86. Karadağ, M.M.; Küpeli, S.; Aryk, F.; Ayhan, A.; Zedef, V.; Döyen, A. Rare earth element (REE) geochemistry and genetic implications of the Mortas bauxite deposit (Seydisehir/Konya—Southern Turkey). *Chem. Erde* **2009**, *69*, 143–159. [CrossRef]
87. Taylor, S.R.; McLennan, S.M. *The Continental Crust: Its Composition and Evolution*; Blackwell: Hoboken, NJ, USA, 1985; p. 328.
88. McLennan, S.M.; Hemming, S.; McDaniel, D.K.; Hanson, G.N. Geochemical approaches to sedimentation, provenance and tectonics. In *Processes Controlling the Composition of Clastic Sediments*; Johnsson, M.J., Basu, A., Eds.; Spec. Pap. 284; Geological Society of America: Boulder, CO, USA, 1993; pp. 21–40.
89. Wang, X.; Griffin, W.L.; Chen, J. Hf contents and Zr/Hf ratios in granitic zircons. *Geochem. J.* **2010**, *44*, 65–72. [CrossRef]
90. Schroll, E.; Sauer, D. Beitrag zur Geochemie von Titan, Chrom, Nickel, Cobalt, Vanadium und Molybdän in bauxitischen Gesteinen. *Trav. ICSOBA* **1968**, *5*, 83–96.
91. Khosravi, M.; Abedini, A.; Alipour, S.; Mongelli, G. The Darzi-Vali bauxite deposit, West-Azarbaidjan Province, Iran: Critical metals distribution and parental affinities. *J. Afr. Earth Sci.* **2017**, *129*, 960–972. [CrossRef]
92. Taylor, S.R.; McLennan, S.M. *Planetary Crusts: Their Composition, Origin and Evolution*; Cambridge University Press: Cambridge, UK, 2009; p. 378.
93. Cantrell, K.J.; Byrne, R.H. Rare earth element complexation by carbonate and oxalate ions. *Geochim. Cosmochim. Acta* **1987**, *51*, 597–605. [CrossRef]
94. Zhuk-Pochetukov, K.A.; Serdobova, L.I.; Kataeva, Z.T.; Andreeva, I.P.; Ryabova, T.V.; Lagunova, E.V. Rare earth elements in anhydrites from Kacharskoe iron-ore deposits. *Geochemistry (USSR)* **1986**, *5*, 630–635.
95. Crnički, J.; Jurković, I. Rare earth elements in Triassic bauxites of Croatia, Yugoslavia. *Trav. ICSOBA* **1990**, *19*, 239–248.
96. Maksimović, Z.; Pantó, G. Contribution to the geochemistry of the rare earth elements in the karst–bauxite deposits of Yugoslavia and Greece. *Geoderma* **1991**, *51*, 93–109. [CrossRef]
97. Wang, X.; Jiao, Y.; Du, Y.; Ling, W.; Wu, L.; Cui, T.; Zhou, Q.; Jin, Z.; Lei, Z.; Weng, S. REE mobility and Ce anomaly in bauxite deposits of northern Guizhou, China. *J. Geochem. Explor.* **2013**, *133*, 103–117. [CrossRef]
98. Mondillo, N.; Boni, M.; Balassone, G.; Rollinson, G. Karst bauxites in the Campania Apennines (southern Italy): A new approach. *Period. Mineral.* **2011**, *80*, 407–432. [CrossRef]
99. Yang, S.; Wang, Q.; Liu, X.; Kan, Z.; Santosh, M.; Deng, J. Global spatio-temporal variations and metallogenic diversity of karst bauxites. *Earth-Sci. Rev.* **2022**, *233*, 104184. [CrossRef]
100. Xu, H.; Zhang, D.; Xiao, D.; Wang, Y.; Zhou, Q.; Li, X. Mineralogical characteristics and occurrence of critical metal elements in lateritic bauxites from the Boké region, Guinea. *Appl. Geochem.* **2026**, *201*, 106758. [CrossRef]
101. Çelik Karakaya, M.; Rüşen, A.; Karakaya, N.; Alkan, M.S. Selection of Mineral Acids for Extraction of Rare Earth Elements and Critical Metals from Bauxite Ore Using the Taguchi Method. *JOM* **2026**. [CrossRef]
102. Rao Borra, C.; Pontikes, Y.; Binnemans, K.; Van Gerven, T. Leaching of rare earths from bauxite residue (red mud). *Miner. Eng.* **2015**, *76*, 20–27. [CrossRef]
103. Reid, S.; Tam, J.; Yang, M.; Azimi, G. Technospheric mining of rare earth elements from bauxite residue (red mud): Process optimization, kinetic investigation, and microwave pretreatment. *Sci. Rep.* **2017**, *7*, 15252. [CrossRef]

Disclaimer/Publisher's Note: The statements, opinions and data contained in all publications are solely those of the individual author(s) and contributor(s) and not of MDPI and/or the editor(s). MDPI and/or the editor(s) disclaim responsibility for any injury to people or property resulting from any ideas, methods, instructions or products referred to in the content.

Supplementary material to

Mineralogical and geochemical variability of the Mamutovac-1a Upper Eocene karst bauxite deposit (Croatian Dinarides) and its CRM potential

Table S1. Mineralogical composition of the bauxite samples from Mamutovac-1a deposit. Mineral abbreviation [70]. Bhm: böhmite. Gbs: gibbsite. Hem: hematite. Gth: goethite. Ant: anatase. Rt: rutile. Kln: kaolinite. Dsp: diaspore. C-V MLM: chlorite-vermiculite mixed-layer minerals. ± refers to trace amounts.

	Bauxite core samples		Bulk mineralogical composition	Clay minerals
1	MAM B-1	0.00-0.05	Bhm. Gbs. Hem. Ant. Kln. 2:1 clay min.	
2	MAM B-1	0.15-0.20	Bhm. Gbs. Hem. Ant. Gth. Kln. 2:1 clay min.	
3	MAM B-1	0.30-0.35	Bhm. Gbs. Hem. Ant. Gth	
4	MAM B-1	0.45-0.50	Bhm. Gbs. Hem. Ant. Gth	
5	MAM B-1	0.7-0.75	Bhm. Gbs. Hem. Ant. Gth. Kln	
6	MAM B-1	1.65-1.70	Bhm. Gbs. Hem. Ant. Gth. Kln (±)	
7	MAM B-1	2.70-2.75	Bhm. Gbs. Hem. Ant. Gth. Kln	
8	MAM B-1	3.65-3.70	Bhm. Gbs. Hem. Ant. Gth	
9	MAM B-1	4.65-4.70	Bhm. Gbs. Hem. Ant. Kln. Gth. 2:1 clay min.	Kln. C-V MLM (±)
10	MAM B-1	5.30-5.35	Bhm. Gbs. Hem. Ant. Gth. Kln (±)	
11	MAM B-1	6.25-6.30	Bhm. Gbs. Hem. Ant. Gth. Kln	
12	MAM B-1	7.60-7.65	Bhm. Gbs. Hem. Ant. Kln. Rt. 2:1 clay min.	Kln. C-V MLM
13	MAM B-1	8.30-8.35	Bhm. Gbs. Hem. Ant. Kln	
14	MAM B-1	8.90-8.95	Bhm. Gbs. Hem. Ant. Gth. 2:1 clay min.	
15	MAM B-1	9.90-9.95	Bhm. Gbs. Hem. Ant. Gth	
16	MAM B-1	10.40-10.45	Bhm. Gbs. Hem. Ant. Kln	
17	MAM B-1	11.50-11.55	Bhm. Gbs. Hem. Ant. Kln	
18	MAM B-1	12.60-12.65	Bhm. Gbs. Hem. Ant. Kln. 2:1 clay min.	
19	MAM B-1	13.75-13.80	Bhm. Gbs. Hem. Ant. Kln	
20	MAM B-1	14.15-14.20	Bhm. Gbs. Hem. Ant. Gth. Kln. 2:1 clay min.	
21	MAM B-1	14.70-14.75	Bhm. Gbs. Hem. Ant. Gth	
22	MAM B-1	15.25-15.30	Bhm. Gbs. Hem. Ant. Kln (±)	
23	MAM B-1	15.70-15.75	Bhm. Gbs. Hem. Ant. Gth. Kln. 2:1 clay min.	Kln. C-V MLM
24	MAM B-1	16.30-16.35	Bhm. Gbs. Hem. Ant. Kln. Gth	
25	MAM B-1	16.80-16.85	Bhm. Gbs. Hem. Ant. Gth. Kln. 2:1 clay min.	
26	MAM B-1	17.40-17.45	Bhm. Gbs. Hem. Ant. Kln. Gth. 2:1 clay min.	
27	MAM B-1	17.90-17.95	Bhm. Gbs. Hem. Ant. Kln. Rt	
28	MAM B-1	18.35-18.40	Bhm. Gbs. Hem. Ant. Kln	
29	MAM B-1	18.50-18.54	Bhm. Gbs. Hem. Ant. Kln. Gth. 2:1 clay min.	
30	MAM B-1	18.90-18.95	Bhm. Gbs. Hem. Ant. Gth. Kln. Rt. 2:1 clay min.	
31	MAM B-1	19.30-19.35	Bhm. Gbs. Gth. Ant. Rt. Kln. Hem (±). 2:1 clay min.. Dsp	Kln. C-V MLM
32	MAM B-1	19.85-19.90	Bhm. Gbs. Gth. Ant. Rt. Kln. Hem (±). 2:1 clay min.	
33	MAM B-1	20.15-20.20	Bhm. Gbs. Ant. Gth. Kln. Hem (±). 2:1 clay min.	
34	MAM B-1	20.75-20.80	Bhm. Gbs. Ant. Gth. Hem. Rt. Kln. 2:1 clay min.	
35	MAM B-1	21.70-21.75	Bhm. Gbs. Ant. Kln. Gth. Rt. Hem (±). 2:1 clay min.. Dsp	Kln. C-V MLM

36	MAM B-1	22.30-22.35	Bhm. Gbs. Ant. Kln. Rt. Hem (±). 2:1 clay min.	
37	MAM B-1	22.75-22.80	Bhm. Gbs. Ant. Gth. Kln. Rt. Hem (±). 2:1 clay min.	
38	MAM B-1	23.25-23.30	Bhm. Gbs. Ant. Gth. Kln. Hem (±). 2:1 clay min.	Kln. C-V MLM
39	MAM B-1	23.90-23.95	Bhm. Gbs. Ant. Kln. Hem	
40	MAM B-1	24.10-24.15	Bhm. Gbs. Ant. Kln. Hem (±). 2:1 clay min.	
41	MAM B-1	24.70-24.75	Bhm. Gbs. Ant. Gth. Kln. Hem. 2:1 clay min.	
42	MAM B-1	25.00-25.10	Bhm. Gbs. Ant. Kln. Gth. Hem (±). 2:1 clay min.. Dsp	Kln. C-V MLM

Table S2. Pearson correlation matrix of major and trace elements.

	SiO_2	*Al_2O_3*	*Fe_2O_3*	*TiO_2*	*MgO*	*CaO*	*Na_2O*	*K_2O*	*P_2O_5*	*MnO*	*Cr_2O_3*	*Ba*	*Ni*	*Be*	*Co*	*Cs*	*Ga*	*Hf*	*Nb*	*Rb*	*Sn*	*Sr*	*Ta*	*Th*	*U*	*V*	*W*	*Zr*
SiO_2	1																											
Al_2O_3	-0.98	1																										
Fe_2O_3	-0.90	0.91	1																									
TiO_2	-0.13	-0.02	-0.04	1																								
MgO	0.81	-0.86	-0.79	0.40	1																							
CaO	0.96	-0.96	-0.94	0.00	0.87	1																						
Na_2O	0.52	-0.60	-0.58	0.50	0.77	0.65	1																					
K_2O	0.85	-0.84	-0.75	0.04	0.89	0.88	0.64	1																				
P_2O_5	0.37	-0.49	-0.44	0.79	0.79	0.48	0.73	0.51	1																			
MnO	0.42	-0.44	-0.61	0.07	0.50	0.58	0.52	0.54	0.25	1																		
Cr_2O_3	-0.70	0.74	0.84	-0.24	-0.77	-0.79	-0.65	-0.63	-0.63	-0.63	1																	
Ba	0.69	-0.74	-0.76	0.35	0.90	0.81	0.80	0.86	0.68	0.77	-0.76	1																
Ni	0.57	-0.51	-0.49	-0.35	0.45	0.59	0.26	0.69	0.05	0.73	-0.43	0.65	1															
Be	-0.04	0.04	0.06	0.22	0.26	0.06	0.26	0.23	0.36	0.20	-0.21	0.29	0.17	1														
Co	0.43	-0.44	-0.56	0.19	0.60	0.57	0.66	0.60	0.46	0.82	-0.64	0.81	0.63	0.29	1													
Cs	0.69	-0.75	-0.73	0.38	0.93	0.79	0.70	0.89	0.71	0.64	-0.75	0.94	0.60	0.29	0.65	1												
Ga	-0.86	0.89	0.83	-0.16	-0.92	-0.88	-0.59	-0.86	-0.61	-0.51	0.77	-0.82	-0.57	-0.20	-0.54	-0.87	1											
Hf	-0.11	-0.05	-0.05	1.00	0.42	0.02	0.51	0.06	0.81	0.06	-0.25	0.36	-0.35	0.22	0.17	0.39	-0.19	1										
Nb	-0.17	0.02	-0.01	1.00	0.36	-0.04	0.47	0.00	0.77	0.03	-0.21	0.31	-0.39	0.22	0.15	0.34	-0.12	1.00	1									
Rb	0.76	-0.79	-0.75	0.26	0.94	0.84	0.73	0.96	0.65	0.62	-0.72	0.94	0.64	0.31	0.69	0.97	-0.87	0.26	0.21	1								
Sn	-0.84	0.76	0.73	0.54	-0.46	-0.76	-0.21	-0.63	0.06	-0.43	0.52	-0.44	-0.67	0.13	-0.38	-0.40	0.66	0.52	0.58	-0.49	1							
Sr	0.45	-0.57	-0.56	0.80	0.86	0.58	0.80	0.57	0.93	0.35	-0.65	0.76	0.04	0.25	0.52	0.76	-0.66	0.81	0.77	0.72	-0.01	1						
Ta	-0.18	0.02	-0.02	0.98	0.32	-0.04	0.46	-0.06	0.74	0.04	-0.22	0.27	-0.43	0.17	0.14	0.28	-0.11	0.98	0.98	0.16	0.56	0.75	1					
Th	-0.59	0.46	0.42	0.85	-0.08	-0.46	0.19	-0.36	0.45	-0.17	0.18	-0.04	-0.55	0.18	-0.05	-0.04	0.32	0.84	0.87	-0.15	0.86	0.40	0.86	1				
U	0.08	-0.22	-0.28	0.91	0.54	0.27	0.67	0.21	0.84	0.21	-0.43	0.49	-0.25	0.23	0.31	0.49	-0.30	0.91	0.90	0.41	0.37	0.86	0.90	0.71	1			
V	0.08	-0.08	0.11	-0.29	-0.15	0.01	-0.05	-0.11	-0.27	0.03	0.25	-0.15	0.10	0.01	-0.20	-0.27	0.09	-0.26	-0.28	-0.24	-0.16	-0.28	-0.24	-0.27	-0.27	1		
W	-0.01	-0.13	-0.11	0.92	0.49	0.10	0.52	0.14	0.80	0.05	-0.26	0.40	-0.28	0.28	0.16	0.42	-0.26	0.93	0.93	0.31	0.43	0.82	0.88	0.70	0.82	-0.18	1	
Zr	-0.12	-0.04	-0.04	1.00	0.41	0.02	0.49	0.05	0.80	0.04	-0.24	0.35	-0.36	0.22	0.16	0.38	-0.18	1.00	1.00	0.26	0.54	0.80	0.98	0.84	0.91	-0.27	0.93	1

Table S3. Pearson correlation matrix of major and rare earth elements.

	SiO_2	*Al_2O_3*	*Fe_2O_3*	*MgO*	*CaO*	*Na_2O*	*K_2O*	*TiO_2*	*P_2O_5*	*MnO*	*Cr_2O_3*	*Sc*	*Y*	*La*	*Ce*	*Pr*	*Nd*	*Sm*	*Eu*	*Gd*	*Tb*	*Dy*	*Ho*	*Er*	*Tm*	*Yb*	*Lu*	*REE*	*LREE*	*HREE*
SiO_2	1																													
Al_2O_3	-0,98	1																												
Fe_2O_3	-0,90	0,91	1																											
MgO	0,81	-0,86	-0,79	1																										
CaO	0,96	-0,96	-0,94	0,87	1																									
Na_2O	0,52	-0,60	-0,58	0,77	0,65	1																								
K_2O	0,85	-0,84	-0,75	0,89	0,88	0,64	1																							
TiO_2	-0,13	-0,02	-0,04	0,40	0,00	0,50	0,04	1																						
P_2O_5	0,37	-0,49	-0,44	0,79	0,48	0,73	0,51	0,79	1																					
MnO	0,42	-0,44	-0,61	0,50	0,58	0,52	0,54	0,07	0,25	1																				
Cr_2O_3	-0,70	0,74	0,84	-0,77	-0,79	-0,65	-0,63	-0,24	-0,63	-0,63	1																			
Sc	-0,77	0,79	0,88	-0,67	-0,77	-0,43	-0,55	-0,09	-0,49	-0,37	0,85	1																		
Y	0,06	-0,17	-0,14	0,49	0,18	0,43	0,36	0,64	0,71	0,33	-0,41	-0,19	1																	
La	0,20	-0,26	-0,22	0,52	0,27	0,35	0,45	0,43	0,69	0,17	-0,46	-0,32	0,85	1																
Ce	-0,09	0,06	-0,16	0,09	0,05	0,24	0,09	0,25	0,08	0,57	-0,19	0,00	0,29	0,07	1															
Pr	0,20	-0,22	-0,18	0,44	0,25	0,26	0,48	0,21	0,53	0,21	-0,41	-0,26	0,76	0,96	0,06	1														
Nd	0,15	-0,16	-0,12	0,38	0,19	0,21	0,45	0,17	0,47	0,20	-0,36	-0,20	0,76	0,93	0,05	0,99	1													
Sm	-0,06	0,08	0,15	0,13	-0,04	0,07	0,29	-0,01	0,23	0,14	-0,11	0,09	0,60	0,73	-0,02	0,86	0,90	1												
Eu	-0,09	0,12	0,20	0,07	-0,08	0,02	0,26	-0,08	0,15	0,11	-0,04	0,14	0,54	0,67	-0,04	0,81	0,86	0,99	1											
Gd	-0,01	0,01	0,10	0,18	0,02	0,09	0,34	0,02	0,26	0,16	-0,15	0,03	0,67	0,77	0,00	0,88	0,92	0,99	0,98	1										
Tb	-0,10	0,11	0,20	0,11	-0,07	0,08	0,28	0,01	0,21	0,13	-0,05	0,15	0,60	0,67	-0,03	0,79	0,85	0,99	0,99	0,98	1									
Dy	-0,13	0,13	0,22	0,13	-0,09	0,13	0,26	0,10	0,27	0,15	-0,05	0,18	0,64	0,69	0,01	0,79	0,84	0,97	0,97	0,96	0,99	1								
Ho	-0,10	0,08	0,16	0,21	-0,04	0,21	0,30	0,23	0,38	0,21	-0,12	0,13	0,75	0,74	0,07	0,80	0,85	0,95	0,94	0,95	0,97	0,99	1							
Er	-0,16	0,12	0,21	0,20	-0,09	0,22	0,25	0,28	0,38	0,22	-0,10	0,18	0,77	0,71	0,12	0,76	0,81	0,91	0,90	0,92	0,95	0,97	0,99	1						
Tm	-0,31	0,27	0,34	0,09	-0,23	0,18	0,12	0,33	0,32	0,18	0,03	0,34	0,68	0,58	0,16	0,63	0,68	0,84	0,83	0,82	0,89	0,93	0,94	0,97	1					
Yb	-0,35	0,31	0,36	0,06	-0,27	0,22	0,08	0,37	0,32	0,18	0,05	0,39	0,65	0,52	0,22	0,55	0,60	0,77	0,76	0,74	0,82	0,87	0,89	0,93	0,99	1				
Lu	-0,36	0,32	0,38	0,07	-0,28	0,20	0,06	0,41	0,33	0,17	0,07	0,41	0,67	0,51	0,23	0,53	0,58	0,74	0,73	0,71	0,80	0,85	0,88	0,92	0,98	1,00	1			
REE	0,06	-0,10	-0,15	0,39	0,17	0,33	0,41	0,34	0,50	0,41	-0,39	-0,15	0,84	0,86	0,48	0,89	0,89	0,78	0,73	0,81	0,74	0,76	0,80	0,79	0,71	0,67	0,66	1		
LREE	0,09	-0,14	-0,21	0,42	0,21	0,35	0,42	0,36	0,52	0,44	-0,43	-0,21	0,83	0,85	0,55	0,86	0,86	0,71	0,65	0,74	0,65	0,67	0,72	0,72	0,63	0,60	0,59	0,99	1	
HREE	-0,12	0,12	0,20	0,15	-0,08	0,14	0,27	0,13	0,29	0,17	-0,08	0,16	0,69	0,72	0,05	0,81	0,86	0,97	0,97	0,97	0,99	1,00	0,99	0,98	0,93	0,87	0,85	0,79	0,71	1

7. BIOGRAPHY OF THE AUTHOR

Erli Kovačević Galović was born on August 11, 1977, in Zagreb, Croatia, where she completed primary school and graduated from the V Gymnasium. In 1996, she enrolled in the study of Geology at the Faculty of Science, University of Zagreb, where she obtained the degree of graduate engineer of geology in 2004. In 2005, she enrolled in the postgraduate doctoral study programme in Geology at the Faculty of Science, University of Zagreb, and began working at the Croatian Geological Survey. Since then, she has advanced through several professional positions, from research assistant and expert associate to senior expert associate, and currently holds the position of expert advisor. She re-enrolled in the doctoral programme in 2017. During her professional career, she has participated in numerous commercial and EU-funded projects related to sustainable management of mineral resources, with particular involvement in county-level mineral resource studies and resource evaluation. Her scientific research is focused primarily on karst bauxites, geochemistry, critical raw materials, and sustainable mineral resource management. She has participated in several professional workshops and training programmes related to mineral resource management and exploration, including DIM ESEE workshops and UNFC training programmes. She has presented her research at numerous scientific conferences, including the 5th, 6th, and 7th Croatian Geological Congress. She is a member of the Croatian Geological Society.

List of published papers:

Kovačević Galović, E., Ilijanić, N., Fajković, H.*, Miko, S., Tomašić, N., Ivkić Filipović, I., Gizdavec, N., Peh, Z., Teskera, D. (2026): Mineralogical and Geochemical Variability of the Mamutovac-1a Upper Eocene Karst Bauxite Deposit (Croatian Dinarides) and Its CRM Potential. – Minerals, 16(5), 547. https://doi.org/10.3390/min16050547

Borojević Šoštarić, S.*, Tomašić, N., Bohanek, V., Kovačević Galović, E., Gizdavec, N., Miko, S. (2026): Croatian Critical Mineral Commodity Letters: Bauxite.- Geologia Croatica, 79/2, accepted for publication. https://doi.org/10.4154/GC.2026.10

Gizdavec, N., Kovačević Galović, E.* (2026): Aligning Croatia's national solid mineral resources classification system with UNFC: a methodological framework and case-based implications.- Geologia Croatica, 79/2, accepted for publication. https://doi.org/10.4154/GC.2026.08

Kovačević Galović, E., Ilijanić, N.*, Gizdavec, N., Miko, S., Peh, Z. (2025): Geochemical insights and mineral resource potential of rare earth elements (REE) in the Croatian karst bauxites. – Minerals, 15(2), 192. https://doi.org/10.3390/min15020192

Ilijanić, N.*, Kovačević Galović, E., Gizdavec, N., Ivkić Filipović, I., Miko, S.*, Peh, Z. (2023): Geochemical records in subaerial exposure environments in Croatia using discriminant function analysis of bauxite data. – Frontiers in Earth Science, 10, 1055435. https://doi.org/10.3389/feart.2022.1055435

Peh, Z.*, Kovačević Galović, E. (2016): Geochemistry of Lower Palaeogene bauxites – Unique signature of the tectonostratigraphic evolution of a part of the Croatian Karst. – Geologia Croatica, 69, 269–279. https://doi.org/10.4154/gc.2016.24

Peh, Z.*, Kovačević Galović, E. (2014): Geochemistry of Istrian Lower Palaeogene bauxites – Is it relevant to the extent of subaerial exposure during Cretaceous times? – Ore Geology Reviews, 63, 296–306. https://doi.org/10.1016/j.oregeorev.2014.05.020

Kovačević Galović, E.*, Ilijanić, N., Peh, Z., Miko, S., Hasan, O. (2012): Geochemical discrimination of early Palaeogene bauxites in Croatia. – Geologia Croatica, 65, 53–65. https://doi.org/10.4154/GC.2012.04